



**Universal Mobile Telecommunications System (UMTS);
LTE;
Universal Terrestrial Radio Access (UTRA)
and Evolved Universal Terrestrial Radio Access (E-UTRA);
Verification of radiated multi-antenna reception performance of
User Equipment (UE)
(3GPP TR 37.977 version 14.3.0 Release 14)**



Reference

RTR/TSGR-0437977vE30

Keywords

LTE,UMTS

ETSI

650 Route des Lucioles
F-06921 Sophia Antipolis Cedex - FRANCE

Tel.: +33 4 92 94 42 00 Fax: +33 4 93 65 47 16

Siret N° 348 623 562 00017 - NAF 742 C
Association à but non lucratif enregistrée à la
Sous-Préfecture de Grasse (06) N° 7803/88

Important notice

The present document can be downloaded from:

<http://www.etsi.org/standards-search>

The present document may be made available in electronic versions and/or in print. The content of any electronic and/or print versions of the present document shall not be modified without the prior written authorization of ETSI. In case of any existing or perceived difference in contents between such versions and/or in print, the only prevailing document is the print of the Portable Document Format (PDF) version kept on a specific network drive within ETSI Secretariat.

Users of the present document should be aware that the document may be subject to revision or change of status.

Information on the current status of this and other ETSI documents is available at

<https://portal.etsi.org/TB/ETSIDeliverableStatus.aspx>

If you find errors in the present document, please send your comment to one of the following services:

<https://portal.etsi.org/People/CommiteeSupportStaff.aspx>

Copyright Notification

No part may be reproduced or utilized in any form or by any means, electronic or mechanical, including photocopying and microfilm except as authorized by written permission of ETSI.

The content of the PDF version shall not be modified without the written authorization of ETSI.

The copyright and the foregoing restriction extend to reproduction in all media.

© European Telecommunications Standards Institute 2017.

All rights reserved.

DECT™, **PLUGTESTS™**, **UMTS™** and the ETSI logo are Trade Marks of ETSI registered for the benefit of its Members.

3GPP™ and **LTE™** are Trade Marks of ETSI registered for the benefit of its Members and of the 3GPP Organizational Partners.

oneM2M logo is protected for the benefit of its Members

GSM® and the GSM logo are Trade Marks registered and owned by the GSM Association.

Intellectual Property Rights

IPRs essential or potentially essential to the present document may have been declared to ETSI. The information pertaining to these essential IPRs, if any, is publicly available for **ETSI members and non-members**, and can be found in ETSI SR 000 314: "*Intellectual Property Rights (IPRs); Essential, or potentially Essential, IPRs notified to ETSI in respect of ETSI standards*", which is available from the ETSI Secretariat. Latest updates are available on the ETSI Web server (<https://ipr.etsi.org>).

Pursuant to the ETSI IPR Policy, no investigation, including IPR searches, has been carried out by ETSI. No guarantee can be given as to the existence of other IPRs not referenced in ETSI SR 000 314 (or the updates on the ETSI Web server) which are, or may be, or may become, essential to the present document.

Foreword

This Technical Report (TR) has been produced by ETSI 3rd Generation Partnership Project (3GPP).

The present document may refer to technical specifications or reports using their 3GPP identities, UMTS identities or GSM identities. These should be interpreted as being references to the corresponding ETSI deliverables.

The cross reference between GSM, UMTS, 3GPP and ETSI identities can be found under <http://webapp.etsi.org/key/queryform.asp>.

Modal verbs terminology

In the present document "**should**", "**should not**", "**may**", "**need not**", "**will**", "**will not**", "**can**" and "**cannot**" are to be interpreted as described in clause 3.2 of the [ETSI Drafting Rules](#) (Verbal forms for the expression of provisions).

"**must**" and "**must not**" are **NOT** allowed in ETSI deliverables except when used in direct citation.

Contents

| | |
|--|----|
| Intellectual Property Rights | 2 |
| Foreword..... | 2 |
| Modal verbs terminology..... | 2 |
| Foreword..... | 8 |
| 1 Scope | 9 |
| 2 References | 9 |
| 3 Definitions, symbols and abbreviations | 10 |
| 3.1 Definitions | 10 |
| 3.2 Symbols..... | 10 |
| 3.3 Abbreviations | 10 |
| 4 Introduction | 11 |
| 4.1 Background | 11 |
| 4.2 Work item objective | 11 |
| 4.3 High level requirements | 12 |
| 5 Performance metrics..... | 13 |
| 5.1 Figure of Merits..... | 13 |
| 5.1.1 Definition of MIMO throughput..... | 13 |
| 5.1.2 Definition of Signal-to-Interference Ratio (SIR) | 13 |
| 5.1.2.1 SIR Control for Multi-Probe Anechoic Chamber Methodology | 14 |
| 5.1.2.2 SIR Control for the reverberation chamber method..... | 15 |
| 5.1.2.3 SIR Control for the reverberation chamber plus channel emulator method | 16 |
| 5.1.2.4 SIR Control for the two-stage methodology | 17 |
| 5.2 Averaging of throughput curves | 19 |
| 5.2.1 Average of power levels | 19 |
| 6 Candidate measurement methodologies..... | 20 |
| 6.1 Void..... | 20 |
| 6.2 Void..... | 20 |
| 6.3 Downlink measurement methodologies | 20 |
| 6.3.1 Methodologies based on Anechoic RF Chamber | 20 |
| 6.3.1.1 Candidate Solution 1 | 20 |
| 6.3.1.1.1 Concept and configuration..... | 21 |
| 6.3.1.1.2 Scalability of the methodology..... | 22 |
| 6.3.1.1.3 Test conditions | 23 |
| 6.3.1.2 Void..... | 24 |
| 6.3.1.3 Candidate solution 3..... | 24 |
| 6.3.1.3.1 Concept and configuration..... | 24 |
| 6.3.1.3.2 Test conditions | 27 |
| 6.3.1.3.3 Overview of calibration procedures specific to the RTS method | 27 |
| 6.3.1.4 Candidate solution 4..... | 28 |
| 6.3.1.4.1 Concept and configuration..... | 28 |
| 6.3.1.4.2 Decomposition approach | 28 |
| 6.3.1.4.3 Conducted test | 30 |
| 6.3.1.4.4 Radiated test | 30 |
| 6.3.1.4.5 Possible extensions of the decomposition method | 31 |
| 6.3.1.5 Candidate solution 5..... | 32 |
| 6.3.1.5.1 Concept and configuration..... | 32 |
| 6.3.1.5.2 Test conditions | 34 |
| 6.3.2 Methodologies based on Reverberation Chamber | 36 |
| 6.3.2.1 Candidate solution 1..... | 36 |
| 6.3.2.1.1 Concept and configuration..... | 37 |
| 6.3.2.1.2 Test conditions | 38 |
| 6.3.2.2 Candidate solution 2..... | 39 |

| | | |
|-----------|---|----|
| 6.3.2.2.1 | Concept and configuration..... | 39 |
| 6.3.2.2.2 | Test conditions | 40 |
| 7 | Base Station (BS) configuration..... | 41 |
| 7.1 | eNodeB emulator settings | 41 |
| 8 | Channel Models..... | 43 |
| 8.1 | Introduction | 43 |
| 8.2 | Channel Model(s) to be validated..... | 43 |
| 8.3 | Verification of Channel Model implementations | 45 |
| 8.3.1 | Measurement instruments and setup..... | 45 |
| 8.3.1.1 | Vector Network Analyzer (VNA) setup..... | 45 |
| 8.3.1.2 | Spectrum Analyzer (SA) setup..... | 46 |
| 8.3.2 | Validation measurements..... | 46 |
| 8.3.2.1 | Power Delay Profile (PDP)..... | 46 |
| 8.3.2.2 | Doppler/Temporal correlation..... | 48 |
| 8.3.2.3 | Spatial correlation | 49 |
| 8.3.2.4 | Cross-polarization | 51 |
| 8.3.3 | Reporting | 52 |
| 8.4 | Channel Model validation results | 54 |
| 8.4.1 | Scope | 54 |
| 8.4.2 | Power Delay Profile (PDP)..... | 54 |
| 8.4.3 | Doppler / Temporal Correlation..... | 57 |
| 8.4.4 | Spatial correlation..... | 58 |
| 8.4.5 | Cross polarization | 60 |
| 8.4.6 | Summary..... | 60 |
| 8.5 | Channel Model emulation of the Base Station antenna pattern configuration | 61 |
| 9 | Reference antennas and devices testing | 61 |
| 9.1 | Reference antennas design | 61 |
| 9.2 | Reference devices | 62 |
| 9.3 | Description of tests with reference antennas and devices..... | 62 |
| 9.3.1 | The Absolute Data Throughput Comparison Framework..... | 62 |
| 9.3.1.1 | Introduction..... | 62 |
| 9.3.1.2 | Antenna pattern data format..... | 63 |
| 9.3.1.3 | Emulation of antenna pattern rotation..... | 64 |
| 9.3.1.4 | Absolute Data Throughput measurement enabler | 65 |
| 9.3.1.5 | Output data format | 66 |
| 9.3.1.6 | Application of the framework and scenarios for comparison..... | 71 |
| 9.3.1.7 | Proof of concept | 73 |
| 9.3.1.7.1 | The first scenario, anechoic based..... | 73 |
| 9.3.1.7.2 | The second scenario, reverberation chamber based..... | 75 |
| 9.3.1.7.3 | The third scenario, reverberation chamber and channel emulator based | 76 |
| 9.4 | Device positioning..... | 78 |
| 9.4.1 | Handheld UE – Browsing mode | 78 |
| 9.4.1.1 | MPAC Positioning Guidelines | 78 |
| 9.4.2 | Handheld UE – Speech mode | 78 |
| 9.4.2.1 | MPAC Positioning Guidelines..... | 78 |
| 9.4.3 | Laptop Mounted Equipment (LME) | 78 |
| 9.4.3.1 | MPAC Positioning Guidelines | 79 |
| 9.4.4 | Laptop Embedded Equipment (LEE)..... | 79 |
| 9.4.4.1 | MPAC Positioning Guidelines | 79 |
| 10 | Measurement results from testing campaigns | 79 |
| 10.1 | Introduction | 79 |
| 10.2 | CTIA test campaign..... | 79 |
| 10.2.1 | Description of the test plan | 79 |
| 10.2.2 | Anechoic chamber method with multiprobe configuration..... | 80 |
| 10.2.3 | Reverberation chamber method using NIST channel model and using channel emulator with short delay spread low correlation channel model..... | 85 |
| 10.2.4 | RTS method results..... | 93 |
| 10.3 | 3GPP harmonization test campaign..... | 97 |
| 10.3.1 | Description of the test plan | 97 |

| | | |
|-----------------|---|------------|
| 10.3.2 | Devices under test..... | 98 |
| 10.3.3 | Measurement uncertainty bound for harmonization | 99 |
| 10.3.4 | Summary of results | 99 |
| 10.3.5 | Harmonization outcome..... | 103 |
| 10.4 | Lab alignment procedures for performance labs | 105 |
| 10.4.1 | General..... | 105 |
| 10.4.2 | Channel model validation data..... | 105 |
| 10.4.3 | Calibration with a specific set of reference dipoles | 105 |
| 10.4.4 | Performance alignment measurements | 106 |
| 10.4.5 | Acceptance criteria | 106 |
| 11 | Void..... | 107 |
| 12 | MIMO OTA test procedures | 107 |
| 12.1 | Anechoic chamber method with multiprobe configuration test procedure..... | 107 |
| 12.1.1 | Base Station configuration..... | 107 |
| 12.1.2 | Channel Models | 107 |
| 12.1.3 | Device positioning and environmental conditions | 107 |
| 12.1.4 | System Description | 107 |
| 12.1.4.1 | Solution Overview | 107 |
| 12.1.4.2 | Configuration | 107 |
| 12.1.4.3 | Calibration..... | 107 |
| 12.1.5 | Figure of Merit..... | 107 |
| 12.1.6 | Test procedure | 107 |
| 12.1.6.1 | Initial conditions | 107 |
| 12.1.6.2 | Test procedure..... | 108 |
| 12.1.7 | Measurement Uncertainty budget | 108 |
| 12.2 | Reverberation chamber test procedure | 108 |
| 12.2.1 | Base Station configuration..... | 108 |
| 12.2.2 | Channel Models | 108 |
| 12.2.3 | Device positioning and environmental conditions | 109 |
| 12.2.4 | System Description | 109 |
| 12.2.4.1 | Solution Overview | 109 |
| 12.2.4.2 | Configuration | 109 |
| 12.2.4.3 | Calibration..... | 109 |
| 12.2.5 | Figure of Merit..... | 109 |
| 12.2.6 | Test procedure | 109 |
| 12.2.6.1 | Initial conditions | 109 |
| 12.2.6.2 | Test procedure..... | 109 |
| 12.2.7 | Measurement Uncertainty budget | 110 |
| 12.3 | RTS method test procedure | 110 |
| 12.3.1 | Base Station configuration..... | 110 |
| 12.3.2 | Channel Models | 110 |
| 12.3.3 | Device positioning and environmental conditions | 110 |
| 12.3.4 | System Description | 110 |
| 12.3.4.1 | Solution Overview | 110 |
| 12.3.4.2 | Configuration | 111 |
| 12.3.4.3 | Calibration..... | 111 |
| 12.3.5 | Figure of Merit..... | 111 |
| 12.3.6 | Test procedure | 111 |
| 12.3.6.1 | Initial conditions | 111 |
| 12.3.6.2 | Test procedure..... | 111 |
| 12.3.7 | Measurement Uncertainty budget | 112 |
| 12.4 | Comparison of methodologies..... | 112 |
| Annex A: | eNodeB Emulator Downlink power verification | 116 |
| A.1 | Introduction | 116 |
| A.2 | Test prerequisites..... | 116 |
| A.3 | Test Methodology | 117 |
| Annex B: | Measurement uncertainty budget | 120 |

| | | |
|-----------------|--|------------|
| B.1 | Measurement uncertainty budget for multiprobe method | 120 |
| B.2 | Measurement uncertainty budget contributors for the RTS method | 123 |
| B.3 | Measurement uncertainty budget for reverberation chamber method..... | 126 |
| B.4 | Measurement uncertainty budget for decomposition method | 129 |
| B.5 | Measurement uncertainty budget for reverberation chamber plus channel emulator method..... | 130 |
| B.6 | Fading channel emulator output uncertainty | 132 |
| B.7 | External Amplifiers Uncertainty Terms | 133 |
| B.7.1 | Stability | 133 |
| B.7.2 | Linearity | 133 |
| B.7.3 | Noise Figure | 133 |
| B.7.4 | Mismatch..... | 133 |
| B.7.5 | Gain..... | 133 |
| Annex C: | Other Environmental Test conditions for consideration..... | 134 |
| C.1 | Scope | 134 |
| C.2 | 3D isotropic Channel Models..... | 134 |
| C.3 | Verification of Channel Model implementations | 136 |
| C.3.1 | Measurement instruments and setup..... | 136 |
| C.3.1.1 | Vector Network Analyzer (VNA) setup | 136 |
| C.3.1.2 | Spectrum Analyzer (SA) setup | 137 |
| C.3.2 | Validation measurements | 138 |
| C.3.2.1 | Power Delay Profile (PDP)..... | 138 |
| C.3.2.2 | Doppler for 3D isotropic models | 140 |
| C.3.2.3 | Base Station antenna correlation for 3D isotropic models | 142 |
| C.3.2.4 | Rayleigh fading..... | 143 |
| C.3.2.5 | Isotropy for 3D isotropic models | 147 |
| C.3.3 | Reporting..... | 149 |
| C.4 | Channel model validation results | 150 |
| C.4.1 | Scope | 150 |
| C.4.2 | Power Delay Profile (PDP) for 3D isotropic models..... | 150 |
| C.4.2.1 | Setup used by harmonization test lab..... | 152 |
| C.4.3 | Doppler for 3D isotropic models..... | 154 |
| C.4.3.1 | Setup used by harmonization test lab..... | 155 |
| C.4.4 | Base Station antenna correlation for 3D isotropic models | 157 |
| C.4.4.1 | Setup used by harmonization test lab..... | 158 |
| C.4.5 | Rayleigh fading for 3D isotropic models | 159 |
| C.4.5.1 | Setup used by harmonization test lab..... | 160 |
| C.4.6 | Isotropy for 3D isotropic models..... | 161 |
| C.4.6.1 | Setup used by harmonization test lab..... | 163 |
| C.4.7 | Summary for 3D Isotropic Models..... | 164 |
| Annex D: | Environmental requirements..... | 165 |
| D.1 | Scope | 165 |
| D.2 | Ambient temperature..... | 165 |
| D.3 | Operating voltage | 165 |
| Annex E: | DUT orientation conditions..... | 166 |
| E.1 | Scope | 166 |
| E.2 | Testing environment conditions | 166 |
| E.2.1 | MPAC Positioning Guidelines | 172 |
| E.2.2 | RTS Positioning Guidelines and test zone dimensions | 176 |
| Annex F: | Calibration..... | 177 |

| | | |
|---|--|------------|
| F.1 | Scope | 177 |
| F.2 | Calibration Procedure – Anechoic chamber method with multiprobe configuration..... | 177 |
| F.2.1 | Example Calibration Procedure..... | 177 |
| F.3 | Calibration Procedure – Reverberation chamber method..... | 179 |
| F.3.1 | Measurement of S-parameters through the chamber for a complete stirring sequence | 179 |
| F.3.2 | Calculation of the chamber reference transfer function..... | 180 |
| F.3.3 | Cable calibration | 180 |
| F.4 | Calibration Procedure: RTS method | 181 |
| Annex G: Test Volume Validation..... | | 183 |
| G.1 | Test Volume Validation for the RC+CE Methodology..... | 183 |
| G.1.1 | Test Volume Validation Setup | 183 |
| G.1.1.1 | Type 1 Reverberation Chamber – With Turntable..... | 183 |
| G.1.1.2 | Type 2 Reverberation Chamber – Without Turntable..... | 185 |
| G.1.2 | Test Volume Validation Procedure | 186 |
| G.1.2.1 | Isotropy | 187 |
| G.1.2.2 | Chamber Statistical Ripple and Repeatability | 187 |
| Annex H: Change history | | 188 |
| History | | 191 |

Foreword

This Technical Report has been produced by the 3rd Generation Partnership Project (3GPP).

The contents of the present document are subject to continuing work within the TSG and may change following formal TSG approval. Should the TSG modify the contents of the present document, it will be re-released by the TSG with an identifying change of release date and an increase in version number as follows:

Version x.y.z

where:

- x the first digit:
 - 1 presented to TSG for information;
 - 2 presented to TSG for approval;
 - 3 or greater indicates TSG approved document under change control.
- y the second digit is incremented for all changes of substance, i.e. technical enhancements, corrections, updates, etc.
- z the third digit is incremented when editorial only changes have been incorporated in the document.

1 Scope

The present document is the technical report for the work item on MIMO OTA, which was approved at TSG RAN#55 [13]. The scope of the WI is to define a 3GPP methodology or set of comparable methodologies for measuring the radiated performance of multiple antenna reception and MIMO receivers in the UE. The test methodology should be relevant for HSPA and LTE technologies, with particular focus on handheld devices and devices embedded in laptop computers.

RAN WG4 has been working on the study item "Measurement of radiated performance for MIMO and multi-antenna reception for HSPA and LTE terminals" with the objective to define a test methodology for measuring the radiated performance of MIMO and multi-antenna UE reception in UMTS and LTE.

RAN4 has done sufficient work to be confident that the definition of a meaningful test methodology is feasible; however RAN4 does not have sufficient evidence yet to conclude on a single test methodology that would fulfil all requirements for standardisation, and the standardisation of multiple test methodologies may be one eventual outcome, with a view to avoid differences in the decision of what is a "good" or "bad" device from the radiated receiver performance perspective.

2 References

The following documents contain provisions which, through reference in this text, constitute provisions of the present document.

- References are either specific (identified by date of publication, edition number, version number, etc.) or non-specific.
- For a specific reference, subsequent revisions do not apply.
- For a non-specific reference, the latest version applies. In the case of a reference to a 3GPP document (including a GSM document), a non-specific reference implicitly refers to the latest version of that document *in the same Release as the present document*.

- [1] 3GPP TR 21.905: "Vocabulary for 3GPP Specifications".
- [2] RP-090352: "Proposed new study item: Measurement of radiated performance for MIMO and multi-antenna reception for HSPA and LTE terminals."
- [3] TD(09) 766, COST2100 SWG 2.2, Braunschweig, Germany, Pekka Kyösti et. al. "Proposal for standardized test procedure for OTA testing of multi-antenna terminals", Elektrobitt.
- [4] 3GPP TS 34.114: "User Equipment (UE) / Mobile Station (MS) Over The Air (OTA) antenna performance; Conformance testing".
- [5] 3GPP TS 25.214: "Physical layer procedures (FDD)"
- [6] TD(09) 742, COST 2100 SWG 2.2, Braunschweig, Germany, February 2009, J. Takada: "Handset MIMO Antenna Testing Using a RF-controlled Spatial Fading Emulator".
- [7] 3GPP TS 36.212: "Evolved Universal Terrestrial Radio Access (E-UTRA); Multiplexing and channel coding".
- [8] 3GPP TS 36.213: "Evolved Universal Terrestrial Radio Access (E-UTRA); Physical layer procedures".
- [9] CTIA: "Test Plan for Wireless Device Over-the-Air Performance ".
- [10] 3GPP TS 36.101: "Evolved Universal Terrestrial Radio Access (E-UTRA); User Equipment (UE) radio transmission and reception".
- [11] 3GPP TR 25.914: "Measurements of radio performances for UMTS terminals in speech mode".
- [12] 3GPP TS 36.521-1: "Evolved Universal Terrestrial Radio Access (E-UTRA); User Equipment (UE) conformance specification Radio transmission and reception; Part 1: Conformance testing"

- [13] RP-120368: Revised WID on "Verification of radiated multi-antenna reception performance of UEs in LTE/UMTS – performance aspects".
- [14] B. Yanakiev, J. O. Nielsen, M. Christensen, G. F. Pedersen: "The AAU 3D antenna pattern format-proposal for IC1004".
- [15] 3GPP TR 25.996: "Spatial channel model for Multiple Input Multiple Output (MIMO) simulations".
- [16] IEC 61000-4-21: "Electromagnetic compatibility (EMC) – Part 4-21: Testing and measurement techniques – Reverberation chamber test methods", Edition 2.0 2011-01.
- [17] IEEE.149-1979.R2008: "IEEE Standard Test Procedures for Antennas," IEEE, October 2003.
- [18] B. Yanakiev, J. Nielsen, M. Christensen, G. Pedersen: "Antennas In Real Environments," EuCAP 2011.
- [19] 3GPP TS 36.508: "Evolved Universal Terrestrial Radio Access (E-UTRA) and Evolved Packet Core (EPC); Common test environments for User Equipment (UE) conformance testing".
- [20] 3GPP TS 36.978: "User Equipment (UE) antenna test function definition for two-stage Multiple Input Multiple Output (MIMO) Over The Air (OTA) test method".
- [21] P.M. Shankar, "Introduction to Wireless Systems," John Wiley & Sons, 2002, Section 2.5.
- [22] D. A. Hill, "Boundary Fields in Reverberation Chambers", IEEE Transactions on Electromagnetic Compatibility, Vol. 47, No. 2, May 2005.

3 Definitions, symbols and abbreviations

3.1 Definitions

For the purposes of the present document, the terms and definitions given in TR 21.905 [1] and the following apply. A term defined in the present document takes precedence over the definition of the same term, if any, in TR 21.905 [1].

3.2 Symbols

For the purposes of the present document, the following symbols apply:

| | |
|----------|---|
| H | Channel matrix |
| ϕ | Adjacent probe separation angle |
| θ | Zenith angle in the spherical co-ordinate system |
| ϕ | Azimuth angle in the spherical co-ordinate system |

3.3 Abbreviations

For the purposes of the present document, the abbreviations given in TR 21.905 [1] and the following apply. An abbreviation defined in the present document takes precedence over the definition of the same abbreviation, if any, in TR 21.905 [1].

| | |
|------|---|
| ADTF | Absolute Data Throughput Framework |
| AoA | Angle of Arrival |
| AoD | Angle of Departure |
| BS | Base Station |
| BSE | Base Station Emulator |
| BTS | Base Transceiver Station |
| COST | Cooperation of Scientific and Technical |
| CTIA | Cellular and Telecommunication Industry Association |
| DL | Downlink |
| DUT | Device Under Test |

| | |
|---------|---|
| FRC | Fixed Reference Measurement Channel |
| FTP | File Transfer Protocol |
| HSPA | High Speed Packet Access |
| HTTP | HyperText Transfer Protocol |
| LTE | Long Term Evolution |
| MCS | Modulation and Coding Scheme |
| MIMO | Multiple Input Multiple Output |
| MPAC | Multi-probe Anechoic |
| OTA | Over-the-Air |
| RC | Reverberation Chamber |
| RC + CE | Reverberation chamber plus channel emulator |
| RTS | Radiated Two-Stage |
| SCM | Spatial Channel Model |
| SCME | Spatial Channel Model Extension |
| SI | Study Item |
| SISO | Single Input Single Output |
| SIR | Signal-to-Interference Ratio |
| SNR | Signal-to-Noise Ratio |
| SS | System Simulator |
| TBS | Transport Block Size |
| TTI | Transmission Time Interval |
| UE | User Equipment |
| UDP | User Datagram Protocol |
| UL | Uplink |
| VRC | Variable Reference Measurement Channel |

4 Introduction

4.1 Background

The use of MIMO and receiver diversity in the UE is expected to give large gains in downlink throughput performance for HSPA and LTE devices. 3GPP already defined conducted tests for MIMO and multiple antenna receivers (type 1 and type 3 in TS 25.101 for HSPA demodulation), but it is clear that the ability to duplicate these gains in the field is highly dependent on the performance of the receive-antenna system.

At TSG RAN#41, Sep 2008, it was indicated that there is a need for a test methodology to be created with the aim of measuring and verifying the radiated performance of multi-antenna and MIMO receiver in UEs for both HSPA and LTE devices. As an outcome of the discussion, an LS was sent to COST 2100 SWG2.2 and CTIA ERP to ask them for feedback on their plans/ongoing work in this area, and also the timescales for which such work could be completed to define such a methodology, with particular focus on handheld devices and devices embedded in laptop computers.

Since then, feedback from COST 2100 and CTIA has suggested they are happy to work on this topic. However, given that 3GPP is the customer for this work as well as being a potential contributor, it is important to aim for commonly-accepted measurement and test methodology to be used across the industry.

4.2 Work item objective

The high level objective of this work item is to define a test methodology (ies) for verifying the radiated performance of multiple antenna reception in the UE and such methodology shall be able to:

- Verify the radiated "Over-The-Air" (OTA) performance of multiple antenna reception in the UE.
- Accurately able to reflect MIMO and SIMO performance under realistic MIMO and SIMO channel conditions. Be able to distinguish between UEs of "Good" and "Bad" multi-Rx antenna OTA performance, and offer a good reflection of the likely experience in the field.
- Offer good reliability, repeatability and an acceptable level of measurement uncertainty.

Such test methodology(ies) shall enable performance verification for:

- Handheld devices, devices embedded in laptop computers, and other devices (such as M2M equipment).
- All transmission modes of LTE and HSDPA, including spatial multiplexing (MIMO) and single spatial layer operation. However the transmission modes used in the test shall be defined as part of the work.
 - Initially tests shall use of LTE Transmission Mode 3, Fixed Reference Channel, and forced Rank 2. As the work progresses, other transmission modes of LTE and HSPA shall be introduced.
 - The utilization of Variable Reference Channels and other-cell interference shall also be studied at a later stage.

The following is required for the analysis phase of this work item:

- In order to compare results across the different methods, absolute throughput shall be used as the Figure of Merit.
- In order to analyse and accurately validate a method(s) the following work shall be performed:
 - eNodeB settings shall be agreed.
 - Realistic MIMO conditions and realistic channel models shall be identified to be used as a reference radio environment.
 - The MIMO conditions and channel models shall be validated for the proposed test methods.
 - Calibration of the power levels in the methodology shall be performed.
 - The absolute throughput measured for each test method shall be compared with the absolute throughput measured in the reference radio environment, in order to identify the capability of each method to provide a measurement result that matches what is observed in realistic environments.
 - In order to minimize the variables associated with testing of production UEs with unknown antenna characteristics, utilize reference antennas in combination with a known UE baseband receiver (verified via conducted RF tests with and without channel impairments). This is intended to verify whether the characteristics of the receive antenna design (i.e. correlation, gain imbalance, etc) affecting receiver performance can be accurately distinguished by proposed test methods.

In the event that more than one test methodology is agreed to be standardised, differences between methodologies in the decision of what is a "good" or "bad" device from the radiated receiver performance perspective shall be avoided.

When selecting the method(s) for specification for LTE MIMO, applicability to LTE-SIMO UMTS-SIMO/MIMO shall be described.

During the course of this Work Item, maintain ongoing communication with COST and CTIA MOSG to ensure industry coordination on this topic and to distribute tasks according to expertise or resource availability.

TSG RAN should contact TSG GERAN to get feedback on the applicability of such a test methodology for GERAN.

4.3 High level requirements

The following high level requirements are agreed by RAN4:

1. Measurement of radiated performance for MIMO and multi-antenna reception for HSPA and LTE terminals must be performed over-the-air, i.e. without RF cable connections to the DUT.
 - NOTE 1: DUTs to the test house will have accessibility to temporary antenna port for conducted purposes.
 - NOTE 2: Temporary antenna port is used to assess to DUT receiver.
 - NOTE 3: UE special function to measure antenna pattern is not desirable for MIMO OTA purposes.
2. The MIMO OTA method(s) must be able to differentiate between a good terminal and a bad terminal in terms of MIMO OTA performance.

3. The desired primary Figure Of Merit (FOM) is absolute throughput. This will easily allow meaningful comparison of the ability of different methods to evaluate MIMO OTA performance.

5 Performance metrics

5.1 Figure of Merits

Absolute throughput performance is used in order to be able to compare the different proposed methodologies in their ability to distinguish good and bad MIMO devices.

The performance metric applies to both HSPA and LTE system.

Other Figure of Merits and their applicability on the assessment of MIMO performance is for further study.

5.1.1 Definition of MIMO throughput

MIMO throughput is defined here as the time-averaged number of correctly received transport blocks in a communication system running an application, where a Transport Block is defined in the reference measurement channel. From OTA perspective, this is also called MIMO OTA throughput.

The MIMO OTA throughput is measured at the top of physical layer of HSPA and LTE system. Therefore, this is also measured at the same point as in the conductive measurement setup: under the use of FRC, the SS transmit fixed-size payload bits to the DUT. The DUT signals back either ACK or NACK to the SS. The SS then records the following:

- Number of ACKs,
- Number of NACKs, and
- Number of DTX TTIs

Hence the MIMO (OTA) throughput can be calculated as

$$MIMO\ (OTA)\ Throughput = \frac{Transmitted\ TBS \times Num\ of\ ACKs}{MeasurementTime}$$

where Transmitted TBS is the Transport Block Size transmitted by the SS, which is fixed for a FRC during the measurement period. MeasurementTime is the total composed of successful TTIs (ACK), unsuccessful TTIs (NACK) and DTX-TTIs.

The time-averaging is to be taken over a time period sufficiently long to average out the variations due to the fading channel. Therefore, this is also called the average MIMO OTA throughput. The throughput should be measured at a time when eventual start-up transients in the system have evanesced.

5.1.2 Definition of Signal-to-Interference Ratio (SIR)

Applicability of SIR to MIMO OTA performance evaluation is FFS.

This definition is applicable to MIMO OTA test cases where control of the signal to interference ratio (SIR) is required (i.e. DUT throughput characterized as a function of SIR shall require control of SIR within the test volume as described in the sub-sections that follow). For test cases where SIR control is not required (i.e. throughput characterized as a function of signal power incident to the DUT antennas, such as RS EPRE) this definition is not applicable.

In real world scenarios the mobile will experience an interference floor higher than the device noise floor. As a consequence, the methodology for quantifying MIMO OTA performance of a device may have to include the use of an external interferer signal. MIMO OTA testing is useful for a situation where, in general, a high signal level is received that is not close to the sensitivity level of the UE and the interference floor is dominated by inter-cell interference and/or other interferers and not the UE noise floor. In most UE performance testing, interference is modelled as AWGN for conducted testing. This proposal intends to align with this assumption and use AWGN for the interference signal.

From a system level point of view, the omnidirectional (isotropic) and uncorrelated nature of the interfering signal to the wanted signal is a crucial assumption. Injecting a noise signal that is correlated to the wanted faded signal is neither a scenario that is typically found in the network nor a scenario for which the UE modem is designed. As a result, we propose the methodology for injecting an omnidirectional (isotropic) and uncorrelated interferer signal.

5.1.2.1 SIR Control for Multi-Probe Anechoic Chamber Methodology

The interference level necessary to achieve a given SIR inside the test zone shall be generated as an independent process at each antenna probe with equal power, regardless of the signal power transmitted through that probe. The SIR shall be decreased by increasing the AWGN power while keeping the signal level constant.

To validate the control of SIR, the measurement setup shown in Figure 5.1.2.1-1 below may be used.

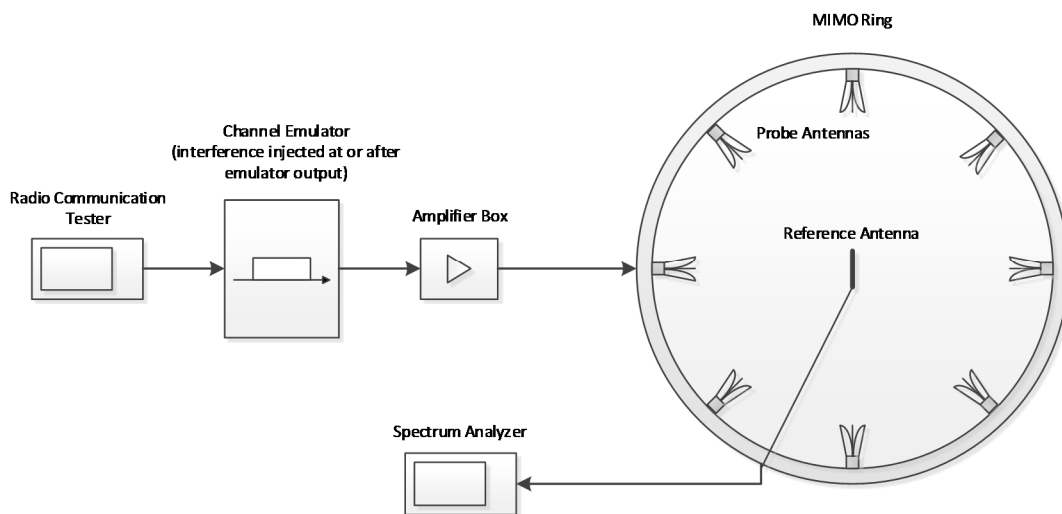


Figure 5.1.2.1-1: Verifying SIR level in the anechoic chamber multi-cluster MIMO OTA setup

The actual system components shown in the diagram, such as amplifier box or the source of the omnidirectional interferer signal, may or may not be present as shown.

The procedure below shall be used to verify SIR control inside the test zone for a given target SIR.

Verification procedure for establishing SIR control:

1. Configure the spectrum analyser with the settings given in Table 5.1.2.1-1 below
2. Load the target channel model into the channel emulator (e.g. SCME UMa, SCME UMi) and start the emulation
3. Configure the system gains for the LTE signal and injected interfering signal paths to achieve the target SIR
4. Disable interfering signal injection (depending on the system configuration this may be configured within the channel emulator itself or in an external signal generator)
5. Connect a vertically polarized reference dipole to the spectrum analyser via a cable and place inside the chamber at the center of the test zone
6. Measure the received power with the spectrum analyser over a duration sufficient to achieve statistical significance as defined in clause 12.1.6.2 and record the value as

$$P_{\text{SIG_MEAS_VER}}$$

7. Compensate for the loss of the cable (α_{CABLE}) and the gain of the dipole (G_{DIPOLE}) such that

$$P_{\text{SIG_VER}} = P_{\text{SIG_MEAS_VER}} - \alpha_{\text{CABLE}} - G_{\text{DIPOLE}}$$

8. Repeat steps 5 to 7 with the magnetic loop and get

$$P_{\text{SIG_HOR}} = P_{\text{SIG_MEAS_HOR}} - \alpha_{\text{CABLE}} - G_{\text{LOOP}}$$

9. Calculate the total signal power received as

$$P_{\text{SIG_TOTAL}} = P_{\text{SIG_VER|LINEAR}} + P_{\text{SIG_HOR|LINEAR}}$$

10. Disable the LTE signal source and enable interference injection (depending on the system configuration this may be configured within the channel emulator itself or in an external signal generator)

11. Connect a reference dipole to the spectrum analyser via a cable and place inside the chamber at the center of the test zone

12. Measure the received interfering signal power with the spectrum analyser over aduration sufficient to achieve statistical significance and record the value as

$$P_{\text{INT_MEAS_VER}}$$

13. Compensate for the loss of the cable (α_{CABLE}) and the gain of the dipole (G_{DIPOLE}) such that

$$P_{\text{INT_VER}} = P_{\text{INT_MEAS_VER}} - \alpha_{\text{CABLE}} - G_{\text{DIPOLE}}$$

14. Repeat steps 11 to 13 with the magnetic loop and get

$$P_{\text{INT_HOR}} = P_{\text{INT_MEAS_HOR}} - \alpha_{\text{CABLE}} - G_{\text{LOOP}}$$

15. Calculate the total interfering signal power received as

$$P_{\text{INT_TOTAL}} = P_{\text{INT_VER|LINEAR}} + P_{\text{INT_HOR|LINEAR}}$$

16. Calculate the achieved signal to interference ratio such that

$$\text{SIR}_{\text{ACHIEVED}} = P_{\text{SIG_TOTAL}} - P_{\text{INT_TOTAL}}$$

and validate that it matches the target SIR.

Table 5.1.2.1-1: Spectrum analyzer settings for SIR control verification

| Item | Unit | Value |
|--|------|--|
| Center frequency | MHz | Downlink center frequency in 3GPP TS 36.508 as required per band |
| Span | MHz | 9 ¹ |
| Resolution BW | kHz | 30 |
| Video BW | MHz | ≥10 |
| Number of points | | > 200 |
| Number of averages | | Sufficient to achieve statistical significance as defined above |
| NOTE 1: Span is shown using the assumption of a 10 MHz LTE RF channel BW and would be adjusted accordingly for an alternate RF channel BW. | | |

Care shall be taken to ensure that the signal level measurement in step 6 and the interfering signal level measurement in step 12 are sufficiently above the noise floor of the measurement system as to not impact the final SIR level. A horizontally polarized reference dipole may be used as opposed to the magnetic loop as long as the theta gain pattern is properly accounted for.

5.1.2.2 SIR Control for the reverberation chamber method

Additive White Gaussian Noise (AWGN) is used as interference for the SIR-controlled test case. Figure 5.1.2.2-1 shows an example setup for adding AWGN to the test environment with the injection point for the AWGN highlighted. The AWGN noise power used to create the desired SIR within the test volume shall be generated as an independent process. It is represented by faded noise driven in an isotropic fashion. The AWGN is injected into the reverberation chamber using a separate chamber antenna and the fading of the signal and the noise will be uncorrelated. The SIR is computed as a long-term average.

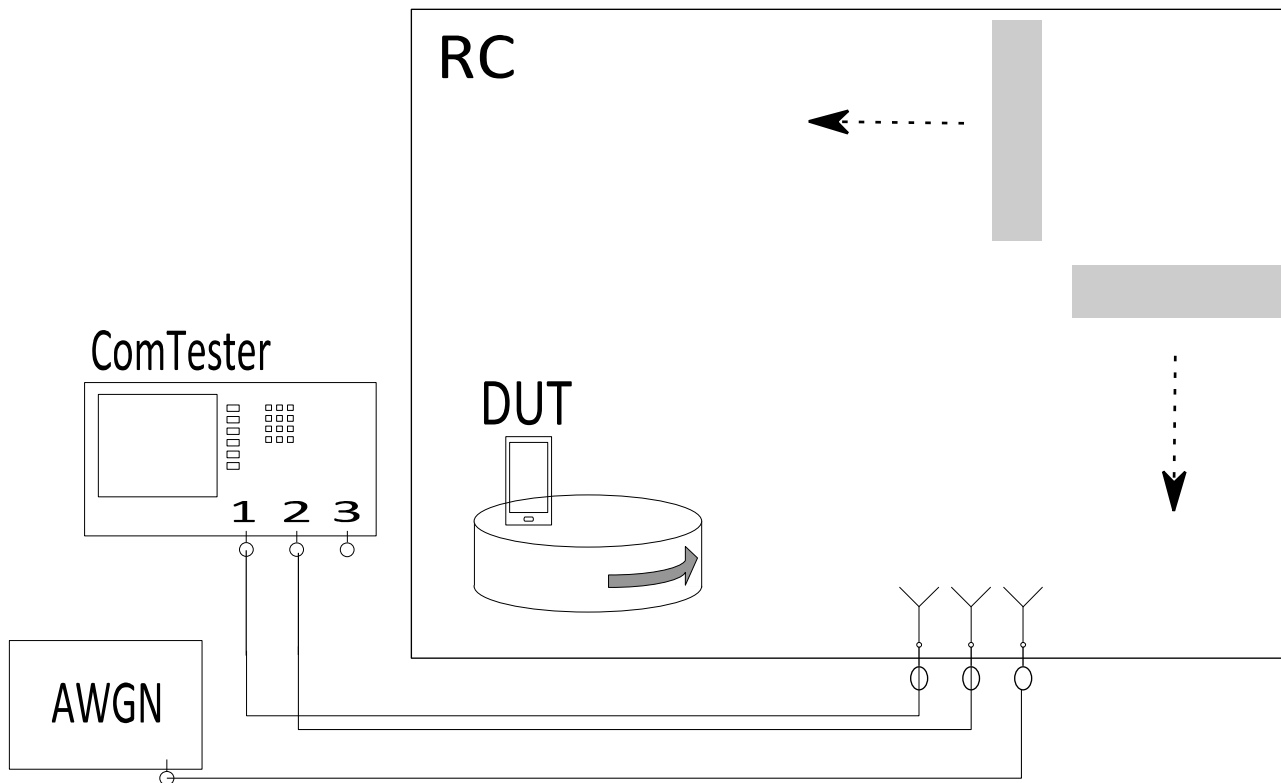


Figure 5.1.2.2-1: Example setup for SIR-controlled test scenario for the reverberation chamber methodology

5.1.2.3 SIR Control for the reverberation chamber plus channel emulator method

AWGN will be used as interference for the SIR-controlled test case. Figure 5.1.2.3-1 shows an example setup for adding AWGN to the test environment with the injection points for the AWGN highlighted. The AWGN noise power used to create the desired SIR within the test volume shall be generated as an independent process with equal power at each output of the channel emulator. It is represented by an un-faded noise driven in an isotropic fashion. The AWGN is combined with the signal at the output of the channel emulator (after the channel emulator fading) but before the signal is fed to the reverberation chamber antennas. The combined signal and AWGN is then fed into the chamber with the same chamber antennas. The SIR is computed as a long-term average.

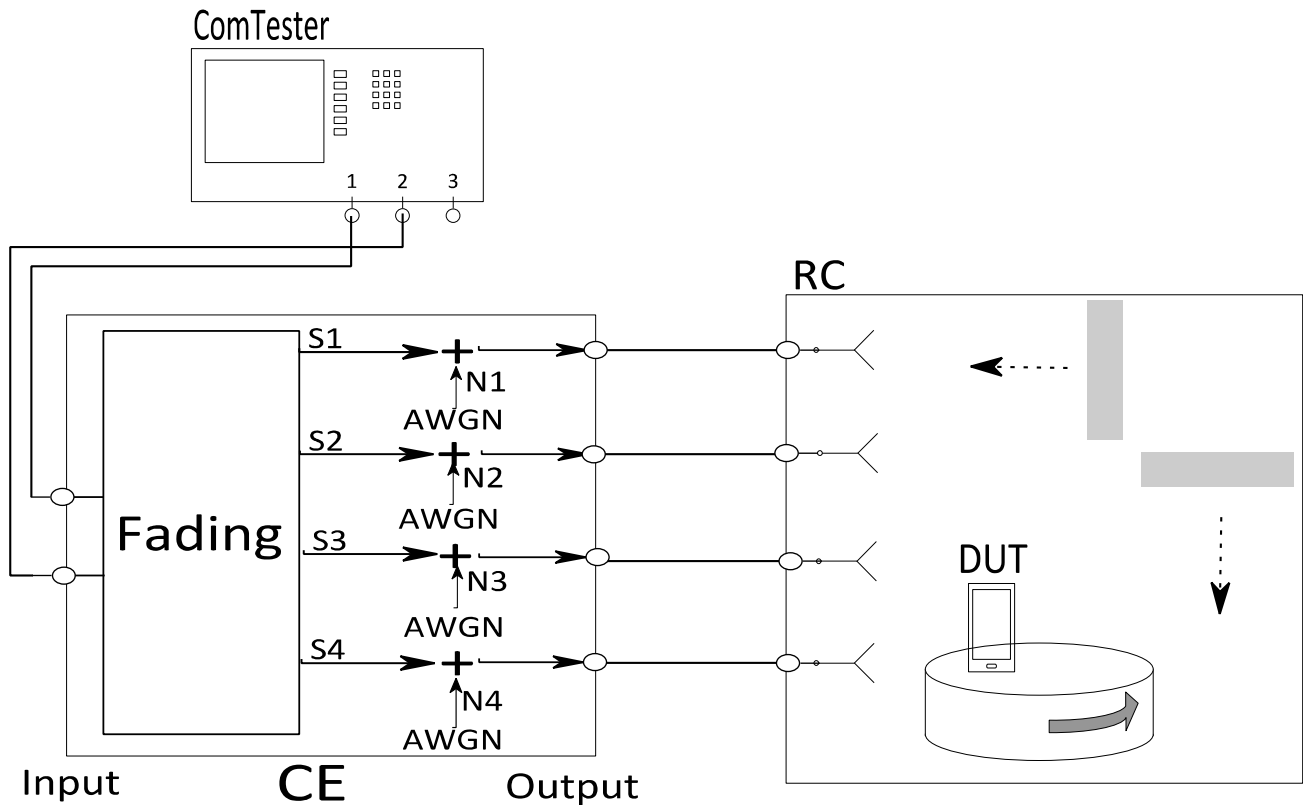


Figure 5.1.2.3-1: Example setup for SIR-controlled test scenario for the reverberation chamber and channel emulator methodology

5.1.2.4 SIR Control for the two-stage methodology

The two-stage method is fundamentally different from the multi-probe boundary array method and this has a significant impact on how omnidirectional AWGN is generated and validated.

In the two-stage method the AWGN is added digitally to the baseband signals. The goal is to emulate omnidirectional AWGN at the UE antennas. Since the signals generated by the second stage of two-stage method represent the signals after applying the effect of the receive antennas this has implications for the addition of AWGN.

If uncorrelated AWGN is added to the second stage signals for each UE receiver this creates a slightly easier test environment where each receiver sees uncorrelated noise. However, when the UE is placed in an actual omnidirectional noise field, the noise reaching each of the receivers is correlated by the same amount as the antennas are correlated. The impact of using uncorrelated AWGN depends on the antennas in question. Highly correlated antennas would see the same AWGN signal at each receiver but very low correlated antennas would expect see uncorrelated AWGN which is easier to process. For typical devices the performance difference has been measured at around 0.5 dB.

To fully represent the impact of omnidirectional AWGN on the wanted signals being generated for each receiver after the antennas, it is therefore necessary to correlate the AWGN according to the antenna correlation for an isotropic field.

To validate the control of SIR, the measurement setup shown in Figure 5.1.2.4-1 below may be used.

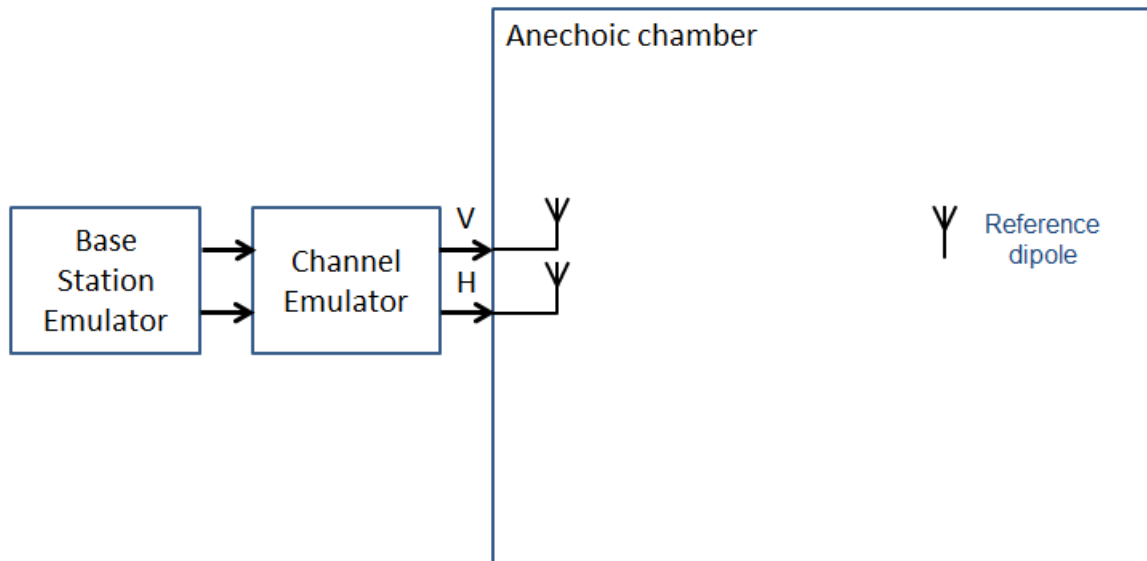


Figure 5.1.2.4-1: Verifying SIR level for the RTS method

Note: The signals from the vertical polarization and horizontal polarization have a different meaning from the multi-probe method. For the multi-probe method, the signal from vertical polarization antenna represents the vertical polarized signal in the real propagation environment. But for RTS method, the signal from the vertical polarization antenna represents the signal intended for one receiver, which has had the dual-polarized channel environment and antenna pattern applied. The same is true for the horizontal antenna. Thus the signals from each probe antenna include AWGN components from both polarizations.

The actual system components shown in the diagram are indicative of functions and may or may not be integrated.

The procedure below shall be used to verify SIR control for a given target SIR.

1. Configure the spectrum analyzer with the settings given in Table 5.1.2.4-1 below
2. Load the target channel model into the channel emulator (e.g. SCME UMa, SCME UMi) and start the emulation
3. Configure the system gains for the LTE signals and interfering signal to achieve the target SIR
4. Disable the interfering signal
5. Connect a vertically polarized reference dipole to the spectrum analyzer via a cable and place inside the chamber at the center of the test zone
6. Measure the received power with the spectrum analyzer over a duration sufficient to achieve statistical significance as defined in clause 12.3.6.2 and record the value as

$$P_{\text{SIG_MEAS_VER}}$$

7. Compensate for the loss of the cable (α_{CABLE}) and the gain of the dipole (G_{DIPOLE}) such that

$$P_{\text{SIG_VER}} = P_{\text{SIG_MEAS_VER}} - \alpha_{\text{CABLE}} - G_{\text{DIPOLE}}$$

8. Repeat steps 5 to 7 with the magnetic loop and get

$$P_{\text{SIG_HOR}} = P_{\text{SIG_MEAS_HOR}} - \alpha_{\text{CABLE}} - G_{\text{LOOP}}$$

9. Disable the LTE signal source and enable interference injection (depending on the system configuration this may be configured within the channel emulator itself or in an external signal generator)
10. Connect a reference dipole to the spectrum analyzer via a cable and place inside the chamber at the center of the test zone

11. Measure the received interfering signal power with the spectrum analyzer over a duration sufficient to achieve statistical significance and record the value as

$$P_{\text{INT_MEAS_VER}}$$

12. Compensate for the loss of the cable (α_{CABLE}) and the gain of the dipole (G_{DIPOLE}) such that

$$P_{\text{INT_VER}} = P_{\text{INT_MEAS_VER}} - \alpha_{\text{CABLE}} - G_{\text{DIPOLE}}$$

13. Repeat steps 10 to 12 with the magnetic loop and get

$$P_{\text{INT_HOR}} = P_{\text{INT_MEAS_HOR}} - \alpha_{\text{CABLE}} - G_{\text{LOOP}}$$

14. Calculate the achieved signal to interference ratio for vertical polarization branch as

$$\text{SIR}_{\text{ACHIEVED_VER}} = P_{\text{SIG_VER}} - P_{\text{INT_VER}}$$

Calculate the achieved signal to interference ratio for horizontal polarization branch as

$$\text{SIR}_{\text{ACHIEVED_HOR}} = P_{\text{SIG_HOR}} - P_{\text{INT_HOR}}$$

and validate that $\text{SIR}_{\text{ACHIEVED_VER}}$ and $\text{SIR}_{\text{ACHIEVED_HOR}}$ matches the target SIR.

Table 5.1.2.4-1: Spectrum analyzer settings for SIR control verification

| Item | Unit | Value |
|--|------|--|
| Center frequency | MHz | Downlink center frequency in 3GPP TS 36.508 as required per band |
| Span | MHz | 9 ¹ |
| Resolution BW | kHz | 30 |
| Video BW | MHz | ≥ 10 |
| Number of points | | > 200 |
| Number of averages | | Sufficient to achieve statistical significance as defined above |
| NOTE 1: Span is shown using the assumption of a 10 MHz LTE RF channel BW and would be adjusted accordingly for an alternate RF channel BW. | | |

Care shall be taken to ensure that the signal level measurement in step 6 and the interfering signal level measurement in step 11 are sufficiently above the noise floor of the measurement system as to not impact the final SIR level. A horizontally polarized reference dipole may be used as opposed to the magnetic loop as long as the theta gain pattern is properly accounted for.

5.2 Averaging of throughput curves

There are different possibilities how to average the curves where throughput (TP) was recorded as function of downlink (DL) power (expressed in RS EPRE) or of Signal-to-Interference (SIR) level. Averages shall be calculated by the following formula.

5.2.1 Average of power levels

The averaging of DL power (or SIR) is the first possibility. The power levels are summed similar to the formula used for TIS evaluation, i.e. using the inverse of power. The formula to use is:

$$P_{\text{avg,inv}}(y) = \frac{N}{\sum_{n=1}^N \frac{1}{P_n(y)}}$$

For every selected TP value y a corresponding power level $P_n(y)$ can be found, and summed over all N conditions. The subscript "inv" is used to indicate that the inverse sum of power values is taken.

The power levels have to be converted to linear values in mW before the summation takes place, and the average then can be reconverted to dBm / 15 kHz for RS EPRE or dB for SIR.

Since the recording of the TP curves is done with fixed steps in power, only few TP values are available. In order to calculate the correct average, the TP curves have to be interpolated, and a fixed set of y values for TP can be used for generating the curve of $P_{avg}(y)$.

In the case that a curve was not recorded down to 0 % TP, it shall be extrapolated from the point taken with lowest TP to TP = 0 using the same power level.

If a curve did not reach nominal TP, it shall be extrapolated in a way that it would reach nominal TP at the lowest power level where it was reaching its individual maximum TP value.

The average TP curve shall only be calculated up to a TP value which equals to the average of all individual maximum TP values.

6 Candidate measurement methodologies

6.1 Void

6.2 Void

6.3 Downlink measurement methodologies

The methodologies defined in this subclause are candidate methodologies being studied for the purpose of defining procedures for performance testing of over the air performance.

Final test procedure for the approved test methodology or methodologies is described in clause 12.

6.3.1 Methodologies based on Anechoic RF Chamber

An OTA method based on the use of an Anechoic RF Chamber is described consisting of a number of test antenna probes located in the chamber transmitting signals with temporal and spatial characteristics for testing multiple antenna devices.

This clause describes the methodologies based on Anechoic RF Chamber, where a number of test antennas are located in different positions of the chamber, and the Device Under Test (DUT) is located at center position. The DUT is tested over the air without RF cables.

6.3.1.1 Candidate Solution 1

An OTA method based on the use of an Anechoic RF Chamber is described consisting of a number of test antennas located in the chamber transmitting signals with temporal and spatial characteristics for testing multiple antenna devices. The method consists of a number of test antennas located in different positions of the chamber, and the device under test (DUT) is located at the center position. The DUT is tested over the air without RF cables.

The Anechoic chamber techniques creates a realistic geometric based spatio-temporal-polarimetric radio channel for testing MIMO performance using Geometric based stochastic channel models as defined in Clause 8.2.

The components of the solution include:

- Anechoic Chamber
- System Simulator (SS)
- N channel RF emulator, with OTA Channel Generation Features
- N linearly polarized antenna elements configured V, H or co-located V&H or slant X polarizations
- K azimuthally separated antenna positions with predefined angles at radius R

- Channel model definition for each test case

An illustration of an anechoic chamber is shown in Figure 6.3.1.1-1 below.

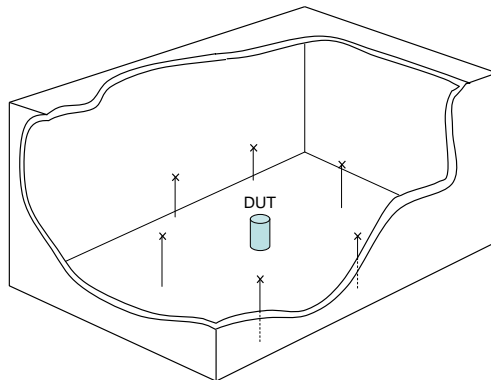


Figure 6.3.1.1-1: N-element Anechoic Chamber approach (Absorbing tiles and cabling not shown)

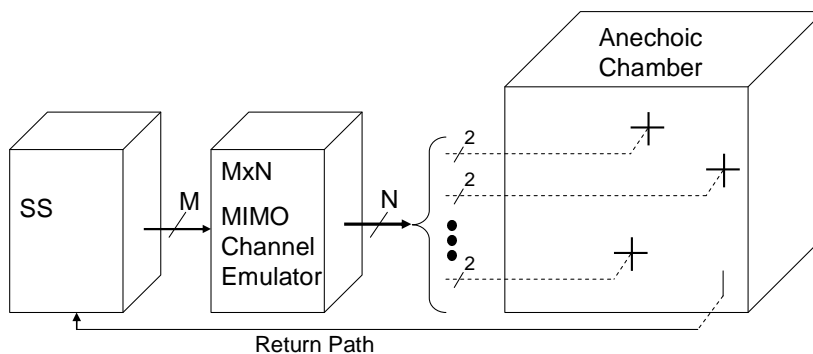


Figure 6.3.1.1-2: OTA system level block diagram

A system level block diagram is shown in Figure 6.3.1.1-2, which includes the SS to generate the M branch MIMO signal, and an RF Channel Emulator with an OTA Channel Generation Feature to properly correlate, fade, scale, delay, and distribute the signal to each test probe in the chamber. For the selected environmental conditions modelled by the SCME UMa and UMi channel models, the minimum setup configuration can be described as below:

Table 6.3.1.1-1: Example of a minimum setup for Boundary Array implementations using the Anechoic Chamber Methodology

| | Full Ring | Single Cluster |
|-------------------------------------|-------------------|---|
| Minimum number of antenna positions | 8 | 3 |
| Antenna spacing | 45° | Determined on the setup |
| Applicable channel model | SCME UMa/SCME UMi | Single Cluster UMa and Single Cluster UMi |

The full SCME or Multi-Cluster channel models are defined in Clause 8.2. The Single-Cluster model, which is not part of the set of channel models validated in clause 8, would be based on the channel models defined in section 8.2 with a set of dithered AoAs around zero degrees.

6.3.1.1.1 Concept and configuration

For MIMO OTA modelling the geometric channel models are mapped into the fading emulator, converting the geometric channel models into the emulator tap coefficients. This process is illustrated in Figure 6.3.1.1.1-1.

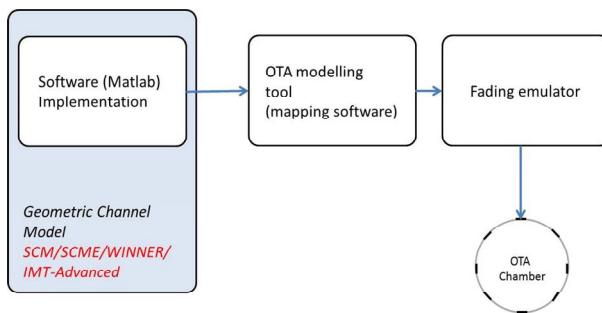
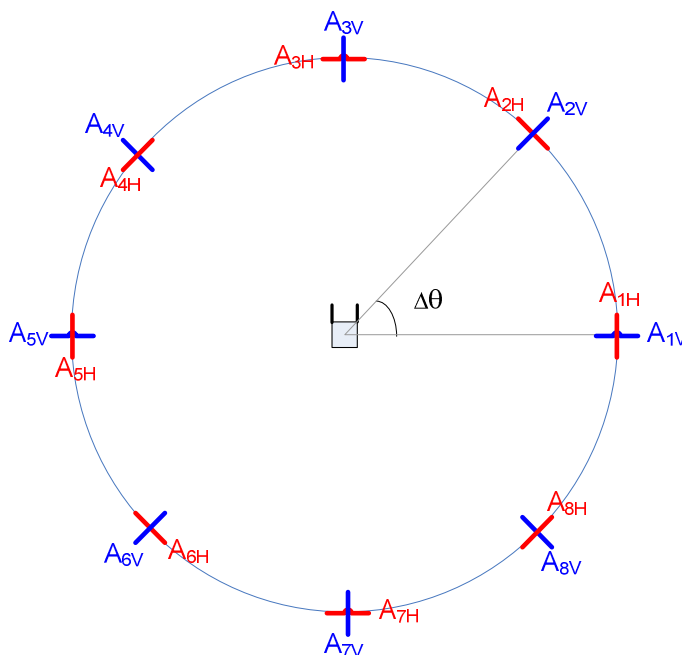


Figure 6.3.1.1.1-1: Modelling process

The setup of OTA chamber antennas with eight antenna positions is depicted in Figure 6.3.1.1.1-2. The DUT is at the center, and the antennas are in a circle around the DUT with uniform spacing (e.g. 45° with 16 elements arranged in 8 positions, where each position contains a vertically and horizontally polarized antenna pair). Denoting directions of K OTA antennas with $\theta_k, k = 1, \dots, K$, and antenna spacing in the angle domain with $\Delta\theta$. Each antenna is connected to a single fading emulator output port. In the figure, for example, antenna A_{1V} denotes the first OTA antenna position and Vertically (V) polarized element, A_{8H} denotes the eight OTA antenna position and horizontally (H) polarized element, etc.



NOTE: In the drawing the V-polarized elements are actually orthogonal to the paper (azimuth plane)

Figure 6.3.1.1.1-2: OTA chamber antenna setup with eight uniformly spaced dual polarized chamber antennas

6.3.1.1.2 Scalability of the methodology

The number of antennas is scalable. In theory, there is no upper limit and the lower limit is one. The required number of channels depends on three main aspects: channel model, DUT size, and polarization. The key question is how accurately the channel model is emulated. Based on the quiet zone discussion, it was proposed to use 8 antennas in the case of single polarization and 16 antennas in the case of dual polarization. However, for single cluster case, fewer antennas may be enough. On the other hand, if elevation is needed, the antenna number will be higher. Additionally, the antenna positions can be adjusted to optimize the accuracy with limited number of antennas.

Another aspect is the channel model. Most of the Geometry-based Stochastic Channel Models (GSCMs) are two-dimensional, i.e. azimuth plane only, but the proposed MIMO OTA concept is not limited to the azimuth plane.

It can also be extended to elevation plane, when we talk about 3D MIMO OTA. However, the 3D MIMO OTA is rather complex and it does not provide very much additional information about the DUT. Therefore, 3D MIMO OTA can be considered as one future development, but it is not the recommended solution in the beginning of MIMO OTA testing.

Downscaling of the proposed method is more attractive due to the possibility to save the cost of the test system.

Full SCME requires multiple antennas, but single cluster SCME can be implemented with lower number of antennas than full SCME. The same downscaling benefits of the single-cluster model apply based on DUT size. The difference between full SCME and Single Cluster model is depicted in Figure 6.3.1.1.2-1. Basically the only difference is that the mean Angle-of-Arrival (AoA) of each cluster is turned to the same primary direction. If all AoA's were identical, it would be a problematic case as it locks all like-angle sub-paths together with identical Doppler, which results in a breakdown of the model. With slight dithering as in the example that the AoAs = [0 -1 1 -2 2 -3] degrees, the angle spread after dithering increases from 35.00 to 35.02 degrees, which is not significant, however the model now performs as expected. Obviously, one primary cluster requires a lower number of antennas than multiple clusters especially when angular spread is narrow, e.g. 35 degrees. The number of fading channels is the same as the number of antennas. Therefore, single cluster SCME would require less fading channels as well.

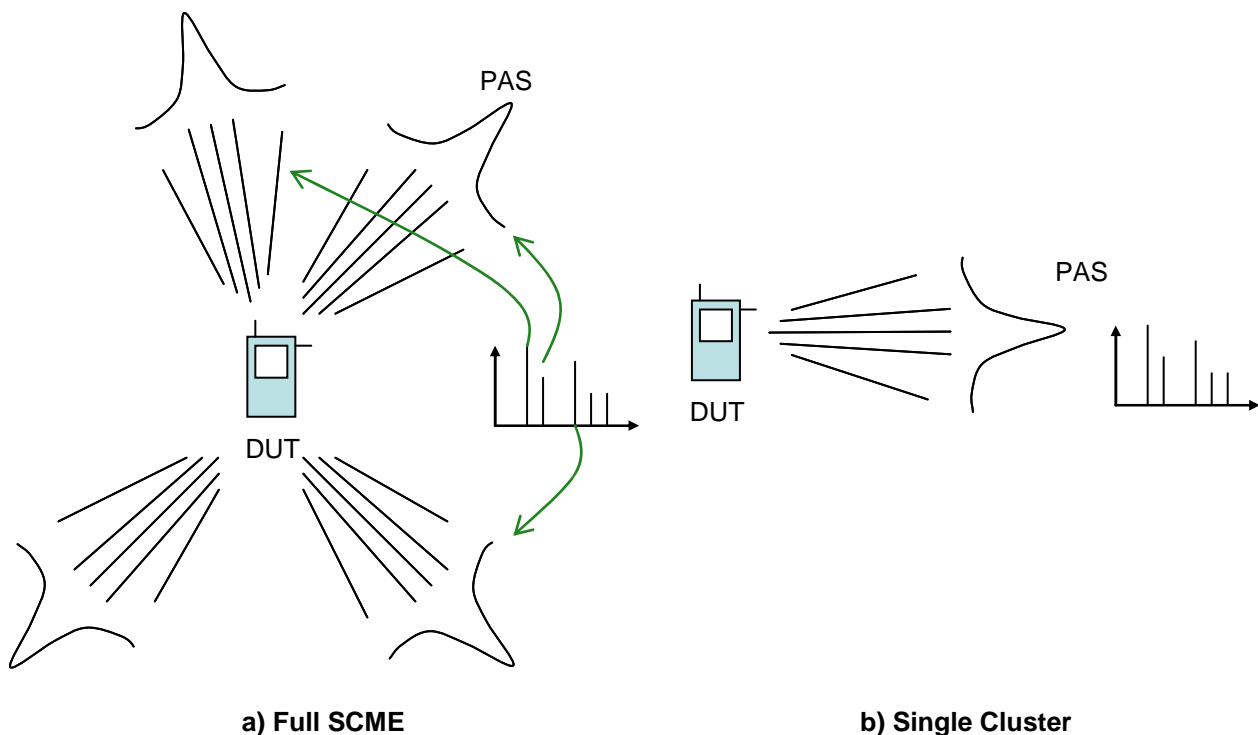


Figure 6.3.1.1.2-1: Full SCME vs. Single Cluster model

6.3.1.1.3 Test conditions

This candidate solution supports testing of different figure of merits and is applicable to any 3GPP release. It supports different channel models from SCM to IMT-Advanced. Due to its generality, it does not restrict the test conditions. However, for simplicity, it is good to start from downlink throughput testing.

The downlink throughput testing can be done e.g. in the following manner.

BS transmits signal through a radio channel emulator. This signal is routed to several antennas in anechoic chamber. The DUT is placed at center of the chamber and the performance is measured from the DUT.

- OTA antennas are located along a circle around the DUT;
- The circular geometry is needed because we need signal from many directions at the same time (requirement from the channel models).

The test steps can be, e.g., according to [3] or as follows:

- 1) Calibrate the full system with a test signal;

- 2) Set the first test case (e.g. channel model) to the fading emulator;
- 3) Generate test signal by the communication tester / BS emulator;
- 4) Measure the DUT performance (downlink throughput);
- 5) If the performance exceeds the specified limit, the DUT passes the test case;
- 6) If all test cases done, go to step 7. Otherwise, set the next test case (e.g. channel model) to the fading emulator and go back to step 3.
- 7) If DUT passed all the test cases, the DUT passes the full MIMO OTA test;
- 8) If DUT failed in at least one test case, the DUT failed the full MIMO OTA test.

6.3.1.2 Void

6.3.1.3 Candidate solution 3

The principle of two-stage MIMO OTA method is based on the assumption that the DUT far-field antenna radiation pattern will contain all the necessary information for evaluation of the DUT's antenna's performance like radiation power, efficiency and correlation and that with channel model approaches, the influence of antenna radiation pattern can be correctly incorporated into the channel model. Thus the method will first measure the DUT's MIMO antenna patterns and then convolve the measured antenna patterns with the chosen MIMO OTA channel models for real-time emulation. The resulting test signal generated by the channel emulator and coupled back into the DUT receivers represents the signal that the DUT receivers would have seen if the DUT had been placed in the desired radiated field. Thus an ideal implementation of the two-stage method provides the same results as an ideal implementation of the boundary antenna array method.

The two-stage method can be used to measure the following figures of merit:

- 1) Throughput
- 2) TRP and TRS
- 3) CQI, BLER
- 4) Antenna efficiency and MEG
- 5) Antenna correlation, MIMO channel capacity.

In order to accurately measure the antenna pattern of the intact device, the DUT chipset needs to support received amplitude and relative phase measurements of the antennas. The validity of antenna pattern measurement is predicated on the assumption that for the frequency being tested, the DUT antenna pattern is static. Devices that can alter their antenna pattern in real time as a function of the radiated environment – sometimes referred to as active antennas – is FFS as noted in Table 12.4-1. The method of coupling the base station emulator and DUT can be through the standard temporary antenna connectors (conducted two-stage method) or by using a specially calibrated radiated connection (radiated two-stage or RTS method) to do the test on throughput, etc., to test how the MIMO antennas will influence the performance. The conducted method of coupling is straightforward but does not capture the impact of radiated leakage from the DUT transmit antennas to the DUT receive antennas, thus in its current form without additional interference estimation the conducted method of coupling in the second stage is not proposed for use in conformance testing. Its description is included for historical completeness of the development of the two-stage method. The radiated method of coupling in the second stage does fully capture radiated leakage and is the method defined for conformance testing in Clause 12.

6.3.1.3.1 Concept and configuration

The assumption of the two-stage MIMO OTA method is that the measured far field antenna pattern of the DUT's multiple antennas can fully capture the mutual coupling of the multiple antenna arrays and their influence on radiated performance.

Thus to do the two-stage MIMO OTA test, the antenna patterns of the antenna array needs to be measured accurately in the first stage. In order to accurately measure the antenna pattern of the intact device, the chipset needs to support amplitude and relative phase measurements of the antennas. To achieve this, two new UE measurements have been

defined called Reference Signal Antenna Power (RSAP) and Reference Signal Relative Antenna Phase (RSARP). These measurements are defined in TR 36.978 [20].

Stage 1: The measurement of the DUT's multiple antennas takes place in a traditional anechoic chamber set up as described in Annex A.2 in [4], where the DUT is put into the chamber and each antenna element's complex far zone pattern is measured using the RSAP and RSARP measurements defined in [20]. The influence of human body loss can also be measured by attaching the DUT to a SAM head and or hand phantom when doing the antenna pattern measurements. The characteristics of the SAM phantom are specified in Annex A.1 of [4]. The chamber is equipped with a positioner, that makes it possible to perform full 3-D far zone pattern measurements for both Tx and Rx radiated performance. As specified in A.2 of [4] the measurement antenna shall be able to measure two orthogonal polarizations (typically linear theta (θ) and phi (ϕ) polarizations as shown in Figure 6.3.1.3.1-1).

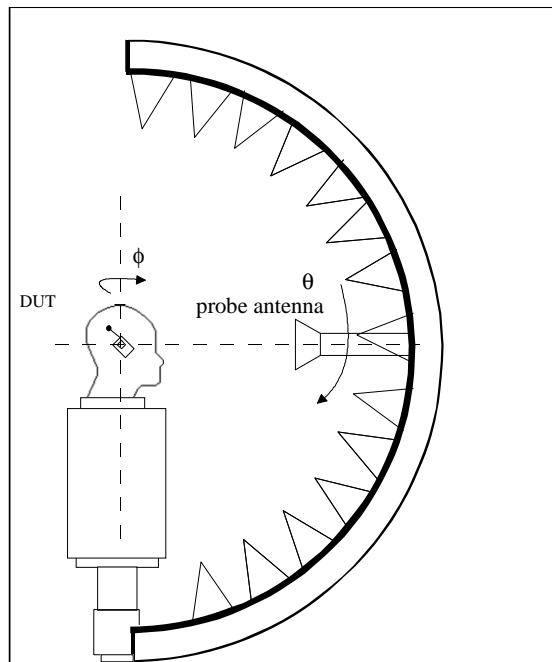


Figure 6.3.1.3.1-1: The coordinate system used in the measurements

Stage 2: Convolve the antenna patterns measured in stage 1 with the chosen MIMO channel model, using a channel emulator and then use the resulting signal to perform the OTA throughput test. The signal is coupled into the DUT using either a cabled or radiated connection.

The two-stage method is illustrated in Figure 6.3.1.3.1-2. In the conducted two-stage method shown in Figure 6.3.1.3.1-2 the BS emulator is connected to the MIMO channel emulator and then to the DUT's temporary antenna ports via approved RF cables. These ports are the standard ones provided for conducted conformance tests. The alternative to using a conducted connection is to use a calibrated radiated connection in an anechoic environment as shown in Figure 6.3.1.3.1-3 is the radiated two-stage (RTS) method. This coupling technique exploits the Eigen modes of the transmission channel in the anechoic chamber to provide isolated radiated connections between the probe antennas and each DUT receiver after the DUT antenna. Throughput with the DUT's MIMO antenna influence can be measured using either coupling method. However, only the radiated coupling method intrinsically includes the effects of DUT self-interference and is the method defined for conformance testing in Clause 12.

There are two different approaches to convolve the DUT antenna patterns with MIMO channel model.

- a) Apply antenna patterns to geometric (Ray-based) channel models. Ray-based models support arbitrary antenna patterns under predefined channel modes in a natural way as described above. If Ray-based models like SCME are specified to be used for MIMO OTA testing, then the channel emulator needs to support SCME channel model emulation and convolution with the measured antenna patterns.
- b) Apply antenna patterns to correlation-based channel models. With a correlation matrix calculation method for arbitrary antenna patterns under multipath channel conditions, the correlation matrix and the antenna imbalance can be calculated and then emulated by the channel emulator.

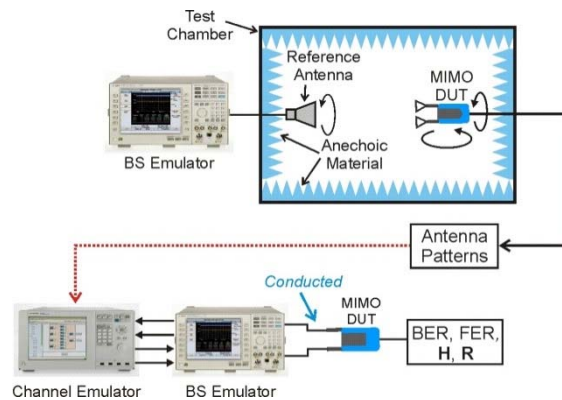


Figure 6.3.1.3.1-2: Proposed conducted two-stage test methodology for MIMO OTA test

An example implementation of the radiated method of connecting to the EUT in the second stage is shown in Figure 6.3.1.3.1-3.

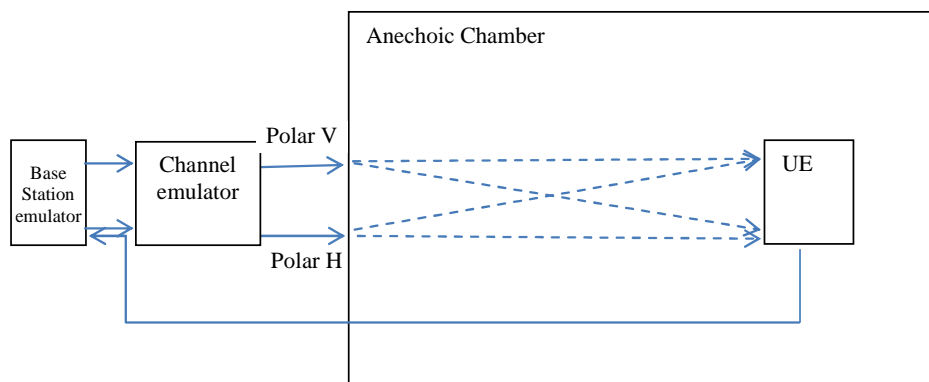


Figure 6.3.1.3.1-3: Alternative connection for the radiated two-stage (RTS) test methodology for MIMO OTA test

Figure 6.3.1.3.1-3 shows the radiated coupling method for the second stage. Two probe antennas with polarization V and H are co-located in the anechoic chamber. Note, unlike in the first stage where the V and H probes are used at different times, in the second stage both V and H probes are used simultaneously. An example implementation of this would be the dual polarized configuration described in Annex A.2.2 of [4]. The only difference between the conducted second stage and the radiated second stage is to replace the RF cables with the radiated channel inside the chamber. Due to the propagation channel in the chamber, signals transmitted from each probe antenna are received by both DUT antennas which is different from the cable conducted case where the signals are isolated by the cables. However, by precoding the transmitted signals using spatial multiplexing techniques it is possible by calculating the radiated channel matrix and by applying its inverse to the transmitted signals, to create an identity matrix allowing the transmitted signals to be received independently at each DUT receiver after the DUT antenna. This precoding recreates the equivalent of the isolated cable conducted conditions at the receiver but with radiated self-interference now included.

The establishment of the radiated connection is explained as follows. Assume x_1 and x_2 are the transmitted signals from the base station emulator, after applying the desired channel model and convolution with the complex antenna pattern we get:

$$f(x_1) \text{ and } f(x_2).$$

The radiated channel matrix between the probe antennas and the DUT antennas is $= \begin{pmatrix} h_{11} & h_{12} \\ h_{21} & h_{22} \end{pmatrix}$.

If the channel emulator applies the inverse of the radiated channel matrix $H^{-1} = \begin{pmatrix} \alpha & \beta \\ \gamma & \delta \end{pmatrix}$ to $f(x_1)$ and $f(x_2)$, the signal received after the DUT antennas is same as the cable-conducted method as follows:

$$\begin{pmatrix} y_1 \\ y_2 \end{pmatrix} = \begin{pmatrix} h_{11} & h_{12} \\ h_{21} & h_{22} \end{pmatrix} \begin{pmatrix} \alpha & \beta \\ \gamma & \delta \end{pmatrix} \begin{pmatrix} f(x_1) \\ f(x_2) \end{pmatrix} = \begin{pmatrix} 1 & 0 \\ 0 & 1 \end{pmatrix} \begin{pmatrix} f(x_1) \\ f(x_2) \end{pmatrix} = \begin{pmatrix} f(x_1) \\ f(x_2) \end{pmatrix}$$

6.3.1.3.2 Test conditions

This candidate solution supports testing of different figure of merits. It is also applicable for any 3GPP Release, and even for other standards.

This method can reuse existing SISO OTA anechoic chambers to make the antenna pattern measurements; the channel emulator number is required to match the number of device receiver inputs regardless of the complexity of the chosen channel model, the method is consequently easily scalable to higher order MIMO due to the reduced number of instruments required; the channel models are highly accurate due to being implemented electronically and are also fully flexible and can be altered to suit any desired operating conditions such as indoor-outdoor, high or low Doppler spread, high or low delay spread, beam width, in 2D or full 3D etc.

This method requires the chipset in the DUT to support amplitude and relative phase measurements of the antennas as defined in TR 36.978 [20]. The conducted coupling method in the second stage cannot directly measure DUT self-desensitization since the antenna pattern measurement does not take account of possible signal leakage from the device transmit antennas into the receive antennas. The radiated coupling method for the second stage does fully characterize any DUT self-desensitization and is the method specified in Clause 12 for conformance testing.

The detailed RTS test procedure can be found in Subclause 12.3.

6.3.1.3.3 Overview of calibration procedures specific to the RTS method

The efficacy of the RTS method is based on the ability to accurately measure the DUT complex antenna pattern and establish an isolated radiated MIMO connection in the second stage.

The output of the first stage is a relative antenna pattern of unknown gain and linearity. The calibration of the antenna pattern occurs in the second stage.

Selection of orientation for the second stage

The second stage starts with the selection of a DUT orientation at which to establish a radiated MIMO connection to the DUT. This orientation is chosen from any point on the measured pattern at which the optimal isolation between the streams can be achieved by application of the inverse channel matrix. A degree of isolation between the received streams for most antenna patterns is achieved through use of different transmit polarizations or by using separate antennas. Improved isolation will be achieved by choosing a DUT orientation that avoids nulls in the antenna pattern. The algorithm for selecting the optimal orientation is left up to implementation. The only criterion is that the selected orientation achieves sufficient isolation.

Calculation of the inverse transmission matrix

Once an orientation is selected an unfaded SISO connection is established from the first probe antenna and the RSAP for each DUT antenna and the RSARP between the antennas is measured. These measurements are repeated using the second probe antenna. From these measurements the optimal transmission matrix from the probe antennas to the DUT receiver can be calculated. When the inverse of this matrix is applied to the probes it is possible to transmit a wanted signal from the first probe to the first receiver and from the second probe to the second receiver with minimal crosstalk.

Calibration of the measured antenna pattern gain

The impact of the unknown gain of the DUT antennas then de-embedded from the test system by setting the downlink power for each probe to the level that returns the same RSAP measurement that was reported for that probe polarization during the first stage at the orientation being used for the second stage. This nulling process is the reason why the absolute accuracy of the RSAP measurement is unimportant since the antenna gain is represented by the change in downlink power necessary to achieve the same RSAP report for the first and second stage at the same DUT orientation.

For example using a -60 dBm nominal level in the first stage for the V antenna assume the DUT for one orientation returns RSAP for receiver 1 of -67 dBm representing an uncorrected gain of -7 dB. This report includes the true gain of the antenna at the V polarization for this orientation (assume -4 dB) plus an unknown error in the RSAP absolute accuracy (-3 dB). In the second stage antenna calibration step, a wanted signal of -60 dBm is transmitted, adjusted to -53 dBm to de-embed the uncorrected gain of -7 dB and the RSAP measured. If the RSAP accuracy were perfect the DUT would report -60 dBm but since the true antenna gain at that orientation is -4 dB, the reported RSAP is higher at -57 dBm. The difference between the first stage RSAP measurement and the second stage RSAP with the uncorrected gain applied then represents the true antenna gain at that orientation referred to the known accuracy of the downlink signal.

Validation of the isolation between the streams

Once the RSAP absolute error has been measured and removed from the measured antenna pattern the isolation of the streams in the second stage can be measured. This could be done with static signals but what matters is the isolation achieved under the more difficult dynamic fading conditions. The isolation can be measured by establishing a connection and, with the channel model and antenna pattern applied, measure the difference in dB between the RSAP reported for each DUT receiver. For a DUT to be usable with the RTS method a minimum isolation has to be achieved of [18] dB averaged over a period of [TBD] frames.

Monotonicity check of RSAP and RSARP

Once the minimum isolation of the radiated second stage has been validated it is necessary to validate the linearity of RSAP and RSARP measurements over the operating range -60 dB, to -80 dBm and +/- 180 degrees. This starts with a monotonicity check using a [1] dB step size for RSAP and a [5] degree step size for RSARP. The step sizes of the monotonicity check determine the accuracy to which the measurements can be linearized. If the monotonicity check fails the RTS method is not usable for the DUT.

Linearization of RSAP and RSARP

Once monotonicity has been validated, the linearity of RSAP can be measured. This is done from the orientation of the peak antenna gain over the range -60 dBm to -80 dBm. The linearity shall be < [1] dB. The linearity of RSARP shall be within [5] degrees over the range ± 180 degrees measured at -60 dBm and -80 dBm. If the uncorrected RSAP or RSARP results do not meet the linearity requirements, calculate and apply a transfer function to the measured patterns to ensure the necessary linearity.

6.3.1.4 Candidate solution 4

6.3.1.4.1 Concept and configuration

In this method an assessment of the antenna's performance in MIMO or Diversity operation is performed. Several simplifications are used in order to optimise the testing.

A test of the UE in an anechoic environment with the help of a base station emulator is proposed, with a limited number of faded channels and transmitting antennas, and in a simple geometrical set-up.

The underlying principle is to decompose the task for evaluating MIMO performance. It combines the radiated measurements in the anechoic chamber where no fading is applied with conducted measurements with fading. The total performance of the UE is decomposed into these two steps, and therefore we name it decomposition approach. Figure 6.3.1.4.1-1 illustrates this approach.

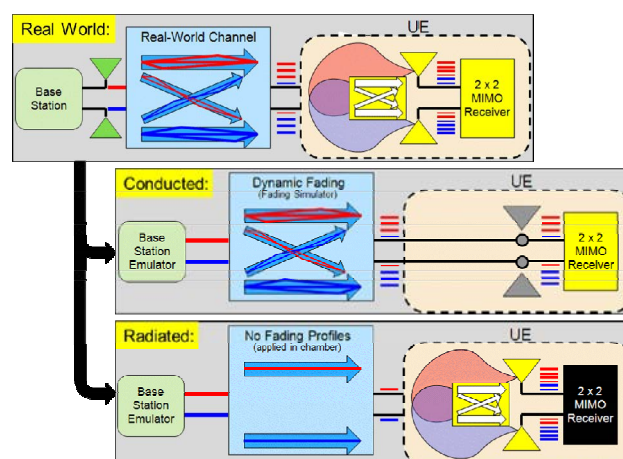


Figure 6.3.1.4.1-1: Diagram of decomposition approach for 2x2 LTE MIMO

6.3.1.4.2 Decomposition approach

To determine the throughput results for the overall MIMO device performance, the following key measurements are needed, as shown in Figure 6.3.1.4.2-1:

- Baseline: the conducted measurement with channel model of the identity matrix
- Conducted: the conducted measurement with the real-world channel model
- Radiated: the average of the radiated measurements for a set of antenna constellations

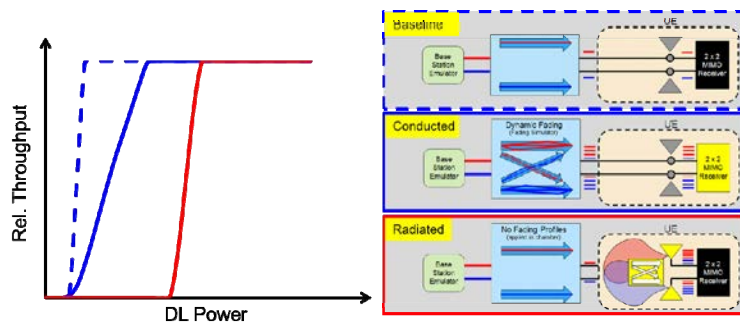


Figure 6.3.1.4.2-1: Key measurements for Decomposition Approach

From these measurements, the receiver MIMO efficiency and the antenna MIMO efficiency are determined as illustrated in Figure 6.3.1.4.2-2. The receiver MIMO efficiency is defined as the difference between the baseline conducted test and the conducted test with dynamic fading as a function of throughput, Figure 6.3.1.4.2-2 (a). Similarly, the antenna MIMO efficiency is defined as the difference between the baseline conducted test and the radiated test for all throughput levels, Figure 6.3.1.4.2-2 (b)

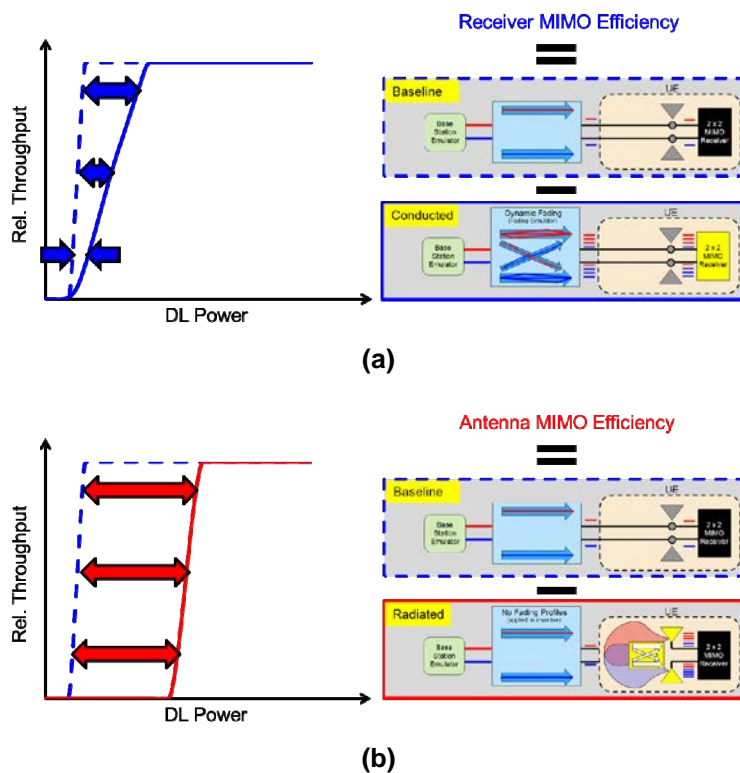


Figure 6.3.1.4.2-2: Definition of (a) receiver MIMO and (b) antenna MIMO efficiencies

The relative Figure Of Merit (FOM) for the UE MIMO performance is subsequently defined as the UE MIMO efficiency that is the sum of the receiver and antenna MIMO efficiencies. By adding this efficiency to the baseline throughput curve, the absolute FOM for the UE MIMO performance, i.e., decomposed throughput curve as a function of DL power level, can be obtained as shown in 6.3.1.4.2-3.

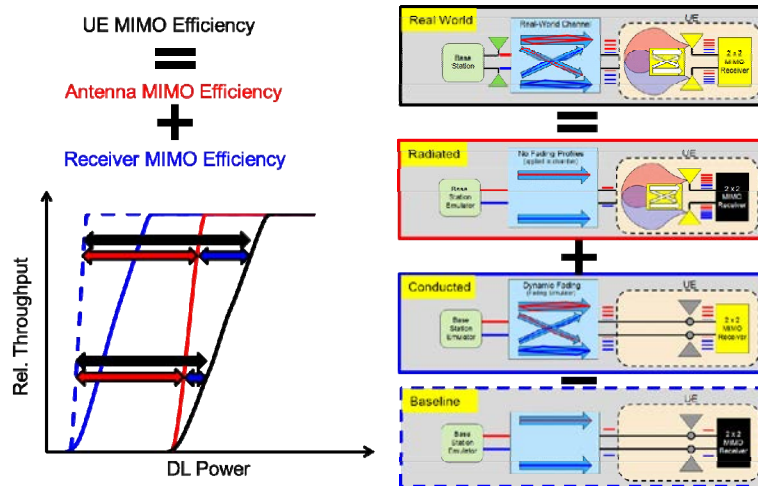


Figure 6.3.1.4.2-3: Illustration of the decomposed throughput curve calculation

6.3.1.4.3 Conducted test

In the conducted tests, measurements with different channel models have to be performed.

The most basic Channel Model (CM) is the identity static channel matrix without fading.

$$CM = \begin{bmatrix} 1 & 0 \\ 0 & 1 \end{bmatrix}$$

This matrix provides a frequency-flat transfer characteristic that does not change over time. Since non-diagonal elements of the channel matrix are zero, each RF port of the UE receives a single LTE data stream. This ideal CM characterizes the noise figure of the MIMO receiver and acts as a "baseline" for further testing.

Another test has to be performed with the CM selected. Typically the channel models are either based on SCME UMa or UMi. Since the channel models are applied in conducted mode, the spatial information of the base station antenna correlation is calculated numerically and implemented as coefficient alpha in the fading model. The coefficient beta describing the correlation at the UE side is set to zero.

6.3.1.4.4 Radiated test

The two-channel method is covering the radiated part of the test where the performance of the UE's antenna subsystem is evaluated. It is using two probe antennas and one azimuth positioner in order to cover a large number of different angle-of-arrival constellations. In each constellation also the polarizations of the two probe antennas are defined.

For an RX MIMO measurement (TM2 or TM3), the two signals from the base station emulator are routed directly to the probe antennas with the chosen polarization.

In order to assess the radiated performance of the MIMO antenna system in 3D, the UE shall be tested for a set of antenna constellations uniformly covering the sphere and generating a wide variety of AoAs. In the radiated test the constellations are categorized as spatial constellations, i.e., the azimuth orientation of the UE and the elevation positions of the two DL antennas and as polarization constellations, i.e., the set of polarizations of the DL antennas used to transmit the LTE MIMO streams. Figure 6.3.1.4.4-1 highlights the key parameters for each constellation category.

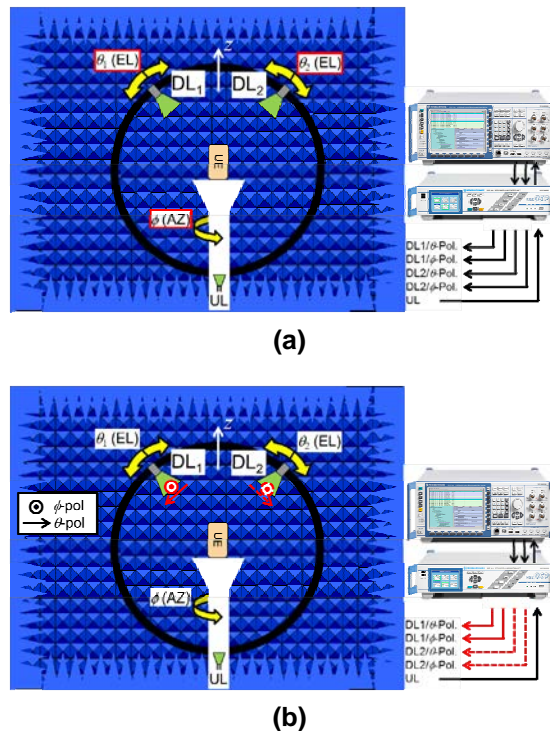


Figure 6.3.1.4.4-1: Overview of (a) spatial and (b) polarization constellations

An optimized constellation approach determines a set of constellations.

The algorithm used has been written specifically for the decomposition approach.

A total of 128 constellations have been identified to be sufficient in order to sample the antenna performance.

For each constellation, a curve of throughput as a function of DL power level or SNR is recorded.

At the end of the test, i.e., 128 constellations, an average of all curves is determined that represents the FOM for the MIMO antenna subsystem performance for a complete set of 3D AoAs.

6.3.1.4.5 Possible extensions of the decomposition method

There are several possible extensions of the method briefly addressed in this Clause.

- The channel information available in the UE can be used to deliver a quick answer to the test system about the current receive quality. If necessary, an explicit scaling from one quantity onto the other one can be made.
- In case of an RX diversity measurement the signal from the base station emulator has to be routed via a two-channel fading to the two probe antennas in the chamber in order to decorrelate the signals.
- In addition of the movements of the probe antennas and the azimuth positioner, the UE may be tilted by some additional rotation around the horizontal axis.
- As a special case it is also possible to test with one antenna where each polarization is transmitting one MIMO data stream.
- As an alternative to moving the antennas by mechanically rotating them it is possible to arrange the antennas in a horizontal plane and to move one antenna with respect to the other in order to vary the angle difference between the two. In that case the positioner rotating the UE will be designed in a more complex way.
- If one wants to extend this method to 3D AoA, a third antenna outside the plane can be used.

The OTA performance can better be described by taking statistical evaluations into account. If, for example, for each test point a relative throughput value is obtained as function of subcarrier power, one can plot the results for different points in a histogram and to obtain some CCDF indicating the conditions for getting at least a given throughput value.

6.3.1.5 Candidate solution 5

The RF-controlled spatial fading emulator can directly reproduce a multipath radio propagation environment by radio waves emitted from antenna-probe units arranged around a handset tested. Moreover, the emulator has an advantage of measuring radiation characteristics of a handset antenna for the present OTA testing in 3GPP as well as the multipath testing because of its RF operation [6].

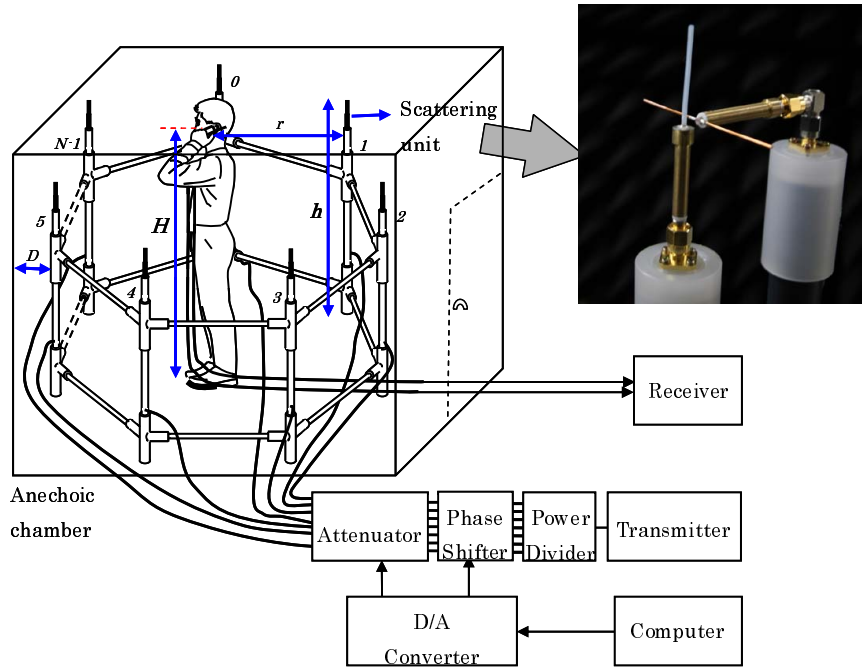
6.3.1.5.1 Concept and configuration

The RF-controlled spatial fading emulator can directly reproduce multipath radio propagation environments both in Line-Of-Sight (LOS) and Non Line-Of-Sight (NLOS) situations by radio waves emitted from antenna probes arranged around a DUT. Thus, the emulator can be easily used for measurement of the MIMO characteristics of a HSPA/LTE multiple antenna device in a multipath fading environment.

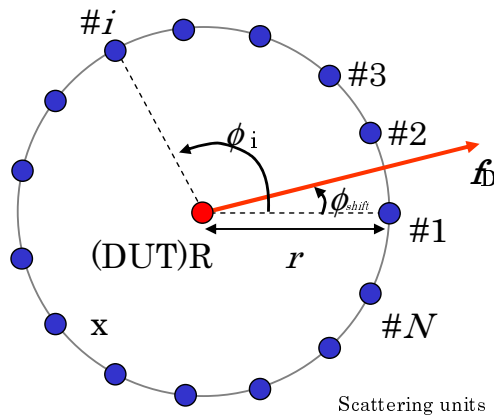
Figure 6.3.1.5.1-1 (a) and (b) show the configuration and arrangement of the antenna probes of the RF spatial fading emulator in an anechoic chamber. In this method, the DUT is designated as any device that possesses multiple antennas, including a HSPA or LTE device.

The height of DUT from the floor of the anechoic chamber is H . The DUT can also be placed at a rotatable turn-table in order to set and vary the horizontal angle of the DUT. The DUT is surrounded by N numbers of antenna probes. The distance between DUT and each antenna probe is r . The antenna probe consists of two antennas. The one is a half-wavelength dipole set vertically for emitting the vertically-polarized wave and the other is a horizontally-located half-wavelength dipole for the horizontally-polarized wave. This configuration of the antenna-probe unit can represent a cross polarization power ratio, XPR, of incoming wave. The separation between vertical and horizontal antennas is d . The height of the antenna probe from the anechoic chamber floor is h . The distance between the ring of antenna probes and the walls of anechoic chamber is D . (Note if the anechoic chamber is not square, then D_1 and D_2 are used).

A reference antenna probe is designated so that it can be used to determine the direction of motion of DUT. This parameter is designated as ϕ_{shift} . The circular angle between antenna probes from the centre of the ring (i.e. DUT) is ϕ_i with respect to the reference antenna probe.



(a) Experimental Setup



(b) Arrangement of the antenna probes

Figure 6.3.1.5.1-1: Experimental setup of the spatial fading emulator

The key features of this method are that it does not use the sophisticated commercial channel emulator. By using the combination of phase shifters, power dividers and attenuators, operating in the RF band, it has been shown that a realistic fading channel environment can be emulated. To reduce the influence from the measurement equipment, the receiver, phase shifter, power divider, transmitter and computer are set outside of the anechoic chamber. Firstly, we describe channel response between the m^{th} base station, BS, antenna and the n^{th} handset antenna for M -by- N MIMO radio communication system. The channel response is calculated by following equation:

$$h_{nm} = \sum_{i=1}^N E_n(\phi_i) \sqrt{\Omega(\phi_i)} \frac{\lambda}{4\pi \cdot r} \exp[-j\{kr + 2\pi \cdot t \cdot f_D \cos(\phi_0 - \phi_i) + \alpha_{mi}\}] \quad (1)$$

where E_n and f_D are radiation component of the n -th handset antenna and the Doppler frequency respectively. ϕ_0 is the direction of motion and ϕ_i is the direction of the i -th antenna probe. α_{mi} is initial phase of the signal radiated from the i -th antenna probe. The waves radiated from each base station (BS) antenna are uncorrelated each other. For the investigation of MIMO antennas, the waves from different BS antenna are represented by different sets of initial phases, α_{mi} , of the waves. According to the propagation models, such as SCM and SCME, the angular power spectrum

Ω of the spatial cluster of incoming waves in the horizontal plane can be modelled by a Laplacian distribution in the following, for instance:

$$\Omega(\phi) = \frac{P}{2\sigma} \exp\left\{-\frac{|\phi - \mu_\phi|}{\sigma}\right\} \quad (2)$$

where P and μ_ϕ are power and average direction of angle of the cluster. σ is a standard deviation of the APS. In this case, the spatial distribution in the vertical plane is modelled by a delta function.

In addition, the strongest point of the spatial fading emulator is to be capable of evaluating radiation characteristics of a handset antenna for the present OTA testing in 3GPP as well as the multipath-fading evaluation since the emulator is operated in a Radio Frequency (RF) band.

A calibration of the RF-controlled spatial fading emulator is carried out using the following procedure:

- 1) Firstly a half-wavelength dipole for the receiving antenna is vertically placed at the center of a circle arranging the antenna probes.
- 2) A radio wave with vertical polarization is radiated only from a vertical dipole of the antenna probe #i ($i=1, 2, \dots, L$), and then, the dipole at the center of the emulator can receive the wave. From this, we can obtain amplitude and phase of the RF signal from the transmitter to the receiver via the vertical dipole of the antenna probe #i.
- 3) The attenuator and phase shifter are adjusted so that the RF signals received by the dipole at the center have the same values in amplitude and phase.
- 4) Secondly the slotted cylindrical antenna is placed at the center of the antenna probes located on the circle.
- 5) A radio wave with horizontal polarization is radiated only from a horizontally-located dipole of the antenna probe #i ($i=1, 2, \dots, L$). From the received signal from the antenna probe #i, we also obtain amplitude and phase of the RF signal from the transmitter to the receiver via the horizontal dipole of the antenna probe #i.
- 6) The attenuator and phase shifter are adjusted so that the RF signals received by the slotted cylindrical antenna at the center have the same values in amplitude and phase.

The calibration procedure above mentioned can be performed by using an electrical-controlled RF switch. Thus, the calibration of the emulator can be done automatically using a computer in our system. Once the calibration is finished, we can vary the attenuators in order to produce a special distribution of the incoming wave and to make a Cross polarization Power Ratio (XPR). Moreover, we can set an initial phase to each antenna probe to create a multipath fading channel.

With regard to the signal-to-noise power ratio, SNR, of incoming wave, the signal power can be determined by an average value of faded signal powers received by a half-wavelength dipole antenna for the vertical polarization and a slotted cylindrical antenna for the horizontal polarization. Both antennas have an omni-directional radiation pattern. Thus, SNR can be obtained as the following equation:

$$SNR = \frac{S_V + S_H}{N_0} \quad (3)$$

where S_V and S_H are the average signal powers received by the dipole and slotted cylindrical antennas, respectively. N_0 is the noise power that was calculated as a thermal noise within the frequency bandwidth of the radio communication.

6.3.1.5.2 Test conditions

In this method, all signals are operated and controlled at RF level. A computer (either a laptop or relatively powerful computer) is used to provide the followings:

- 1) Graphical User Interface (GUI) to set the input parameters, determine the measured parameters to be collected, setting of calibration parameters and setting of DUT parameters.
- 2) Generating control signals to manipulate the phase angle of each Phase Shifter.
- 3) Collecting measured raw data obtained via the DUT.

- 4) Post-processing the measured raw data to derive the desired figure of merits (i.e. minimum requirements for DUT).
- 5) To initiate the BS emulator and start the testing session (by establishing a communication session with DUT).

The RF signals transmitted from the BS emulator's antenna connector are fed to a bank of Power Dividers. Each power divider provides identical RF signal from each of the output ports. The number of Power Dividers required is determined by N .

Each Power Divider output is then fed to a Phase Shifter. The Phase Shifter is used to change the phase of the RF signal according to the parameter setting input to the computer earlier. Note that the control signal from the computer is digital-to-analogue, D/A, converted, before used to control the Phase Shifter. By controlling the phase of each RF signal, a Rayleigh distributed or other relevant multipath distribution can be obtained. The number of Phase Shifters required is determined by N .

The output of the Phase Shifters is connected to the antenna probes. The signal from each Phase Shifter is fed to the vertical and horizontal antennas and radiates toward the DUT. The DUT then measures the signals from each antenna probe and the measurement data is reported back to the computer. The amount of measurement data to be collected can be controlled by the computer by setting the sampling rate, R .

An example below illustrated the principle of creating Rayleigh faded signal by control the phase of each component wave in Figure 6.3.1.5.2-1.

Number of antenna probes N : 15
 Direction of motion ϕ_0 : 10 deg.
 Doppler frequency f_D : 20 Hz
 Sampling frequency f_s : 400 Hz
 Radius of circle arranging antenna probes r : 1.0 m
 Operating frequency : 2.14 GHz
 Receiving antenna (Rx) : half-wavelength Dipole
 Radiation pattern of Rx $E_n(\phi)$: omni
 APS, $\Omega(\phi)$: Uniform

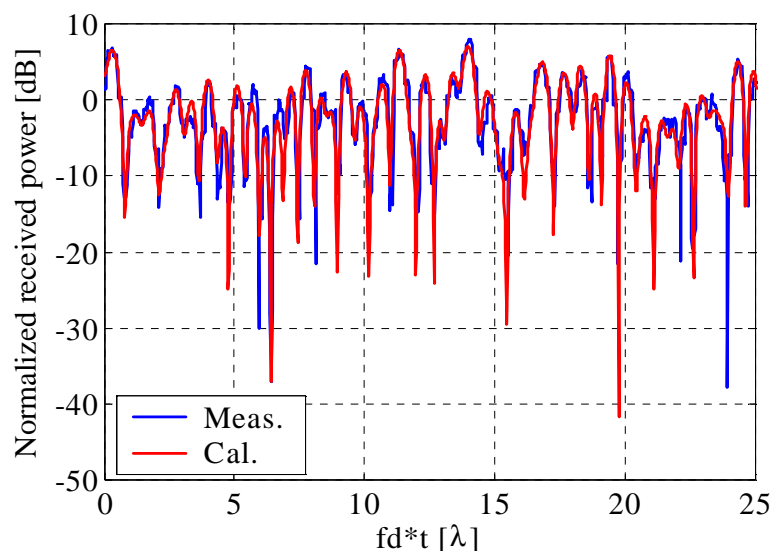


Figure 6.3.1.5.2-1: Rayleigh faded signal by control the phase of each component wave

6.3.2 Methodologies based on Reverberation Chamber

6.3.2.1 Candidate solution 1

The Reverberation Chamber is a metallic cavity or cavities that can emulate an isotropic multi-path environment which represents a reference environment for systems designed to work during fading, similar to how the free space "anechoic" reference environment is used for tests of Line-Of-Sight systems. The Rayleigh environment in a reverberation chamber is well known as a good reference for urban and indoor environments, but does not well represent rural and suburban environments.

For a future multi-antenna OTA measurement standard it is important to have a fast and repeatable test method to evaluate and compare multi-antenna devices in the environments and under the conditions where most people will use them. The overwhelming majority of calls/data connections with mobile phones are made indoors and in urban areas which can be very well represented by the reverberation chamber. These environments are well characterised by multi-path and 3D distribution of the communication signals and it makes sense to use the reverberation chamber for optimizing/evaluating devices with both single and multiple antenna configurations to be used indoors and in urban areas.

The test setup for testing UE receiver diversity performance is composed of a Base Station (BS) emulator, a reverberation chamber equipped with fixed BS wall-mounted antennas, a switch to direct the base station signal to/from one of the BS wall mounted antennas, mechanical metallic stirrers and a rotating platform to hold the DUT (Figure 6.3.2.1-1).

Alternatively, the chamber may contain one or more cavities coupled through waveguides or slotted plates (Figure 7.1-2).

Reverberation chambers have no quiet zone. As long as the DUT is placed at least 0.5 wavelengths from the wall or metallic stirrers the result will be the same within the standard deviation of the chamber.

Mechanical stirrers and switching among different fixed BS wall-mounted antennas (monopoles used for polarization stirring) allow simulating the Rayleigh fading at each antenna of the terminal inside the chamber. Accuracy can even be increased by rotating the platform holding the device.

Each position of the mechanical stirrers for each position of the platform and each fixed BS antenna, represents a point of the Rayleigh distribution in terms of receive power on the device antennas. In that way a Rayleigh fading is artificially created.

In that way, several UE metrics can be measured: throughput with RX-DIV, TRP, TIS (Total Isotropic Sensitivity), etc.

For each point of the Rayleigh distribution created by the different configurations of the chamber, the metric is noted. This method can be used to measure UE sensitivity and UE radiated power.

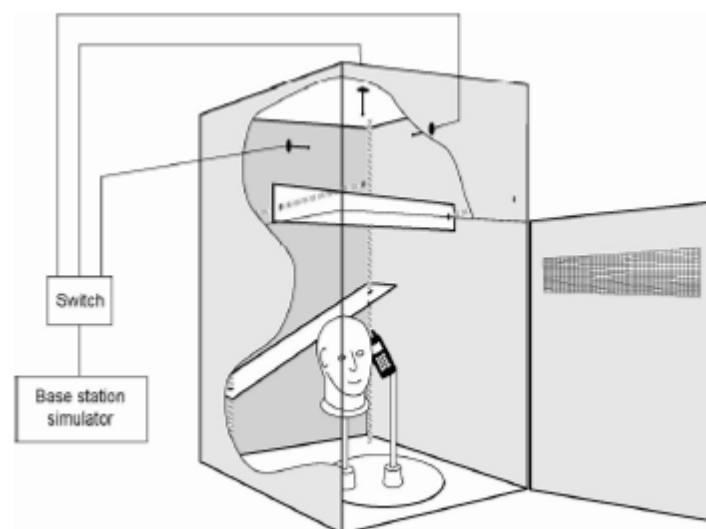


Figure 6.3.2.1-1: Reverberation chamber setup for devices testing with Single Cavity
[source: Bluetest AB]

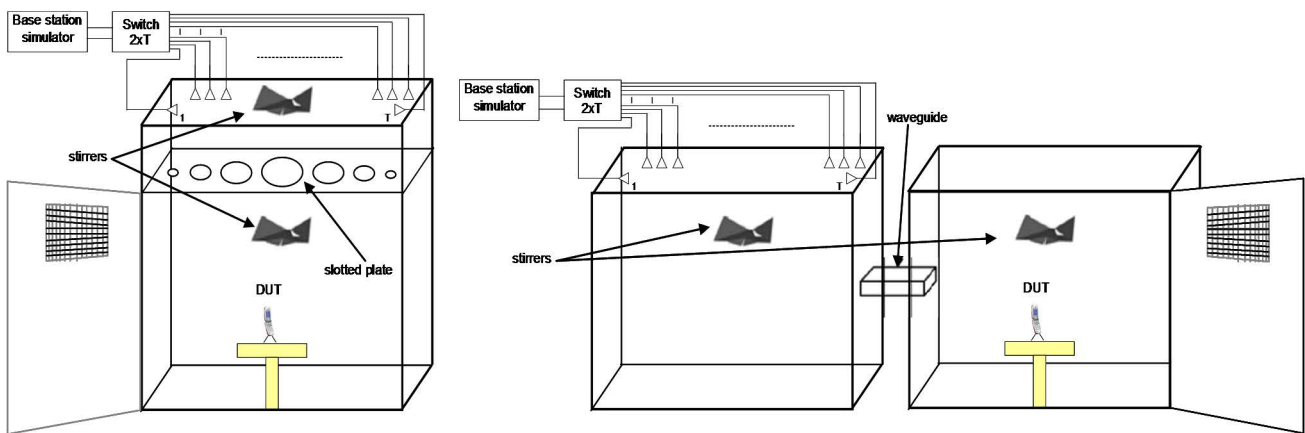


Figure 6.3.2.1-2: Reverberation Chambers with Multiple Cavities
 [source: EMITE Ing]

6.3.2.1.1 Concept and configuration

In order to calibrate the reverberation chamber a broadband antenna can be used to measure the losses in the chamber with a network analyzer. This takes < 10 minutes. CTIA RCSG is working on a standard methodology for reverberation chamber calibration.

There are no active electronics in the measurement path that needs to be calibrated.

Reflections in turntables, cables, doors, etc, do not degrade accuracy. Reflections increase the richness of the channel in the reverberation chamber.

Existing studies show that low standard deviation (good accuracy) can be achieved by measuring the DUT in sufficient number of different positions and calculate the average of the values. Some analysis (see relevant references in [2]) show a typical standard deviation less than 0.5 dB at about 800 MHz, in a reverberation chamber with a size of 1.2m x 1.75m x 1.8m and continuous mode stirring. At higher frequencies or with a chamber of larger dimensions the standard deviation decreases and accuracy increases.

The following figure presents an example for an HSDPA receive diversity test configuration in a reverberation chamber.

For these tests we emulate an HSDPA call with a Node B emulator. The latter is connected to one of the 3 BS wall-mounted antennas through a switch. A fourth antenna allows measuring the DL received signal in the chamber with a spectrum analyzer.

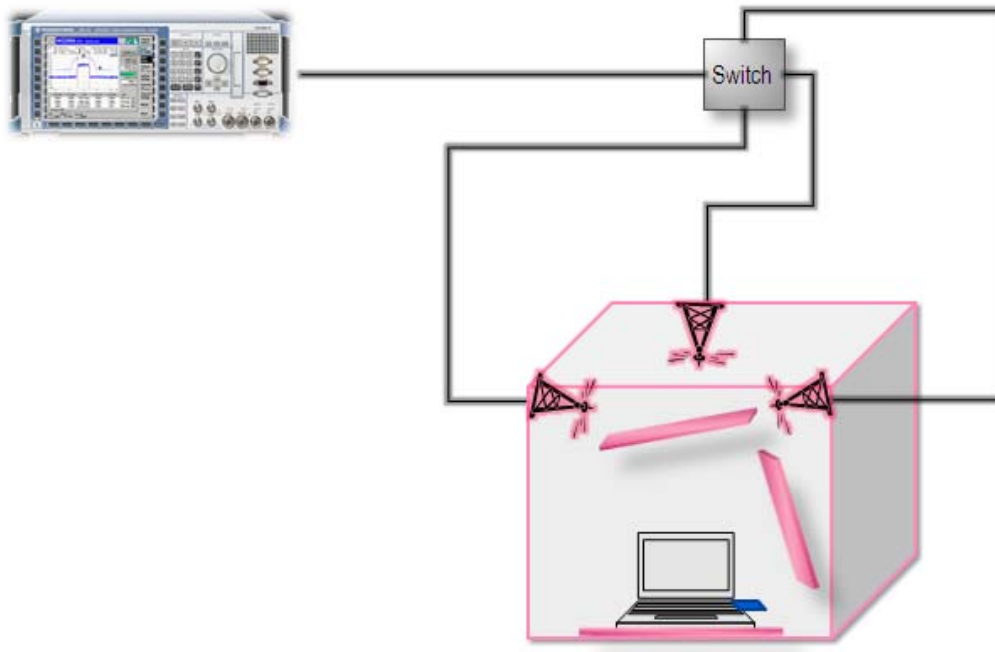


Figure 6.3.2.1.1-1: Test bench configuration for testing in reverberation chamber

In order to create a Rayleigh fading environment, we've got 3 types of parameters that can be set using a tool on a computer plugged to the chamber:

- Antenna among the 3, installed at the top of the cavity with different polarizations, is chosen;
- Turning the platform that holds the DUT;
- The 2 metallic stirrers near the walls can be moved on their axes.

6.3.2.1.2 Test conditions

Once the chamber is calibrated, the downlink throughput testing can be performed as follows to get one throughput averaged measurement:

- The DUT is placed in the chamber at least 0.5 wavelengths from the wall or from the metallic stirrers.
- An HSDPA call is emulated using the NodeB emulator with a pre-defined BS TX power.
- To get one measurement sample we set up one of the following possible combinations: position of the rotating platform $\{0, \pi/2, \pi, 3\pi/2, \text{etc.}\}$ + position of the metallic stirrers $\{0, 25, 50, 75, 100, \text{etc.}\}$ + antenna from $\{1, 2, 3\}$.
- For each one of these combinations we can record CQI, DL Throughput and DL Power in the chamber. The latter is measured using a fourth antenna and a spectrum analyzer. This constitutes one measurement sample. For each measurement sample, the link adaptation is performed manually or automatically on the NodeB emulator as follows: the HS-DSCH is configured (modulation, transport block size, number of HS-DSCH) depending on the CQI (Channel Quality Indicator) reported by the UE (User Equipment) according to the mapping table in 3GPP TS 25.214 [5].
- Once enough different DL throughput measurement samples (ideally ≥ 100), corresponding to different Antenna, rotating platform's position and stirrers' position combinations, are recorded for the same NodeB emulator DL TX power, they can be averaged to have the averaged DL throughput measurement.

The test duration can be significantly reduced if all these steps are automated. With a Variable Reference Channel (VRC) and continuous mode stirring total measurement time of less than 10 minutes could be possible.

6.3.2.2 Candidate solution 2

The reverberation chamber by itself has a limited range of channel modelling capabilities. Specifically,

- The power/delay profile is limited to a single decaying exponential.
- The Doppler spectrum and maximum Doppler is limited by the relatively slow motion of the stirrers.
- It is difficult to impart a specific, repeatable MIMO fading correlation on the downlink waveform.

These limitations can be overcome when a MIMO channel emulator and reverberation chamber are cascaded.

The Power/Delay Profile (PDP) can be enhanced beyond the single decaying exponential by programming the channel emulator with fading taps set at the desired excess delays. The resulting PDP will be the convolution of the taps provided by the channel.

The fading taps provided by the channel emulator allow much higher Doppler spreads than from the reverberation chamber alone. If a classical fading spectrum with a maximum Doppler of 100 Hz is desired, the channel emulator is configured to provide this. The resulting overall Doppler spectrum that results is the convolution of the channel emulator's Doppler spectrum with that of the reverberation chamber.

The fading produced by the cascaded channel emulator and reverberation chamber has a double-Rayleigh amplitude distribution. Because performance simulations generally use Rayleigh fading, simulation results for the double-Rayleigh case are not available.

The benefit is testing with a much higher maximum Doppler, on the order of 100 Hz or higher, than is possible with the reverberation chamber alone. Under these conditions, the reverberation chamber-induced fading will effectively be constant while the channel emulator-induced fading will dominate. Therefore, while a receiver's performance under such circumstances will definitely be different than under normal Rayleigh fading conditions, it should not undermine the receiver's ability to demodulate. Tests have shown that this is indeed the case. However, due to the lack of double-Rayleigh simulation results, measured results should only be compared with other devices using these same test conditions.

The correlation of fading between the downlink MIMO transmission paths can be adjusted using the channel emulator. This is also known as "BS correlation", reflecting the fact that it is controlled on the BS side of the link. The way to set this correlation using the channel emulator is as follows: using the Kronecker model of fading correlation, set the desired correlation of the transmit or BS correlation matrix. The receiver or MS correlation matrix should be set to identity. An example is given for a 2x2 MIMO system:

$$R_{BS} = \begin{bmatrix} 1 & \rho \\ \rho & 1 \end{bmatrix}, \quad R_{MS} = \begin{bmatrix} 1 & 0 \\ 0 & 1 \end{bmatrix}, \quad R_{chan} = R_{BS} \otimes R_{MS}$$

The value for ρ is the desired correlation between the two downlink paths. Note that it is not possible to control the phase of the correlation, only the amplitude.

The downlink antennas in the chamber are typically referred to as "wall" antennas. There should be a number of them equal to the number of spatial streams supported by the DUT. The spacing of the wall antennas is not very important. Tests have shown that as the spacing between them is changed over a range between 6 and 80 mm, the measured correlation changes very little, on the order of 5% to 10%.

6.3.2.2.1 Concept and configuration

The general configuration to be used for testing is shown in Figure 6.3.2.2.1-1. The specific example shown there is for two BS antennas. If higher order MIMO devices are to be tested, additional antennas are required. The channel emulator is placed between the (e)NodeB emulator and the reverberation chamber. Two calibrations are performed:

- 1) Calibration of reverberation chamber loading to set the proper chamber impulse response. Most of the time, the chamber will be loaded to produce a specific, desired chamber RMS delay spread. This is achieved using such devices as a phantom head, tank filled with liquid, and RF absorbing foam. For use with the channel emulator, it is desirable to set the chamber RMS delay spread as low as is allowable (approximately 55 ns - see Note), although higher RMS delay spreads are also legitimate, depending on the desired overall PDP.

NOTE: If the delay spread is reduced to below this point, the chamber's ability to produce the desired Rayleigh amplitude distribution at the DUT is degraded.

- 2) Calibration of the losses from (e)NodeB emulator to DUT location. This is already described in the test methodology for the reverberation chamber alone (subclause 6.3.2.1).

The calibrations are performed in this order, using a test antenna as the DUT antenna, and with the DUT in the chamber as it will be during the test. The contents of the chamber should not be disturbed after the calibration is complete. More information about the calibration procedures are found in Annex F.

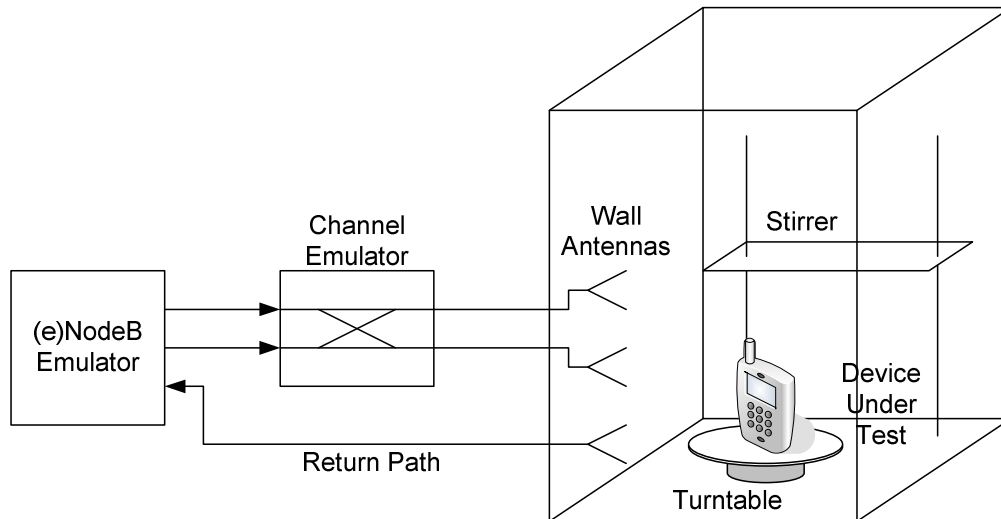


Figure 6.3.2.2.1-1: Test bench configuration for test using channel emulator and reverberation chamber for a 2x2 MIMO configuration

6.3.2.2.2 Test conditions

After the chamber is calibrated, the emulator is configured for the desired channel model, including the end-to-end PDP, the desired fading spectrum and Doppler spread, and the MIMO fading correlation. At this point, the system is ready to test the DUT, and a procedure appropriate to the Figure Of Merit (FOM) being measured is carried out.

There are three (3) operating methods, dependent on the motion of the stirrers and the state of the fading in the channel emulator.

In method 1, the stirrers, turntable or source antennas and channel emulator to operate continuously while the specific FOM is measured. A good example of this use would be throughput measurements under the conditions of a high Doppler rate, or, measured while the signal levels are varied over a wide range.

In method 2, the stirrers and turntable or source antennas are positioned in a number of combinations as described in 6.3.2.1.2. The channel emulator is allowed to run for a fixed length of time (usually 1 or 2 seconds is enough) and paused. The FOM is measured while the stirrers and turntable are not in motion, and the channel emulator is paused. In this method, the number of fixed positions and emulator states must be at least enough to guarantee the proper amplitude distribution. Automation of this entire procedure will significantly reduce the test time.

In method 3, the stirrers and turntable and/or source antennas are positioned as in method 2, but for each position, the channel emulator is allowed to run the fading channel model. The FOM is measured with the stirrers and turntable or source antenna stirring fixed and the channel emulator fading. This method is most analogous to the anechoic method which fixes the device rotation and runs the fading channel emulator while the FOM is measured. This method may also facilitate simulation.

7 Base Station (BS) configuration

7.1 eNodeB emulator settings

The eNodeB emulator parameters shall be set according to Table 7.1-1 for FDD and Table 7.1-2 for TDD. The settings for DL stream 1 and stream 2 are the same.

Table 7.1-1: Settings for FDD eNodeB emulator

| eNodeB settings (Note 1) | Unit | Value |
|--|--------------|--|
| Physical channel | | |
| Connection mode of UE | | Connection established |
| DL MIMO mode | | 2 x 2 open loop spatial multiplexing |
| Duplex mode | | FDD |
| Operating band (UL channel, DL channel) | | Band 7 (21100, 3100) Band 20 (24300, 6300) |
| Schedule type | | Reference Measurement Channel (RMC) |
| Reference Channel | | R.35 (Note 2) |
| Bandwidth DL | MHz | 10 |
| Number of RBs DL | | 50 |
| Start RB DL | | 0 |
| Modulation DL | | 64QAM |
| Maximum Theoretical Throughput | Mbps | 35.424 |
| TBS Idx DL | | 18 (RMC defined, Note 2) |
| Bandwidth UL | MHz | 10 |
| Number of RBs UL | | 50 |
| Start RB UL | | 0 |
| Modulation UL | | QPSK |
| TBS Idx UL | | 6 (RMC defined) |
| Transmit power control | dBm | -10/10 MHz, open loop (Note 3) |
| PDSCH power offset relative to RS EPRE | dB | $\rho_A = -3$ $\rho_B = -3$ |
| Number of HARQ transmissions | | 1 (no HARQ re-transmissions) |
| AWGN | | OFF |
| DL power level (RS EPRE) | dBm / 15 kHz | Set at eNodeB simulator with correction from calibration |
| Number of subframes for FOM measurement | | 2000 minimum for static channel 20000 minimum for faded channel (Note 4) |
| NOTE 1: This set of parameters is aligned with R&S CMW500, Anritsu MTC8820C, AT4 S3110B, and Agilent E6621A (to be confirmed). | | |
| NOTE 2: This RMC is defined in 3GPP TS 36.521-1 [12], Table A.3.3.2.1-1. R.35 subframes 1-4 and 6-9 utilize DL TBS 18, while R.35 subframe 0 utilizes TBS 17 (See Table A.3.3.2.1-1 Fixed Reference Channel two antenna ports in 3GPP TS 36.521-1 [12]). | | |
| NOTE 3: No uplink power control. | | |
| NOTE 4: These values might need to be increased for frequency and mobile speed reasons. | | |

Table 7.1-2: Settings for TDD eNodeB emulator

| eNodeB settings | Unit | Value |
|--|--------------|--|
| Physical channel | | |
| Connection mode of UE | | Connection established |
| DL MIMO mode | | 2 x 2 open loop spatial multiplexing |
| Duplex mode | | TDD |
| Operating band (UL / DL channel) | | Band 38 (38000) Band 39 (38450) Band 40 (39150) Band 41 (40620) |
| Schedule tyoe | | Reference Measurement Channel (RMC) |
| Reference Channel | | Table 7.1-3 |
| Up/Downlink Frame Configuration | | 1 |
| Special Frame configuration | | 7 |
| Bandwidth DL | MHz | 20 |
| Number of RBs DL | | 100 |
| Start RB DL | | 0 |
| Modulation DL | | 64QAM |
| TBS Idx DL | | 16 (RMC defined, NOTE 1) |
| Bandwidth UL | MHz | 20 |
| Number of RBs UL | | 100 |
| Start RB UL | | 0 |
| Modulation UL | | QPSK |
| TBS Idx UL | | 6 |
| Transmit power control | dBm | -10/20 MHz, open loop (NOTE 2) |
| PDSCH power offset relative to RS EPRE | dB | $\rho_A = -3$ $\rho_B = -3$ |
| Number of HARQ transmissions | | 1 (no HARQ re-transmissions) |
| AWGN | | OFF |
| DL power level (RS EPRE) | dBm / 15 kHz | Set at eNodeB simulator with correction from calibration |
| Number of subframes for FOM measurement | | 2000 minimum for static channel 20000 minimum for faded channel (NOTE 3) |
| NOTE 1: This RMC is defined in Table 7.1-3. Subframes 0, 1, 4, 6 and 9 utilize DL TBS 16, subframe 5 is unused for DL data transimission and other subframes are for UL. | | |
| NOTE 2: No uplink power control. | | |
| NOTE 3: These values might need to be increased for frequency and mobile speed reasons. | | |

Table 7.1-3: Fixed Reference Channel two antenna ports for 20MHz TD-LTE

| Parameter | Unit | Value |
|--|------|----------|
| Channel bandwidth | MHz | 20 |
| Allocated resource blocks (Note 3) | | 100 |
| Uplink-Downlink Configuration (Note 1) | | 1 |
| Allocated subframes per Radio Frame (D+S) | | 4+2 |
| Modulation | | 64QAM |
| Target Coding Rate | | 0.4 |
| Information Bit Payload (Note 3) | | |
| For Sub-Frames 4,9 | Bits | 32856 |
| For Sub-Frames 1,6 | | 24496 |
| For Sub-Frame 5 | Bits | N/A |
| For Sub-Frame 0 | Bits | 32856 |
| Number of Code Blocks (Notes 2 and 3) | | |
| For Sub-Frames 4,9 | | 5 |
| For Sub-Frames 1,6 | | 4 |
| For Sub-Frame 5 | | N/A |
| For Sub-Frame 0 | | 5 |
| Binary Channel Bits (Note 3) | | |
| For Sub-Frames 4,9 | Bits | 82800 |
| For Sub-Frames 1,6 | | 67968 |
| For Sub-Frame 5 | Bits | N/A |
| For Sub-Frame 0 | Bits | 80712 |
| Max. Throughput averaged over 1 frame (Note 3) | Mbps | 14.756 |
| UE Category | | ≥ 1 |
| NOTE 1: As per Table 4.2-2 in TS 36.211 [4]. | | |
| NOTE 2: If more than one Code Block is present, an additional CRC sequence of L = 24 Bits is attached to each Code Block (otherwise L = 0 Bit). | | |
| NOTE 3: Given per component carrier per codeword | | |

8 Channel Models

8.1 Introduction

In order to understand how different methodologies are able to similarly distinguish good and bad MIMO devices, it is important to ensure that the radio propagation conditions that are implying to a particular DUT are the same or similar to a certain extent.

The different channel models are used as a simple way to create complex multipath radio propagation conditions and RAN4 has agreed to compare the realization of those channel models across the different methods.

8.2 Channel Model(s) to be validated

Editor's Note: Initially a small set of representative channel models shall be agreed and use to validate channel model realization. Other channel models could be used at a later stage.

This clause shall also contain the identification of the main properties that characterize a given channel model as well as the expected results when realizing a channel model regardless of the methodology.

The following channel models are to be used in evaluation of MIMO OTA methodologies.

The generic models are

- SCME Urban micro-cell, and

- SCME Urban macro-cell.

In addition, the BS antenna assumptions defined in subclause 8.5 also apply when emulating the channel models.

In the following we define the cross polarization power ratio a propagation channel as $XPR = XPR_V = XPR_H$, where

$$XPR_V = \frac{S_{VV}}{S_{HV}} \quad \text{and} \quad XPR_H = \frac{S_{HH}}{S_{VH}}$$

and

- S_{VV} is the coefficient for scattered/reflected power on V-polarization and incident power on V-polarization;
- S_{VH} is the coefficient for scattered/reflected power on V-polarization and incident power on H-polarization;
- S_{HV} is the coefficient for scattered/reflected power on H-polarization and incident power on V-polarization;
- S_{HH} is the coefficient for scattered/reflected power on H-polarization and incident power on H-polarization.

NOTE: For Vertical only measurements, the powers per delay are used without regard to the specified XPR values.

The following SCME Urban Micro-cell is unchanged from the original SCME paper, with added XPR values, Direction of Travel, and Velocity.

Table 8.2-1: SCME urban micro-cell channel model

| SCME Urban micro-cell | | | | | | | | |
|--|------------|-----|-----|------------|-------|-------|---------|-------------------|
| Cluster # | Delay [ns] | | | Power [dB] | | | AoD [°] | AoA [°] |
| 1 | 0 | 5 | 10 | -3.0 | -5.2 | -7.0 | 6.6 | 0.7 |
| 2 | 285 | 290 | 295 | -4.3 | -6.5 | -8.3 | 14.1 | -13.2 |
| 3 | 205 | 210 | 215 | -5.7 | -7.9 | -9.7 | 50.8 | 146.1 |
| 4 | 660 | 665 | 670 | -7.3 | -9.5 | -11.3 | 38.4 | -30.5 |
| 5 | 805 | 810 | 815 | -9.0 | -11.2 | -13.0 | 6.7 | -11.4 |
| 6 | 925 | 930 | 935 | -11.4 | -13.6 | -15.4 | 40.3 | -1.1 |
| Delay spread [ns] | | | | | | | | 294 |
| Cluster AS AoD / AS AoA [°] | | | | | | | | 5 / 35 |
| Cluster PAS shape | | | | | | | | Laplacian |
| Total AS AoD / AS AoA [°] | | | | | | | | 18.2 / 67.8 |
| Mobile speed [km/h] / Direction of travel [°] | | | | | | | | 3, 30 / 120 |
| XPR (NOTE: V & H components based on assumed BS antennas) | | | | | | | | 9 dB |
| Mid-paths Share Cluster parameter values for: | | | | | | | | AoD, AoA, AS, XPR |

The following SCME Urban Macro-cell is unchanged from the original SCME paper, with added XPR values, Direction of Travel, and Velocity.

Table 8.2-2: SCME urban macro-cell channel model

| SCME Urban macro-cell | | | | | | | | |
|--|------------|------|------|------------|-------|-------|---------|-------------------|
| Cluster # | Delay [ns] | | | Power [dB] | | | AoD [°] | AoA [°] |
| 1 | 0 | 5 | 10 | -3 | -5.2 | -7 | 82.0 | 65.7 |
| 2 | 360 | 365 | 370 | -5.2 | -7.4 | -9.2 | 80.5 | 45.6 |
| 3 | 255 | 260 | 265 | -4.7 | -6.9 | -8.7 | 79.6 | 143.2 |
| 4 | 1040 | 1045 | 1050 | -8.2 | -10.4 | -12.2 | 98.6 | 32.5 |
| 5 | 2730 | 2735 | 2740 | -12.1 | -14.3 | -16.1 | 102.1 | -91.1 |
| 6 | 4600 | 4605 | 4610 | -15.5 | -17.7 | -19.5 | 107.1 | -19.2 |
| Delay spread [ns] | | | | | | | | 839.5 |
| Cluster AS AoD / AS AoA [°] | | | | | | | | 2 / 35 |
| Cluster PAS shape | | | | | | | | Laplacian |
| Total AS AoD / AS AoA [°] | | | | | | | | 7.9 / 62.4 |
| Mobile speed [km/h] / Direction of travel [°] | | | | | | | | 3, 30 / 120 |
| XPR (NOTE: V & H components based on assumed BS antennas) | | | | | | | | 9 dB |
| Mid-paths Share Cluster parameter values for: | | | | | | | | AoD, AoA, AS, XPR |

The parameters of the channel models are the expected parameters for the MIMO OTA channel models. However, the final channel model achieved for different methods could be a combined effect of the chamber and the channel emulator.

The Rayleigh fading may be implementation specific. However, the fading can be considered to be appropriate as long as the statistics of the generated Rayleigh fading are within standard requirement on Rayleigh fading statistics.

Editor's Note: NIST channel model is not ruled out, but before it can be used, more information on the AoA values would need to be provided.

8.3 Verification of Channel Model implementations

Channel Models have been specified in Clause 8.2.

This clause describes the MIMO OTA validation measurements, in order to ensure that the channel models are correctly implemented and hence capable of generating the propagation environment, as described by the model, within a test area. Measurements are done mainly with a Vector Network Analyser (VNA) and a spectrum analyzer.

Note that the term "**OTA antenna configuration**" used in this subclause refers only to the physical antennas used to perform the validation. The BS antenna assumptions defined as part of the channel model in subclause 8.5 apply in addition to the physical antenna configuration.

8.3.1 Measurement instruments and setup

The measurement setup includes the following equipment:

Table 8.3.1-1: Measurement equipment list for the verification procedure

| Item | Quantity | Item |
|------|----------|-------------------|
| 1 | 1 | Channel Emulator |
| 2 | 1 | Signal Generator |
| 3 | 1 | Spectrum Analyzer |
| 4 | 1 | VNA |
| 5 | 1 | Magnetic Dipole |
| 6 | 1 | Sleeve Dipole |

8.3.1.1 Vector Network Analyzer (VNA) setup

Most of the measurements are performed with a VNA. An example set of equipment required for this set-up is shown in Figure 8.3.1.1-1. VNA transmits frequency sweep signals through the MIMO OTA test system.

A test antenna, within the test area, receives the signal and VNA analyzes the frequency response of the system.

A number of traces (frequency responses) are measured and recorded by VNA and analyzed by a post processing SW, e.g., Matlab. Special care has to be taken into account to keep the fading conditions unchanged, i.e. frozen, during the short period of time of a single trace measurement. The fading may proceed only in between traces. This setup can be used to measure PDP, Spatial Correlation and Polarization of the Channel models defined in clause 8.2.

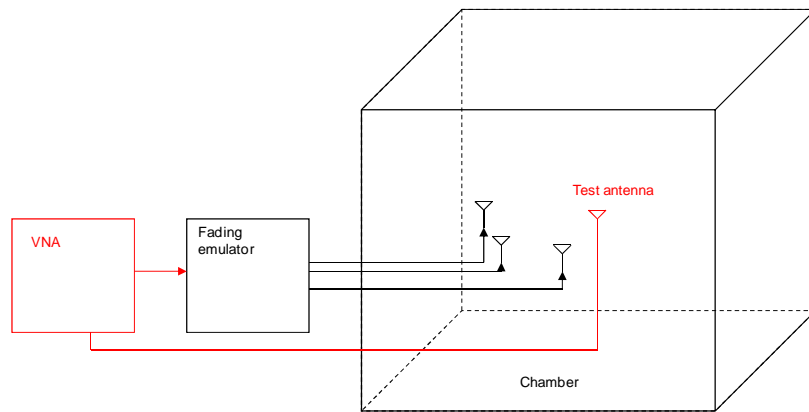


Figure 8.3.1.1-1: Setup for VNA measurements

8.3.1.2 Spectrum Analyzer (SA) setup

The Doppler spectrum is measured with a spectrum analyzer as shown in Figure 8.3.1.2-1. In this case a signal generator transmits CW signal through the MIMO OTA test system. The signal is received by a test antenna within the test area. Finally the signal is analyzed by a spectrum analyzer and the measured spectrum is compared to the target spectrum. This setup can be used to measure Doppler Spectrum of the Channel models defined in Clause 8.2.

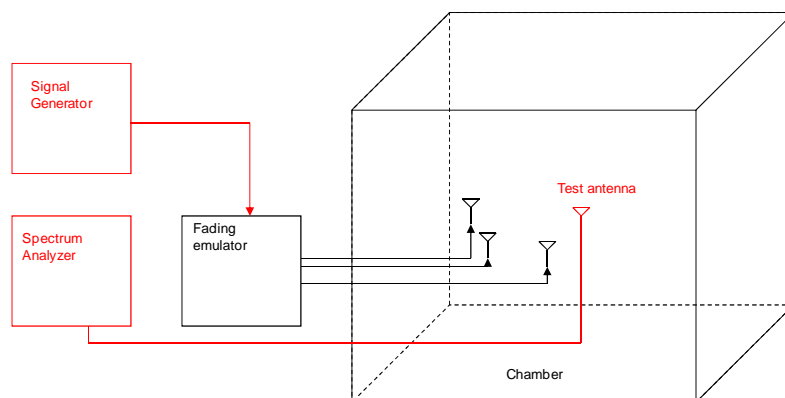


Figure 8.3.1.2-1: Setup for VNA measurements

8.3.2 Validation measurements

8.3.2.1 Power Delay Profile (PDP)

This measurement checks that the resulting Power Delay Profile (PDP) is like defined in the channel model.

Method of measurement:

Step the emulation and store traces from VNA. I.e. run the emulation to CIR number 1, pause, measure VNA trace, run the emulation to CIR number 10, pause, measure VNA trace. Continue until 1000 VNA traces are measured.

VNA settings:

Table 8.3.2.1-1: VNA settings for PDP

| Item | Unit | Value |
|--|--|---|
| Center frequency | MHz | Downlink center frequency in 3GPP TS 36.508 [19] as required per band |
| Span | MHz | 200 [TDB] |
| RF output level | dBm | -15 |
| Number of traces | | 1000 |
| Distance between traces in channel model | wavelength (Note) | > 2 |
| Number of points | | 1101 |
| Averaging | | 1 |
| NOTE: | Time [s] = distance [λ] / MS speed [λ/s] MS speed [λ/s] = MS speed [m/s] / Speed of light [m/s] * Center frequency [Hz] | |

Channel model specification:

Table 8.3.2.1-2: Channel model specification for PDP

| Item | Unit | Value |
|-----------------------|------------|---|
| Center frequency | MHz | Downlink center frequency in 3GPP TS 36.508 [19] as required per band |
| Channel model samples | wavelength | > 2000 |
| Channel model | | As specified in Clause 8.2 |

Method of measurement result analysis:

Measured VNA traces (frequency responses $H(t,f)$) are saved into a hard drive. The data is read into, e.g., Matlab. The analysis is performed by taking the Fourier transform of each FR. The resulting impulse responses $h(t,\tau)$ are averaged in power over time:

$$P(\tau) = \frac{1}{T} \sum_{t=1}^T |h(t, \tau)|^2$$

Finally the resulting PDP is shifted in delay, such that the first tap is on delay zero. The reference PDP plots from Table 8.2-1 and Table 8.2-2 are shown in Figure 8.3.2.1-1.

OTA antenna configuration: For e.g. 1 full ring (or single cluster configuration) of V polarized elements.

Measurement antenna: For e.g. Vertically oriented sleeve dipole.

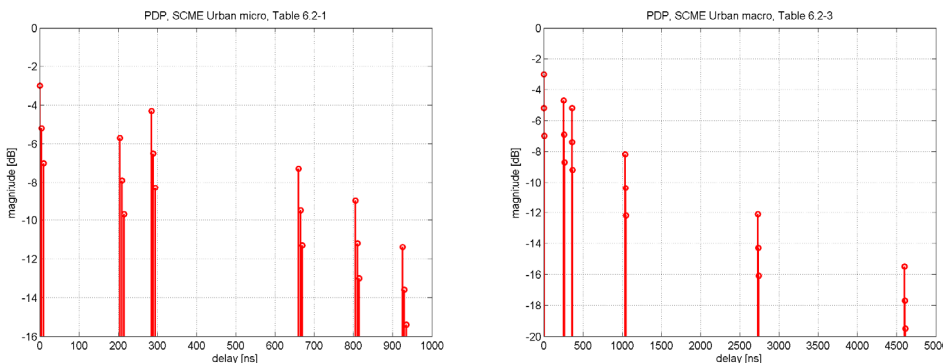


Figure 8.3.2.1-1: Reference PDP values for SCME Urban Macro / SCME Urban Micro plotted from Table 8.2-1 and Table 8.2-2

8.3.2.2 Doppler/Temporal correlation

This measurement checks the Doppler/temporal correlation.

Method of measurement:

Sine wave (CW, carrier wave) signal is transmitted from the signal generator. The signal is connected from the signal generator to fading emulator via cables. The fading emulator output signals are connected to power amplifier boxes via cables. The amplified signals are then transferred via cables to the probe antennas. The probe antennas radiate the signals over the air to the test antenna. The Doppler spectrum is measured by the spectrum analyzer and the trace is saved.

Signal generator settings:

Table 8.3.2.2-1: Signal generator settings for Doppler/Temporal correlation

| Item | Unit | Value |
|------------------|------|---|
| Center frequency | MHz | Downlink center frequency in 3GPP TS 36.508 [19] as required per band |
| Output level | dBm | -15 |
| Modulation | | OFF |

Spectrum analyzer settings:

Table 8.3.2.2-2: Spectrum analyzer settings for Doppler/Temporal correlation

| Item | Unit | Value |
|------------------|------|---|
| Center frequency | MHz | Downlink center frequency in 3GPP TS 36.508 [19] as required per band |
| Span | Hz | 4000 |
| RBW | Hz | 1 |
| VBW | Hz | 1 or use FFT |
| Number of points | | 8001 |
| Averaging | | 100 |

Channel model specification:

Table 8.3.2.2-3: Channel model specification for Doppler/Temporal correlation

| Item | Unit | Value |
|------------------|------|---|
| Center frequency | MHz | Downlink center frequency in 3GPP TS 36.508 [19] as required per band |
| Channel model | | As specified in Clause 8.2 |
| Mobile speed | km/h | 100 |

Method of measurement result analysis: Measurement data file (Doppler power spectrum) is saved into hard drive. The data is read into, e.g., Matlab.

The analysis is performed by taking the Fourier transformation of the Doppler spectrum.

The resulting temporal correlation function $R_t(\Delta t)$ is normalized such that $\max(\text{Re}(R_t(\Delta t))) = 1$.

Then the function values left from the maximum is cut out.

Further on the function values after, e.g. seven periods is cut out.

The reference temporal correlation plots from Table 8.2-1 and 8.2-2 are shown in Figure 8.3.2.2-1 and Figure 8.3.2.2-2.

OTA antenna configuration: For e.g. 1 full ring (or single cluster configuration) of V polarized elements.

Measurement antenna: For e.g. vertically oriented dipole.

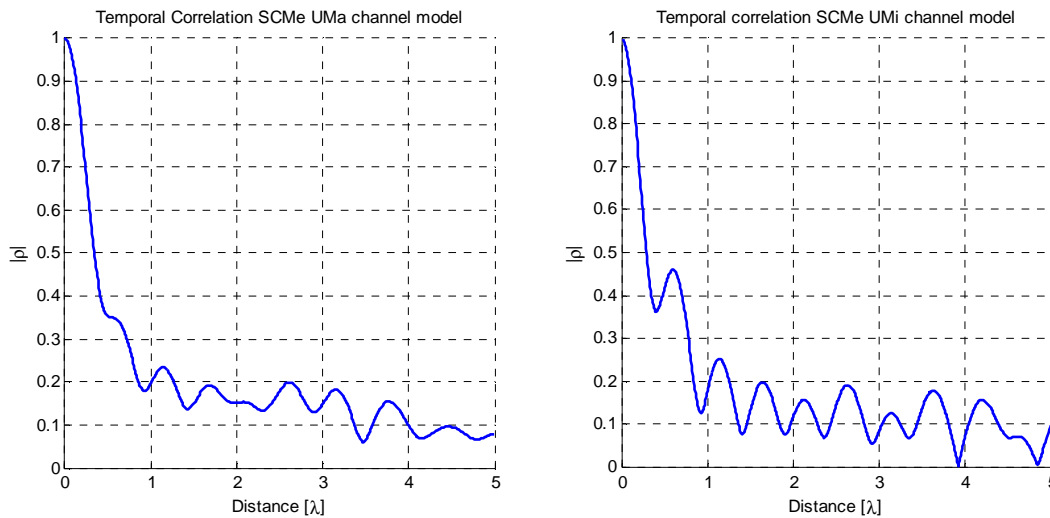


Figure 8.3.2.2-1: Reference Temporal Correlation Functions for SCME Urban Macro (left) and SCME Urban Micro (right) plotted from Table 8.2-1 and Table 8.2-2

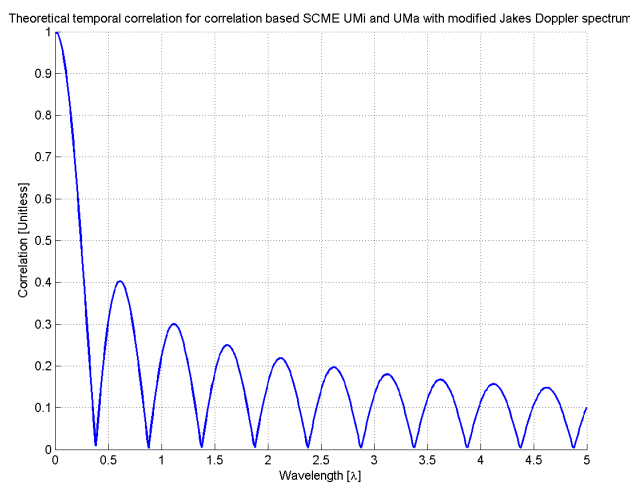


Figure 8.3.2.2-2: Reference Temporal Correlation Function for correlation implementation of SCME UMa and UMi with Jake's Doppler spectrum plotted from Table 8.2-1 and Table 8.2-2

8.3.2.3 Spatial correlation

This measurement checks whether the measured correlation curve follows the theoretical curve.

Method of measurement:

Step the emulation and store traces from VNA. I.e. run the emulation to CIR number 1, pause, measure VNA traces in 11 different DUT positions, run the emulation to CIR number 10, pause, measure VNA traces in 11 different DUT positions, ... etc. Continue until frequency response of 1000 CIRs in 11 positions (=1000*11 VNA traces) are measured.

11 test antenna positions sample a segment of line of length 1 wavelength with sampling interval of 0.1 wavelengths. Antenna spacing (wave lengths): -0.5 to +0.5 step of 0.1.

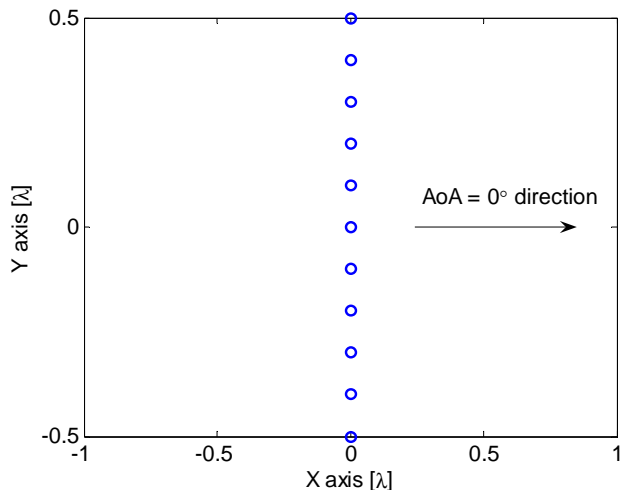


Figure 8.3.2.3-1: Test antenna positions

VNA settings:

Table 8.3.2.3-1: VNA settings for spatial correlation

| Item | Unit | Value |
|---|-------------------|---|
| Center frequency | MHz | Downlink center frequency in 3GPP TS 36.508 [19] as required per band |
| Span | MHz | 10 |
| RF output level | dBm | -15 |
| Number of traces | | 1000 |
| Distance between traces in channel model | Wavelength (Note) | > 2 |
| Number of points | | 1 (or the smallest possible) |
| Averaging | | 1 |
| NOTE: Time in seconds = distance [λ] / MS speed [λ/s] | | |
| MS speed [λ/s] = MS speed [m /s] / Speed of light [m/s] * Center frequency [Hz] | | |

Channel model specification:

Table 8.3.2.3-2: Channel model specification for spatial correlation

| Item | Unit | Value |
|-----------------------|------------|---|
| Center frequency | MHz | Downlink center frequency in 3GPP TS 36.508 [19] as required per band |
| Channel model samples | Wavelength | > 2000 |
| Channel model | | As specified in Clause 8.2 |
| Mobile speed | km/h | 30 |

Measurement Procedure

CALIBRATE

OPEN corrVNATrace trace file

FOR EACH gridPoint **IN** [test zone grid set]

MOVE measurement antenna to gridPoint

FOR EACH chanIRNumber **IN** [0:SD:1000*SD]

MEASURE Freq Resp with VNA

SAVE freq resp trace to trace file

END

END

CLOSE corrVNATrace_<calibMethod>_<polarization> trace file

Method of Measurement Results Analysis

Calculate correlation of 1000 x 11 matrix $\mathbf{H}(f)$ of frequency response samples. The procedure is to correlate sixth column (the trace measured at the centre of chamber) with the 10 other columns as follows (Matlab example)

```
for ind = 1:11;
    Corr(:, :, ind) = abs(corrcoef(H(:, 1), H(:, ind)));
end
Correlation = squeeze(Corr(1, 2, :));
```

The reference spatial correlation plots from Table 8.2-1 and 8.2-2 are shown in Figure 8.3.2.3-2.

OTA antenna configuration: For e.g. 1 full ring (or a single cluster configuration) of V polarized elements.

Measurement antenna: For e.g. Sleeve dipole.

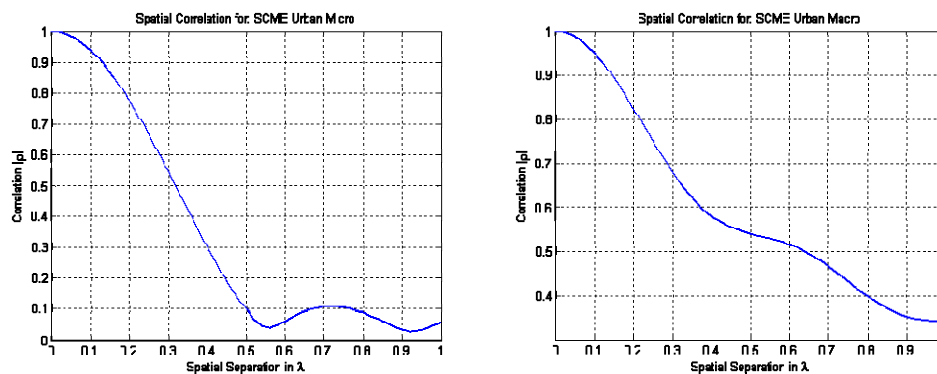


Figure 8.3.2.3-2: Reference Spatial Correlation Functions for SCME Urban Macro / SCME Urban Micro plotted from Table 8.2-1 and Table 8.2-2

8.3.2.4 Cross-polarization

This measurement checks how well the measured vertically or horizontally polarized power levels follow expected values.

Method of measurement: Step the emulation and store traces from VNA.

VNA settings:

Table 8.3.2.4-1: VNA settings for cross-polarization

| Item | Unit | Value |
|---|-------------------|---|
| Center frequency | MHz | Downlink Center Frequency in 3GPP TS 36.508 [19] as required per band |
| Span | MHz | 10 |
| RF output level | dBm | -15 |
| Number of traces | | 1000 |
| Distance between traces in channel model | Wavelength (Note) | > 2 |
| Number of points | | 201 |
| Averaging | | 1 |
| NOTE: Time [s] = distance [λ] / MS speed [λ /s] MS speed [λ /s] = MS speed [m /s] / Speed of light [m/s] * Center frequency [Hz] | | |

Channel model specification:**Table 8.3.2.4-2: Channel model specification for cross-polarization.**

| Item | Unit | Value |
|-----------------------|------------|---|
| Center frequency | MHz | Downlink center frequency in 3GPP TS 36.508 [19] as required per band |
| Channel model samples | wavelength | > 2000 |
| Channel model | | As specified in Clause 8.2 |
| Mobile speed | km/h | 30 |

Measurement Procedure

1. Play or step through the channel model -> SCME UMi, or UMa X Corr.
2. Measure the absolute power received at the center of the array, averaged over a statistically significant number of fades.
 - a. Use a vertically polarized sleeve dipole to measure the V component.
 - b. Use a horizontally polarized (vertically oriented) magnetic loop dipole, or a horizontally polarized sleeve dipole measured in two orthogonal horizontal positions and summed to measure the H component.
3. Calculate the V/H ratio.
4. Compare it with the theory -> 0.83dB for UMi, and 8.13dB for UMa.

Expected measurement results

V/H ratio (composite, i.e. all 6 paths combined) of the 3GPP SCME Umicro model is 0.83 dB and for Umacro 8.13 dB. The BS antennas are isotropic dipoles with +/- 45 degrees slant and subject to a foreshortening of the slanted radiating element. See channel model details specified in clause 8.2.

8.3.3 Reporting

The tolerance for the channel model measurements is defined in tables 8.3.3-2, 8.3.3-3, 8.3.3-4 and 8.3.3-5.

These tolerances are based on what can practically be measured for each metric in order that pass/fail limits can be defined for validation of acceptable channel model implementation. Studies of the impact on non-ideal channel model implementation have not been carried out and therefore it may be necessary in the future when a better understanding of the impact of the channel model implementation on throughput measurements is found, that these tolerance values may need to be revised.

Table 8.3.3-1: Void

Table 8.3.3-2: Limits for PDP

| | |
|--|--|
| Maximum Power Deviation per Cluster | Maximum Excess Delay Deviation per Cluster |
| $\pm 0.85\text{dB}$ | $\pm 11\text{ns}$ |
| NOTE: The PDP must be postprocessed with a running average of 9 elements | |

Table 8.3.3-3: Limits for Doppler / Temporal Correlation for the geometric implementation

| λ | Lower Limit | Upper Limit |
|-----------|-------------|-------------|
| 0 | 0.95 | 1 |
| 0.1 | 0.8 | 1 |
| 0.3 | 0.27 | 0.57 |
| 0.4 | 0.27 | 0.5 |
| 0.45 | 0.27 | 0.5 |
| 0.6 | 0.37 | 0.5 |
| 0.75 | 0.1 | 0.5 |
| 0.8 | 0.06 | 0.37 |
| 0.93 | 0.06 | 0.25 |
| 1.05 | 0.06 | 0.31 |
| 1.15 | 0.15 | 0.31 |
| 1.25 | 0.075 | 0.31 |
| 1.35 | 0 | 0.21 |
| 1.45 | 0 | 0.21 |
| 1.5 | 0 | 0.25 |
| 1.65 | 0.1 | 0.25 |
| 1.75 | 0 | 0.25 |
| 5 | 0 | 0.2 |

Table 8.3.3-4: Limits for Spatial Correlation

| λ | Lower Limit | Upper Limit |
|-----------|-------------|-------------|
| 0 | 0.99 | 1.015 |
| 0.1 | 0.9 | 0.975 |
| 0.2 | 0.70 | 0.83 |
| 0.3 | 0.46 | 0.63 |
| 0.4 | 0.22 | 0.4 |
| 0.5 | 0 | 0.21 |
| 0.6 | 0 | 0.18 |
| 0.7 | 0 | 0.18 |
| 0.8 | 0 | 0.2 |
| 0.9 | 0.08 | 0.32 |
| 1 | 0.23 | 0.56 |

Table 8.3.3-5: Limits for Cross Polarization

| |
|------------------------------|
| V/H Maximum Deviation |
| ± 0.9 dB |

8.4 Channel Model validation results

8.4.1 Scope

Clauses 8.4.2-6 contain the validation results of channel models defined in Clause 8.2 for companies using methods as described in Clauses 6.3.1.1 , 6.3.1.2 and 6.3.1.3. These results are based on three different types of channel emulators and setup vendors, and all three sets of results are included here for comparison.

8.4.2 Power Delay Profile (PDP)

The power delay profiles of the channel models specified in Clause 8.2 have been measured according to the procedures in 8.3.2.1. Figure 8.4.1-1 below illustrates the measured results for Band 13 for both channel emulators.

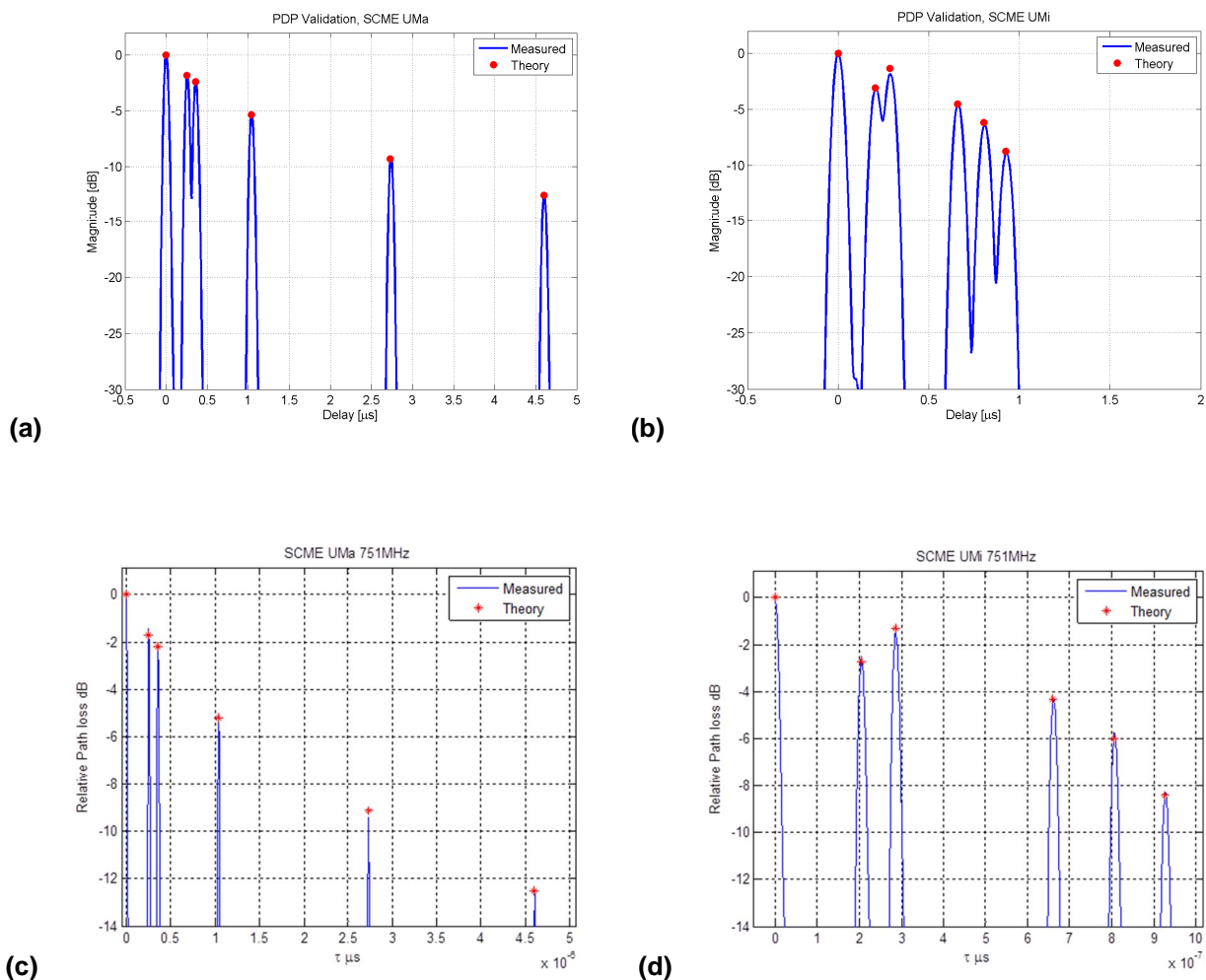


Figure 8.4.2-1: For Band 13, SCMe UMa (a) and SCMe UMi (b) PDP verification measurement for channel emulator A; SCMe UMa (c) and SCMe UMi (d) PDP verification measurement for channel emulator B

Table 8.4.2-1 below summarizes the PDP verification results.

Table 8.4.2-1: Summary of PDP verification results at Band 13 for both channel emulator vendors

| SCMe UMa | Channel Emulator A | | | Channel Emulator B | | |
|----------|----------------------|---------------------|-------|----------------------|---------------------|-------|
| Cluster | Simulated Power (dB) | Measured Power (dB) | Delta | Simulated Power (dB) | Measured Power (dB) | Delta |
| 1 | 0 | 0 | 0 | 0 | 0 | 0 |
| 2 | -1.8 | -1.9 | -0.1 | -1.7 | -1.6 | +0.1 |
| 3 | -2.4 | -2.45 | -0.05 | -2.2 | -2.25 | -0.05 |
| 4 | -5.35 | -5.35 | 0 | -5.2 | -5.35 | -0.15 |
| 5 | -9.2 | -9.2 | 0 | -9.1 | -9.25 | -0.15 |
| 6 | -12.6 | -12.6 | 0 | -12.5 | -12.6 | -0.1 |
| SCMe UMi | Channel Emulator A | | | Channel Emulator B | | |
| Cluster | Simulated Power (dB) | Measured Power (dB) | Delta | Simulated Power (dB) | Measured Power (dB) | Delta |
| 1 | 0 | 0 | 0 | 0 | 0 | 0 |
| 2 | -3.09 | -3.09 | 0 | -2.7 | -2.75 | -0.05 |
| 3 | -1.33 | -1.85 | -0.52 | -1.3 | -1.35 | -0.05 |
| 4 | -4.54 | -4.52 | +0.02 | -4.3 | -4.35 | -0.05 |
| 5 | -6.17 | -6.41 | -0.24 | -6.0 | -5.95 | +0.05 |
| 6 | -8.76 | -8.9 | -0.14 | -8.4 | -8.45 | -0.05 |

The results for the RTS method with geometric implementation are shown in Figures 8.4.2-2:

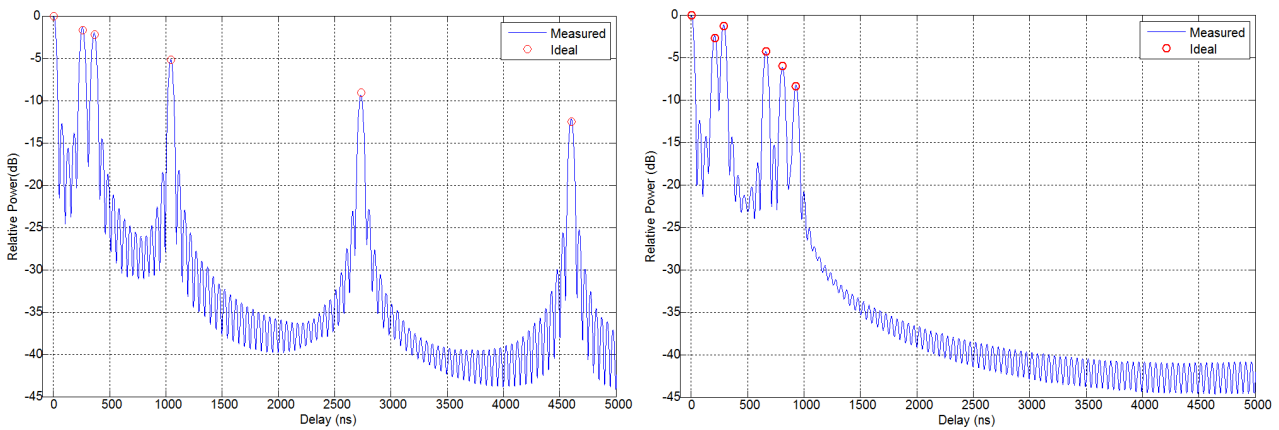


Figure 8.4.2-2: For Band 13, SCMe UMa and UMi PDP verification measurement for the RTS method with geometric implementation

The results for the RTS method with correlation implementation (Jake’s Doppler spectrum) are shown in Figures 8.4.2-3:

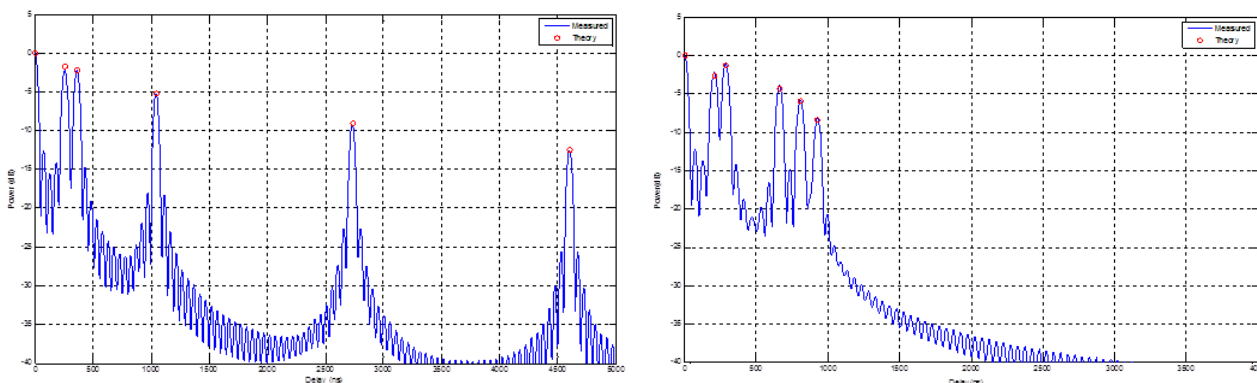


Figure 8.4.2-3: For Band 13, SCMe UMa and UMi PDP verification measurement for the RTS method with correlation implementation (Jake's Doppler spectrum)

The summarized results can be found in Tables 8.4.2-2 and 8.4.2-3:

Table 8.4.2-2: Summary of PDP verification results at Band 13 for the RTS method with geometric implementation

| SCME Urban Macro | | | | | | |
|------------------|------------|----------|------------|------------|----------|------------|
| Cluster | Delay (ns) | | | Power (dB) | | |
| | Theory | Measured | Delta (ns) | Theory | Measured | Delta (dB) |
| 1 | 0 | 0 | 0 | 0 | 0 | 0 |
| 2 | 255 | 256 | 1 | -1.7 | -2 | -0.3 |
| 3 | 360 | 360 | 0 | -2.2 | -2.2 | 0 |
| 4 | 1040 | 1040 | 0 | -5.2 | -5.2 | 0 |
| 5 | 2730 | 2728 | -2 | -9.1 | -9.4 | -0.3 |
| 6 | 4600 | 4600 | 0 | -12.5 | -12.5 | 0 |
| SCME Urban Micro | | | | | | |
| Cluster | Delay (ns) | | | Power (dB) | | |
| | Theory | Measured | Delta (ns) | Theory | Measured | Delta (dB) |
| 1 | 0 | 0 | 0 | 0 | 0 | 0 |
| 2 | 205 | 208 | 3 | -2.7 | -2.6 | 0.1 |
| 3 | 285 | 288 | 3 | -1.3 | -1.2 | 0.1 |
| 4 | 660 | 664 | 4 | -4.3 | -4.5 | -0.2 |
| 5 | 805 | 808 | 3 | -6 | -6.1 | -0.1 |
| 6 | 925 | 928 | 3 | -8.4 | -8.3 | 0.1 |

Table 8.4.2-3: Summary of PDP verification results at Band 13 for the RTS method with correlation implementation (Jake's Doppler spectrum)

| SCME Urban Macro | | | | | | |
|------------------|------------|----------|------------|------------|----------|------------|
| Cluster | Delay (ns) | | | Power (dB) | | |
| | Theory | Measured | Delta (ns) | Theory | Measured | Delta (dB) |
| 1 | 0 | 0 | 0 | 0 | 0 | 0 |
| 2 | 255 | 256 | 1 | -1.7 | -1.6 | 0.1 |
| 3 | 360 | 360 | 0 | -2.2 | -2.1 | 0.1 |
| 4 | 1040 | 1040 | 0 | -5.2 | -5.2 | 0 |
| 5 | 2730 | 2728 | -2 | -9.1 | -9.7 | -0.6 |
| 6 | 4600 | 4600 | 0 | -12.5 | -12.3 | 0.2 |
| SCME Urban Micro | | | | | | |
| Cluster | Delay (ns) | | | Power (dB) | | |
| | Theory | Measured | Delta (ns) | Theory | Measured | Delta (dB) |
| 1 | 0 | 0 | 0 | 0 | 0 | 0 |
| 2 | 205 | 208 | 3 | -2.7 | -2.9 | 0.2 |
| 3 | 285 | 288 | 3 | -1.3 | -1.4 | -0.1 |
| 4 | 660 | 664 | 4 | -4.3 | -4.9 | -0.6 |
| 5 | 805 | 808 | 3 | -6 | -6 | 0 |
| 6 | 925 | 928 | 3 | -8.4 | -8.3 | 0.1 |

8.4.3. Doppler / Temporal Correlation

The Doppler spread and temporal correlation of the channel models defined in clause 8.2 have been characterized according to clause 8.3.2.2. Figure 8.4.3-1 below illustrates the measured results for Band 13.

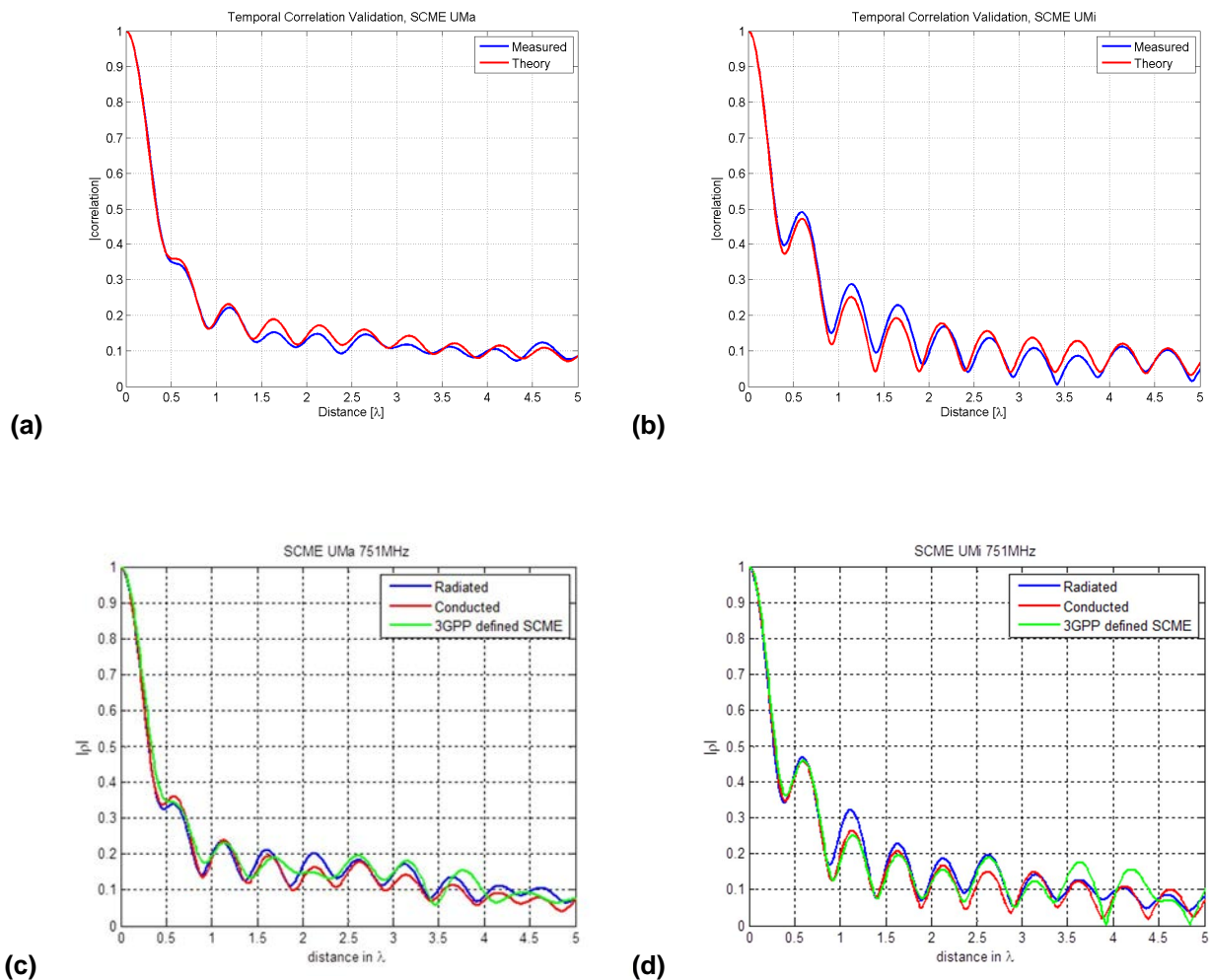


Figure 8.4.3-1: For Band 13, temporal correlation measurements of SCMe UMa (a) and SCMe UMi (b) emulated by channel emulator A; SCMe UMa (c) and SCMe UMi (d) with channel emulator B, both for Band 13

Figure 8.4.3-2: Void

Figure 8.4.3-3: Void

The temporal correlation results for the RTS method using the geometric implementation are shown in Figure 8.4.3-4:

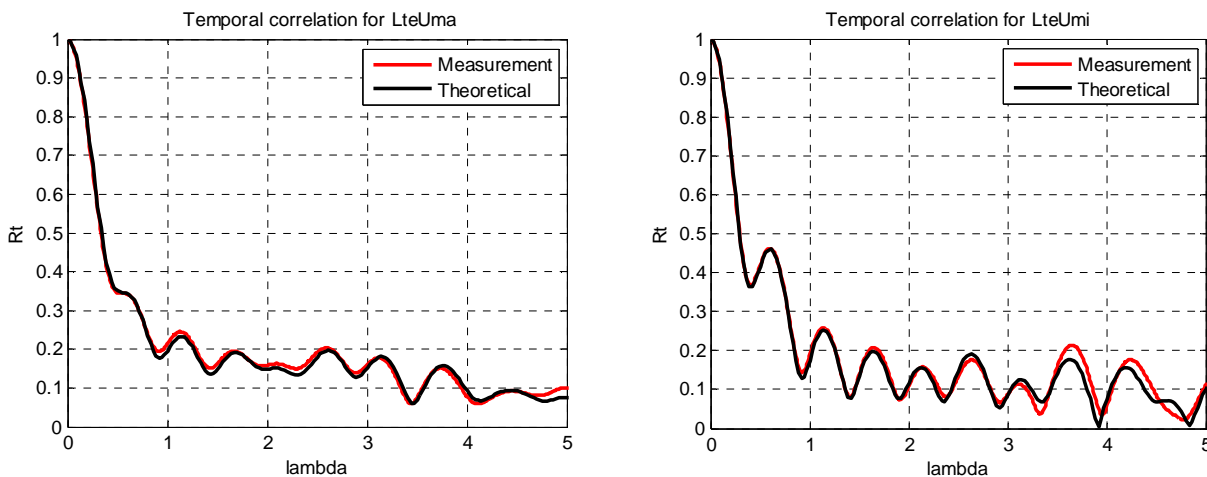


Figure 8.4.3-4: Band 13 temporal correlation measurements of SCME UMa and UMi for the RTS method with geometric implementation

The temporal correlation results for the radiated two-stage method using correlation implementation of SCME (Jake's Doppler spectrum) are shown in Figure 8.4.3-5:

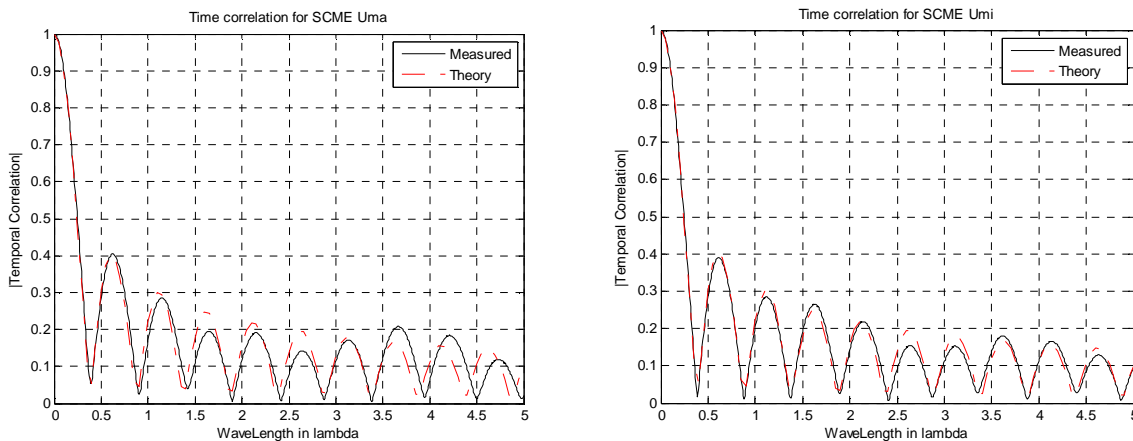
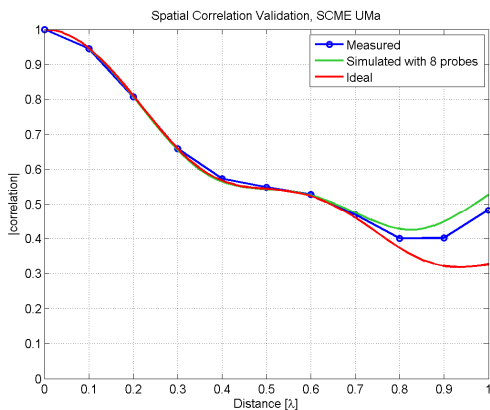


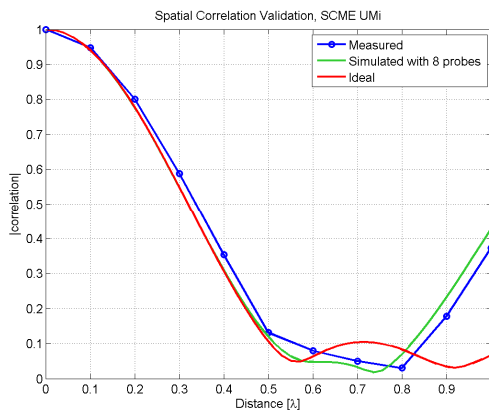
Figure 8.4.3-5: Band 13 Temporal correlation measurements for the radiated two-stage method using correlation implementation of SCME UMa and UMi with with correlation implementation (Jake's Doppler spectrum)

8.4.4 Spatial correlation

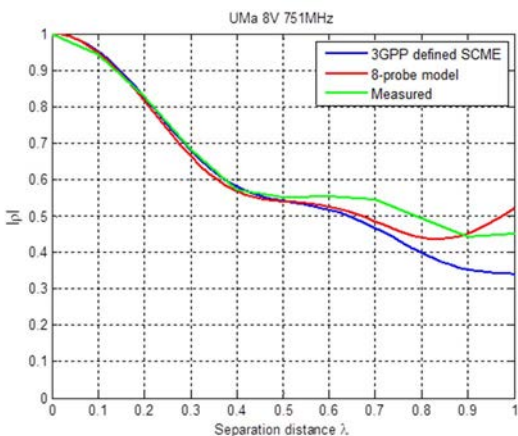
The spatial correlation properties of the channel models defined in clause 8.2 have been characterized according to clause 8.3.2.3. Figure 8.4.4-1 below illustrates the measured results for Band 13.



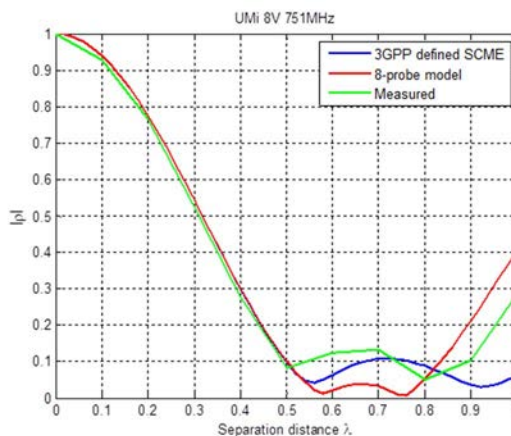
(a)



(b)



(c)



(d)

Figure 8.4.4-1: For Band 13 spatial correlation measurements of SCMe UMa (a) and SCMe UMi (b) emulated by channel emulator A; SCMe UMa (c) and SCMe UMi (d) with channel emulator B, both for Band 13

Figure 8.4.4-2: Void

Figure 8.4.4-3: Void

The spatial correlation results for the RTS method using correlation implementation of SCME (Jake's Doppler spectrum) are shown in Figure 8.4.4-4.

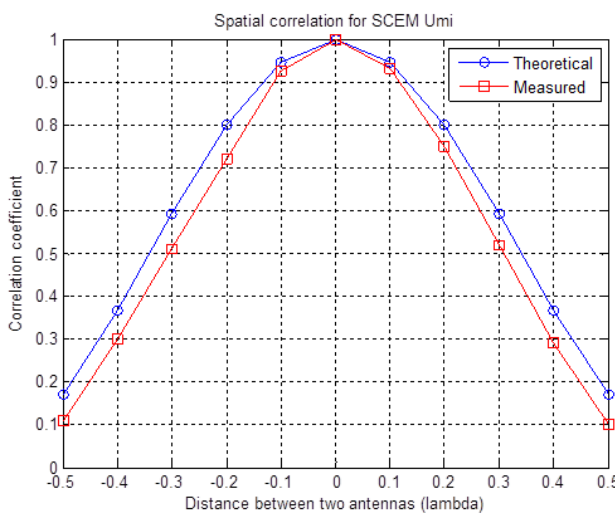
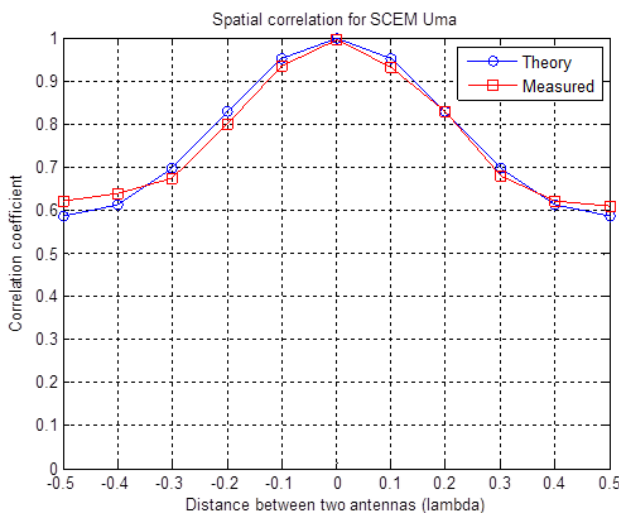


Figure 8.4.4-4: Band 13 spatial correlation measurements for the radiated two-stage method using correlation implementation of SCME UMa and UMi (Jake's Doppler spectrum)

The spatial correlation results for the RTS method using geometric implementation of SCME are shown in Figure 8.4.4-5.

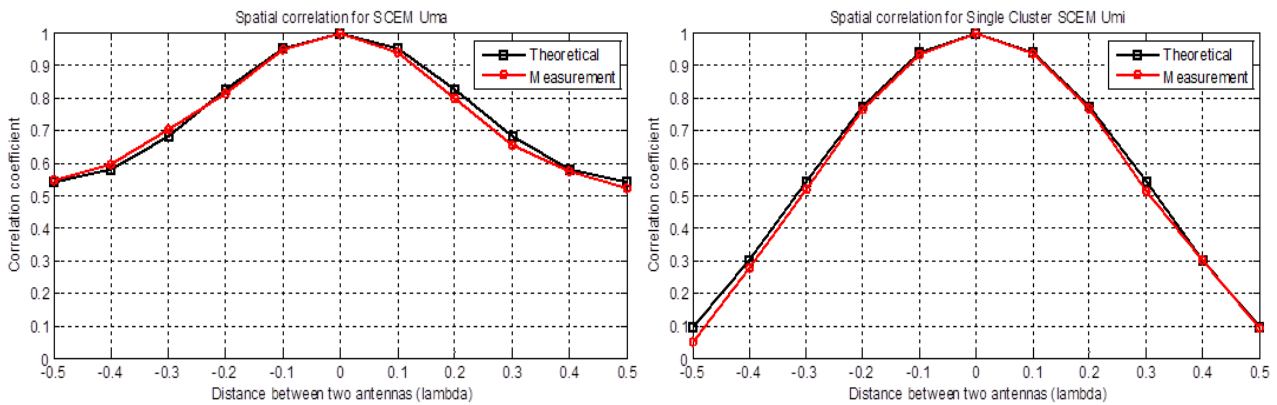


Figure 8.4.4-5: Band 13 spatial correlation measurements for the RTS method using geometric implementation of SCME UMa and UMi

8.4.5 Cross polarization

The cross polarization properties of the channel models defined in clause 8.2 have been characterized according to clause 8.3.2.3. The measured results shown in Table 8.4.5-1 below are reported considering the antenna gain difference of the reference antennas.

Table 8.4.5-1: Summary of cross polarization verification results for Band 13

| | Channel emulator A | | Channel emulator B | |
|---|--------------------|----------|--------------------|--------------------|
| | SCMe UMi | SCMe UMa | SCMe UMi | SCMe UMa |
| Target | 0.83 dB | 8.13 dB | To be added (Note) | To be added (Note) |
| Measurement considering antenna gain difference | 2.0 dB | 9.0 dB | To be added (Note) | To be added (Note) |
| Deviation | 1.2dB | 0.9dB | To be added (Note) | To be added (Note) |
| NOTE: XPR values for channel emulator B will be added at a later stage. | | | | |

The cross-polarization results for the RTS method using geometric implementation of SCME are shown in Table 8.4.5.2:

Table 8.4.5-2: Summary of cross polarization verification results for Band 13 with geometric implementation

| Channel model | V/H ratio | Theory | Deviation |
|---------------|-----------|--------|-----------|
| UMa MC | 8.1 | 8.13 | 0.03 |
| UMi MC | 0.8 | 0.83 | 0.03 |

The cross-polarization results for the RTS method using correlation implementation of SCME (Jake's Doppler spectrum) are shown in Table 8.4.5.3:

Table 8.4.5-3: Summary of cross polarization verification results for Band 13 with correlation implementation (Jake's Doppler spectrum)

| Channel model | V/H ratio | Theory | Deviation |
|---------------|-----------|--------|-----------|
| UMa | 7.9 | 8.13 | -0.23 |
| UMi | 0.8 | 0.83 | -0.03 |

8.4.6 Summary

The summary of the channel model validation activity is provided in Table 8.4.6-1 below.

Table 8.4.6-1: Summary of channel model validation results

| Item | Parameter | Result | Tolerances | Comments |
|---|--------------------------------|-----------|------------|----------|
| 1 | Power delay profile | See 8.4.2 | FFS (Note) | |
| 2 | Doppler / Temporal Correlation | See 8.4.3 | FFS (Note) | |
| 3 | Spatial Correlation | See 8.4.4 | FFS (Note) | |
| 4 | Cross Polarization | See 8.4.5 | FFS (Note) | |
| NOTE: Further investigation of channel model validation metrics and their corresponding tolerances is on-going within the framework of measurement uncertainty budget development | | | | |

8.5 Channel Model emulation of the Base Station antenna pattern configuration

Editor's Note: To include the agreed X-polarized method. Any additional approach would need to be clearly specified.

The emulated BS antennas to be used for all emulation of the channel models defined in subclause 8.2 shall be assumed to be dual polarized equal power elements with a fixed θ_λ separation, 45 degrees slanted.

The slant 45 degree antenna is an "X" configuration and is modelled as an ideal dipole with isotropic gain and subject to a foreshortening of the slanted radiating element, which is observed to vary as a function of the path angle of departure. This foreshortening with AoD is a typical slanted dipole behaviour and is a source of power variation in the channel model. The effective antenna pattern for this antenna is illustrated in Figure 8.5-1.

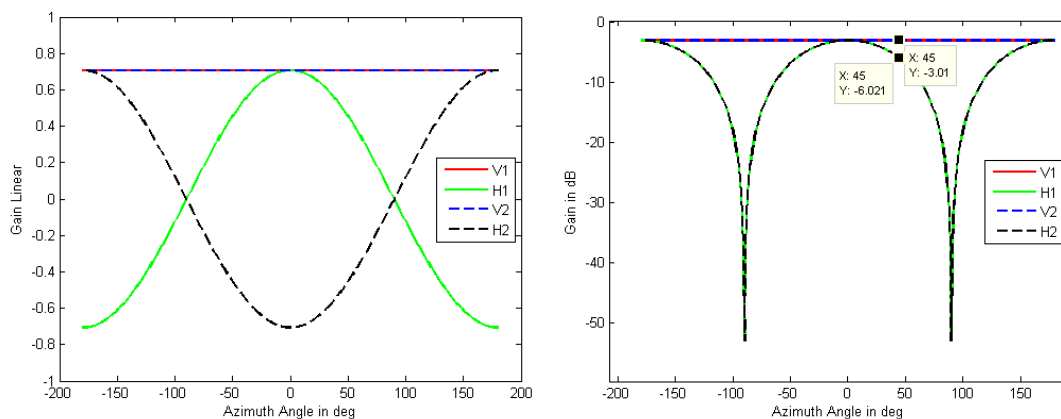


Figure 8.5-1: X antenna gain assumption (a) Linear gain (b) dB gain

9 Reference antennas and devices testing

9.1 Reference antennas design

Editor's Note: Text to be added

9.2 Reference devices

9.3 Description of tests with reference antennas and devices

9.3.1 The Absolute Data Throughput Comparison Framework

9.3.1.1 Introduction

In an effort to compare different MIMO OTA methodologies' results to conducted results under the implementations of channel models defined in clause 8.2, the absolute data throughput comparison framework has been defined. By utilizing the reference antennas (clause 9.1) and reference devices (clause 9.2), this framework shall be used to compare each MIMO OTA testing method's ability to emulate the specified network and channel propagation characteristics based on an absolute data throughput metric.

The framework consists of a set of conducted (Figure 9.3.1.1-1) and radiated (Figure 9.3.1.1-2) measurements of MIMO throughput (clause 5.1.1). The details for the application of this framework are described in clause 9.3.1.6.

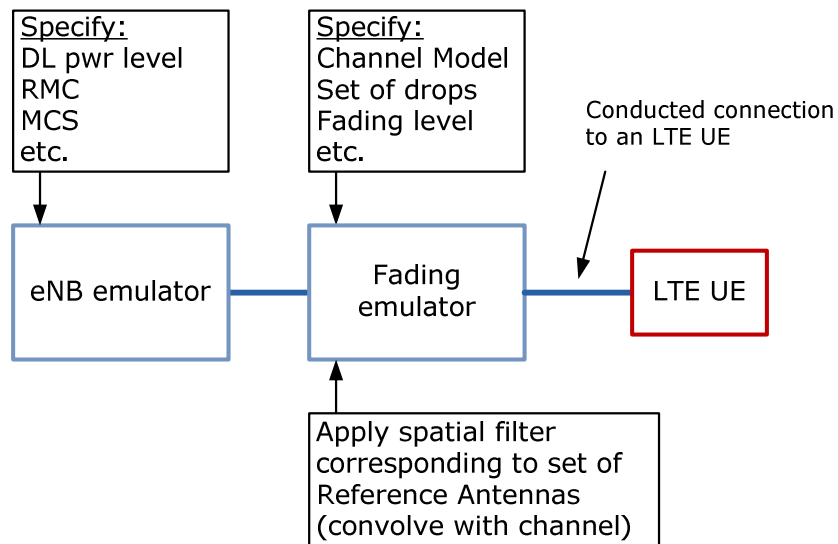


Figure 9.3.1.1-1: Method of measuring the conducted absolute throughput reference performance

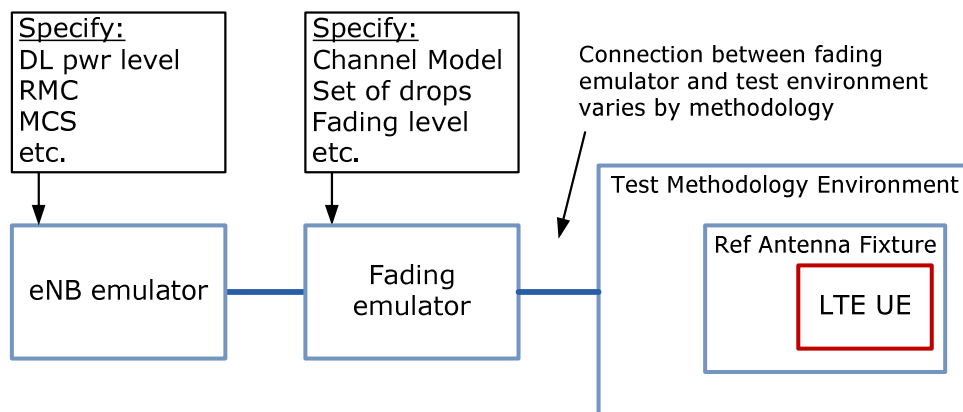


Figure 9.3.1.1-2: Method of measuring the absolute radiated data throughput metric with the reference antennas

The following subclauses define the antenna pattern data format, emulation of antenna pattern rotation, absolute data throughput measurement enabler, and the output data format.

9.3.1.2 Antenna pattern data format

The antenna pattern data format—used in the conducted portion of the measurements — shall be in the 3D AAU format as defined by COST IC1004 [14]. Table 9.3.1.2-1 and 9.3.1.2-2 below illustrates the header structure with a sample data set respectively.

Table 9.3.1.2-1: Auxiliary informational header

| Line(s) | Pos. | Description | Values - examples or defaults |
|--|------|---|-------------------------------|
| 1 | 1 | Pattern frequency | free (750) |
| | 2 | Frequency units | {Hz,KHz,MHz,GHz} |
| | 3 | Port index (to resolve antennas automatically) | free (1) |
| | 4 | Pattern type (Directivity, Gain, Realized Gain, E-field) | {D,G,Gr,E} - possible more |
| | 5 | Units format (as in touchstone plus the E-field format) | {DB,MA,RI,V/m} |
| NOTE: There is no freedom in the column arrangement but the labels can vary. Done for ease of use. | | | |
| 2 | 1 | θ scan stepping - must be constant | Theta [deg] |
| | 2 | ϕ scan stepping - must be constant | Phi [deg] |
| | 3 | Absolute of the field X(1-4) in [units(1-5)] | Abs X [units] |
| | 4 | θ polarized field X(1-4) in [units(1-5)] | XTh [units] |
| | 5 | phase of the θ polarized field - always in degrees | phase Th [deg] |
| | 6 | ϕ polarized field X(1-4) in [units(1-5)] | XPh [units] |
| | 7 | phase of the ϕ polarized field - always in degrees | phase Ph [deg] |
| 3,4 ... | N/A | NOTE: Any number additional lines can be added, always beginning with Matlab comment sign % Some custom comment, ID etc. | % File version 1.0 |

Note: A semicolon should be used as a delimiter in the header.

Table 9.3.1.2-2: 3D AAU file format example

| 750; MHz; 1; G; DB | | | | | | |
|--------------------|---------------|---------------|---------------|----------------|---------------|----------------|
| Theta [deg] | Phi [deg] | Abs G [dB] | GTh [dB] | phase Th [deg] | GPh [dB] | phase Ph [deg] |
| File version 1.0 | | | | | | |
| 0.0000000e+00 | 0.0000000e+00 | 7.1488243e+00 | 8.8275753e+00 | 2.9473810e+02 | 1.2089176e+01 | 2.9741836e+02 |
| 5.0000000e+00 | 0.0000000e+00 | 5.9290614e+00 | 6.9276561e+00 | 2.8631853e+02 | 1.2802746e+01 | 2.9300649e+02 |
| 1.0000000e+01 | 0.0000000e+00 | 4.6884986e+00 | 5.2974347e+00 | 2.8098081e+02 | 1.3521536e+01 | 2.8790096e+02 |
| 1.5000000e+01 | 0.0000000e+00 | 3.5323323e+00 | 3.9212541e+00 | 2.7745182e+02 | 1.4204563e+01 | 2.8204220e+02 |
| 2.0000000e+01 | 0.0000000e+00 | 2.4979324e+00 | 2.7615381e+00 | 2.7503474e+02 | 1.4797363e+01 | 2.7547303e+02 |
| 2.5000000e+01 | 0.0000000e+00 | 1.5926370e+00 | 1.7843443e+00 | 2.7333007e+02 | 1.5239593e+01 | 2.6841058e+02 |
| ... | ... | ... | ... | ... | ... | ... |

In this table we further define the following parameters:

- Position 1 on Line 1 shall indicate the measurement frequency.
- Position 2 on Line 1 shall indicate the frequency units to be MHz.
- Position 3 on Line 1 shall indicate the antenna index 1 or 2.
- Antenna index is defined as: antenna index 1 defined as left antenna (portrait front view, from RF enclosure side).
- Antenna index 2 defined as right antenna (portrait front view, from RF enclosure side).
- Position 4 on Line 1 shall be G.
- Position 5 on Line 1 shall be dBi.
- Positions 3, 4, and 6 on Line 2 shall describe the measured gain in dBi.

The file name format shall be defined as "(lab acronym)_(antenna serial number)_CTIA_MIMO 2x2_Band(B7, B13..Bxx)_(Good, Nominal, or Bad)_Ant(1 or 2).3daau".

Based on experiments taken with low (<1GHz) and high (>1.8GHz) frequency band antennas, the magnitude of the complex correlation coefficient generated from measured data remains unchanged from higher resolution antenna pattern measurements up to 15 degrees resolution in theta and phi orientations. To align with current COST IC1004 TWGO MIMO OTA topic group proposed resolution for 3D MIMO OTA complex radiation pattern measurements, the antenna pattern measurement step size in theta and phi shall be no more than 5 degrees. In the specific case of 2D measurements theta is fixed at 90 degrees.

9.3.1.3 Emulation of antenna pattern rotation

For the conducted portion of the absolute data throughput framework, it is necessary to generate the spatially filtered channel impulse response per polarization and then combine to generate the emulated channel impulse response coefficients. The measured antenna pattern shall be interpolated to match the spatial resolution of the angles of arrival of the SCME channel emulator (this value is typically 1 degrees). Figure 9.3.1.3-1 below illustrates an example of this procedure using a simplified antenna pattern and channel PAS.

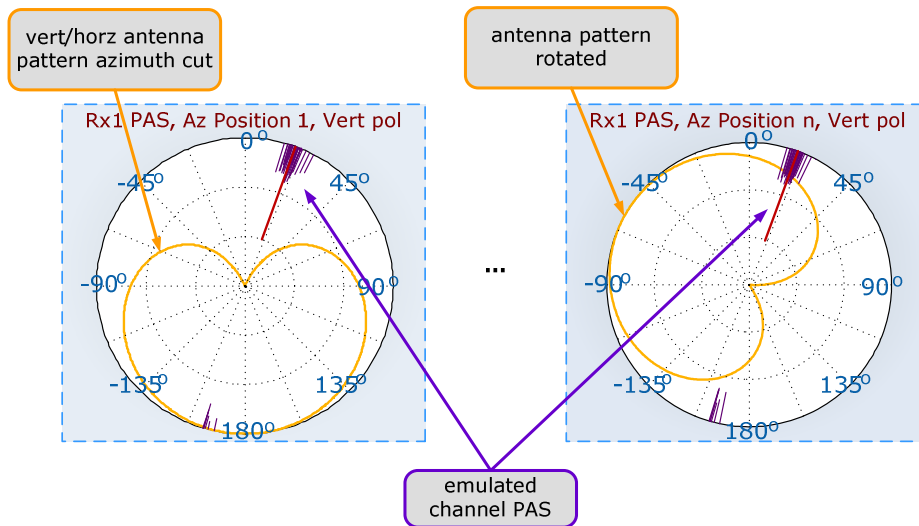


Figure 9.3.1.3-1: Rotation of antenna pattern over azimuth positions

In general, the emulation of antenna pattern rotation is specific to the channel model. For 2D channel models antenna pattern rotation shall be performed over 360 degrees in 30 degree steps (12 total positions). For other channel models this process is FFS.

A spatial filtering operation alone does not capture the behaviour of the 2D channel model as a function of DUT rotation. Figure 9.3.1.3-2 below illustrates the geometric parameters of the 2D channel model [15] for two DUT rotations.

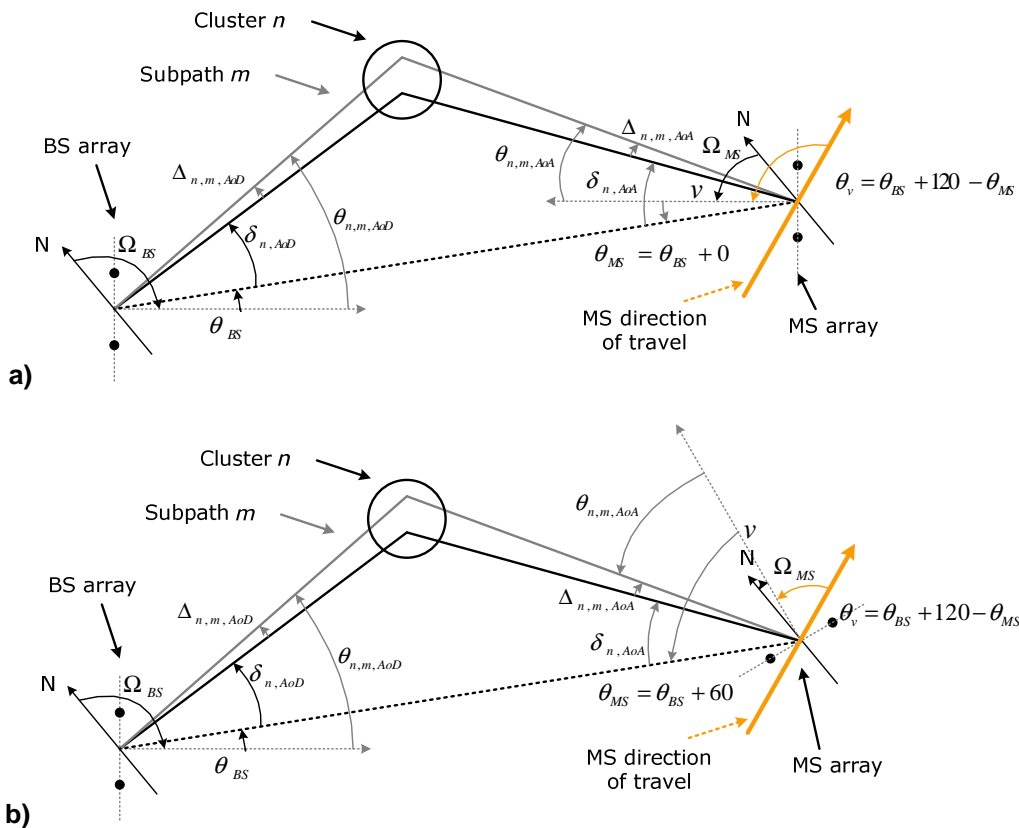


Figure 9.3.1.3-2: (a) 2D channel model geometric parameters for MS array direction = 0 degrees; (b) MS array direction = 60 degrees

For a given rotation of the DUT, the angle of the MS array relative to the cluster angles of arrival changes. Thus, MS array rotation together with the spatial filtering operations described above is necessary to emulate the conducted portion of the framework properly. Doppler spread, which is a function of the MS direction of travel relative to the channel model clusters' angles of arrival, shall remain the same for all rotations of the DUT.

Calculation of the required spatial filtering operations as a function of DUT orientation for channel emulators using a geometric implementation is self-evident from Figures 9.3.1.3-1 and 9.3.1.3-2. For channel emulators implementing the alternative correlation-based approach, the same spatial filtering operations are carried out by computing the correlation matrix and power imbalance for the specific channel model used and then applying the calculated correlation matrix and power in the channel emulation. The detail for how this is done is considered implementation specific and is not elaborated further here. It is noted that the correlation implementation results in a Doppler spectrum and corresponding temporal correlation that is independent of DUT orientation.

This process may be automated with channel emulator control software or performed manually. The output data format is described in clause 9.3.1.5.

9.3.1.4 Absolute Data Throughput measurement enabler

The fundamental enabler for the adoption of the Absolute Data Throughput metric is the ability to apply the complex radiation pattern to the channel for the conducted portion of the test. Such conducted measurements can be performed manually; however, without an application (SW) to rotate the loaded antenna complex radiation pattern, the measurement may become very time consuming and prone to human errors. Automation of this process is highly recommended.

9.3.1.5 Output data format

A unified data format for recording the conducted and radiated test results by each lab is defined in Tables 9.3.1.5-1 and 9.3.1.5-2 below.

Table 9.3.1.5-1: Conducted measurement data table format

| | | | | |
|---|--|-------------------------------|-------------|---------------|
| Absolute data throughput: conducted measurement data | | | | |
| ID | <measurement ID> | | | |
| Lab info | <lab name, location, chamber ID> | | | |
| Date | <YYYY-MM-DD> | | | |
| eNodeB emulator | <manufacturer name, model number, serial number> | | | |
| eNodeB emulator version | <hardware and firmware version numbers> | | | |
| eNodeB test application name and version | <test application name and version> | | | |
| eNodeB ant config | Clause 8.5 | | | |
| eNodeB PHY config | Clause 7.1 | | | |
| Band | <band num> | | | |
| DL channel | <channel num | | | |
| UL channel | <channel num | | | |
| RMC | <R.11 or R.35> | | | |
| Transmission Mode | <TM2 or TM3> | | | |
| Num subframes per SIR pt | | | | |
| Channel emulator | <manufacturer name, model number, serial number> | | | |
| Channel emulator version | <hardware and firmware version numbers> | | | |
| Channel model config | Clause 8.2 | | | |
| Channel model | <UMi, UMa, etc> | | | |
| Emulated vehicular speed | <speed in km/h> | | | |
| Reference antenna classification | <good, nominal, or bad> | | | |
| Ant1 pattern | <filename of reference antenna data as described in Clause 9.3.1.2> | | | |
| Ant2 pattern | <filename of reference antenna data as described in Clause 9.3.1.2> | | | |
| UE manufacturer | <manufacturer name> | | | |
| UE model | <model name> | | | |
| UE ID | <IMEI and possible additional unique ID number> | | | |
| Max theoretical throughput | <kbps> | | | |
| Num theta positions | Clause 9.3.1.3 | | | |
| Theta positions | Clause 9.3.1.3 | | | |
| Num phi positions | Clause 9.3.1.3 | | | |
| Phi positions | Clause 9.3.1.3 | | | |
| Test plan name and version | | | | |
| Comments | | | | |
| Test points per single position below | Skip if not applicable | | | |
| Theta (deg) | Phi (deg) | RS EPRE (dBm/15 kHz) | DL SIR (dB) | DL TPT (kbps) |
| 90 | 0 | r_max | s_max | TPT_max |
| ... | ... | ... | ... | ... |
| 90 | 0 | r_1 | s_1 | TPT_1 |
| 90 | 0 | r_2 | s_2 | TPT_2 |
| ... | ... | ... | ... | ... |
| 90 | 0 | r_min | s_min | TPT_min |
| 90 | 30 | r_max | s_max | TPT_max |
| ... | ... | ... | ... | ... |
| 90 | 30 | r_1 | s_1 | TPT_1 |
| 90 | 30 | r_2 | s_2 | TPT_2 |
| ... | ... | ... | ... | ... |
| 90 | 30 | r_min | s_min | TPT_min |
| Spatial average results below | | | | |
| RS EPRE (dBm/15 kHz) | DL SIR (dB) | AVG DL TPT (kbps) | Comments | |
| r_max | s_max | TPT_max | | |

| | | | | |
|-------|-------|---------|--|--|
| ... | ... | ... | | |
| r_1 | s_1 | TPT_1 | | |
| r_2 | s_2 | TPT_2 | | |
| ... | ... | ... | | |
| r_min | s_min | TPT_min | | |

Table 9.3.1.5-2: Radiated measurement data table format

| | | | | |
|---|---|-------------------------------|-------------|---------------|
| Absolute data throughput: radiated measurement data | | | | |
| ID | <measurement ID> | | | |
| Lab info | <lab name, location, chamber ID> | | | |
| Date | <YYYY-MM-DD> | | | |
| Test methodology | | | | |
| eNodeB emulator | <manufacturer name, model number, serial number> | | | |
| eNodeB emulator version | <hardware and firmware version numbers> | | | |
| eNodeB test application name and version | <test application name and version> | | | |
| eNodeB ant config | Clause 8.5 | | | |
| eNodeB PHY config | Clause 7.1 | | | |
| Band | <band num> | | | |
| DL channel | <channel num | | | |
| UL channel | <channel num | | | |
| RMC | <R.11 or R.35> | | | |
| Transmission Mode | <TM2 or TM3> | | | |
| Num subframes per SIR pt | | | | |
| Channel emulator | <manufacturer name, model number, serial number> | | | |
| Channel emulator version | <hardware and firmware version numbers> | | | |
| Channel model config | Clause 8.2 | | | |
| Channel model | <UMi, UMa, etc> | | | |
| Emulated vehicular speed | <speed in km/h> | | | |
| Reference antenna classification and serial number | <(good, nominal, or bad)_SN> | | | |
| Ant 1 | <Tx/Rx port of the UE> | | | |
| Ant 2 | <Rx port of the UE> | | | |
| UE manufacturer | <manufacturer name> | | | |
| UE model | <model name> | | | |
| UE ID | <IMEI and possible additional unique ID number> | | | |
| Max theoretical throughput | <kbps> | | | |
| Num theta positions | <if applicable> | | | |
| Theta positions | <if applicable> | | | |
| Num phi positions | <if applicable> | | | |
| Phi positions | <if applicable> | | | |
| Configuration of testing antennas in chamber | <detailed description> | | | |
| Test plan name and version | | | | |
| Comments | | | | |
| Test points per single position below | Skip if not applicable | | | |
| Theta (deg) | Phi (deg) | RS EPRE (dBm/15 kHz) | DL SIR (dB) | DL TPT (kbps) |
| 90 | 0 | r_max | s_max | TPT_max |
| ... | ... | ... | ... | ... |
| 90 | 0 | r_1 | s_1 | TPT_1 |
| 90 | 0 | r_2 | s_2 | TPT_2 |
| ... | ... | ... | ... | ... |
| 90 | 0 | r_min | s_min | TPT_min |
| 90 | 30 | r_max | s_max | TPT_max |
| ... | ... | ... | ... | ... |
| 90 | 30 | r_1 | s_1 | TPT_1 |
| 90 | 30 | r_2 | s_2 | TPT_2 |
| ... | ... | ... | ... | ... |
| 90 | 30 | r_min | s_min | TPT_min |
| Spatial average results below | | | | |

| RS EPRE (dBm/15 kHz) | DL SIR (dB) | AVG DL TPT (kbps) | Comments | |
|----------------------|--------------|-------------------|----------|--|
| r_max | s_max | TPT_max | | |
| ... | ... | ... | | |
| r_1 | s_1 | TPT_1 | | |
| r_2 | s_2 | TPT_2 | | |
| ... | ... | ... | | |
| r_min | s_min | TPT_min | | |

9.3.1.6 Application of the framework and scenarios for comparison

This framework is methodology agnostic, and shall be used to compare each MIMO OTA testing method's ability to emulate the specified network and channel propagation characteristics based on an absolute data throughput metric (Clause 5.1.1).

The purposes of this framework are:

- For the agreed Channel Models, currently SCME Umi and Uma, to understand and quantify what are the deviations (if any) introduced by the chamber used in radiated mode compared to the conducted mode (when reference antennas are embedded). This shall be applied inter labs for the same method and inter methods.
- For methods that are able to reproduce channel models that are not agreed in the present document, it can be used to define the channel model details that need to be injected in the conducted test to obtain same results in the radiated part. And therefore it is easier to reproduce those conditions across methods.

The above use cases for the framework are required to be conducted for inter methodology comparison. Other applications for the framework are optional and not excluded.

And more concretely, the following scenarios for comparison are defined:

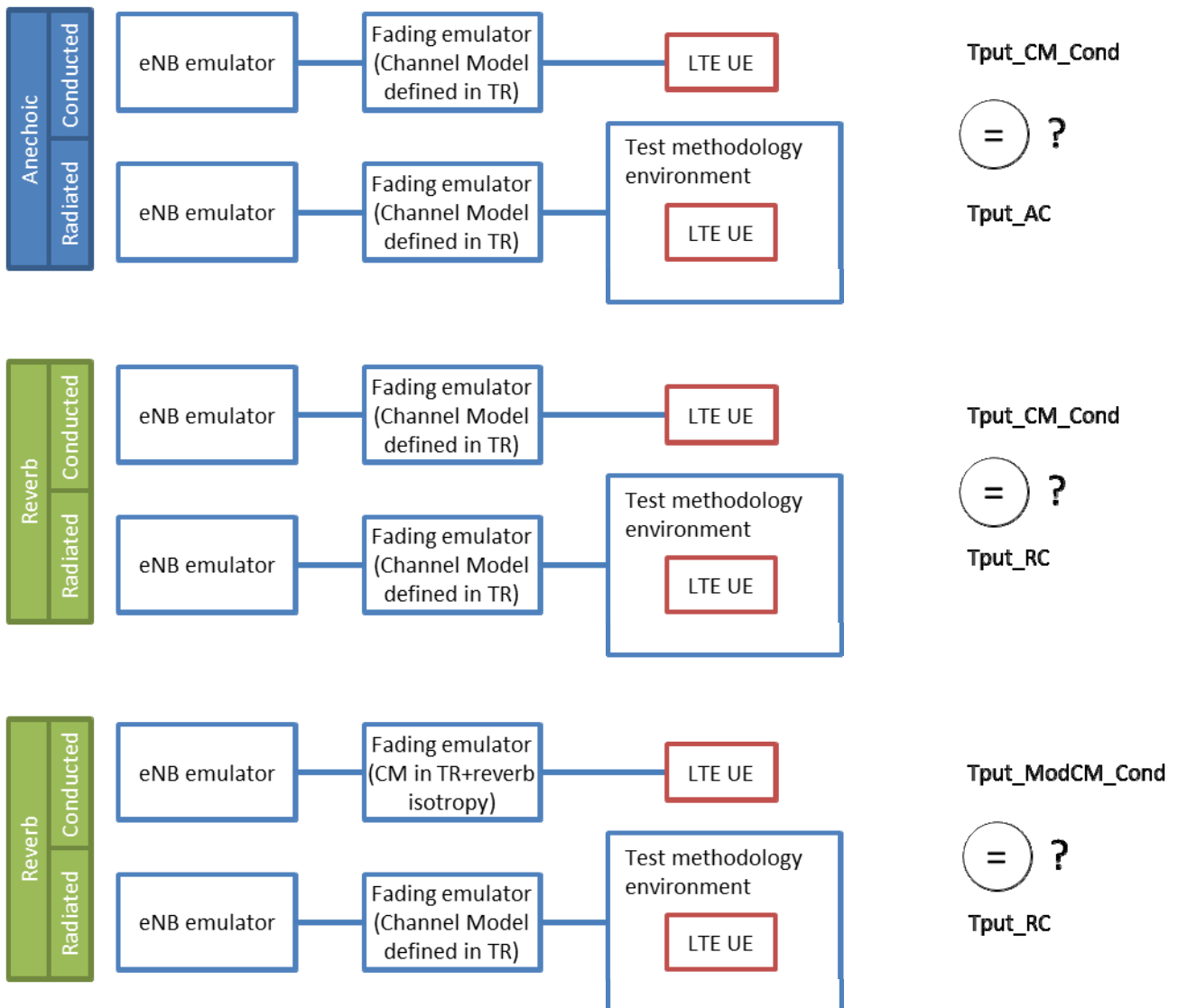


Figure 9.3.1.6-1: Application of the framework and scenarios for comparison

These scenarios are intended to address the following aspects:

1. **The first scenario**, anechoic based: intended to compare the conducted portion of the test (with embedded radiation pattern antennas) with the same results of the radiated test. Throughputs are compared to understand any artifacts introduced by the setup.
2. **The second scenario**, reverberation based: intended to compare the conducted portion of the test (with embedded radiation pattern antennas) with the same results of the radiated test. Throughputs are compared to understand any artifacts introduced by the setup.
3. **The third scenario**, reverberation based: intended to compare the conducted portion of the test (with embedded radiation pattern antennas) and with 3D isotropic channel model with the same results of the radiated test. Throughputs are compared to understand any artifacts introduced by the setup. Additionally this scenario will help to define the 3D isotropic properties of the channel model as perceived by the UE in the reverb chamber, and compare its realization in the conducted portion.

NOTE: If scenario2 holds true, it would mean that for the agreed setup anechoic method and reverberation method provides comparable results for the agreed channel models in the present document, currently 2D SCME.

9.3.1.7 Proof of concept

9.3.1.7.1 The first scenario, anechoic based

The implementation of the Absolute Data Throughput Framework based in the first scenario; i.e. anechoic chamber ring of probes; is defined in Clause 9.3.1.6 and table 9.3.1.7.1-1.

Figure 9.3.1.7.1-2 indicates variation equal or less than 0.5dB when comparing OTA measurements with correspondent conducted measurements, therefore validating the framework concept.

Table 9.3.1.7.1-1: Absolute Data Throughput proof of concept measurement setup

| Anechoic based measurement setup | Conducted | Radiated |
|----------------------------------|------------------------|------------------------|
| Lab | Conducted lab "A" | Radiated "B" |
| Methodology | Conducted | Radiated |
| eNodeB emul. | model "A" | model "A" |
| eNodeB ant config | Clause 7.2 | Clause 7.2 |
| eNodeB PHY config | Clause 7.1 | Clause 7.1 |
| Band | 13 | 13 |
| DL channel | 5230 | 5230 |
| UL channel | 23230 | 23230 |
| RMC | R11 | R11 |
| Num subframes per SNR pt | 20000 | 20000 |
| Channel emul. | model "B1" | model "B2" |
| Channel model config | Clause 8.2 | Clause 8.2 |
| Channel model | SCME Umi, SCME Uma | SCME Umi, SCME Uma |
| Emul. veh. speed | 30 km/h | 30 km/h |
| UE mfg | Commercially available | Commercially available |
| Transmission Mode | TM3 | TM3 |

Band 13, SCME Umi & SCME Uma, 16 QAM, abs TP Framework

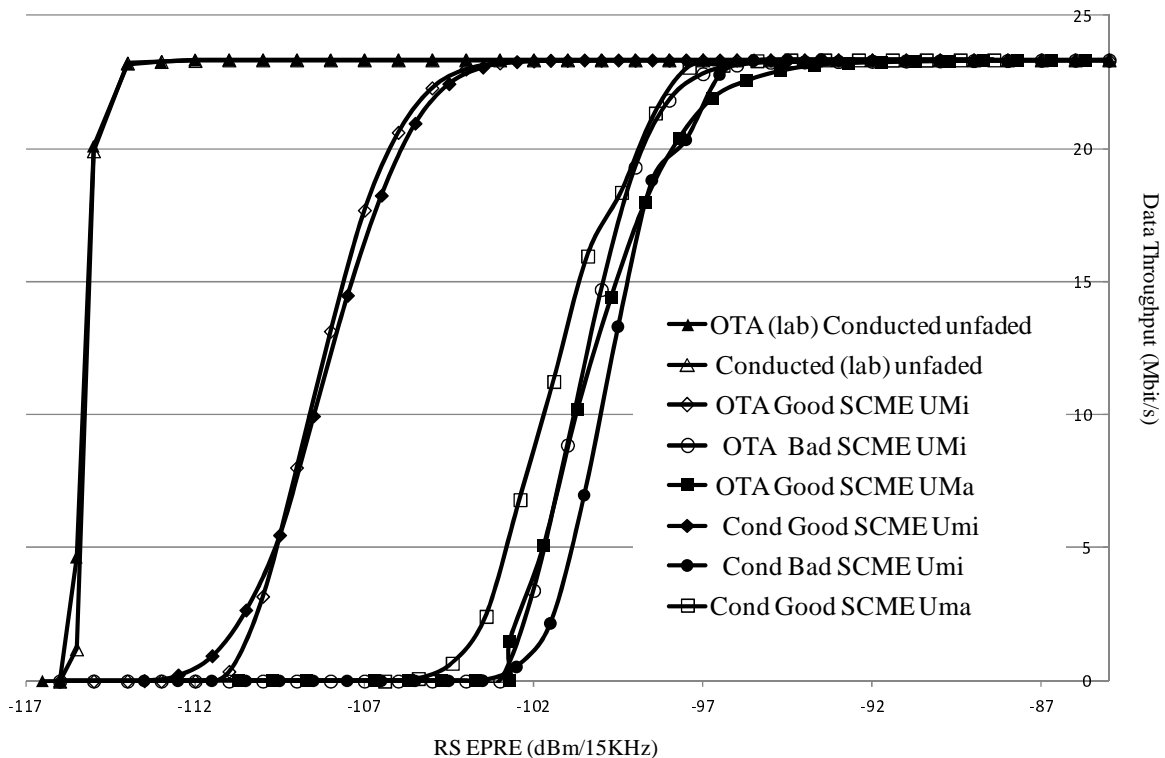


Figure 9.3.1.7.1-1: First Scenario (anechoic based) proof of concept, measurement results

The implementation of the Absolute Data Throughput Framework based on the anechoic RTS method is defined in clause 9.3.1.6 and Table 9.3.1.7.1-2.

Figure 9.3.1.7.1-2 indicates variation equal or less than 0.5dB when comparing OTA measurements with correspondent conducted measurements, therefore validating the framework concept. These results were generated using the correlation-based channel model implementation.

Table 9.3.1.7.1-2: Absolute Data Throughput proof of concept measurement setup

| RTS measurement setup | Conducted | Radiated |
|--------------------------|--------------------|--------------------|
| Lab | Conducted lab "A" | Radiated lab "B" |
| Methodology | Conducted | Radiated |
| eNodeB emul. | Agilent PXT | Agilent PXT |
| eNodeB ant config | Clause 7.2 | Clause 7.2 |
| eNodeB PHY config | Clause 7.1 | Clause 7.1 |
| Band | 13 | 13 |
| DL channel | 5230 | 5230 |
| UL channel | 23230 | 23230 |
| RMC | R11 | R11 |
| Num subframes per SNR pt | 20000 | 20000 |
| Channel emul. | Agilent PXB | Agilent PXB |
| Channel model config | Clause 8.2 | Clause 8.2 |
| Channel model | SCME Umi, SCME UMa | SCME Umi, SCME UMa |
| Emul. veh. speed | 30 km/h | 30 km/h |
| UE mfg | HTC ADR6425LVW | HTC ADR6425LVW |
| Transmission Mode | TM3 | TM3 |

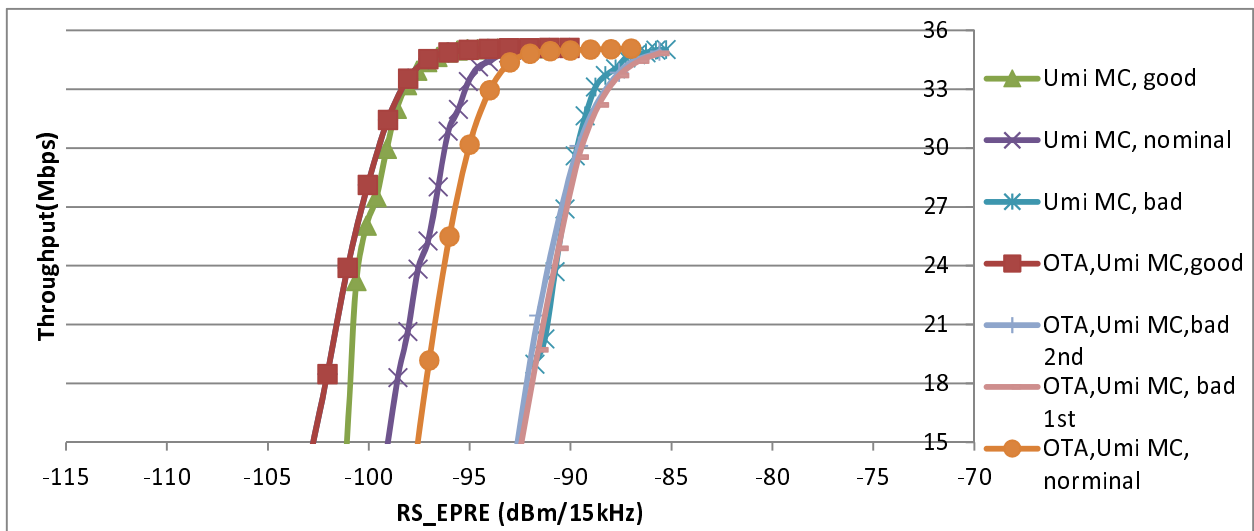


Figure 9.3.1.7.1-3: Radiated vs Cable-conducted Absolute Throughput Test for Umi MC Model using correlation-based channel model

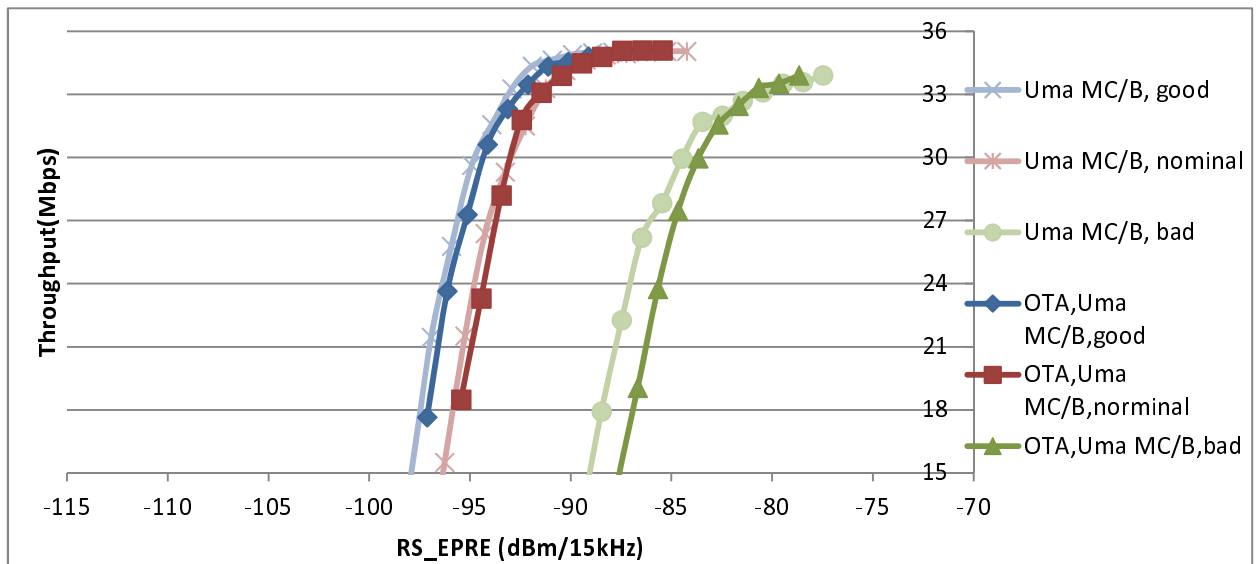


Figure 9.3.1.7.1-4: Radiated vs Cable-conducted Absolute Throughput Test for Uma MC Model using correlation-based channel model

9.3.1.7.2 The second scenario, reverberation chamber based

Figure 9.3.1.7.2-1 shows results from measurements using the absolute data throughput comparison framework for the reverberation chamber methodology, implementing the isotropic channel model based on NIST. The conducted and radiated results align within +/- 0.5 dB (comparing the 70 % throughput level), therefore validating the framework concept.

Details about the measurement setup are given in Table 9.3.1.7.2-1.

Table 9.3.1.7.2-1: Measurement setup for the reverberation chamber methodology

| Reverberation chamber based measurement setup | Conducted | Radiated |
|---|------------------------|------------------------|
| Lab | A | A |
| Methodology | Conducted | Radiated |
| eNodeB emul. | model "A.1" | model "A.1" |
| eNodeB ant config | Uncorrelated | Uncorrelated |
| eNodeB PHY config | Clause 7.1 | Clause 7.1 |
| Band | 13 | 13 |
| DL channel | 5230 | 5230 |
| UL channel | 23230 | 23230 |
| RMC | R35 | R,35 |
| Num subframes per power level | 96000 | 96000 |
| Channel emul. | model "A.2" | N/A |
| Channel model config | Annex C.2 | Annex C.2 |
| Channel model | Isotropic NIST | Isotropic NIST |
| Emul. veh. speed | 1 km/h | N/A |
| UE mfg | Commercially available | Commercially available |
| Transmission Mode | TM3 | TM3 |

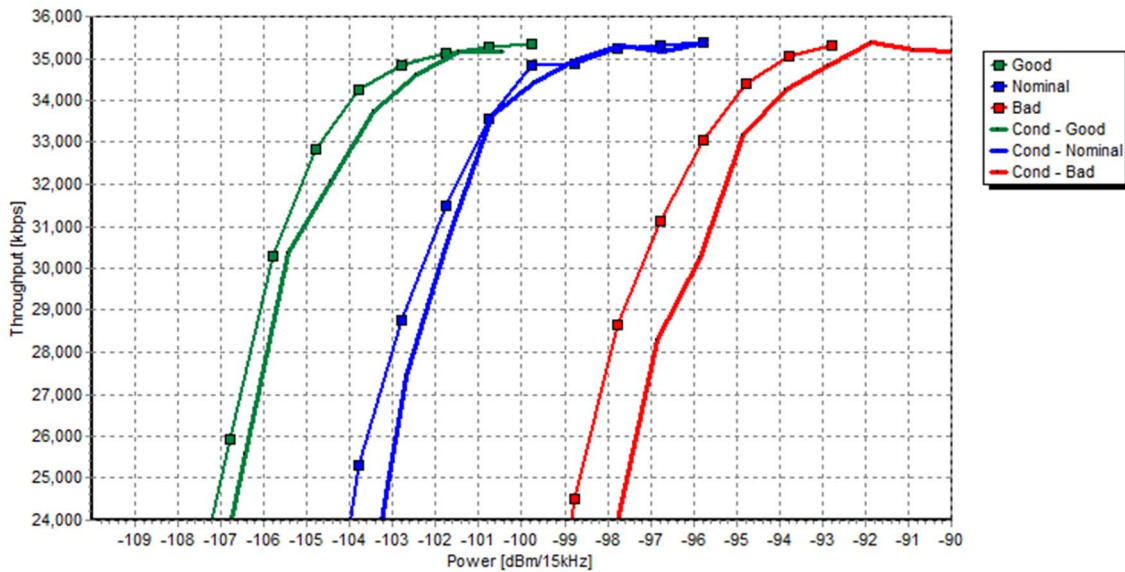


Figure 9.3.1.7.2-1: Proof of concept for the reverberation chamber methodology, implementing the isotropic channel model based on NIST

9.3.1.7.3 The third scenario, reverberation chamber and channel emulator based

Figure 9.3.1.7.3-1 and Figure 9.3.1.7.3-2 show results from measurements using the absolute data throughput comparison framework for the reverberation chamber and channel emulator methodology, implementing the short delay spread low correlation and the long delay spread high correlation channel model. The conducted and radiated results align within +/- 1 dB (comparing the 70 % throughput level), therefore validating the framework concept.

Details about the measurement setups are given in Table 9.3.1.7.3-1 and Table 9.3.1.7.3-2.

Table 9.3.1.7.3-1: Measurement setup for the reverberation chamber and channel emulator methodology

| Reverberation chamber based measurement setup | Conducted | Radiated |
|---|--|--|
| Lab | A | A |
| Methodology | Conducted | Radiated |
| eNodeB emul. | model A.1 | model A.1 |
| eNodeB ant config | Clause 8.5 | Clause 8.5 |
| eNodeB PHY config | Clause 7.1 | Clause 7.1 |
| Band | 13 | 13 |
| DL channel | 5230 | 5230 |
| UL channel | 23230 | 23230 |
| RMC | R35 | R,35 |
| Num subframes per power level | 96000 | 96000 |
| Channel emul. | model A.2 | model A.2 |
| Channel model config | Annex C.2 | Annex C.2 |
| Channel model | Isotropic short delay spread low correlation | Isotropic short delay spread low correlation |
| Emul. veh. speed | 30 km/h | 30 km/h |
| UE mfg | Commercially available | Commercially available |
| Transmission Mode | TM3 | TM3 |

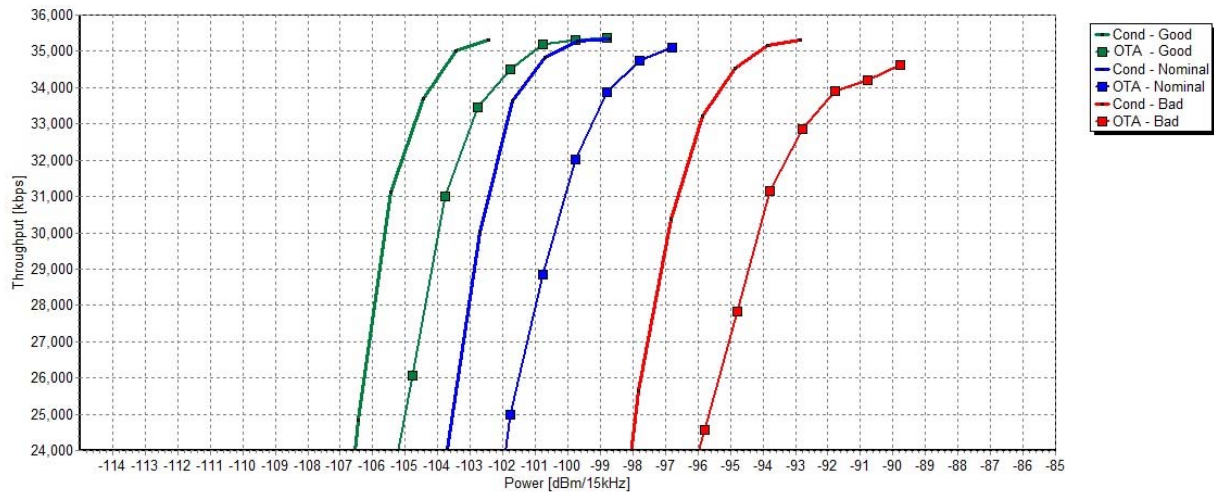


Figure 9.3.1.7.3-1: Proof of concept for the reverberation chamber and channel emulator methodology emulating the short delay spread low correlation channel model

Table 9.3.1.7.3-2: Measurement setup for the reverberation chamber and channel emulator methodology

| Reverberation chamber based measurement setup | Conducted | Radiated |
|---|--|--|
| Lab | A | A |
| Methodology | Conducted | Radiated |
| eNodeB emul. | model A.3 | model A.3 |
| eNodeB ant config | Clause 8.5 | Clause 8.5 |
| eNodeB PHY config | Clause 7.1 | Clause 7.1 |
| Band | 13 | 13 |
| DL channel | 5230 | 5230 |
| UL channel | 23230 | 23230 |
| RMC | R35 | R,35 |
| Num subframes per power level | 96000 | 96000 |
| Channel emul. | model A.4 | model A.4 |
| Channel model config | Annex C.2 | Annex C.2 |
| Channel model | Isotropic long delay spread high correlation | Isotropic long delay spread high correlation |
| Emul. veh. speed | 30 km/h | 30 km/h |
| UE mfg | Commercially available | Commercially available |
| Transmission Mode | TM3 | TM3 |

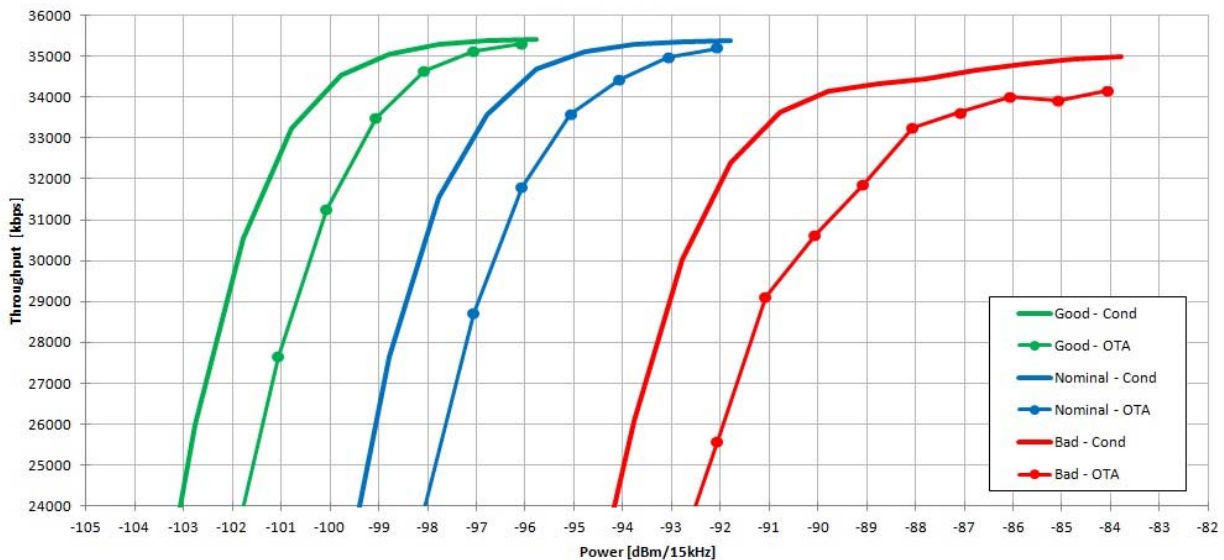


Figure 9.3.1.7.3-2: Proof of concept for the reverberation chamber and channel emulator methodology emulating the long delay spread high correlation channel model

9.4 Device positioning

9.4.1 Handheld UE – Browsing mode

Handheld UE is a device which is primarily used in a handgrip like normal mobile/smart phones when they are used for browsing.

Browsing mode testing method is used for MIMO OTA performance measurements in case of handheld types of UE form factors as defined in 3GPP TR 25.914 [11] subclause 5.1.7.

9.4.1.1 MPAC Positioning Guidelines

The MPAC positioning guidelines of the handheld UE in browsing mode in the MPAC system shall follow the requirements in Annex E.2.1.

9.4.2 Handheld UE – Speech mode

Handheld UE which supports VoLTE is primarily used in speech mode when doing a voice call.

Speech mode is simulation of a voice call user case. DUT is placed in to a hand phantom which is holding the DUT against SAM head phantom. Speech mode testing is used for MIMO OTA performance measurements as defined in 3GPP TR 25.914 [11] subclause 5.1.6.

9.4.2.1 MPAC Positioning Guidelines

The MPAC positioning guidelines of the handheld UE in speech mode in the MPAC system shall follow the requirements in Annex E.2.1.

9.4.3 Laptop Mounted Equipment (LME)

Laptop Mounted Equipment (LME) type UE is a plug-in device that hosts on the laptop (like USB dongles).

A laptop ground plane phantom is used for radiated MIMO OTA performance measurements in case of LME plug-in DUT as defined in TR 25.914 [11] subclauses 5.1.3 and 5.1.4.

9.4.3.1 MPAC Positioning Guidelines

The MPAC positioning guidelines of an LME DUT in the MPAC system shall follow the requirements in Annex E.2.1.

9.4.4 Laptop Embedded Equipment (LEE)

Laptop Embedded Equipment (LEE) are notebook PC's or tablets.

A notebook PC is a portable personal computer combining the computer, keyboard and display in one form factor. Typically the keyboard is built into the base and the display is hinged along the back edge of the base. The largest single dimension for a notebook is limited to 0.42 m.

As notebooks are not body worn equipment nor recommended for use placed directly on the lap, the notebook shall be tested in a free space configuration without head and hand phantoms.

LEE Notebook PC's shall be tested in free space configuration as defined in TR 25.914 [11] subclause 5.3.1.

Tablet positioning is FFS.

9.4.4.1 MPAC Positioning Guidelines

The MPAC positioning guidelines of an LEE DUT in the MPAC system shall follow the requirements in Annex E.2.1.

10 Measurement results from testing campaigns

10.1 Introduction

Subclause 10.2 contains measurement results that are considered valid for the devices with reference antennas, and test conditions used. These results represent the ability of the methodologies described hereafter to distinguish good from bad devices in terms of their MIMO OTA performance under the conditions described in clause 10.2.1.

10.2 CTIA test campaign

10.2.1 Description of the test plan

This clause summarizes the test environment used within CTIA during execution of the "Phase 2" Inter Laboratory and Inter-Technique (IL/IT) comparison activity. The settings utilized during execution of this test activity have been summarized here according to the applicable clauses, tables and annexes of the present document.

Table 10.2.1-1: Summary of settings used in the test plan for IL/IT testing campaign

| | Settings used in test plan | Observations |
|---|--|--|
| eNodeB | Table 7.1-1 | Initial Downlink RS-EPRE of -85 dBm/15 kHz |
| Channel Models | Clause 8 and Annex C | Additional channel models were also included in the CTIA Phase 2 test campaign |
| Channel Model emulation of the Base Station antenna pattern configuration | Clause 8.5 | None |
| Frequency bands | Band 7 and 13 | Band 13 mandatory Band 7 recommended |
| SIR | Not used | None |
| Transmission Mode | TM3 according to Table 7.1-1 | None |
| Devices | Clause 9.2 | None |
| Reference antennas | Clause 9.1 | None |
| Measurements performed | Absolute throughput performance in conducted and radiated modes Channel model verification (Clause 8 and Annex C) Absolute data throughput verification (Clause 9.3.1) | None |

10.2.2 Anechoic chamber method with multiprobe configuration

Inter-Lab/Inter-Technique (IL/IT) campaigns have been performed in CTIA MOSG LTE MIMO OTA by the Anechoic Chamber test methodology. The results are produced here in Figures 10.2.2-1 to 10.2.2-9.

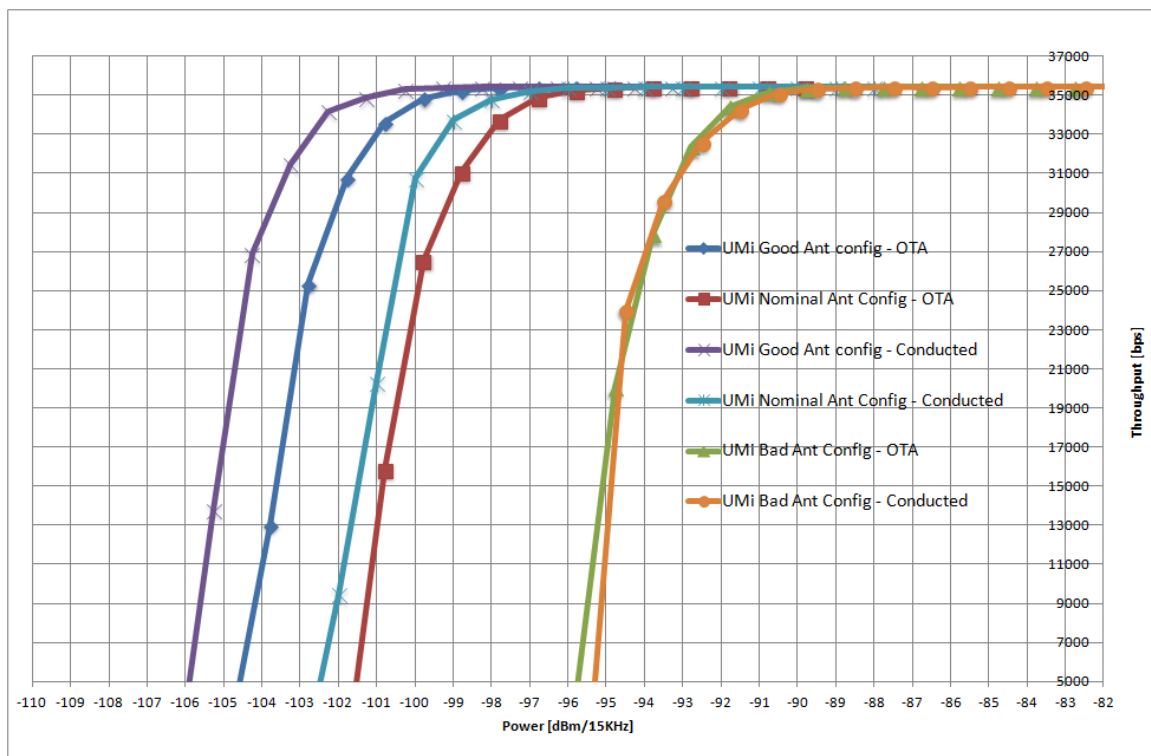


Figure 10.2.2-1: Absolute data throughput framework results for the SCME UMi Channel model for SATIMO

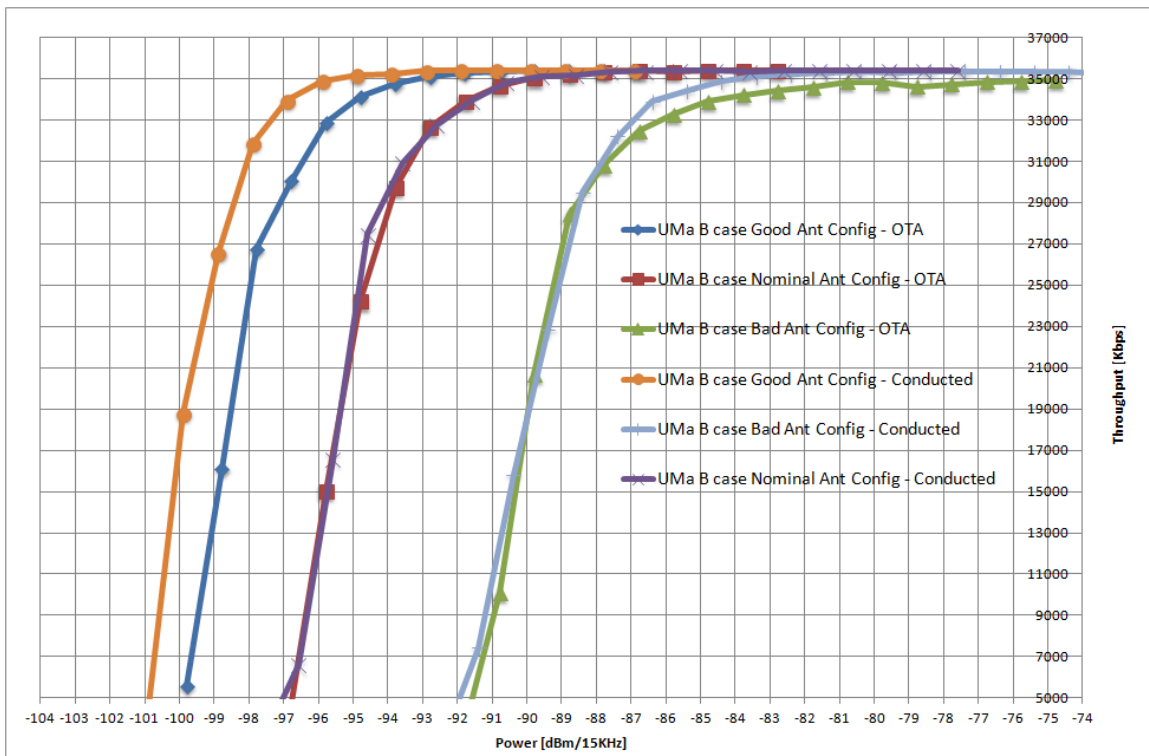


Figure 10.2.2-2: Absolute data throughput framework results for the SCME UMa-B Channel model for SATIMO

Further, from Figure 10.2.2-2, it can be noted that the max deviation between the absolute data throughput and OTA measurements is around 1.5dB at 70% throughput. This can be observed for the Good antenna system and SCME UMi case with the absolute data throughput outperforming the OTA measurements. There is also a deviation of around 1dB for the following case - SCME UMi with Nominal antenna and SCME UMa B case with Good antenna. Very little deviation is noted for the Bad antenna and both SCME UMi, and UMa B case.

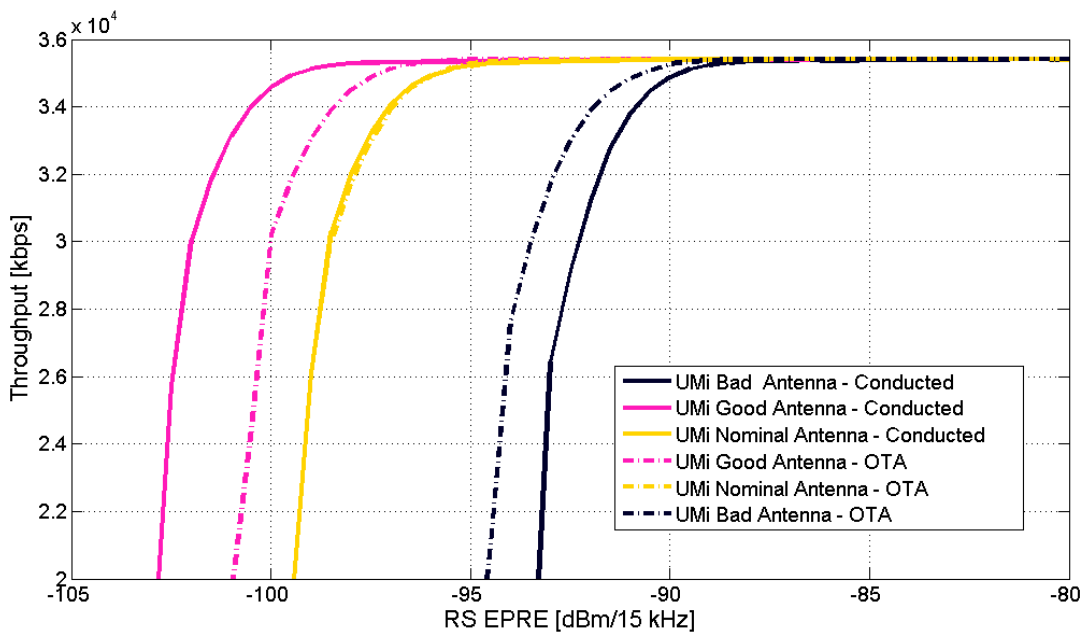


Figure 10.2.2-3 Absolute data throughput framework results for the SCME UMi Channel model for Intel

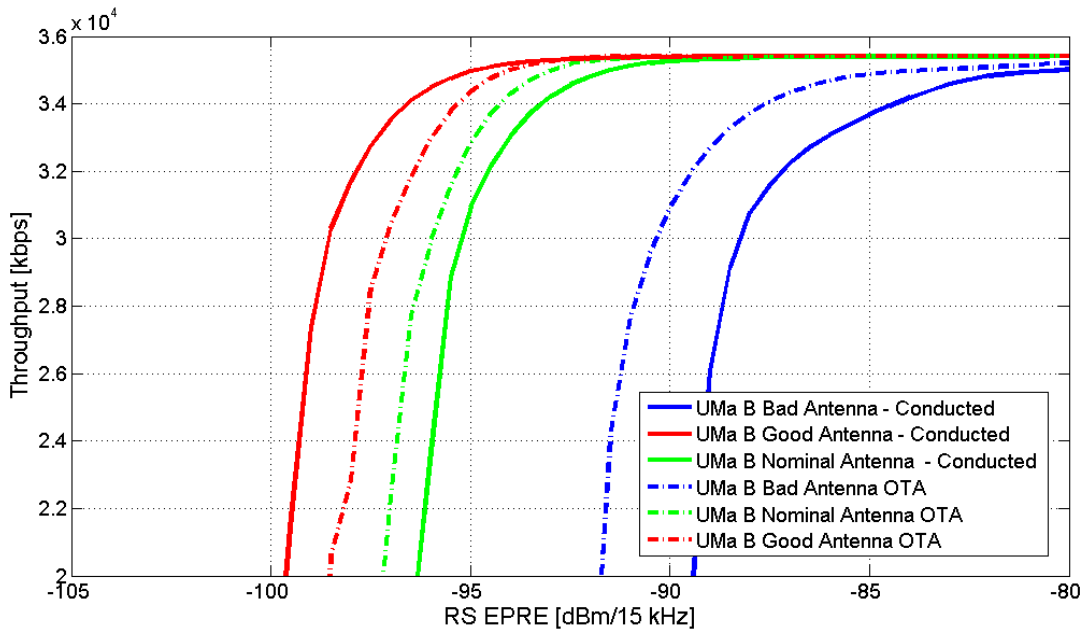


Figure 10.2.2-4 Absolute data throughput framework results for the SCME UMa B Channel model for Intel

Figure 10.2.2-3 and Figure 10.2.2-4 show a results agreement within the specified margins.

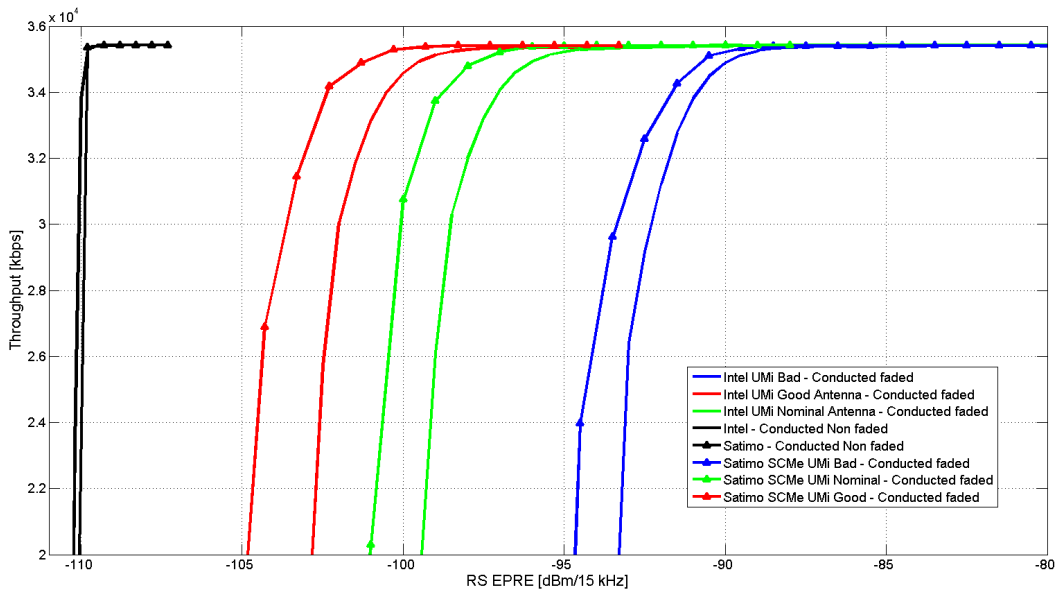


Figure 10.2.2-5: Comparison between the conductive measurements between Intel and SATIMO for the SCME UMi channel model

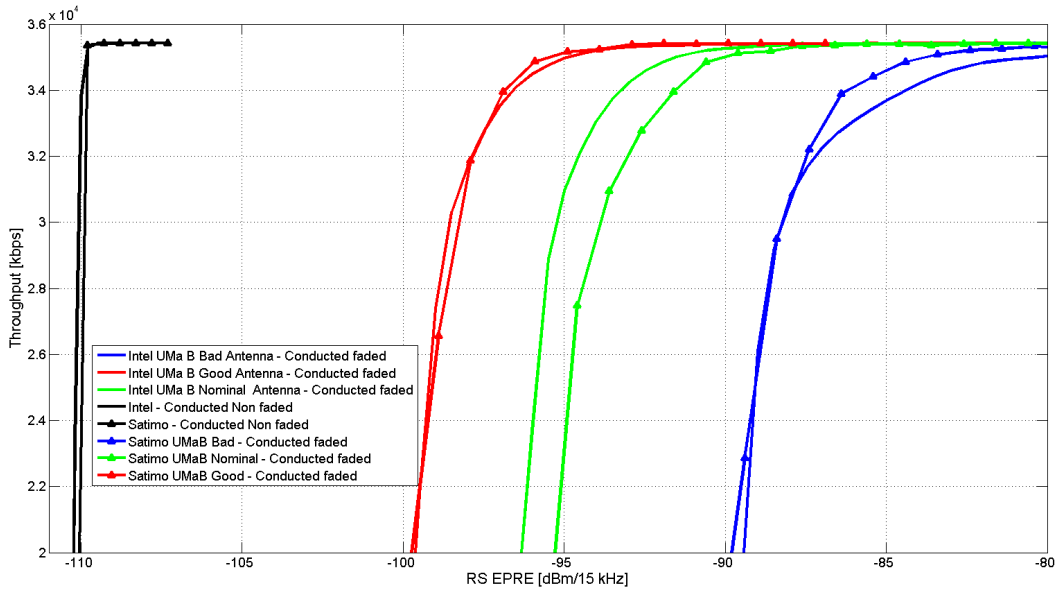


Figure 10.2.2-6: Comparison between the conductive measurements between Intel and SATIMO for the SCME UMaB channel model

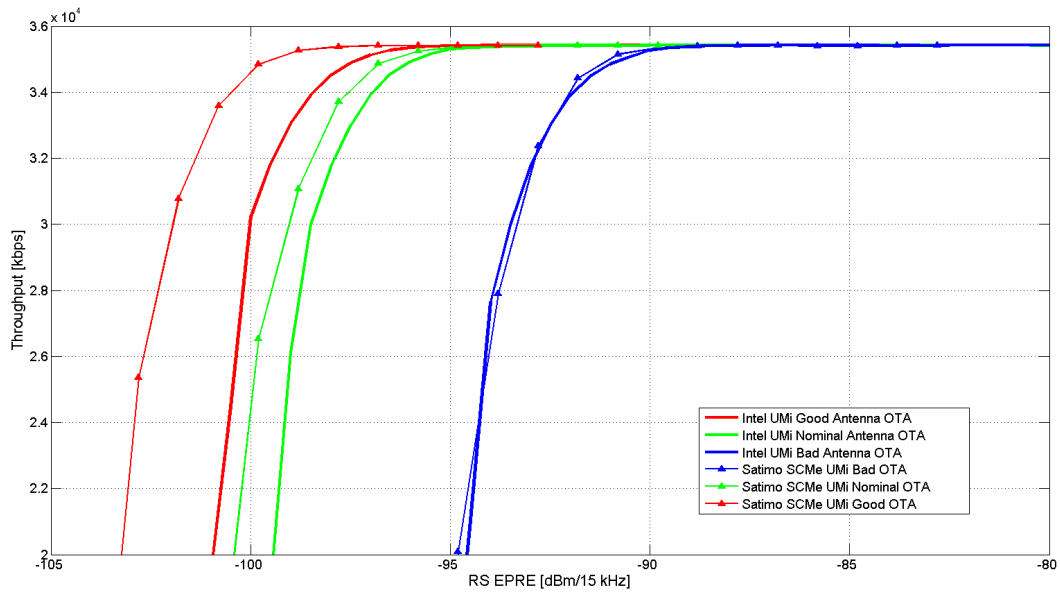


Figure 10.2.2-7: Average radiated throughput comparison under SCMe UMi OTA for Intel and SATIMO

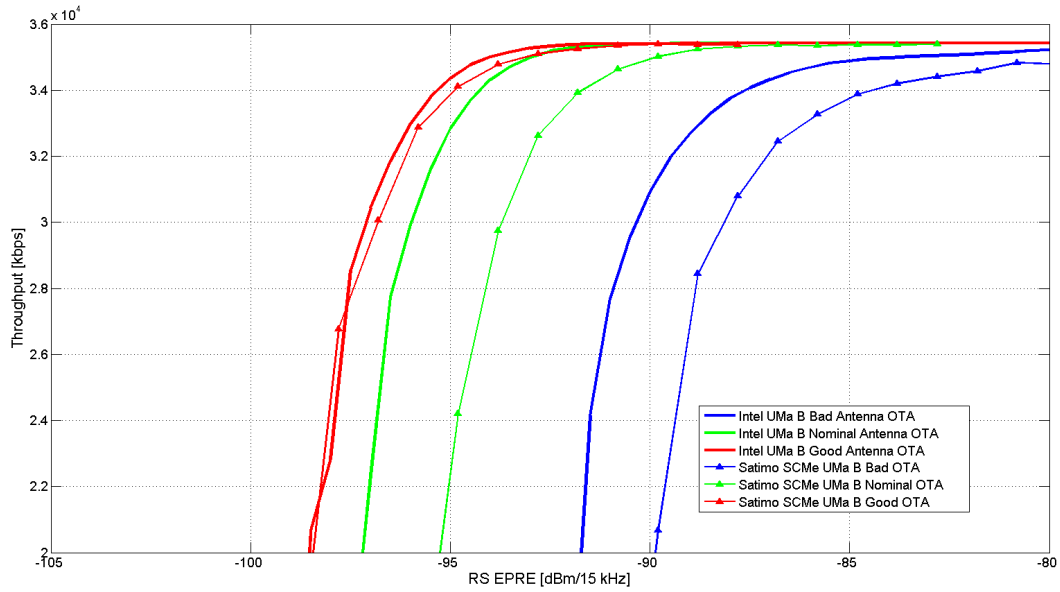


Figure 10.2.2-8: Average radiated throughput comparison under SCMe UMa-B OTA for Intel and SATIMO

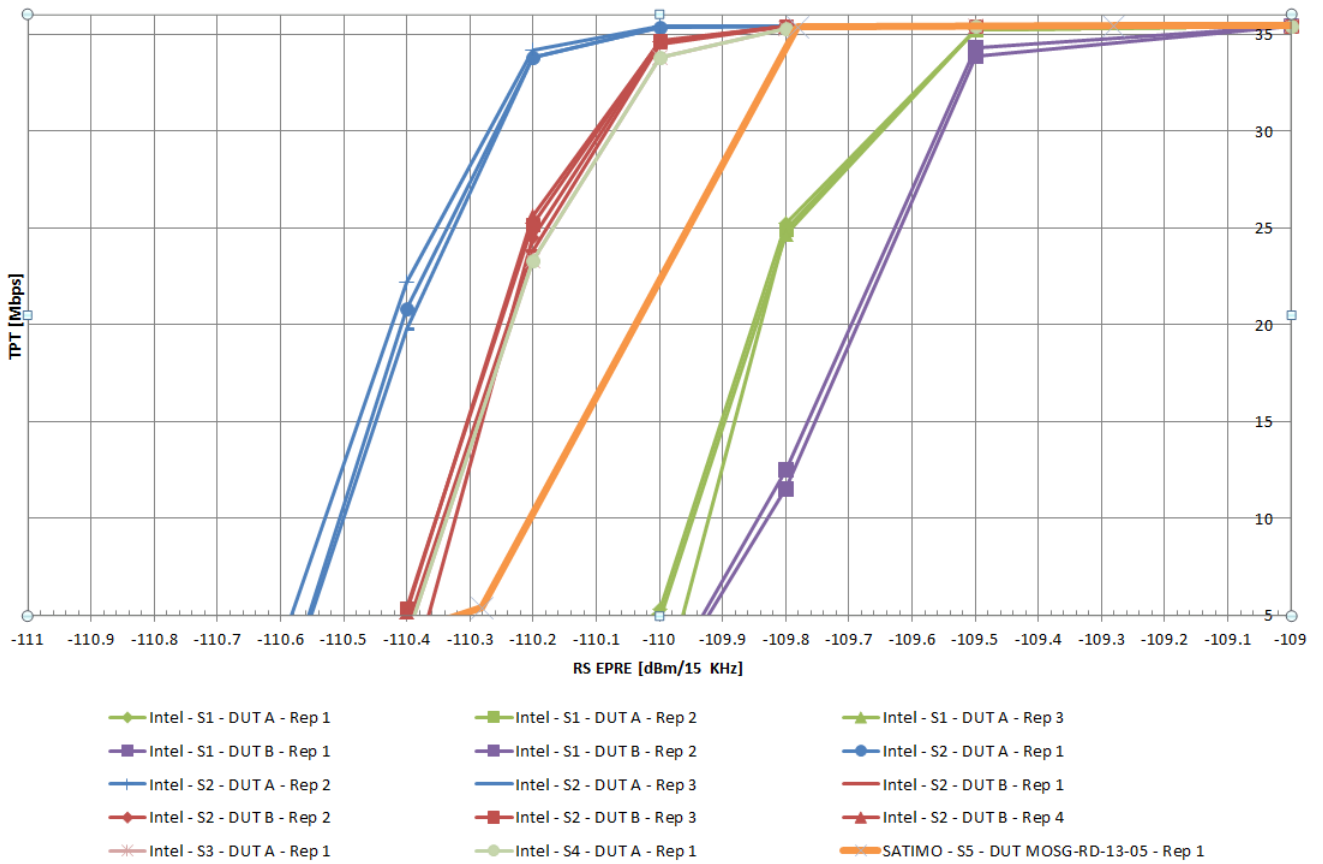


Figure 10.2.2-9: Conducted non-faded measurements comparison between Intel and SATIMO

The legend in the Figure 10.2.2-9 should be read as indicated in Table 10.2.2-1.

Table 10.2.2-1: Explanation of the legend for Figure 10.2.2-9

| DUT/Setups | Category | Lab | Comment |
|---------------|----------|-----------------|---|
| S1 – 4 S5 | Setup | Intel SATIMO | Different base station emulators and cable calibrations |
| DUT A/B | Phone | Intel | Details below |
| MOSG-RD-13-05 | Phone | SATIMO | Details below |

The references for the different phones are provided in Table 10.2.2-2.

Table 10.2.2-2: Explanation of the legend for Figure 10.2.2-9

| Device ID | DUT A | DUT B | MOSG-RD-13-05 |
|------------------|-----------------------------|-----------------------------|---------------|
| Manufacturer | HTC | HTC | HTC |
| Model | Rezound | Rezound | Rezound |
| Operating system | Android 4.0.3 | Android 4.0.3 | Android |
| Software number | 4.03.605.2 710RD | 4.03.605.2 710RD | NA |
| Baseband version | 2.22.10.0801r,2.22.10.0803r | 2.22.10.0801r,2.22.10.0803r | NA |
| Serial Number | HT1APS201087 | HT1APS201196 | HT18KS200216 |
| IMEI | 990000338088158 | 990000338089248 | NA |
| HTC version | Sense 3.6 | Sense 3.6 | NA |
| PRI Version | 1.16_002-3.01_002 | 1.16_002-3.01_002 | NA |
| PRL Version | 00000 | 00666 | NA |
| ERI Version | 5 | 5 | NA |
| Kernel | 3.0.16-g480e1b0 | 3.0.16-g480e1b0 | NA |
| Lab | Intel | Intel | SATIMO |

And finally Rep. in the legend stands for repetition number.

10.2.3 Reverberation chamber method using NIST channel model and using channel emulator with short delay spread low correlation channel model

The IL/IT test results from CTIA MOSG LTE MIMO OTA Round Robin campaign for the reverberation chamber candidate methodology 1 (RC) using the NIST model are reproduced in figures 10.2.3-1 to 10.2.3-4. A maximum standard deviation uncertainty value for inter-chamber comparison of NIST of 0.7 dB STD has been found, showing that IL/IT consistency has been achieved using the reverberation chamber methodology 1 (RC).

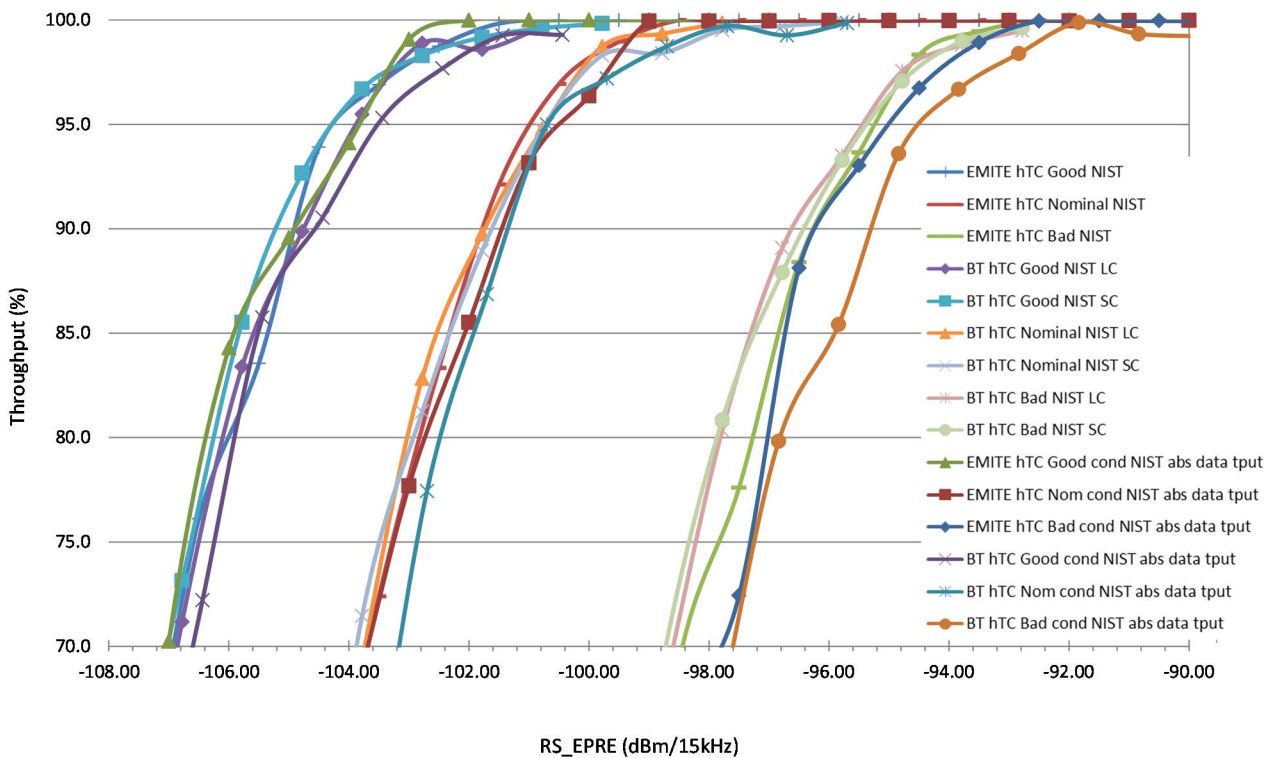


Figure 10.2.3-1: IL/IT results consistency for Reverberation Chamber candidate methodology 1 (RC) measurements implementing the NIST channel model (all reference antennas)

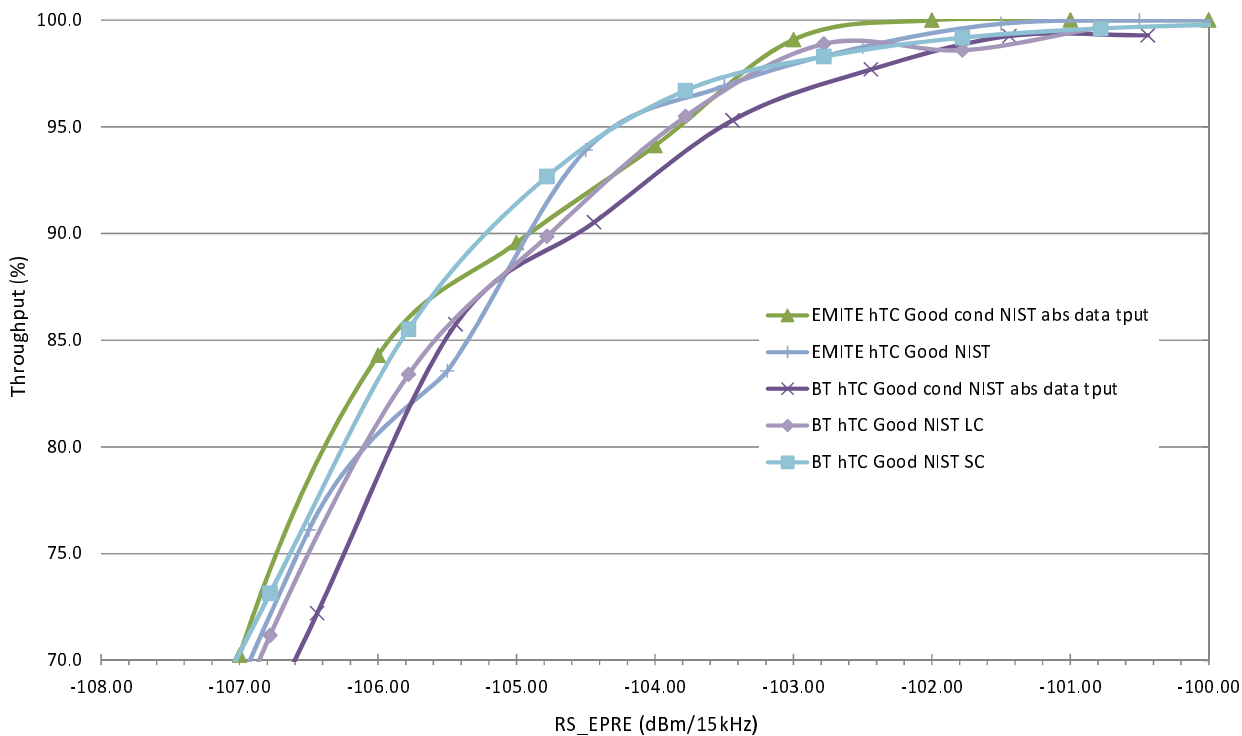


Figure 10.2.3-2: IL/IT results consistency for Reverberation Chamber candidate methodology 1 (RC) measurements implementing the NIST channel model with the Good reference antennas

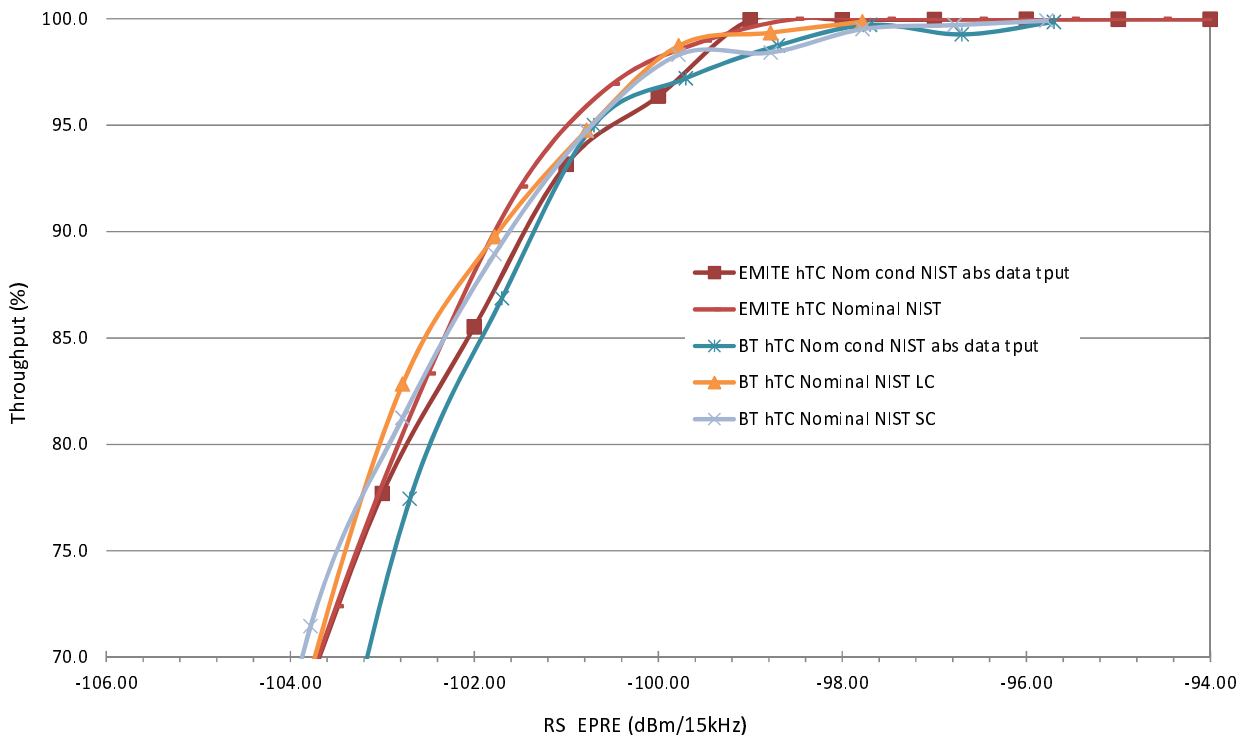


Figure 10.2.3-3: IL/IT results consistency for Reverberation Chamber candidate methodology 1 (RC) measurements implementing the NIST channel model with the Nominal reference antennas

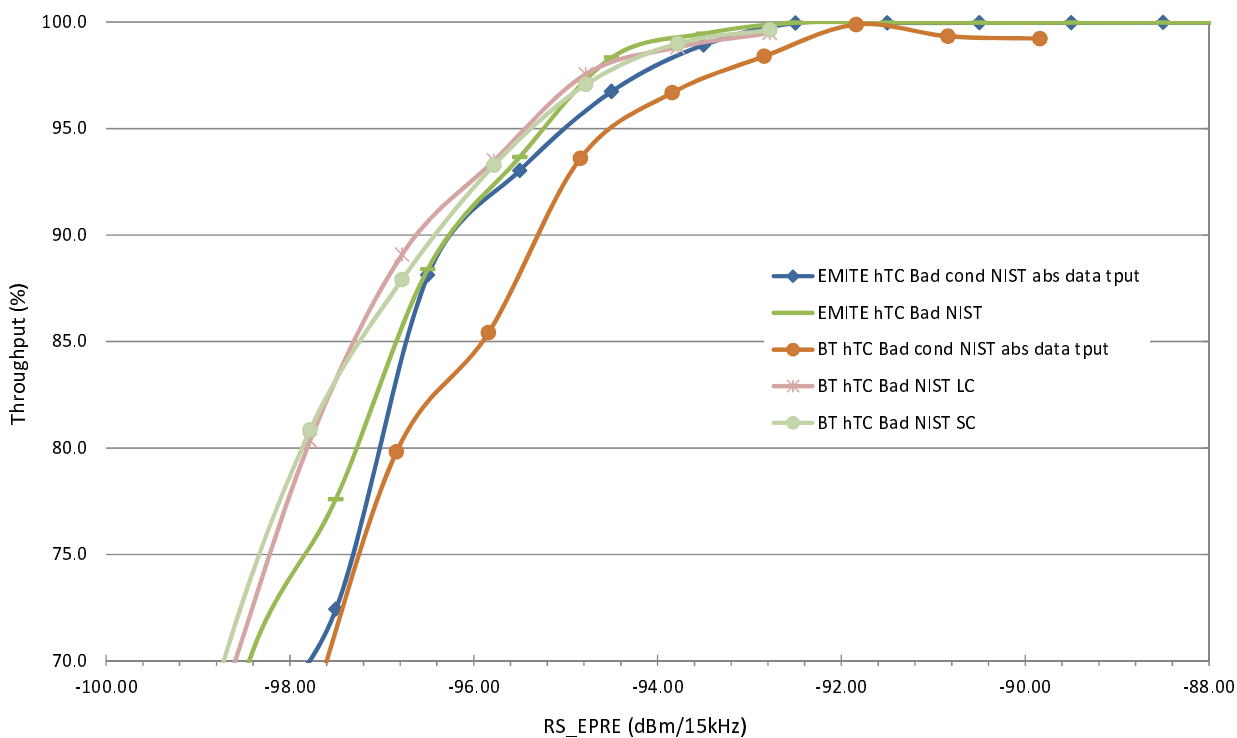


Figure 10.2.3-4: IL/IT results consistency for Reverberation Chamber candidate methodology 1 (RC) measurements implementing the NIST channel model with the Bad reference antennas

The IL/IT test results from CTIA MOSG LTE MIMO OTA Round Robin campaign for the reverberation chamber candidate methodology 2 (RC+CE) using the Short Delay Spread Low Correlation model are reproduced in Figures

10.2.3-5 to 10.2.3-8. A maximum standard deviation uncertainty value for inter-chamber comparison of Short Delay Spread Low Correlation of 1.7 dB STD has been found, showing that IL/IT consistency has been achieved using the reverberation chamber methodology 2 (RC+CE).

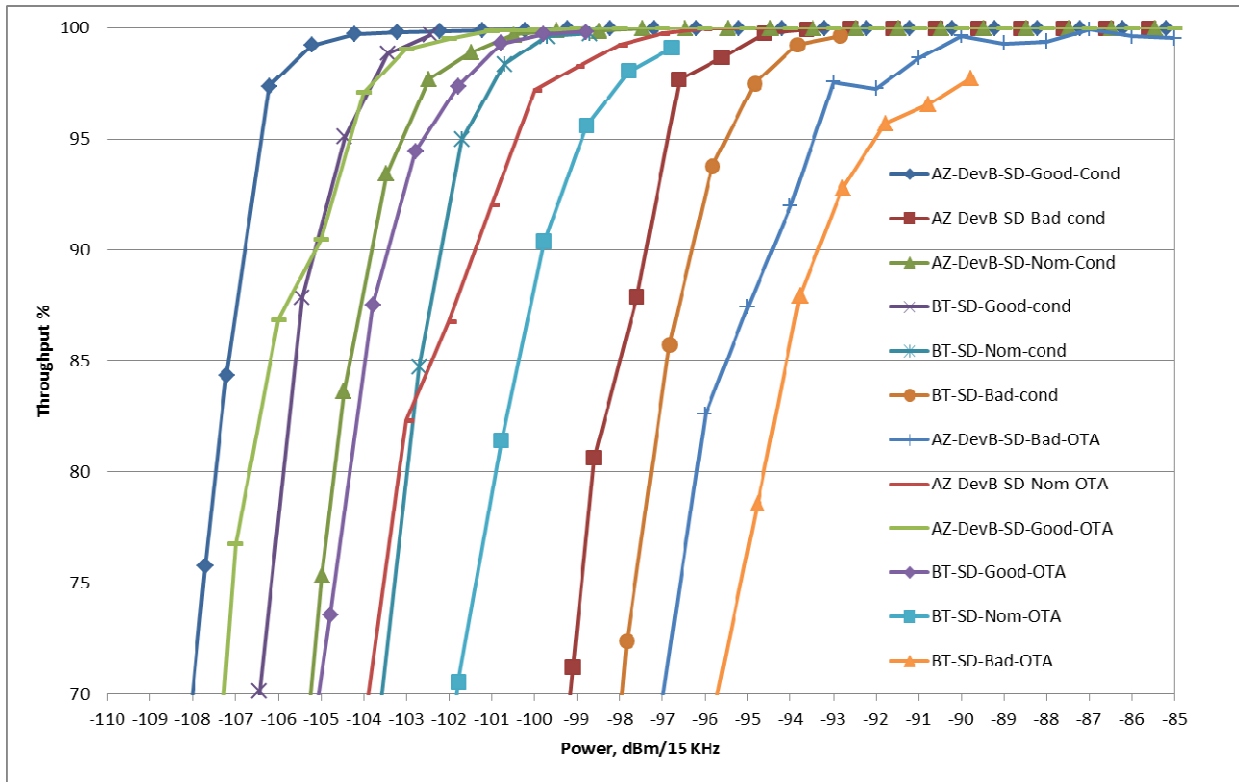


Figure 10.2.3-5: IL/IT results consistency for Reverberation Chamber candidate methodology 2 (RC+CE) measurements implementing the Short Delay channel model (all antennas)

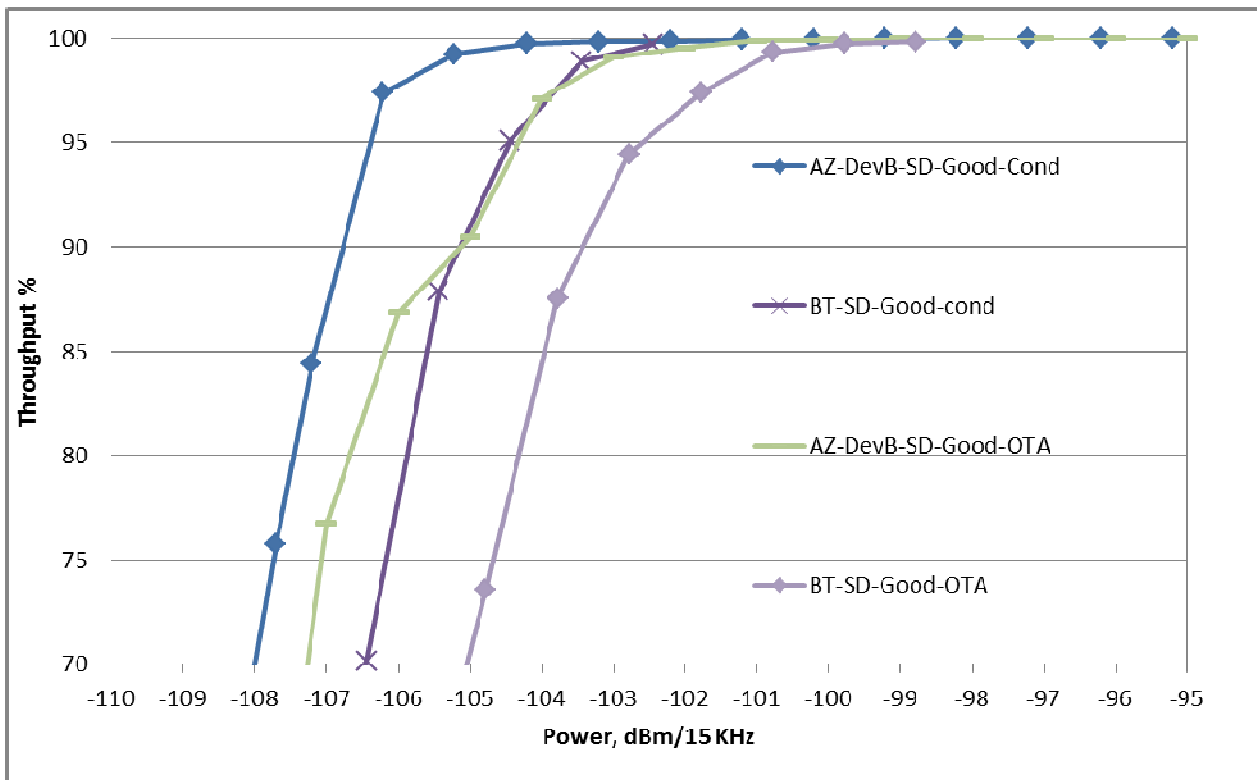


Figure 10.2.3-6: IL/IT results consistency for Reverberation Chamber candidate methodology 2 (RC+CE) measurements implementing the Short Delay channel model with the Good reference antennas

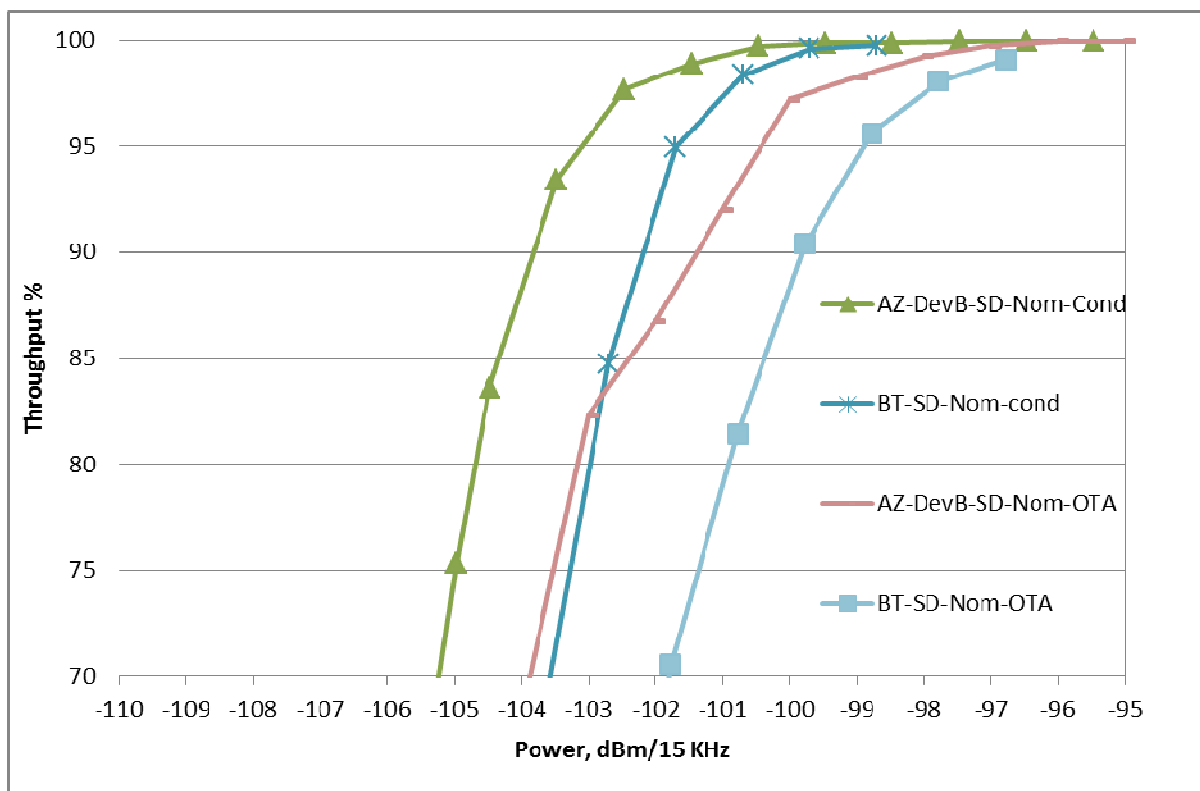


Figure 10.2.3-7: IL/IT results consistency for Reverberation Chamber candidate methodology 2 (RC+CE) measurements implementing the Short Delay channel model with the Nominal reference antennas

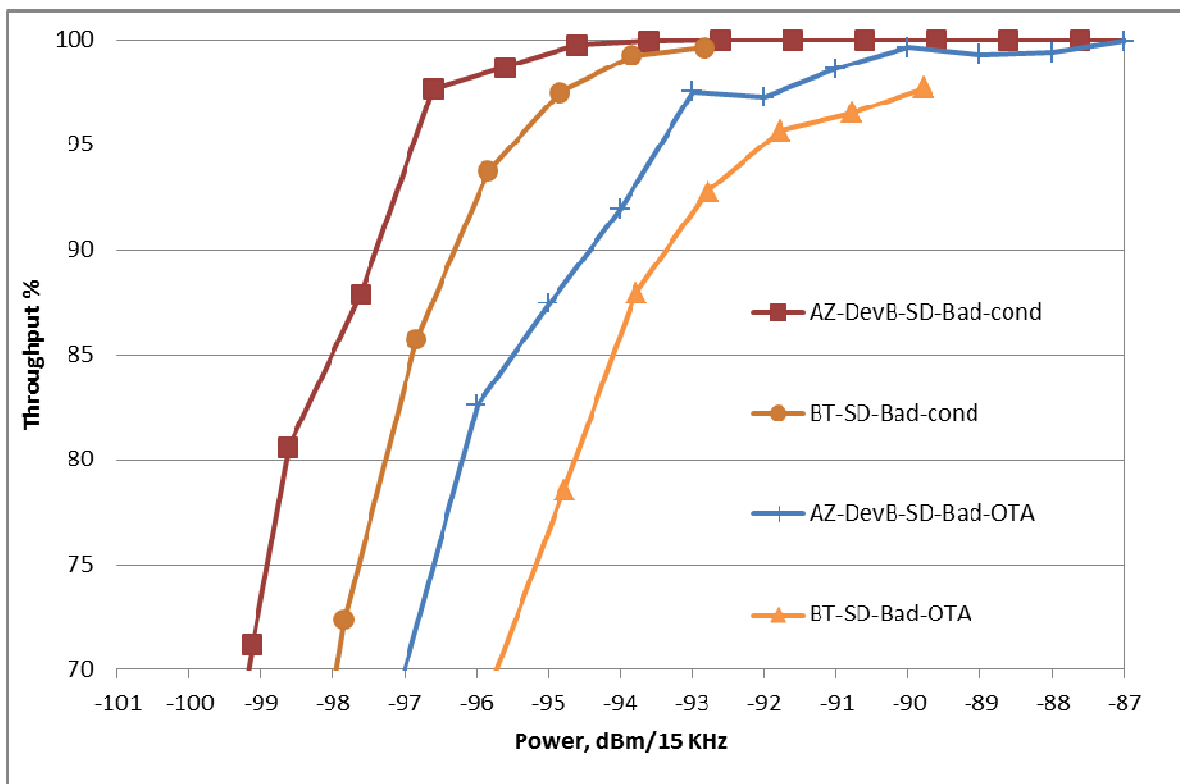


Figure 10.2.3-8: IL/IT results consistency for Reverberation Chamber candidate methodology 2 (RC+CE) measurements implementing the Short Delay channel model with the Bad reference antennas

The IL/IT test results from CTIA MOSG LTE MIMO OTA Round Robin campaign for the reverberation chamber candidate methodology 2 (RC+CE) using the Long Delay Spread High Correlation model are reproduced in figures 10.2.3-9 to 10.2.3-12. A maximum standard deviation uncertainty value for inter-chamber comparison of Long Delay Spread High Correlation of 1.86 dB STD has been found, showing that IL/IT consistency has been achieved using the reverberation chamber methodology 2 (RC+CE).

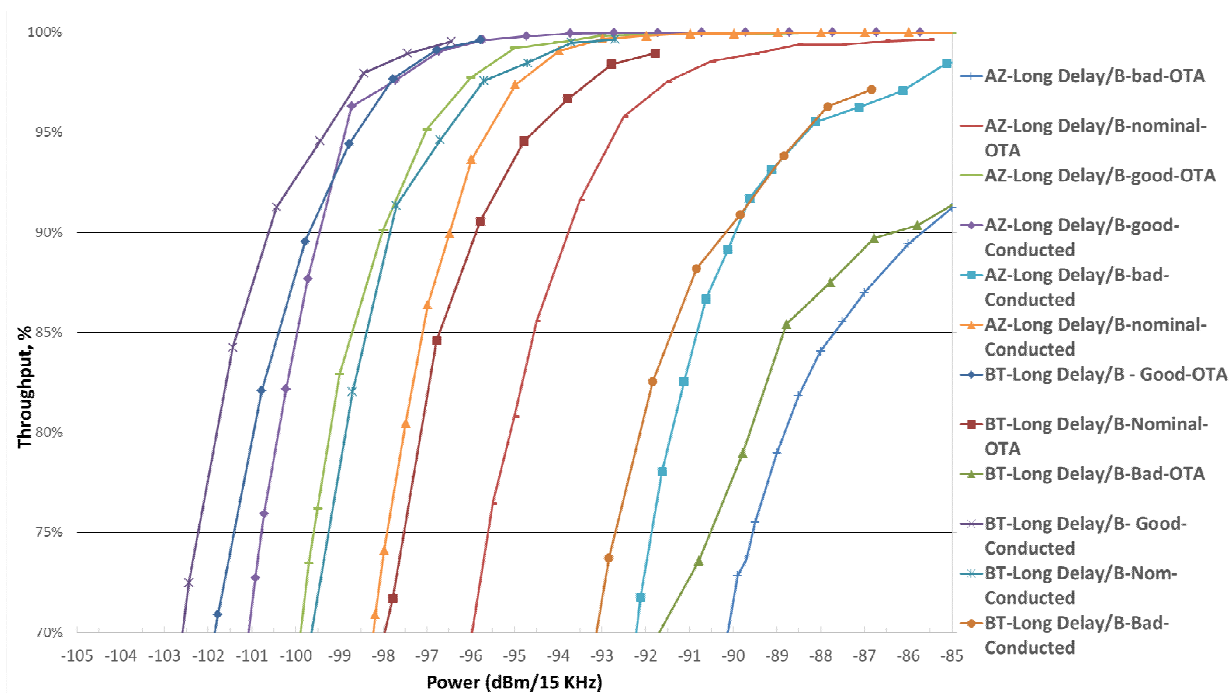


Figure 10.2.3-9: IL/IT results consistency for reverberation chamber methodology 2 (RC+CE) measurements implementing the Long Delay Spread High Correlation channel model (all antennas)

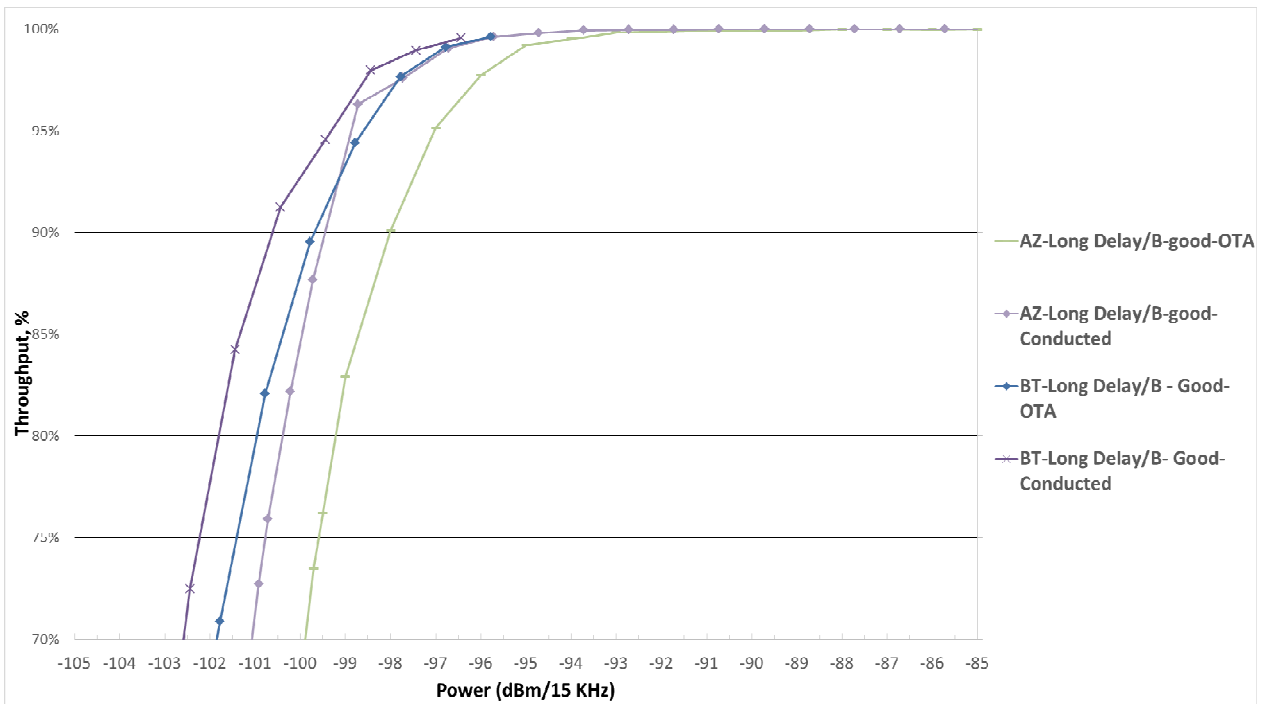


Figure 10.2.3-10: IL/IT results consistency for reverberation chamber methodology 2 (RC+CE) measurements implementing the Long Delay Spread High Correlation channel model with Good reference antenna only

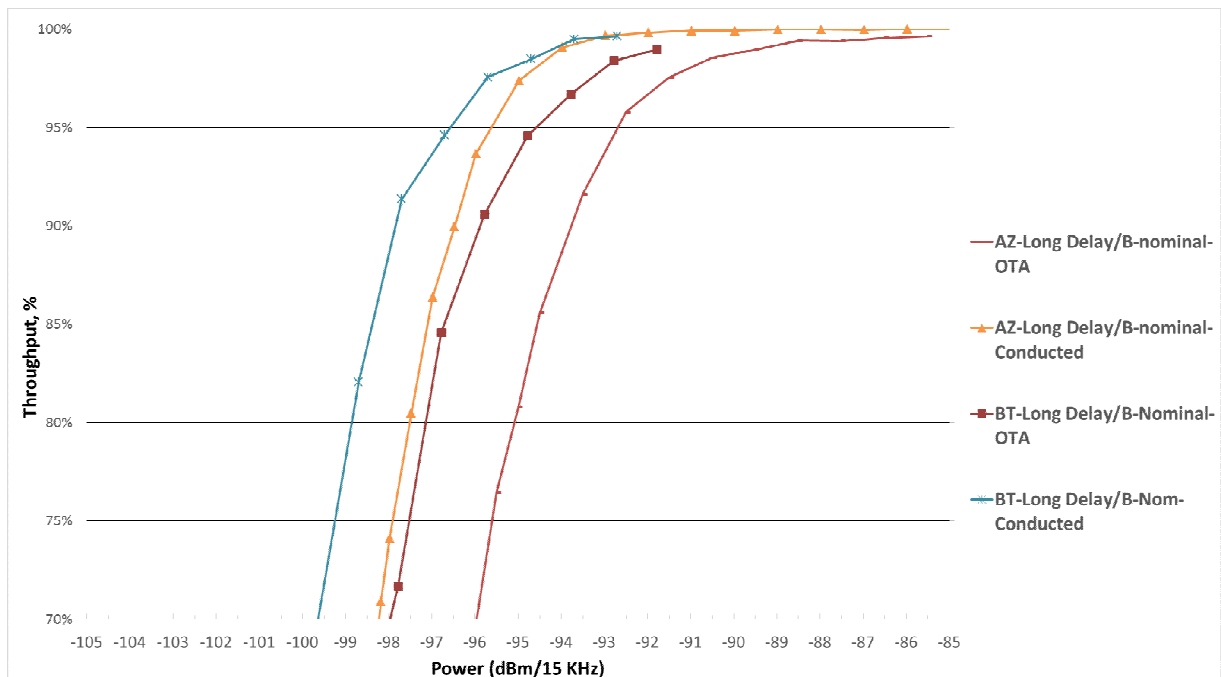


Figure 10.2.3-11: IL/IT results consistency for reverberation chamber methodology 2 (RC+CE) measurements implementing the Long Delay Spread High Correlation channel model with Nominal reference antenna only

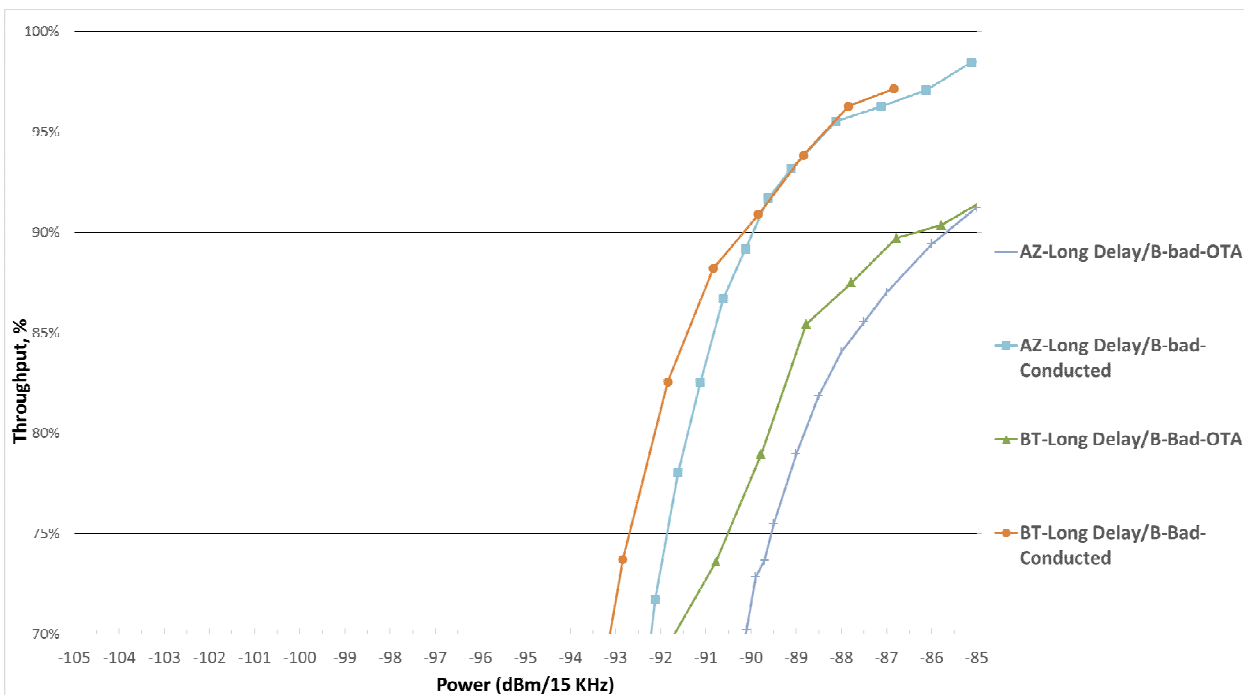


Figure 10.2.3-12: IL/IT results consistency for reverberation chamber methodology 2 (RC+CE) measurements implementing the Long Delay Spread High Correlation channel model with Bad reference antenna only

The case for conducted non-faded measurements is shown in Figure 10.2.3-13.

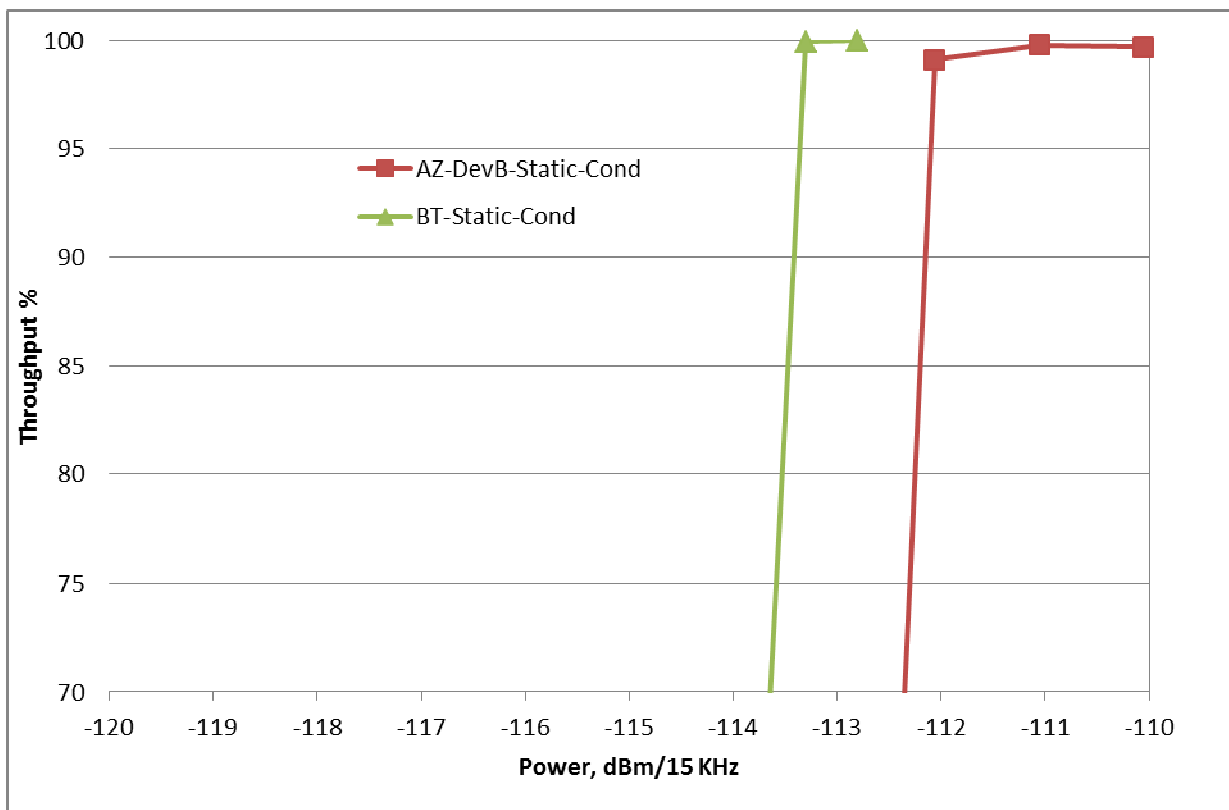


Figure 10.2.3-13: Conducted non-faded measurements comparison between Bluetest and Azimuth

In all cases for Figures 10.2.3-5 through 10.2.3-13 the following applies:

- AZ: Azimuth
- BT: Bluetest

The details on the devices used in all cases for Figures 10.2.3-5 through 10.2.3-13 are given in the table below.

Table 10.1.2-1

| | Azimuth Lab | Bluetest Lab |
|----------------------|--------------------|---------------------|
| Device ID | Dev B | MOSG-RD-13-03 |
| Manufacturer | HTC | HTC |
| Model | Rezound | Rezound |
| Model Number | ADR6425LVW | ADR6425LVW |
| Serial Number | HT1AXS201238 | HT18KS200207 |
| IMEI Number | 990000338748983 | 990000327075521 |

10.2.4 RTS method results

Inter-Lab/Inter-Technique (IL/IT) campaigns have been performed in CTIA MOSG LTE MIMO OTA by the RTS test methodology by Agilent's lab and CATR using the GTS lab. Both labs used the correlation implementation of the SCME channel model with the Jake's Doppler spectrum.

The static conducted baseline measurements for Agilent and GTS are provided in Figure 10.2.4-1.

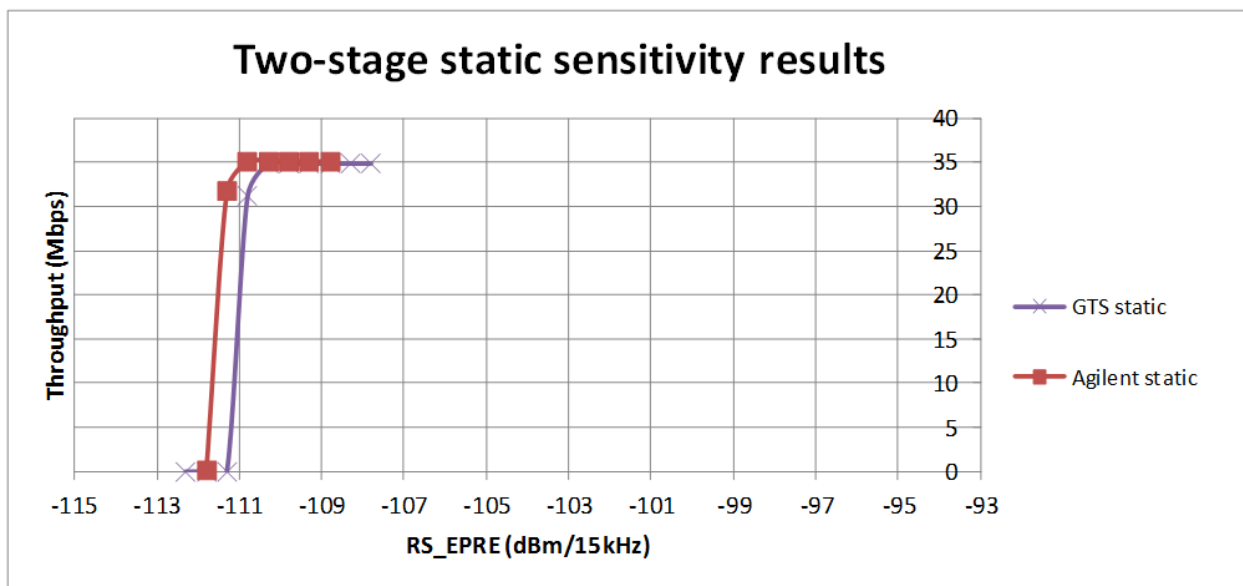


Figure 10.2.4-1: Static conducted reference results for Agilent and GTS

The absolute data throughput framework proof of concept for the RTS method is in Clause 9.3.1.7.

The absolute data throughput measurements for the new GTS lab to demonstrate equivalence between conducted and radiated measurements was performed for the UMi channel model are shown in Figures 10.2.4-2 and 10.2.4-3.

These results show approximately +/- 0.2 dB consistency for UMi and +/- 0.6 dB consistency for UMa/B.

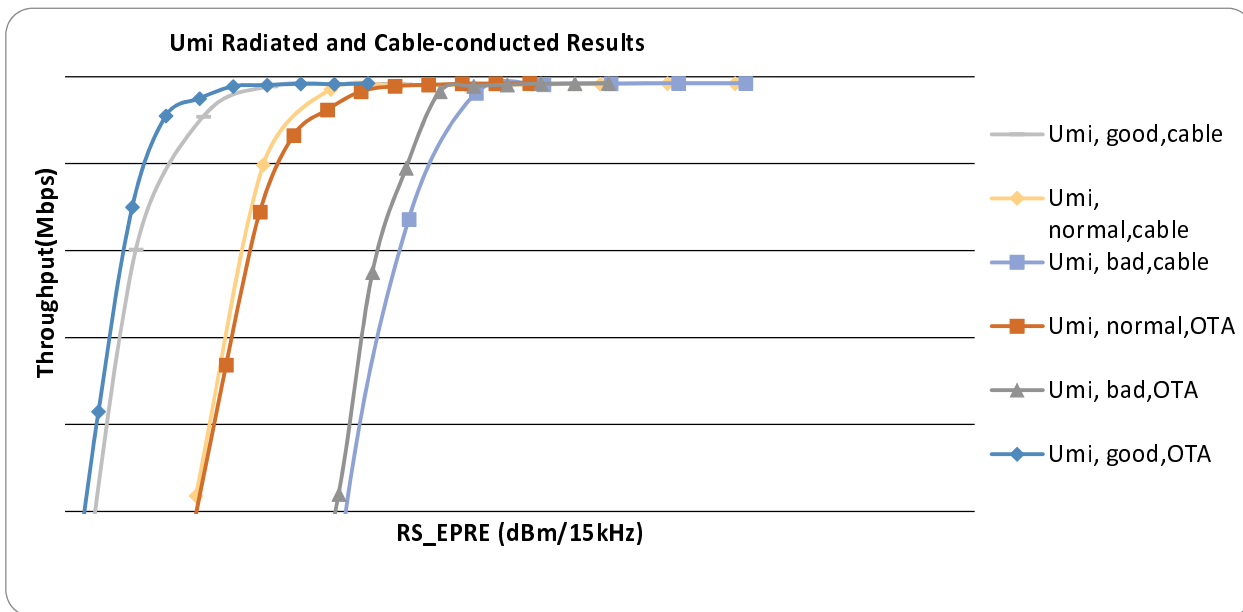


Figure 10.2.4-2: Radiated vs Cable-conducted Absolute Throughput Test for UMi Model for the GTS lab

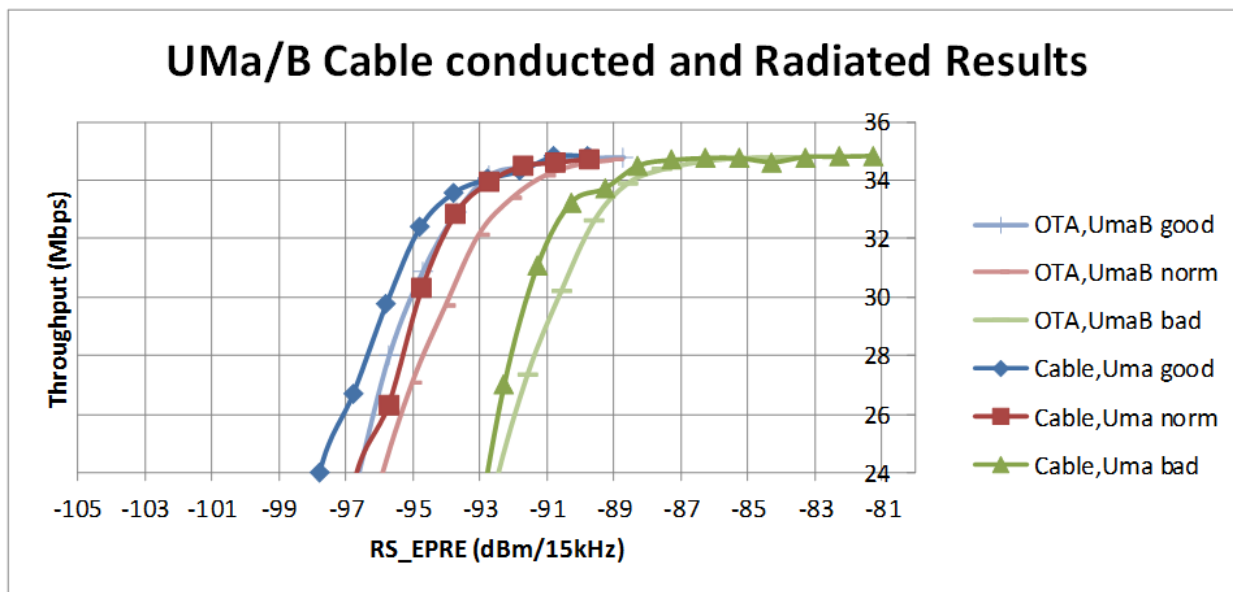


Figure 10.2.4-3: Radiated vs. Cable-conducted Absolute Throughput Test for UMa/B Model for the GTS lab

A comparison between both RTS labs is shown in Figures 10.2.4-4 and 10.2.4-5.

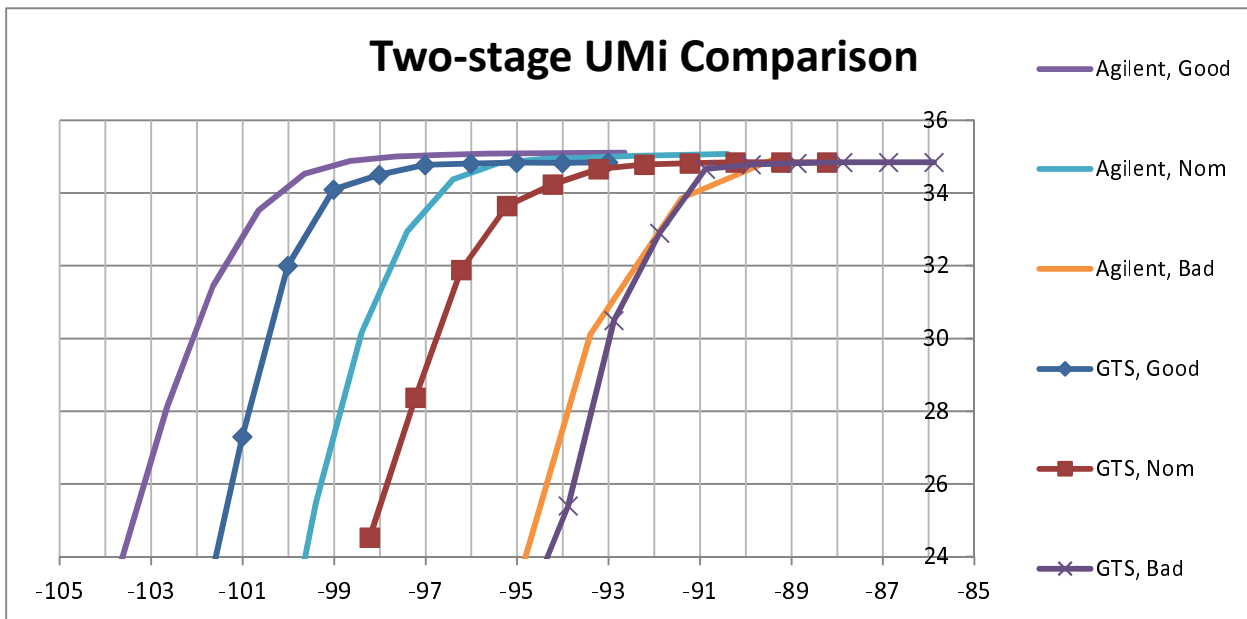


Figure 10.2.4-4: Comparison of RTS results for UMi

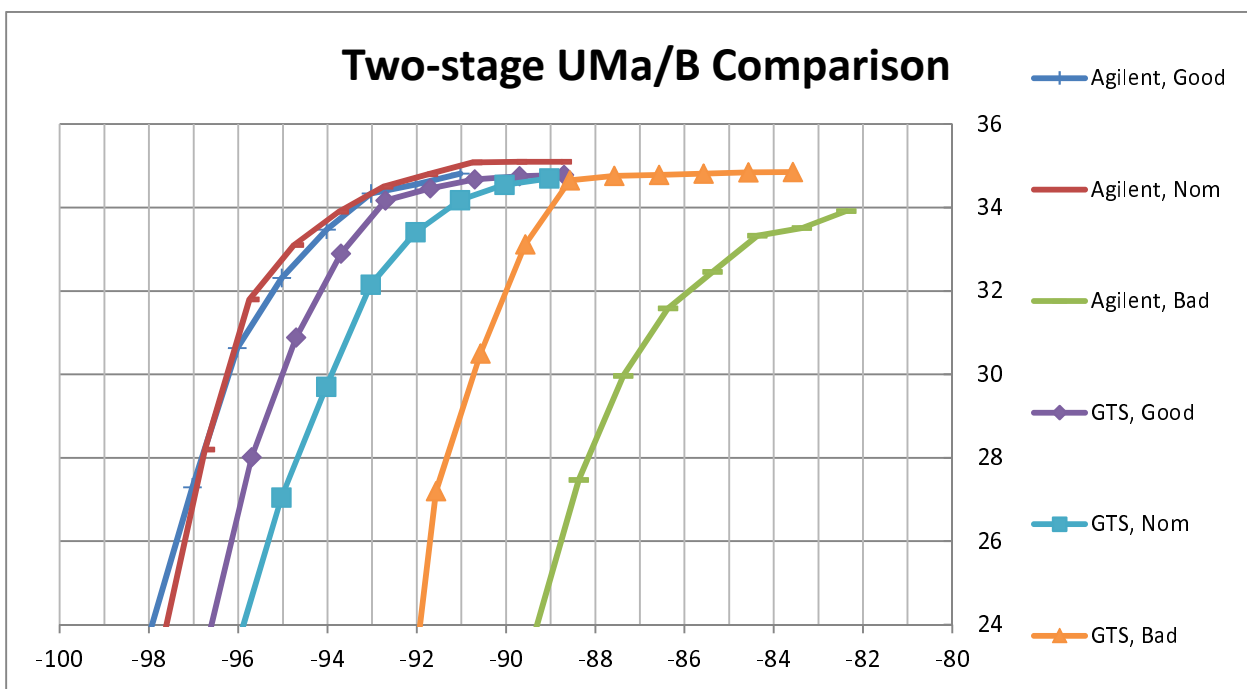


Figure 10.2.4-5: Comparison of RTS results for UMa/B

The RTS UMi results compared against Intel and SATIMO anechoic are shown in Figure 10.2.4-6.

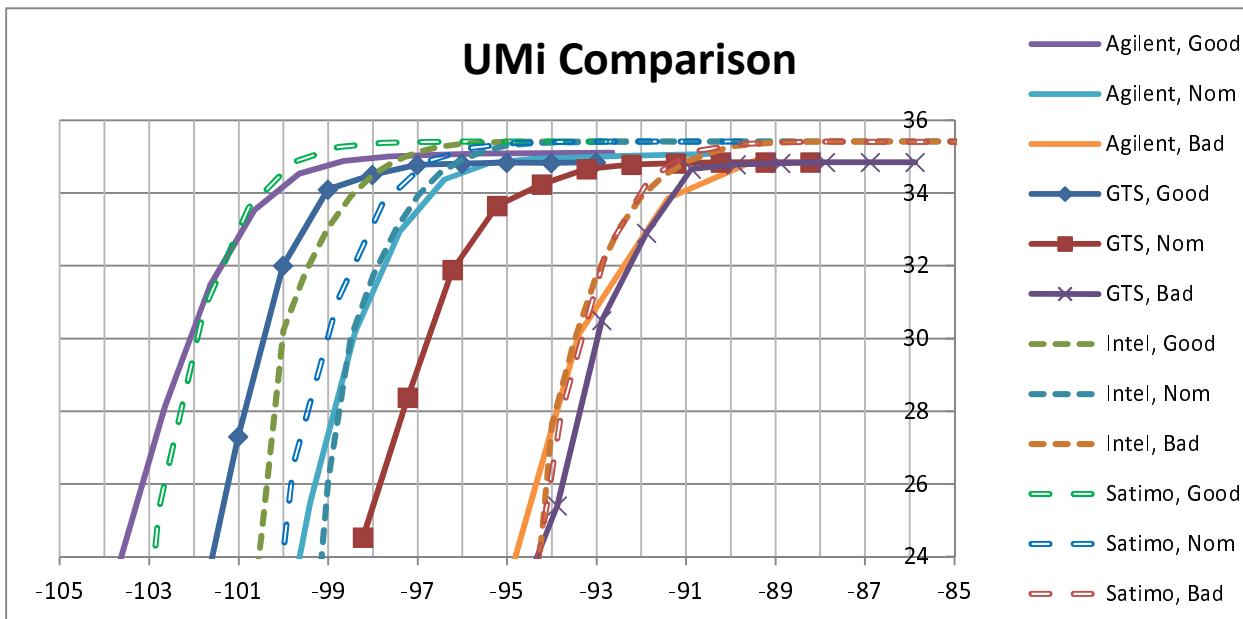


Figure 10.2.4-6: Absolute Throughput Test for UMi Model

The RTS UMa results compared against Intel and SATIMO anechoic are shown in Figure 10.2.4-7.

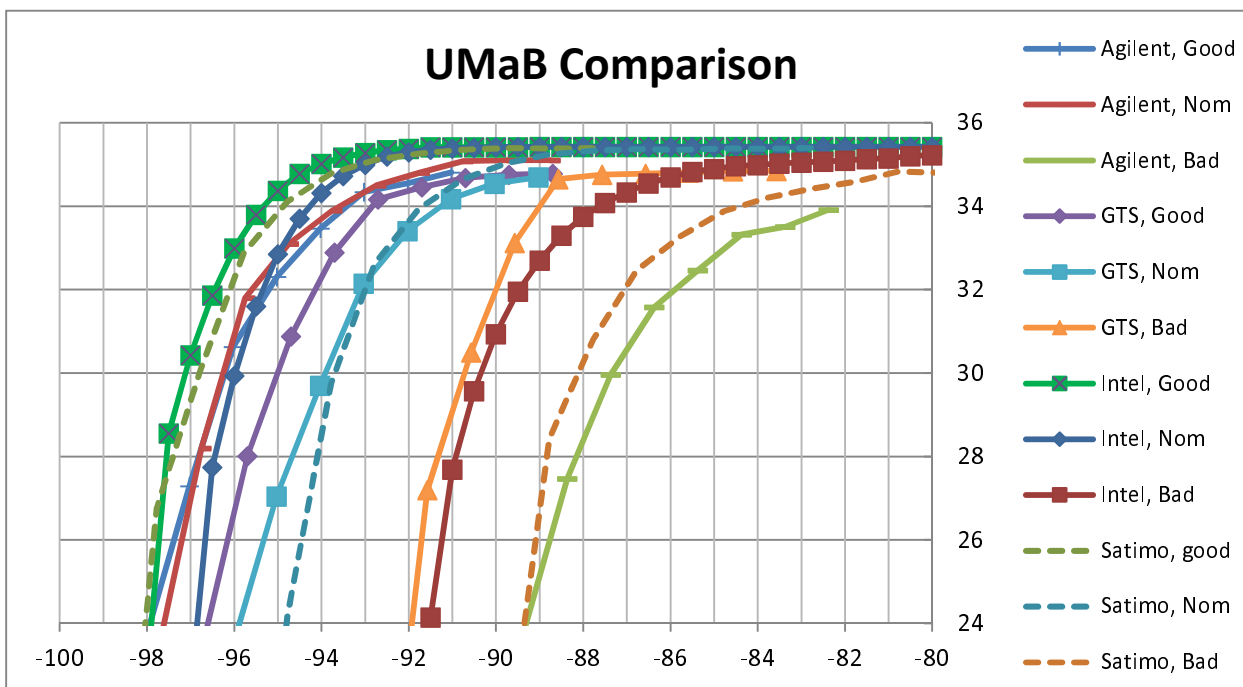


Figure 10.2.4-7: Absolute Throughput Test for UMa/B Model

A tabular comparison of all the results at 70% throughput is given in Tables 10.2.4-1 and 10.2.4-2.

Table 10.2.4-1: Summary of UMi results at 70% throughput

| | Good (dBm) | Nominal (dBm) | Bad (dBm) |
|-------------------|------------|---------------|-----------|
| Agilent | -103.6 | -99.4 | -94.7 |
| GTS | -101.5 | -98.2 | -94.2 |
| Intel | -100.5 | -99 | -94.2 |
| SATIMO | -102.8 | -100 | -94.2 |
| Spread +/- | +/- 1.55 | +/- 0.9 | +/- 0.25 |

Table 10.2.4-2. Summary of UMa results at 70% throughput

| | Good (dBm) | Nominal (dBm) | Bad (dBm) |
|-------------------------|------------|---------------|-----------|
| Agilent | -97.9 | -97.6 | -89.2 |
| GTS | -96.6 | -95.8 | -92 |
| Intel | -98 | -96.8 | -91.5 |
| SATIMO | -98 | -94.7 | -89.3 |
| Spread (all) +/- | +/- 0.7 | +/- 1.45 | +/- 1.4 |

10.3 3GPP harmonization test campaign

10.3.1 Description of the test plan

The objective of the harmonization measurement campaign is to capture comparable data from the different MIMO OTA methodologies, whose procedures are described in Clause 12, and to draw conclusions based on this data on the ability to harmonize across two or more methodologies.

The free space (FS) testing condition is used in this measurement campaign.

1. Eight device orientations are used for testing with the MPAC and RTS methodologies. With the vertical portrait orientation defined as (0,0,0) of (yaw, pitch, roll), these are: Portrait - (0°, 0°, roll)
2. Portrait tilt down - (0°, -45°, roll)
3. Portrait tilt up - (0°, 45°, roll)
4. Face up - (0°, 90°, roll)
5. Face down - (0°, -90°, roll)
6. Landscape - (90°, 0°, roll)
7. Landscape tilt down - (90°, -45°, roll)
8. Landscape tilt up - (90°, 45°, roll),

where the roll is represented by the rotation around the turntable axis to produce a single cut.

For MPAC and RTS methodologies a complete Throughput versus Power curve is obtained over 12 azimuth angles per device orientation. The total number of subframes (TNS) per power step is 20,000 to enable post-processing of the result using the agreed FoM working assumptions.

For RC and RC+CE, device orientation is not applicable, but the following other conditions apply. At least 100 samples and 400 subframes per power step and sample (giving a total of 40,000 TNS per power step) are be measured to enable post-processing of the results using the FoM working assumptions. Additionally, an MU analysis on the TNS will be completed by measuring all the devices with at least 100 samples and 20,000 subframes per power step and sample (giving a total of TNS=2,000,000 per power step), with the aim of validating the use of the small number of subframes through a comparison of their final averaged outage values. Results for both stepwise and continuous stirring modes are measured.

For any method, the power step is 0.5 dB from 95% down to 60%.

The following channel models are emulated by the different methodologies:

RC: NIST channel model (Table C.2-3)

RC+CE: Short delay spread low correlation (SDLC; Table C.2-1) and long delay spread high correlation (LDHC; Table C.2-2)

MPAC: SCMe UMi (Table 8.2-1) and SCMe UMa (Table 8.2-2)

RTS: SCMe UMi (Table 8.2-1) and SCMe UMa (Table 8.2-2)

The following is the working assumption on the figure of merit to be used for the analysis of harmonization testing campaign results:

Option 1: statistic of outages per throughput curve

Option 2: outage point from the average throughput curve

In addition to these procedures, each methodology also performs absolute data throughput framework tests in order to derive the measurement uncertainty bound for harmonization (as defined in Clause 10.3.3). The AC methodologies utilize a single free space portrait 90° device orientation, with the MIMO reference antenna placed at 90° elevation, and the RF enclosure door facing the 0° azimuth. The RC test methodologies conduct their measurements in stepstirred mode only. The lab performing RC and RC+CE methodologies can determine the optimal number of subframes per stirring state and per power level for the ADTF analysis only. All methodologies use the channel models defined in Clauses 8.2 and Annex C. ADTF results for each methodology, band, and channel model include 5 conducted ADTF results and 5 radiated results. The ADTF repeatability results for the MPAC methodology were impacted by additional measurement uncertainty due to re-cabling and test system re-configuration during the repeatability testing period.

10.3.2 Devices under test

The devices used in the harmonization testing campaign are listed in Tables 10.3.2-1 and 10.3.2-2 below.

Table 10.3.2-1: Devices used in the harmonization testing campaign: device set 1

| | | MPAC | RC | RC+CE | RTS |
|--------------|---------------|------|------|-------|--------------------------------|
| Band 13 | DUT01 | Done | Done | Done | Done |
| | DUT02 | Done | Done | Done | DUT does not support |
| | DUT03 (Black) | Done | Done | Done | Done |
| Band 13 ADTF | DUT04 (White) | Done | Done | Done | Done |
| Band 7 | DUT02 | Done | Done | Done | DUT does not support |
| | DUT05 | Done | Done | Done | Done |
| | DUT06 | Done | Done | Done | Done |
| Band 7 ADTF | DUT05 | Done | Done | Done | Done |
| Band 41 | DUT07 | Done | Done | Done | RTS does not support TDD bands |
| | DUT08 | Done | Done | Done | |
| | DUT09 | Done | Done | Done | |
| Band 41 ADTF | DUT08 | Done | Done | Done | |

Table 10.3.2-2: Devices used in the harmonization testing campaign: device set 2

| | | MPAC | RC | RC+CE | RTS |
|---------|-------|------|------|-------|--------------------------------|
| Band 13 | KS1 | Done | Done | Done | Done |
| | KS2 | Done | Done | Done | Done |
| Band 7 | KS2 | Done | Done | Done | Done |
| | SP1 | Done | Done | Done | DUT does not support |
| Band 41 | CMCC1 | Done | Done | Done | DUT does not support TDD bands |

10.3.3 Measurement uncertainty bound for harmonization

10.3.4 Summary of results

Harmonization evaluations across methodologies are carried out by defining harmonization options. Table 10.3.4-1 below lists harmonization options and their associated parameters.

Table 10.3.4-1: Harmonization options

| Option | Channel models | MPAC/RTS positions | Averaging type |
|---|---|--------------------------------------|----------------|
| C | UMi, NIST, LCLD | AVG {P 45,L 45,P 90} | inverse |
| D | UMi, NIST, LCLD | AVG {P 45,L 45,P 90} | linear |
| G (3 orientations) | UMa, UMi, NIST, LCSD, HCLD NIST is compared to both UMa/HCLD and UMi/LCSD | AVG {P 45,L 45,P 90} | linear |
| G (2 orientations P45, L45) | UMa, UMi, NIST, LCSD, HCLD NIST is compared to both UMa/HCLD and UMi/LCSD | AVG {P 45,L 45} | linear |
| G (1 orientation, all 3 combinations) | UMa, UMi, NIST, LCSD, HCLD NIST is compared to both UMa/HCLD and UMi/LCSD | 1 orientation, all 3 combinations | linear |
| H (3 orientations) | UMa, UMi, NIST, LCSD, HCLD | AVG {P 45,L 45,P 90} | inverse |
| I | UMa, NIST, HCLD | AVG {P 45,L 45,P 90} | linear |
| J | UMa, NIST, HCLD | AVG {P 45,L 45,P 90} | inverse |

For each option, each band, and each pair of methodologies (i.e. MPAC/RC, MPAC/RC+CE, and MPAC/RTS), harmonization offsets are selected and harmonization residuals are calculated. Table 10.3.4-2 below lists the harmonized MU terms (h), within the parameters of each option. In this table the inter-methodology offsets were optimized across the measurements obtained from device set 1 and device set 2 at 70% throughput.

Table 10.3.4-2: Harmonized MU (h) with offsets optimized across UEs from device set 1 and device set 2

| Option | Band | RC&MPAC | RC+CE/MPAC | RTS/MPAC |
|-----------------------|---------|---------|------------|----------|
| C | Band 13 | 4.2 | 4.2 | 3.1 |
| | Band 7 | 3.2 | 3.4 | 3.1 |
| | Band 41 | 2.9 | 3.6 | |
| D | Band 13 | 4.4 | 4.4 | 3.4 |
| | Band 7 | 3.4 | 3.4 | 3.1 |
| | Band 41 | 2.9 | 3.6 | |
| G (3 orientations) | Band 13 | 7.2 | 4.6 | 3.6 |
| | Band 7 | 5.9 | 3.5 | 3.3 |

| | | | | |
|---|---------|-----|-----|-----|
| | Band 41 | 6.1 | 4.3 | |
| G (2 orientations P45, L45) | Band 13 | 7.3 | 4.9 | 3.3 |
| | Band 7 | 5.9 | 4.3 | 3.8 |
| | Band 41 | 6.4 | 4.5 | |
| G (1 orientation, all 3 combinations) | Band 13 | 8.2 | 5.7 | 4.4 |
| | Band 7 | 6.8 | 5.7 | 4.9 |
| | Band 41 | 7.7 | 5.5 | |
| H (3 orientations) | Band 13 | 7.0 | 4.6 | 3.1 |
| | Band 7 | 8.9 | 3.9 | 3.8 |
| | Band 41 | 6.1 | 4.2 | |
| I | Band 13 | 4.6 | 4.5 | 3.6 |
| | Band 7 | 3.3 | 2.9 | 3.3 |
| | Band 41 | 3.5 | 4.1 | |
| J | Band 13 | 4.5 | 4.5 | 3.0 |
| | Band 7 | 3.8 | 3.5 | 3.8 |
| | Band 41 | 3.4 | 4.2 | |

Table 10.3.4-3 below lists the robustness bias terms (b). In this table the inter-methodology offsets were optimized only across the measurements obtained from device set 1 at 70% throughput.

Table 10.3.4-3: Robustness bias terms (b) without optimizing offsets after UEs from device set 2 were added

| Option | Band | RC&MPAC | RC+CE/MPAC | RTS/MPAC |
|-----------------------|---------|---------|------------|----------|
| C | Band 13 | 1.3 | 2.7 | 0.8 |
| | Band 7 | 0.0 | 0.5 | 0.1 |
| | Band 41 | 0.0 | 1.2 | |
| D | Band 13 | 1.0 | 2.3 | 1.0 |
| | Band 7 | 0.2 | 0.4 | 0.2 |
| | Band 41 | 0.0 | 1.1 | |
| G (3 orientations) | Band 13 | 0.8 | 2.1 | 0.2 |
| | Band 7 | 0.0 | 0.4 | 0.1 |
| | Band 41 | 0.0 | 1.2 | |
| | Band 13 | 0.0 | 3.6 | 0.6 |
| | Band 7 | 0.0 | 0.9 | 0.0 |

| | | | | |
|---|---------|-----|-----|-----|
| G (2 orientations P45, L45) | Band 41 | 0.7 | 1.1 | |
| G (1 orientation, all 3 combinations) | Band 13 | 0.0 | 0.3 | 1.1 |
| | Band 7 | 0.0 | 0.2 | 0.0 |
| | Band 41 | 0.0 | 0.4 | |
| H (3 orientations) | Band 13 | 1.5 | 2.9 | 0.0 |
| | Band 7 | 0.0 | 0.1 | 0.0 |
| | Band 41 | 0.3 | 1.2 | |
| I | Band 13 | 0.8 | 2.2 | 1.0 |
| | Band 7 | 0.0 | 0.4 | 0.0 |
| | Band 41 | 0.0 | 1.6 | |
| J | Band 13 | 1.5 | 3.0 | 0.2 |
| | Band 7 | 0.0 | 0.3 | 0.0 |
| | Band 41 | 0.4 | 2.4 | |

Table 10.3.4-4 below lists the delta of residuals between 70% and 95% throughput. In this table the inter-methodology offsets were optimized across the measurements obtained from device set 1 and device set 2 at 70% throughput.

Table 10.3.4-4: Delta of residuals (r) between 95% and 70% throughput

| Option | Band | RC&MPAC | RC+CE/MPAC | RTS/MPAC |
|-----------------------------------|---------|---------|------------|----------|
| C | Band 13 | 0.4 | -0.4 | 0.0 |
| | Band 7 | 1.6 | -0.1 | -0.1 |
| | Band 41 | 2.0 | -0.6 | 0.0 |
| D | Band 13 | 0.7 | -0.4 | 0.4 |
| | Band 7 | 1.6 | 0.1 | 0.1 |
| | Band 41 | 2.1 | -0.4 | 0.0 |
| G (3 orientations) | Band 13 | 1.1 | -0.4 | 0.2 |
| | Band 7 | 1.7 | 0.1 | -0.1 |
| | Band 41 | 1.9 | -0.4 | 0.0 |
| G (2 orientations P45, L45) | Band 13 | -0.3 | -0.3 | 0.0 |
| | Band 7 | 1.8 | -0.3 | 0.0 |
| | Band 41 | 2.9 | -0.2 | 0.0 |
| | Band 13 | | | |
| | Band 7 | | | |

| | | | | |
|---|---------|-----|------|------|
| G (1 orientation, all 3 combinations) | Band 41 | | | |
| H (3 orientations) | Band 13 | 0.6 | -0.4 | 0.1 |
| | Band 7 | 1.8 | 0.2 | -0.1 |
| | Band 41 | 1.4 | -0.3 | 0.0 |
| I | Band 13 | 1.1 | -0.1 | 0.2 |
| | Band 7 | 1.7 | -0.2 | -0.1 |
| | Band 41 | 1.9 | -0.6 | 0.0 |
| J | Band 13 | 0.6 | -0.4 | 0.2 |
| | Band 7 | 1.8 | -0.1 | -0.1 |
| | Band 41 | 1.4 | -0.3 | 0.0 |

Table 10.3.4-5 below list the informational flags.

Table 10.3.4-5: Informational Flags

| Informational Flags (UEs from device set 1) | |
|--|---|
| UE | Flag |
| Z3 | RC&CE: Z3 did not reach 95% TP for 1/120 states for UMa channel model in Band 13 |
| Z3 | RC&CE: Z3 did not reach 95% TP for 2/120 states for UMa channel model in Band 7 |
| S5 | RC&CE: S5 did not reach 95% TP for 1/120 states for UMa channel model in Band 41 |
| Informational Flags (UEs from device set 2) | |
| UE | Flag |
| KS1 | MPAC: In Band 13, KS1 did not reach 95% TP in 1/12 AZ positions in Landscape 45 orientation |
| KS1 | MPAC: In Band 13, KS1 did not reach 95% TP in 4/12 AZ positions in Portrait 90 orientation |
| KS1 | RTS: In Band 7, KS1 did not reach 95% TP in 6/12 AZ positions in Portrait 45 orientation, in 4/12 AZ positions in Portrait 90 orientation, and in 5/12 AZ positions in Landscape 45 orientation |
| KS1 | RTS: In Band 7, KS1 did not reach 95% TP in 2/12 AZ positions in Portrait 45 orientation |
| KS2 | RTS: In Band 13, KS2 did not reach 95% TP in 12/12 AZ positions in P45 orientation and 3/12 AZ positions in L45 orientation for UMa channel model |
| KS2 | RC+CE: In Band 13, KS2 did not reach 95% TP in 4/120 stirring modes for UMa channel model |
| SP1 | MPAC: In Band 7, SP1 did not reach 70% TP in 10/12 AZ positions in P45, in 11/12 AZ positions in P90, and 12/12 AZ positions in L45 orientation for UMa channel model |
| SP1 | MPAC: In Band 7, SP1 did not reach 95% TP in 12/12 AZ positions in all three orientations (P45, P90, L45) for UMa channel model |

| | |
|-------------------------|--|
| SP1 | RC+CE: In Band 7, SP1 did not reach 70% and 95% TP in 120/120 stirring modes for UMa channel model |
| SP1 | RC+CE: In Band 7, SP1 did not reach 70% and 95% TP in 120/120 stirring modes for UMa channel model |
| Additional Flags | |
| UE | Flag |
| SP1 | As this device did not achieve 70% in many cases, further analysis of the raw data using throughput averaging was performed to estimate the performance delta in dB between MPAC and RC+CE. The deltas are as follows after applying the optimized fixed offsets. RC+CE to MPAC difference at 12.5Mbps: P45: -11 dB P90: -14 dB L45: +18.5 dB Average(P45,P90,L45): -11.75 dB |
| KS2 | B13 UMa – RTS does not provide a 95% outage while MPAC does – This is probably due to subtle differences in the channel conditions for a device near its limit |
| KS1 | B13 UMa – MPAC does not provide a 95% outage while RTS does – This was due to too low a starting power to try to save test time |
| KS1 | B7 UMi – RTS does not provide a 95% outage while MPAC does |
| KS1 | B7 UMa – RTS does not provide a 95% outage while MPAC does – This is due to insufficient power from the amplifier for this particularly bad device |

10.3.5 Harmonization outcome

Harmonization cost has been calculated among the options in Table 10.3.4-1 and is defined as $c = \max(h_{B7}, h_{B13}, h_{B41}) - m_{MPAC}$. Table 10.3.5-1 below lists the cost values per option and methodology combination.

Table 10.3.5-1: Harmonization cost

| Option | RC&MPAC | RC+CE&MPAC | RTS&MPAC | RC+CE&RTS&MPAC | RC&RC+CE&RTS&MPAC |
|--|---------|------------|----------|----------------|-------------------|
| C | 1.6 | 1.6 | 0.5 | 1.6 | 1.6 |
| D | 1.8 | 1.8 | 0.7 | 1.8 | 1.9 |
| G (3 orientations) | 4.5 | 2 | 1 | 2 | 4.5 |
| G (2 orientations P45, L45) | 4.9 | 2.3 | 1.2 | 2.3 | 4.9 |
| G (1 orientation, all 3 combinations) | 5.5 | 3.2 | 2.3 | 4 | 6.6 |
| H (3 orientations) | 4.4 | 2 | 1.2 | 2 | 4.4 |
| I | 2 | 1.8 | 1 | 1.8 | 2 |
| J | 1.9 | 1.9 | 1.2 | 1.9 | 1.9 |
| NOTE: RTS cannot test TDD (as of today) and requires UE support. | | | | | |

Additionally, as offsets were optimized for 70% throughput, a check is made at 95% to determine the change in the residuals (r). Table 10.3.5-2 below lists the cost check values per option and methodology combination.

Table 10.3.5-2: Harmonization cost check at 95% outage

| Option | RC&MPAC | RC+CE&MPAC | RTS&MPAC | RC+CE&RTS&MPAC | RC&RC+CE&RTS&MPAC |
|--------------------|---------|------------|----------|----------------|-------------------|
| C | 1.9 | 0 | 0 | 0 | 1.4 |
| D | 2.1 | 0.1 | 0.4 | 0.1 | 1.6 |
| G (3 orientations) | 1.9 | 0.1 | 0.2 | 0.1 | 1.7 |
| G (2 orientations) | 2.5 | -0.2 | 0 | -0.3 | 1.8 |
| H (3 orientations) | 1.7 | 0.1 | 0.1 | 0.1 | 1.7 |
| I | 1.9 | -0.1 | 0.2 | -0.1 | 1.7 |
| J | 1.8 | -0.1 | 0.2 | -0.1 | 1.7 |

The following agreements have been made:

1. Final harmonization cannot be successfully claimed. But potential for harmonization can be found. In this situation, a single method shall be selected according to WID, while work on improving harmonization is deemed possible and needed
2. Select MPAC methodology, and start new activity on performance requirement phase for MPAC
3. Select UMi channel model, and inverse averaging. Option C
4. Select the following KPIs: 70% and 95%
5. How to treat failing of devices:
 1. For 95% tput: 2 orientations/azimuth rotations that fail are allowed. If more orientations fail then device fails test
 2. For 70% tput: 1 orientation /azimuth rotations that fail is allowed. If more orientations fail then device fails test
6. Start follow-up harmonization activity in parallel to Performance requirement activity above, for the pair or pairs of methods that have potential harmonization
 1. This follow-up activity will increase the number of devices to be tested with the aim to augment and improve harmonization
 2. This follow-up activity will also increase the bands to be considered for harmonization
 3. Add UMa only option (Option J) for harmonization it in this follow-up harmonization activity which will be tested in parallel to UMi harmonization. UMa is not excluded from future performance work
7. Due to robustness check at 95%, methods involving RC-only shall not be considered
8. RC+CE&MPAC, RTS&MPAC and RC+CE&RTS&MPAC shall be considered in the harmonization activity
9. Everything can be done in the same WI
10. Bands for performance requirement definition activity: 1,2,3,4,5,7, 8,12,13,19,20,28,32,38,40,41,42,46
11. The first set of bands to define requirements for and to perform harmonization activity are 2 FDD low bands, 2 FDD high bands and 2 TDD bands
12. if harmonization fails for a particular set of corresponding channel models, then that method is not applicable for testing in that particular set of corresponding channel model
13. Sample size for performance requirement: 100 measurements as a minimum
14. How to claim new harmonization activity is successful
 1. Same bands (or set) as in the performance activity will be addressed in the same order, and harmonization will be checked after the performance requirement for each band (or set) is finalized.

2. How many measurements samples per band: 30 of devices used for Performance requirement phase will be used for this harmonization activity. And tested in the same lab to minimize MUs with a controlled environment

15. Add Rayleigh validation procedure for RC+CE method

The following open items have been identified:

1. Study how to perform averaging across orientations that did not fail the KPI
2. Add how to extend the concept of devices failing in MPAC as agreed in slide 5 to RC+CE method
3. Development of the procedure to validate Rayleigh
4. Think what happens if we don't find a single lab with a controllable environment
5. Include statistical analysis to determine when to stop testing more devices for harmonization
6. Study how to find the offset
7. Study the distribution of residuals when analysing the cost
8. Study how to calculate the cost and threshold

10.4 Lab alignment procedures for performance labs

10.4.1 General

Labs intending to contribute to the performance requirement part of the work shall complete the lab alignment measurements and report the results to RAN4 in the approved data format.

10.4.2 Channel model validation data

If the lab implements a commercial test solution for which the test solution provider has already submitted channel model validation data to RAN4 and which results have been included in TR 37.977, then a submission of the channel model validation data is not required.

If the lab implements a commercial test solution for which the test solution provider has not yet submitted channel model validation data to RAN4, then the channel model validation data shall be provided by the solution provider. If the lab implements a custom test solution, then the lab (as the test solution provider) shall provide channel model validation data to RAN4, such that

- The measurements are made according to the procedures described in Clause 8.3 of TR 37.977
- Using the channel models defined in 8.1.1 of TS 37.144
- The results are submitted to RAN4 as a CR to TR 37.977
- The testing frequencies are the center frequencies corresponding to LTE bands 13 and 7

10.4.3 Calibration with a specific set of reference dipoles

A set of reference dipoles shall be used by the lab to perform the chamber range calibration in both the V and H polarizations as well as to verify the sum of the power in vertical and horizontal polarizations during the alignment activity. This set shall be shipped together with the alignment devices. Table 10.4.3-1 below lists the calibration reference antennas in the set.

Table 10.4.3-1: Calibration reference antennas

| Reference antenna ID | Reference antenna type | Operating Band | Availability | Current location |
|----------------------|------------------------|----------------|--------------|------------------|
| TBD | Sleeve dipole | 13 | TBD | TBD |
| TBD | Sleeve dipole | 7 | TBD | TBD |

For each operating band listed in Table 10.4.3-1, the lab shall report the measured power in the V polarization for the SCMe UMi channel model and, optionally, for the UMa channel model, as defined in 8.2 of TR 37.977.

10.4.4 Performance alignment measurements

The lab shall perform alignment measurements according to the following parameters:

- Using the performance alignment devices (PAD) and bands listed in Table 10.4.4-1.
- Using the testing conditions as defined in 8.1.1 of TS 37.144.
- Recording and reporting the measured data in the agreed spreadsheet format.

Table 10.4.4-1: Performance alignment devices (PAD)

| UE | Operating Band(s) | Availability | Current location |
|-------|-------------------|--------------|------------------|
| PAD_1 | FDD7, FDD13 | Now | China |
| PAD_2 | FDD7, FDD13 | Now | USA |
| PAD_3 | TDD41 | TBD | TBD |
| PAD_4 | TDD41 | TBD | TBD |

Total tests with the PAD set: 6 device-band combinations x 3 orientations = 18 tests.

Optionally, the lab may perform additional alignment measurements according to the following parameters:

- Using the additional alignment devices (AAD), bands, and UE orientations listed in Table 10.4.4-2.
- Using the SCMe UMa channel model as defined in 8.2 of TR 37.977.
- Recording and reporting the measured data in the agreed spreadsheet format.

Table 10.4.4-2: Additional alignment devices (AAD) with UMa

| UE | Operating Band | UE orientation | Availability | Current location |
|-------|----------------|----------------|--------------|------------------|
| AAD_1 | FDD7 | L0 & P0 | Now | Europe |
| AAD_2 | FDD13 | P0 & Face Down | Now | Europe |
| AAD_3 | FDD13 | P0 & L -45 | Now | USA |

Total tests with the AAD set: 3 device-band combinations x 2 orientations = 6 tests.

The alignment procedures are applicable to MPAC.

10.4.5 Acceptance criteria

The criteria for accepting the outcome of the lab alignment activity for a given lab are listed in Table 10.4.5-1 below.

Table 10.4.5-1: Performance alignment acceptance criteria

| Aspect | Case | Band | Acceptance criterion |
|---------------------------|----------------------|--------|--|
| Channel model validation | PDP | {13,7} | 8.4.6 |
| | Temporal correlation | {13,7} | 8.4.6 |
| | Spatial correlation | {13,7} | 8.4.6 |
| | Cross-polarization | {13,7} | 8.4.6 |
| Power verification PAD | (V) for UMi | {13,7} | TBD |
| | PAD_1 | 13 | Maximum deviation of $S_{Mode,x} \leq 1.0$ dB, Maximum deviation of TRMS \leq TBD |
| | PAD_1 | 7 | |
| | PAD_2 | 13 | |
| | PAD_2 | 7 | |
| | PAD_3 | 41 | |
| PAD_4 | 41 | | |

11 Void

12 MIMO OTA test procedures

12.1 Anechoic chamber method with multiprobe configuration test procedure

12.1.1 Base Station configuration

The SS parameter settings shall be set according to Clause 7.1.

The emulated antenna array configuration shall be set according to Clause 8.5.

12.1.2 Channel Models

The applicable channel models are defined in Clause 8.2.

12.1.3 Device positioning and environmental conditions

The positioning of the device under test within the test volume shall be set as defined in Clause 9.4.

The environmental requirements for the device under test shall be set as defined in Annex D.

12.1.4 System Description

12.1.4.1 Solution Overview

The setup described in Clause 6.3.1.1 shall be used.

12.1.4.2 Configuration

The concept and configuration of the test setup is given in Clause 6.3.1.1.1.

12.1.4.3 Calibration

The calibration procedure is specific to the test concept and configuration, therefore is unique for each implementation. The calibration procedure shall be documented by each lab, with enough details to allow third party verification. Examples for signal level calibration are given in Annex F.

12.1.5 Figure of Merit

The performance metric is given in Clause 5.

12.1.6 Test procedure

12.1.6.1 Initial conditions

Initial conditions are a set of test configurations the UE shall be tested in and the steps for the SS to take with the UE to reach the correct measurement state for each test case.

1. Ensure environmental requirements of Annex A are met.

2. Configure the test system according to Clauses 12.1.1 and 12.1.2 for the applicable test case.
3. Verify the implementation of the channel model as specified in Clause 12.1.2.

NOTE: The verification of the channel model implementation can be part of the laboratory accreditation process i.e. performed once for each channel model, and will remain valid as long as the setup and instruments remain unchanged. Otherwise the channel model validation may need to be performed prior to starting each throughput test.

4. Position the UE in the chamber according to Clause 12.1.3.
5. Power on the UE.
6. Set up the connection.

12.1.6.2 Test procedure

The following steps shall be followed in order to evaluate MIMO OTA performance of the DUT:

1. Measure MIMO OTA throughput from one measurement point. MIMO OTA throughput is the minimum downlink power (or SIR) resulting in a throughput value of 70% of the maximum theoretical throughput. The downlink power (or SIR) step size shall be no more than 0.5 dB when RF power level is near the LTE MIMO sensitivity level. Measurement duration shall be sufficient to achieve statistical significance that is TBD.

NOTE 1: The initial RS EPRE can be set to the user's freely selectable level. Recommended initial RS EPRE is found in Tables 7.1-1 and 7.1-2. For the SIR control tests, ensure that the default signal level is set such that the target SIR values can be achieved when utilizing the SIR validation procedure defined in clause 5.1.2.1.

NOTE 2: The throughput value target DL power level (or SIR) can be changed using user's freely selectable algorithm.

NOTE 3: Assuming that the default signal level meets the criteria in NOTE 1, the interference level will be adjusted to achieve the target SIR.

2. Rotate the UE around vertical axis of the test system by 30 degrees and repeat from step 1 until one complete rotation has been measured i.e. 12 different UE azimuth rotations.
3. Repeat the test from step 1 for each specified device orientation. A list of orientations is given in Annex E.
4. The postprocessing method to calculate the average MIMO Throughput is defined in 5.2.1.

12.1.7 Measurement Uncertainty budget

The measurement uncertainty budget for the test methodology is given in Annex B.

12.2 Reverberation chamber test procedure

12.2.1 Base Station configuration

The SS parameter settings shall be set according to Clause 7.1.

The emulated antenna array configuration shall be set according to Clause 8.5. For the isotropic channel model based on NIST, the base station antennas shall be uncorrelated.

12.2.2 Channel Models

The applicable channel models are defined in Annex C.

12.2.3 Device positioning and environmental conditions

The positioning of the device under test within the test volume shall be set as defined in Clause 9.4.

The environmental requirements for the device under test shall be set as defined in Annex D.

12.2.4 System Description

12.2.4.1 Solution Overview

The setup described in Clause 6.3.2.1 or Clause 6.3.2.2 shall be used, depending on the applicable test case.

12.2.4.2 Configuration

The concept and configuration of the test setup is given in Clause 6.3.2.1 or Clause 6.3.2.2, depending on the applicable test case.

12.2.4.3 Calibration

The calibration procedure is specific to the test concept and configuration, therefore is unique for each implementation. The calibration procedure shall be documented by each lab, with enough details to allow third party verification. Examples for signal level calibration are given in Annex F.

12.2.5 Figure of Merit

The performance metric is given in Clause 5.

12.2.6 Test procedure

12.2.6.1 Initial conditions

Initial conditions are a set of test configurations the UE shall be tested in and the steps for the SS to take with the UE to reach the correct measurement state for each test case.

1. Ensure environmental requirements of Annex A are met.
2. Configure the test system according to Clauses 12.2.1 and 12.2.2 for the applicable test case.
3. Verify the implementation of the channel model as specified in Clause 12.2.2.

NOTE: The verification of the channel model implementation can be part of the laboratory accreditation process i.e. performed once for each channel model, and will remain valid as long as the setup and instruments remain unchanged. Otherwise the channel model validation may need to be performed prior to starting each throughput test.

4. Position the UE in the chamber according to Clause 12.2.3.
5. Power on the UE.
6. Set up the connection.

12.2.6.2 Test procedure

The following steps shall be followed in order to evaluate MIMO OTA performance of the DUT:

1. Generate a test signal by the SS. The SS transmits the signal through the test system to the DUT.
2. Search for the minimum average DL RS ERPE (or SIR) level resulting in a MIMO OTA throughput of at least 70 % of the maximum theoretical throughput. The measurement procedure shall be based on sending a pre-defined number of subframes for each throughput sample for each DL RS EPRE (or SIR) level. When all

samples have been collected for a specific DL RS EPRE (or SIR) level, the procedure is repeated for other DL RS EPRE (or SIR) levels. Alternatively, the search can be performed for each stirring combination and then average the RS EPRE (or SIR) levels when all throughput samples have been collected.

NOTE 1: The initial RS EPRE (or SIR) can be set to the user's freely selectable level.

Recommended initial RS EPRE is found in Tables 7.1-1 and 7.1-2. For the SIR control tests, ensure that the default signal level is set such that the target SIR values can be achieved when utilizing the SIR validation procedure defined in clauses 5.1.2.2 and 5.1.2.3.

NOTE 2: To meet the throughput value target DL RS EPRE (or SIR) level can be changed using user's freely selectable algorithm.

NOTE 3: The average throughput calculated from all samples collected for each RS EPRE (or SIR) level is reported as the MIMO OTA throughput.

NOTE 4: The downlink RS EPRE (or SIR) step size shall be no more than 0.5 dB, when RF power level is near the MIMO OTA throughput sensitivity level.

NOTE 5: Assuming that the default signal level meets the criteria in NOTE 1, the interference level will be adjusted to achieve the target SIR.

3. The minimum average DL RS EPRE (or SIR) level that results in a MIMO OTA throughput of at least 70 % of the maximum theoretical throughput shall be reported.

12.2.7 Measurement Uncertainty budget

The measurement uncertainty budget for the test methodology is given in Annex B.

12.3 RTS method test procedure

12.3.1 Base Station configuration

The SS parameter settings shall be set according to Clause 7.1.

The emulated antenna array configuration shall be set according to Clause 8.5.

12.3.2 Channel Models

The applicable channel models are defined in Clauses 8.2 and Annex C.

12.3.3 Device positioning and environmental conditions

The positioning of the device under test within the test volume shall be set as defined in Clause 9.4.

The environmental requirements for the device under test shall be set as defined in Annex D.

12.3.4 System Description

12.3.4.1 Solution Overview

The setup described in Clause 6.3.1.3 shall be used.

Use of the RTS method for conformance test depends on the specification of the UE antenna test function which is defined in TR 36.978 [20].

12.3.4.2 Configuration

The concept and configuration of the test setup is given in Clause 6.3.1.3.

12.3.4.3 Calibration

The calibration procedure is specific to the test concept and configuration, therefore is unique for each implementation. The calibration procedure shall be documented by each lab, with enough details to allow third party verification. Examples for signal level calibration are given in Annex F.

12.3.5 Figure of Merit

The performance metric is given in Clause 5.

12.3.6 Test procedure

12.3.6.1 Initial conditions

Initial conditions are a set of test configurations the UE shall be tested in and the steps for the SS to take with the UE to reach the correct measurement state for each test case.

1. Ensure environmental requirements of Annex A are met.
2. Configure the test system according to Clauses 12.3.1 and 12.3.2 for the applicable test case.
3. Verify the implementation of the channel model as specified in Clause 12.3.2.

NOTE: The verification of the channel model implementation can be part of the laboratory accreditation process i.e. performed once for each channel model, and will remain valid as long as the setup and instruments remain unchanged. Otherwise the channel model validation may need to be performed prior to starting each throughput test.

4. Position the UE in the chamber according to Clause 12.3.3.
5. Power on the UE.
6. Set up the connection.

12.3.6.2 Test procedure

The following steps shall be followed in order to evaluate MIMO OTA performance of the DUT:

1. Measure the DUT complex antenna pattern at a nominal -60 dBm downlink power as described in subclause 6.3.1.3 first stage.
2. Select an appropriate orientation from the measured antenna pattern and establish a radiated MIMO connection to the DUT using the V and H probes as described in subclause 6.3.1.3 second stage. Measure the transmission matrix in the chamber and apply the inverse matrix to the MIMO signal. The DUT orientation at which this is done is selected to optimize the achievable isolation. The unknown gain of the DUT antennas represented by the absolute accuracy of the RSAP measurement is then de-embedded from the measured antenna pattern. This is done by comparing the RSAP measurement from the first stage at the orientation being used in the second stage, to a second RSAP measurement made in the second stage using a nominal signal of -60 dBm adjusted by the uncorrected antenna gain for that orientation. The difference in the RSAP measurements represents the true antenna gain for that orientation.
3. With the desired channel model applied, measure the isolation in dB between each stream as seen by the DUT receiver and ensure it is at least [18] dB averaged over a period of [TBD] frames.
4. Using the calibrated radiated connection validate monotonicity of the DUT RSAP and RSARP measurements over the range -60 dB, to -80 dBm and +/- 180 degrees. The step size for RSAP shall be [1] dB and the step size for RSARP shall be [5] degrees.

5. Once monotonicity has been validated, check the linearity of RSAP at the orientation of the peak antenna gain over the range -60 dBm to -80 dBm is $< [1]$ dB. Check the linearity of RSARP is within $[5]$ degrees over the range ± 180 degrees. If the uncorrected RSAP or RSARP results do not meet the linearity requirements, calculate and apply a transfer function to the measured patterns to ensure the necessary linearity.
6. Convolve the antenna patterns from stage 1, linearized if necessary, with the channel model in the channel emulator and perform the throughput test.
7. Record the throughput for each DUT orientation controlled by the channel emulator and each RS EPRE level.
8. Identify and report the RS EPRE (or SIR) level achieving 70% throughput for averaged throughput.

NOTE 1: The initial RS EPRE can be set to the user's freely selectable level.

Recommended initial RS EPRE is found in Tables 7.1-1 and 7.1-2. For the SIR control tests, ensure that the default signal level is set such that the target SIR values can be achieved when utilizing the SIR validation procedure defined in clause 5.1.2.4.

NOTE 2: To meet the throughput value target DL RS EPRE level can be changed using user's freely selectable algorithm.

NOTE 3: Assuming that the default signal level meets the criteria in NOTE 1, the interference level will be adjusted to achieve the target SIR.

12.3.7 Measurement Uncertainty budget

The measurement uncertainty budget for the test methodology is given in Annex B.

12.4 Comparison of methodologies

The methodologies which tests plans are described Clause 12, can be broadly classified into 3 categories:

- 1) Reverberation Chamber (RC);
- 2) Anechoic Chamber (AC);
- 3) Multi-stage Method.

The content of the Table 12.4-1 is based on what has been validated as well as currently available state-of-the-art information, and may be reconsidered when the state of the art technology progresses.

Table 12.4-1: Simplified methodology comparison

| Attribute | Reverberation Chamber | | Anechoic Chamber | Multi-stage methods |
|--|---|---|---|--|
| | RC | RC + CE | Multi probe | 2 stage method rad. |
| Channel Modelling aspects | | | | |
| 2D/3D dimension over which the signals simultaneously arrive at the DUT location | 3D ¹ | 3D ¹ | 2D | 2D ¹¹ |
| Directional distribution of angles of arrival | Random | Random | Selected as defined by SCME channel model in Clause 8 | Selected as defined by SCME channel model in Clause 8 |
| Channel model with controllable spatial characteristics | no | no | Yes ² | Yes ² |
| Angular spread | Statistically isotropic | Statistically isotropic | Selected as defined by SCME channel model in Clause 8 | Selected as defined by SCME channel model in Clause 8 |
| Ability to control angular spread | no | no | Yes ² | Yes ² |
| Power delay profile | Exponential decay | Selected as defined by channel model in Annex C | Selected as defined by SCME channel model in Clause 8 | Selected as defined by SCME channel model in Clause 8 |
| Ability to control power delay profile | Partly controllable ^{2,3} | Yes ² | Yes ² | Yes ² |
| UE speed | Approximately 1Km/h | 30Km/h | 30Km/h | 30Km/h |
| Ability to control UE speed | No | Yes ² | Yes ² | Yes ² |
| UE direction of travel | N/A | N/A | 120° as specified in Clause 8 | 120° as specified in Clause 8 |
| Ability to control direction of travel | N/A | N/A | Yes ² | Yes ² |
| Supported channel models | NIST | Short Delay Spread Long Deay Spread | SCME Uma SCME Umi | SCME Uma SCME Umi |
| BS antenna configuration | Uncorrelated | Selected as defined in Clause 8.5 | Selected as defined in Clause 8.5 | Selected as defined Clause 8.5 |
| Ability to control BS antenna configuration | No | Yes ² | Yes ² | Yes ² |
| XPR (defined in Clause 8.2) | N/A | N/A | 9dB | 9dB |
| V/H ratio | 0dB on average | 0dB on average | 0.83 dB for SCME UMi 8.13 dB for SCME UMa | 0.83 dB for SCME UMi 8.13 dB for SCME UMa |
| Ability to control XPR and V/H | No | No | Yes ² | Yes ² |
| MIMO OTA attributes not yet tested | | | | |
| Ability to control noise and interference direction | Limited ⁴ | Limited ⁴ | Yes ² | Yes ² |
| DUT size constraints | Depends on chamber size ⁵ and stirrer size | Depends on chamber size ⁵ and stirrer size | Depends on chamber size ⁵ , and number of active antenna probes and channel emulator ports to fit required active antenna probes | Depends on chamber size ⁵ (SISO chamber quiet zone) |
| Other Considerations | | | | |
| Non-intrusive test mode for DUT antenna pattern measurement | Not required | Not required | Not required | Required |
| Ability to distinguish performance based on device orientation relative to the field | No | No | Yes | Yes |
| Major equipment elements for MIMO OTA test setup (all need MIMO BS emulator) | MIMO capable reverberation chamber | MIMO capable reverberation chamber and channel emulator | MIMO capable anechoic chamber to fit antenna probes and channel emulator | SISO anechoic chamber with additional antenna and channel emulator |
| Number of channel emulator ports ⁷ | N/A | 4 | 16 ⁶ | 2 |
| DUT antenna polarization discrimination ⁸ | No | No | Yes | Yes |
| DUT Antenna radiation pattern adaptation, performance discrimination | Feasibility study not yet performed | Feasibility study not yet performed | Yes ⁹ | Feasibility study not yet performed ¹⁰ |

| | | | | |
|---|---|---|---------------------------------------|--|
| Number of independent measurements | 1 after sufficient number of stirrers states to ensure isotropy ¹² | 1 after sufficient number of stirrers states to ensure isotropy ¹² | 12 device rotations for 2D evaluation | Measurement of radiation pattern in 1 st stage and measurement in radiated stage for 12 rotations for 2D evaluation |
| <p>Note 1: Random distribution of angles of arrival. Isotropy is achieved after sufficient amount of test time as per Annex C.</p> <p>Note 2: Requires validation.</p> <p>Note 3: PDP modification will require new loading of chamber.</p> <p>Note 4: Feasibility study under progress.</p> <p>Note 5: Chamber size depends on the size of the UE and the frequency of the test.</p> <p>Note 6: Minimum setup configuration as per table 6.3.1.1-1.</p> <p>Note 7: Configuration reflects what has been tested. Optimization may be possible.</p> <p>Note 8: Assuming that correlation, gain imbalance, total efficiency are equivalent among DUT, purely isolating antennas polarization.</p> <p>Note 9: Based on preliminary feasibility study.</p> <p>Note 10: It will require DUT feedback mechanism.</p> <p>Note 11: 3D is possible without new test setup if 3D channel models are specified. It requires validation.</p> <p>Note 12: Isotropy is achieved after sufficient amount of isotropic states as per Annex C. The guideline for TRS, number of independent samples should be larger than 100, preferable 200 or 400 (3GPP TS 34.114 [4]).</p> | | | | |

Annex A: eNodeB Emulator Downlink power verification

A.1 Introduction

The measurements described in this clause serve three primary purposes; to confirm that:

- 1) the PDSCH total power is balanced between the MIMO transmit ports of an eNodeB emulator;
- 2) the PDCCH-EPRE vs. PDSCH-EPRE is balanced per eNodeB emulator antenna port within a given RB;
- 3) the RS-EPRE vs. PDSCH-EPRE ratio is correct per eNodeB emulator antenna port within a given RB.

A.2 Test prerequisites

The parameters specified in Table A.1-1 and Table A.1-2 below are based on the eNodeB emulator settings described in Table 7.1-1 and Table 7.1-2.

Table A.1-1: FDD eNodeB Emulator Configuration for Downlink Power Verification

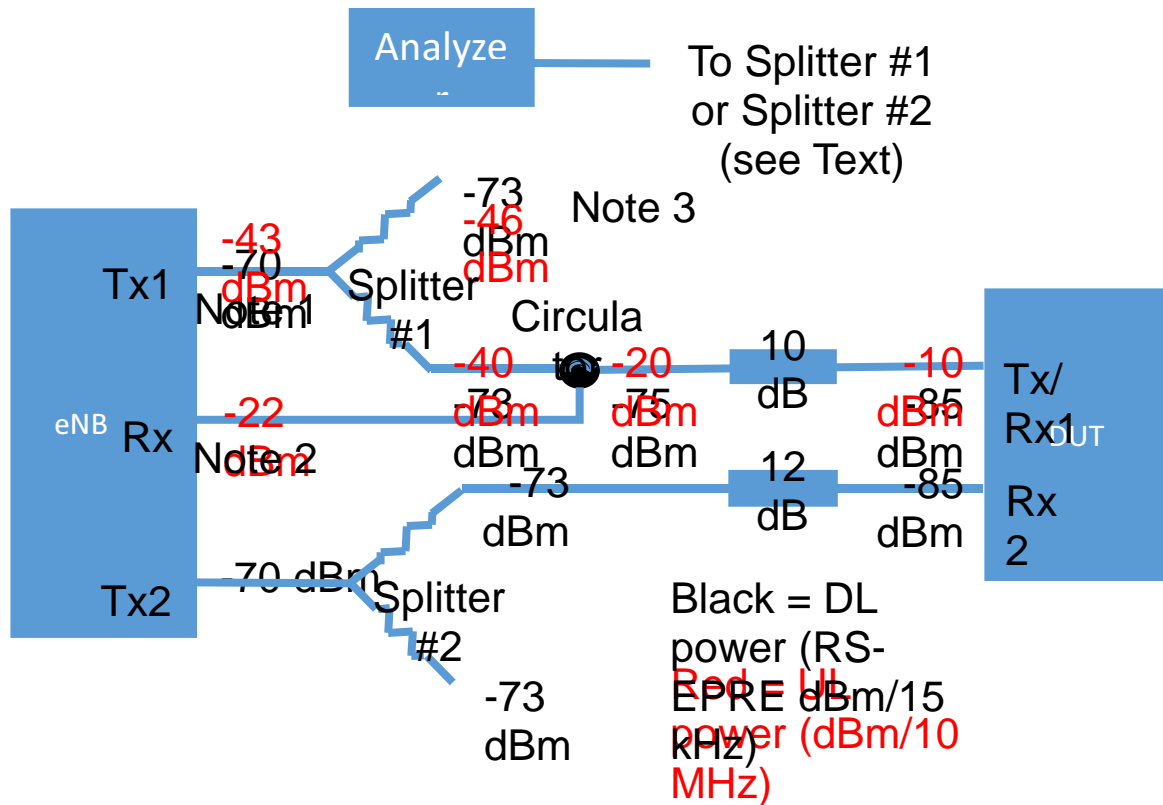
| Parameter | Value | |
|--|--|------------------|
| Operating Band/Channel (see Note) | Band 7 (3100 DL/21100 UL) Band 13 (5230 DL/23230 UL) Band 20 (6300 DL/24300 UL) | |
| Downlink Bandwidth | 10 MHz | |
| Duplex Mode | FDD | |
| Schedule Type | Reference Measurement Channel (RMC) | |
| Downlink Reference Channel | R.11 FDD | R.35 FDD |
| Downlink Modulation | 16QAM | 64QAM |
| Downlink TBS Index | 13 (RMC Defined) | 24 (RMC Defined) |
| Downlink MIMO Mode | 2x2 Open Loop Spatial Multiplexing | |
| Number of Downlink RBs | 50 | |
| Downlink RB _{Start} | 0 | |
| Downlink Power Level, eNodeB emulator | -50 dBm/15 kHz (RS-EPRE at each eNodeB emulator port) | |
| Uplink Bandwidth | 10 MHz | |
| Uplink Modulation | QPSK | 16QAM |
| Uplink TBS Index | 6 (RMC Defined) | 19 (RMC Defined) |
| Number of Uplink RBs | 50 | |
| Uplink RB _{Start} | 0 | |
| Transmit Power Control | 10 dB below the nominal maximum output power defined by the DUT power class (e.g. +13 dBm/10 MHz for a DUT with UE Power Class 3) | |
| PDSCH Power Offset Relative to RS EPRE | $\rho_A = -3$ dB $\rho_B = -3$ dB | |
| HARQ Transmissions | 1 (No HARQ) | |
| AWGN | Off | |
| OCNG | Off | |
| NOTE: | Labs executing this test may use any one of the three bands listed in Table A.1-1 according to test UE availability and band support in the eNodeB emulator. | |

Table A.1-2: TDD eNodeB Emulator Configuration for Downlink Power Verification

| Parameter | Value | |
|---|--|------------------|
| Operating Band / Channel (see Note) | Band 38 (38000) Band 39 (38450) Band 40 (39150) Band 41 (40620) | |
| Downlink Bandwidth | 20 MHz | |
| Duplex Mode | TDD | |
| Schedule Type | Reference Measurement Channel (RMC) | |
| Downlink Reference Channel | R.30 TDD | R.31-4 TDD |
| Downlink Modulation | 16QAM | 64QAM |
| Downlink TBS Index | 13 (RMC defined) | 26 (RMC defined) |
| Up/Downlink Frame Configuration | 1 | |
| Special Frame configuration | 7 | |
| Downlink MIMO Mode | 2x2 Open Loop Spatial Multiplexing | |
| Number of Downlink RBs | 100 | |
| Downlink RB _{Start} | 0 | |
| Downlink Power Level, eNodeB emulator | -50 dBm/15 kHz (RS-EPRE at each eNodeB emulator port) | |
| Uplink Bandwidth | 20 MHz | |
| Uplink Modulation | QPSK | 16QAM |
| Uplink TBS Index | 6 (RMC Defined) | 19 (RMC Defined) |
| Number of Uplink RBs | 100 | |
| Uplink RB _{Start} | 0 | |
| Transmit Power Control | 10 dB below the nominal maximum output power defined by the DUT power class (e.g. +13 dBm/20 MHz for a DUT with UE Power Class 3) | |
| PDSCH Power Offset Relative to RS EPRE | $\rho_A = -3$ dB $\rho_B = -3$ dB | |
| HARQ Transmissions | 1 (No HARQ) | |
| AWGN | Off | |
| OCNG | Off | |
| NOTE: | Labs executing this test may use any one of the four bands listed in Table A.1-2 according to test UE availability and band support in the eNodeB emulator. | |

A.3 Test Methodology

For the purpose of verifying channel power levels called for in this document, the eNodeB emulator shall be connected to a test UE (DUT) according to the configuration shown in Figure A.3-1 below:



NOTE 1: TX Port #1 is used as transmit-only on eNodeB emulators with a separate uplink RX port.

NOTE 2: If the eNodeB emulator supports full duplex operation on TX port #1, the circulator's RX port shall be terminated in a 50 Ohm load.

NOTE 3: These splitter ports will be used to provide a downlink RF sample to the analyzer and shall be terminated in a 50 Ohm load when not in use.

Figure A.3-1: eNodeB Connections for Downlink Power Verification

The analyzer shown in Figure A.3-1 above must be capable of measuring the eNodeB emulator's average PDCCH power independent of the eNodeB emulator's average PDSCH power, expressed as a PSD in dBm/15 kHz. The analyzer must also be capable of measuring RS EPRE and PDSCH EPRE in dBm/15 kHz. Any instrument capable of making these measurements is acceptable.

The following eight measurements shall be made while the UE is in an active data session and sending continuous uplink data to the eNodeB emulator using the settings described in Table A.1-1 and Table A.1-2:

- 1) Average power at TX Port 1 (through Splitter 1) of all PDCCH RBs expressed as a PSD in dBm/15 kHz
- 2) Average power at TX Port 1 (through Splitter 1) of all PDSCH RBs expressed as a PSD in dBm/15 kHz
- 3) PDSCH-EPRE at TX Port 1 (through Splitter 1) in dBm/15 kHz
- 4) RS-EPRE at TX Port 1 (through Splitter 1) in dBm/15 kHz for the Reference Signals in DL
- 5) Average power at TX Port 2 (through Splitter 2) of all PDCCH RBs expressed as a PSD in dBm/15 kHz
- 6) Average power at TX Port 2 (through Splitter 2) of all PDSCH RBs expressed as a PSD in dBm/15 kHz
- 7) PDSCH-EPRE at TX Port 2 (through Splitter 2) in dBm/15 kHz
- 8) RS-EPRE at TX Port 2 (through Splitter 2) in dBm/15 kHz

From the eight measurements described above, calculate the following:

- eNodeB TX Port 1/TX Port 2 PDCCH average power balance (in dB) across all DL RBs

- eNodeB TX Port 1/TX Port 2 PDSCH average power balance (in dB) across all DL RBs
- eNodeB RS-EPRE to PDSCH-EPRE power ratio (in dB), TX Port 1
- eNodeB RS-EPRE to PDSCH-EPRE power ratio (in dB), TX Port 2

To be considered compliant with 3GPP TS 36.521-1 [12], the following criteria must be met:

- a. eNodeB PDCCH-EPRE TX Port1/TX Port 2 power balance must be 0 dB, +/- 0.7 dB
- b. eNodeB PDSCH-EPRE TX Port 1/TX Port 2 power balance must be 0 dB, +/- 0.7 dB
- c. eNodeB PDCCH-EPRE to PDSCH-EPRE TX Port 1 power ratio must be 0 dB, +/- 0.7 dB
- d. eNodeB PDCCH-EPRE to PDSCH-EPRE TX Port 2 power ratio must be 0 dB, +/- 0.7 dB

In addition, the following criteria must be met per antenna based on the PDSCH EPRE power offset relative to RS EPRE called for in Table A.1-1 and Table A.1-2:

- e. eNodeB RS-EPRE to PDSCH-EPRE ratio must be +3 dB, +/- 0.7 dB for TX Port 1
- f. eNodeB RS-EPRE to PDSCH-EPRE ratio must be +3 dB, +/- 0.7 dB for TX Port 2

Annex B: Measurement uncertainty budget

B.1 Measurement uncertainty budget for multiprobe method

Table B.1-1: Measurement uncertainty budget for multiprobe method

| # | Description of uncertainty contribution | Details in | MPAC | | |
|----|---|-------------------------------------|--|---|----------------------|
| | | | Example Value [dB] | Prob Distr | Std Uncertainty [dB] |
| | Stage 1-DUT measurement | | | | |
| 1 | Mismatch of transmitter chain (i.e. between fixed measurement antenna and base station simulator) | TS 34.114, E.1-E.2 | 0.00 | u-shape | 0.00 |
| 2 | Insertion loss of transmitter chain | TS 34.114, E.3-E.5 | 0.00 | rect | 0.00 |
| 3 | Influence of the fixed measurement antenna cable | TS 34.114, E.6 | 0.00 | rect | 0.00 |
| 4 | Uncertainty of the absolute antenna gain of the fixed measurement antenna | TS 34.114, E.7 | 0.00 | rect | 0.00 |
| 5 | Base station simulator: uncertainty of the absolute output level | TS 34.114, E.17 [TS 36.521-1 F.1.3] | 1.00 | rect | 0.58 |
| 6 | Throughput measurement: output level step resolution | TS 34.114, E.18 | 0.25 | rect | 0.14 |
| 7 | Statistical uncertainty of throughput measurement | TS34.114, E.19 | FFS (negligible and partially included in repeatability) | | |
| 8 | Fading channel emulator output uncertainty (if used) - absolute output power - output signal stability - output stability with temperature | B.6 | 1.5dB 0.5dB 0.4dB | normal (output power) rect (stability) | 0.84 |
| 9 | AWGN flatness within LTE band | TBD (NOTE 4) | | | FFS |
| 10 | Signal-to noise ratio uncertainty, averaged over downlink transmission Bandwidth | TBD (NOTE 4) | | | FFS |
| 11 | Channel model implementation (NOTE 2) | TBD | FFS | | FFS |
| 12 | Chamber statistical ripple and repeatability | TS 34.114, E.26.A | N/A | | 0.00 |
| 13 | Additional power loss in EUT chassis | TS 34.114, E.26.B | N/A | | 0.00 |
| 14 | Quality of the quiet zone | TS 34.114, E.10 | 0.50 | std | 0.50 |
| 15 | Measurement Distance - VSWR - Chamber Standing Wave | TS 34.114, E.9 | 0.00 | | 0.00 |
| 16 | Positioner error (2nd stage RTS) (assuming < 0.5 degrees) | | N/A | | 0.00 |
| 17 | DUT sensitivity drift | TS 34.114, E.21 | 0.20 | rect | 0.12 |
| 18 | Uncertainty related to the use of the phantoms: | TR 25.914 | | | 0.00 |
| | a) Uncertainty of dielectric properties and shape of the hand phantom | A.12.3 | | | 0.00 |
| | b) Uncertainty related to the use of laptop ground plane phantom | A.12.4 | | | 0.00 |
| 19 | Random uncertainty (repeatability) | TS 34.114, E.14 | 0.20 | rect | 0.12 |
| 20 | Uncertainty associated with the stirring method and number of subframes (NOTE 3) | | N/A | | 0.00 |
| | Stage 2-Calibration measurement | | | | 0.00 |
| 21 | Uncertainty of network analyzer - Receiver and Source VNA - Receiver VNA Calibration prior to measurement | TS 34.114, E.15 | 0.50 | rect | 0.29 |
| 22 | Mismatch of transmitter chain | TS 34.114, E.1-E.2 | 0.20 | u-shape | 0.14 |

| | | | | | |
|----|--|--------------------|------|------|-------------|
| 23 | Insertion loss of transmitter chain | TS 34.114, E.3-E.5 | 0.00 | | 0.00 |
| 24 | Mismatch in the connection of calibration antenna | TS 34.114, E.1 | 0.00 | rect | 0.00 |
| 25 | Influence of the calibration antenna feed cable | TS 34.114, E.6 | | | 0.00 |
| 26 | Influence of the transmitter antennas/probes cables | TS 34.114, E.6 | 0.00 | rect | 0.00 |
| 27 | Uncertainty of the absolute gain of the transmitter antennas/probes | TS 34.114, E.7 | 0.00 | rect | 0.00 |
| 28 | Uncertainty of the absolute gain/radiation efficiency of the calibration antenna | TS 34.114, E.16 | 0.50 | std | 0.50 |
| 29 | Chamber statistical ripple and repeatability | TS 34.114, E.26.A | | | 0.00 |
| 30 | Phase Center Offset (when using horn to calibrate) | TS 34.114, E.9 | 0.00 | rect | 0.00 |
| 31 | Quality of the quiet zone (Range Ref. Antenna) | TS 34.114, E.10 | 0.50 | rect | 0.29 |
| 32 | Impact of ATF pattern error on TP - DUT RSAP measurement uncertainty TR - DUT RSARP measurement uncertainty TR | TR 37.978 10.1&2 | N/A | | 0.00 |
| 33 | Impact of non-ideal isolation between streams in radiated 2nd stage (assuming 15 dB isolation) | | N/A | | 0.00 |
| | External Amplifiers | | | | 0.00 |
| 34 | Stability | B.7.1 | 0.30 | rect | 0.17 |
| 35 | Linearity | B.7.2 | 0.10 | rect | 0.06 |
| 36 | Noise Figure | B.7.3 | 0.30 | rect | 0.17 |
| 37 | Mismatch | B.7.4 | 0.00 | rect | 0.00 |
| 38 | Gain | B.7.5 | 0.00 | rect | 0.00 |

NOTE 1: 0dB if fading for RTS is done in baseband; same as RC&CE and MPAC if fading is not in baseband

NOTE 2: assumption is that MU set to 0dB with channel model validation pass/fail limits (FFS) that have negligible impact on TP FOM; MU for channel model validation is FFS

NOTE 3: Analysis of the element associated with stirring method and number of subframes is based on existing harmonization test campaign data and can be further augmented by additional measurements. The following combinations of stirring modes and number of subframes have been identified as common use cases with the following standard uncertainties (different combinations require separate validation):

A: stepped stirring mode with 20k SF per stirring state: 0dB

B: stepped stirring mode with 400 SF per stirring state: 0.22dB

C: continuous stirring mode with 20k SF per sample: FFS

D: continuous stirring mode with 400 SF per sample: FFS

Until MU elements for continuous stirring modes have been defined, the test plan shall only consider stepped stirring approach

NOTE 4: As the applicability of SIR to MIMO OTA performance evaluation is FFS, the measurement uncertainty treatment for SIR related items will remain FFS. When the applicability of SIR is confirmed, the measurement uncertainty treatment defined in 3GPP TS 36.521-1 [12] Table F.1.4-1 for line item 8.2.1.3.1 should be considered along with the related test system constraints. Any adjustments to the test system limits or uncertainty definitions necessary for MIMO OTA performance testing should be applied.

B.2 Measurement uncertainty budget contributors for the RTS method

Table B.2-1: Measurement uncertainty budget contributors for the RTS method

| # | Description of uncertainty contribution | Details in | RTS | | |
|----|---|-------------------------------------|--|------------|----------------------|
| | | | Example Value [dB] | Prob Distr | Std Uncertainty [dB] |
| | Stage 1-DUT measurement | | | | |
| 1 | Mismatch of transmitter chain (i.e. between fixed measurement antenna and base station simulator) | TS 34.114, E.1-E.2 | 0.00 | u-shape | 0.00 |
| 2 | Insertion loss of transmitter chain | TS 34.114, E.3-E.5 | 0.00 | rect | 0.00 |
| 3 | Influence of the fixed measurement antenna cable | TS 34.114, E.6 | 0.00 | rect | 0.00 |
| 4 | Uncertainty of the absolute antenna gain of the fixed measurement antenna | TS 34.114, E.7 | 0.00 | rect | 0.00 |
| 5 | Base station simulator: uncertainty of the absolute output level | TS 34.114, E.17 [TS 36.521-1 F.1.3] | 1.00 | rect | 0.58 |
| 6 | Throughput measurement: output level step resolution | TS 34.114, E.18 | 0.25 | rect | 0.14 |
| 7 | Statistical uncertainty of throughput measurement | TS34.114, E.19 | FFS (negligible and partially included in repeatability) | | |
| 8 | Fading channel emulator output uncertainty (if used) - absolute output power - output signal stability - output stability with temperature | B.6 | 0 (NOTE 1) | | 0.00 |
| 9 | AWGN flatness within LTE band | TBD (NOTE 4) | | | FFS |
| 10 | Signal-to noise ratio uncertainty, averaged over downlink transmission Bandwidth | TBD (NOTE 4) | | | FFS |
| 11 | Channel model implementation (NOTE 2) | TBD | FFS | | FFS |
| 12 | Chamber statistical ripple and repeatability | TS 34.114, E.26.A | N/A | | 0.00 |
| 13 | Additional power loss in EUT chassis | TS 34.114, E.26.B | N/A | | 0.00 |
| 14 | Quality of the quiet zone | TS 34.114, E.10 | 0.50 | std | 0.50 |
| 15 | Measurement Distance - VSWR - Chamber Standing Wave | TS 34.114, E.9 | 0.00 | | 0.00 |
| 16 | Positioner error (2nd stage RTS) (assuming < 0.5 degrees) | | | | 0.00 |
| 17 | DUT sensitivity drift | TS 34.114, E.21 | 0.20 | rect | 0.12 |
| 18 | Uncertainty related to the use of the phantoms: | TR 25.914 | | | 0.00 |
| | a) Uncertainty of dielectric properties and shape of the hand phantom | A.12.3 | | | 0.00 |
| | b) Uncertainty related to the use of laptop ground plane phantom | A.12.4 | | | 0.00 |
| 19 | Random uncertainty (repeatability) | TS 34.114, E.14 | 0.20 | rect | 0.12 |
| 20 | Uncertainty associated with the stirring method and number of subframes (NOTE 3) | | N/A | | 0.00 |
| | Stage 2-Calibration measurement | | | | 0.00 |
| 21 | Uncertainty of network analyzer - Receiver and Source VNA - Receiver VNA Calibration prior to measurement | TS 34.114, E.15 | 0.50 | rect | 0.29 |
| 22 | Mismatch of transmitter chain | TS 34.114, E.1-E.2 | 0.00 | u-shape | 0.00 |

| | | | | | |
|----|--|--------------------|------|------|-------------|
| 23 | Insertion loss of transmitter chain | TS 34.114, E.3-E.5 | 0.00 | | 0.00 |
| 24 | Mismatch in the connection of calibration antenna | TS 34.114, E.1 | 0.00 | rect | 0.00 |
| 25 | Influence of the calibration antenna feed cable | TS 34.114, E.6 | | | 0.00 |
| 26 | Influence of the transmitter antennas/probes cables | TS 34.114, E.6 | 0.00 | rect | 0.00 |
| 27 | Uncertainty of the absolute gain of the transmitter antennas/probes | TS 34.114, E.7 | 0.00 | rect | 0.00 |
| 28 | Uncertainty of the absolute gain/radiation efficiency of the calibration antenna | TS 34.114, E.16 | 0.50 | std | 0.50 |
| 29 | Chamber statistical ripple and repeatability | TS 34.114, E.26.A | | | 0.00 |
| 30 | Phase Center Offset (when using horn to calibrate) | TS 34.114, E.9 | 0.00 | rect | 0.00 |
| 31 | Quality of the quiet zone (Range Ref. Antenna) | TS 34.114, E.10 | 0.50 | rect | 0.29 |
| 32 | Impact of ATF pattern error on TP - DUT RSAP measurement uncertainty TR - DUT RSARP measurement uncertainty TR | TR 37.978 10.1&2 | 0.20 | std | 0.20 |
| 33 | Impact of non-ideal isolation between streams in radiated 2nd stage (assuming 15 dB isolation) | | 0.20 | std | 0.20 |
| | External Amplifiers | | | | 0.00 |
| 34 | Stability | B.7.1 | | | 0.00 |
| 35 | Linearity | B.7.2 | | | 0.00 |
| 36 | Noise Figure | B.7.3 | | | 0.00 |
| 37 | Mismatch | B.7.4 | | | 0.00 |
| 38 | Gain | B.7.5 | | | 0.00 |

NOTE 1: 0dB if fading for RTS is done in baseband; same as RC&CE and MPAC if fading is not in baseband

NOTE 2: assumption is that MU set to 0dB with channel model validation pass/fail limits (FFS) that have negligible impact on TP FOM; MU for channel model validation is FFS

NOTE 3: Analysis of the element associated with stirring method and number of subframes is based on existing harmonization test campaign data and can be further augmented by additional measurements. The following combinations of stirring modes and number of subframes have been identified as common use cases with the following standard uncertainties (different combinations require separate validation):

A: stepped stirring mode with 20k SF per stirring state: 0dB

B: stepped stirring mode with 400 SF per stirring state: 0.22dB

C: continuous stirring mode with 20k SF per sample: FFS

D: continuous stirring mode with 400 SF per sample: FFS

Until MU elements for continuous stirring modes have been defined, the test plan shall only consider stepped stirring approach

NOTE 4: As the applicability of SIR to MIMO OTA performance evaluation is FFS, the measurement uncertainty treatment for SIR related items will remain FFS. When the applicability of SIR is confirmed, the measurement uncertainty treatment defined in 3GPP TS 36.521-1 [12] Table F.1.4-1 for line item 8.2.1.3.1 should be considered along with the related test system constraints. Any adjustments to the test system limits or uncertainty definitions necessary for MIMO OTA performance testing should be applied.

B.3 Measurement uncertainty budget for reverberation chamber method

Table B.3-1: Measurement uncertainty budget for reverberation chamber method

| # | Description of uncertainty contribution | Details in | RC | | |
|----|---|-------------------------------------|--|------------|----------------------|
| | | | Example Value [dB] | Prob Distr | Std Uncertainty [dB] |
| | Stage 1-DUT measurement | | | | |
| 1 | Mismatch of transmitter chain (i.e. between fixed measurement antenna and base station simulator) | TS 34.114, E.1-E.2 | 0.02 | u-shape | 0.01 |
| 2 | Insertion loss of transmitter chain | TS 34.114, E.3-E.5 | 0.00 | rect | 0.00 |
| 3 | Influence of the fixed measurement antenna cable | TS 34.114, E.6 | 0.00 | rect | 0.00 |
| 4 | Uncertainty of the absolute antenna gain of the fixed measurement antenna | TS 34.114, E.7 | 0.00 | rect | 0.00 |
| 5 | Base station simulator: uncertainty of the absolute output level | TS 34.114, E.17 [TS 36.521-1 F.1.3] | 1.00 | rect | 0.58 |
| 6 | Throughput measurement: output level step resolution | TS 34.114, E.18 | 0.25 | rect | 0.14 |
| 7 | Statistical uncertainty of throughput measurement | TS34.114, E.19 | FFS (negligible and partially included in repeatability) | | |
| 8 | Fading channel emulator output uncertainty (if used) - absolute output power - output signal stability - output stability with temperature | B.6 | 0.00 | | 0.00 |
| 9 | AWGN flatness within LTE band | TBD (NOTE 4) | | | FFS |
| 10 | Signal-to noise ratio uncertainty, averaged over downlink transmission Bandwidth | TBD (NOTE 4) | | | FFS |
| 11 | Channel model implementation (NOTE 2) | TBD | FFS | | FFS |
| 12 | Chamber statistical ripple and repeatability | TS 34.114, E.26.A | 0.30 | std | 0.30 |
| 13 | Additional power loss in EUT chassis | TS 34.114, E.26.B | 0.10 | rect | 0.06 |
| 14 | Quality of the quiet zone | TS 34.114, E.10 | N/A | | 0.00 |
| 15 | Measurement Distance - VSWR - Chamber Standing Wave | TS 34.114, E.9 | N/A | | 0.00 |
| 16 | Positioner error (2nd stage RTS) (assuming < 0.5 degrees) | | N/A | | 0.00 |
| 17 | DUT sensitivity drift | TS 34.114, E.21 | 0.20 | rect | 0.12 |
| 18 | Uncertainty related to the use of the phantoms: | TR 25.914 | | | 0.00 |
| | a) Uncertainty of dielectric properties and shape of the hand phantom | A.12.3 | | | 0.00 |
| | b) Uncertainty related to the use of laptop ground plane phantom | A.12.4 | | | 0.00 |
| 19 | Random uncertainty (repeatability) | TS 34.114, E.14 | 0.20 | rect | 0.12 |
| 20 | Uncertainty associated with the stirring method and number of subframes (NOTE 3) | | see NOTE 3 | std | see NOTE 3 |
| | Stage 2-Calibration measurement | | | | 0.00 |
| 21 | Uncertainty of network analyzer - Receiver and Source VNA - Receiver VNA Calibration prior to measurement | TS 34.114, E.15 | 0.50 | rect | 0.29 |
| 22 | Mismatch of transmitter chain | TS 34.114, E.1-E.2 | 0.00 | u-shape | 0.00 |

| | | | | | |
|----|--|---------------------|------|------|-------------|
| 23 | Insertion loss of transmitter chain | TS 34.114, E.3-E.5 | 0.00 | | 0.00 |
| 24 | Mismatch in the connection of calibration antenna | TS 34.114, E.1 | 0.00 | rect | 0.00 |
| 25 | Influence of the calibration antenna feed cable | TS 34.114, E.6 | | | 0.00 |
| 26 | Influence of the transmitter antennas/probes cables | TS 34.114, E.6 | 0.00 | rect | 0.00 |
| 27 | Uncertainty of the absolute gain of the transmitter antennas/probes | TS 34.114, E.7 | 0.00 | rect | 0.00 |
| 28 | Uncertainty of the absolute gain/radiation efficiency of the calibration antenna | TS 34.114, E.16 | 0.50 | std | 0.50 |
| 29 | Chamber statistical ripple and repeatability | TS 34.114, E.26.A | 0.30 | std | 0.30 |
| 30 | Phase Center Offset (when using horn to calibrate) | TS 34.114, E.9 | N/A | | 0.00 |
| 31 | Quality of the quiet zone (Range Ref. Antenna) | TS 34.114, E.10 | N/A | | 0.00 |
| 32 | Impact of ATF pattern error on TP - DUT RSAP measurement uncertainty TR - DUT RSARP measurement uncertainty TR | TR 37.978 10.1&2 | N/A | | 0.00 |
| 33 | Impact of non-ideal isolation between streams in radiated 2nd stage (assuming 15 dB isolation) | | N/A | | 0.00 |
| | External Amplifiers | | | | 0.00 |
| 34 | Stability | B.7.1 | | | 0.00 |
| 35 | Linearity | B.7.2 | | | 0.00 |
| 36 | Noise Figure | B.7.3 | | | 0.00 |
| 37 | Mismatch | B.7.4 | | | 0.00 |
| 38 | Gain | B.7.5 | | | 0.00 |

NOTE 1: 0dB if fading for RTS is done in baseband; same as RC&CE and MPAC if fading is not in baseband

NOTE 2: assumption is that MU set to 0dB with channel model validation pass/fail limits (FFS) that have negligible impact on TP FOM; MU for channel model validation is FFS

NOTE 3: Analysis of the element associated with stirring method and number of subframes is based on existing harmonization test campaign data and can be further augmented by additional measurements. The following combinations of stirring modes and number of subframes have been identified as common use cases with the following standard uncertainties (different combinations require separate validation):

A: stepped stirring mode with 20k SF per stirring state: 0dB

B: stepped stirring mode with 400 SF per stirring state: 0.22dB

C: continuous stirring mode with 20k SF per sample: FFS

D: continuous stirring mode with 400 SF per sample: FFS

Until MU elements for continuous stirring modes have been defined, the test plan shall only consider stepped stirring approach

NOTE 4: As the applicability of SIR to MIMO OTA performance evaluation is FFS, the measurement uncertainty treatment for SIR related items will remain FFS. When the applicability of SIR is confirmed, the measurement uncertainty treatment defined in 3GPP TS 36.521-1 [12] Table F.1.4-1 for line item 8.2.1.3.1 should be considered along with the related test system constraints. Any adjustments to the test system limits or uncertainty definitions necessary for MIMO OTA performance testing should be applied.

B.4 Measurement uncertainty budget for decomposition method

Table B.4-1: Measurement uncertainty budget for decomposition method

| Description of uncertainty contribution | Details in |
|---|--------------------------------------|
| Step 1, UE radiated measurement | |
| 1) Mismatch of transmitter chain (i.e. between probe antenna and base station simulator) | TS 34.114, E.1-E.2 |
| 2) Insertion loss of transmitter chain | TS 34.114, E.3-E.5 |
| 3) Influence of the probe antenna cable | TS 34.114, E.6 |
| 4) Uncertainty of the absolute antenna gain of the probe antenna | TS 34.114, E.7 |
| 5) Base station simulator: uncertainty of the absolute output level | TS 34.114, E.17, [TS 36.521-1 F.1.3] |
| 6) Throughput measurement: output level step resolution | TS 34.114, E.18 |
| 7) Statistical uncertainty of throughput measurement | TBD |
| 8) Channel flatness within LTE band | TBD |
| 9) Measurement distance: a) offset of UE phase centre from axis(es) of rotation b) mutual coupling between the UE and the probe antenna c) phase curvature across the UE | TS 34.114, E.9 |
| 10) Quality of quiet zone | TS 34.114, E.10 |
| 11) UE sensitivity drift | TS 34.114, E.21 |
| 12) Uncertainty related to the use of the phantoms: a) Uncertainty of dielectric properties and shape of the hand phantom. b) Uncertainty related to the use of laptop ground plane phantom: | TR 25.914 A.12.3 A.12.4 |
| 13) Geometrical and polarization constellations | TBD |
| 14) Random uncertainty (repeatability) | TS 34.114, E.14 |
| Step 2, Calibration measurement, network analyzer method, TR 34.114 figure B.1 | |
| 15) Uncertainty of network analyzer | TS 34.114, E.15 |
| 16) Mismatch in the connection of transmitter chain (i.e. between probe antenna and NA) | TS 34.114, E.1-E.2 |
| 17) Insertion loss of transmitter chain | TS 34.114, E.3-E.5 |
| 18) Mismatch in the connection of calibration antenna | TS 34.114, E.1 |
| 19) Influence of the calibration antenna feed cable | TS 34.114, E.6 |
| 20) Influence of the probe antenna cable | TS 34.114, E.6 |
| 21) Uncertainty of the absolute gain of the probe antenna | TS 34.114, E.7 |
| 22) Uncertainty of the absolute gain/radiation efficiency of the calibration antenna | TS 34.114, E.16 |
| 23) Measurement distance: a) Offset of calibration antenna's phase centre from axis(es) of rotation b) Mutual coupling between the calibration antenna and the probe antenna c) Phase curvature across the calibration antenna | TS 34.114 E.9 |
| 24) Quality of quiet zone | TS 34.114, E.10 |
| Step 3, UE conducted measurements, baseband fader | |
| 25) Mismatch uncertainty between UE antenna system radiated connectivity and UE conducted mode test connectivity | TBD |
| 26) Insertion loss of transmitter chain | TS 34.114, E.3-E.5 |
| 27) Base station simulator: uncertainty of the absolute output level | TS 34.114, E.17, [TS 36.521-1 F.1.3] |
| 28) Channel flatness within LTE band | TBD |
| 29) Channel model implementation | TBD |
| 30) Throughput measurement: output level step resolution | TS 34.114, E.18 |
| 31) Statistical uncertainty of throughput measurement | TBD |

B.5 Measurement uncertainty budget for reverberation chamber plus channel emulator method

Table B.5-1: Measurement uncertainty budget for reverberation chamber plus channel emulator method

| # | Description of uncertainty contribution | Details in | RC&CE | | |
|----|---|-------------------------------------|--|---|----------------------|
| | | | Example Value [dB] | Prob Distr | Std Uncertainty [dB] |
| | Stage 1-DUT measurement | | | | |
| 1 | Mismatch of transmitter chain (i.e. between fixed measurement antenna and base station simulator) | TS 34.114, E.1-E.2 | 0.04 | u-shape | 0.03 |
| 2 | Insertion loss of transmitter chain | TS 34.114, E.3-E.5 | 0.00 | rect | 0.00 |
| 3 | Influence of the fixed measurement antenna cable | TS 34.114, E.6 | 0.00 | rect | 0.00 |
| 4 | Uncertainty of the absolute antenna gain of the fixed measurement antenna | TS 34.114, E.7 | 0.00 | rect | 0.00 |
| 5 | Base station simulator: uncertainty of the absolute output level | TS 34.114, E.17 [TS 36.521-1 F.1.3] | 1.00 | rect | 0.58 |
| 6 | Throughput measurement: output level step resolution | TS 34.114, E.18 | 0.25 | rect | 0.14 |
| 7 | Statistical uncertainty of throughput measurement | TS34.114, E.19 | FFS (negligible and partially included in repeatability) | | |
| 8 | Fading channel emulator output uncertainty (if used) - absolute output power - output signal stability - output stability with temperature | B.6 | 1.5dB 0.5dB 0.4dB | normal (output power) rect (stability) | 0.84 |
| 9 | AWGN flatness within LTE band | TBD (NOTE 4) | | | FFS |
| 10 | Signal-to noise ratio uncertainty, averaged over downlink transmission Bandwidth | TBD (NOTE 4) | | | FFS |
| 11 | Channel model implementation (NOTE 2) | TBD | FFS | | FFS |
| 12 | Chamber statistical ripple and repeatability | G.1.2.2 | 0.40 | std | 0.40 |
| 13 | Additional power loss in EUT chassis | TS 34.114, E.26.B | 0.10 | rect | 0.06 |
| 14 | Quality of the quiet zone | TS 34.114, E.10 | N/A | | 0.00 |
| 15 | Measurement Distance - VSWR - Chamber Standing Wave | TS 34.114, E.9 | N/A | | 0.00 |
| 16 | Positioner error (2nd stage RTS) (assuming < 0.5 degrees) | | N/A | | 0.00 |
| 17 | DUT sensitivity drift | TS 34.114, E.21 | 0.20 | rect | 0.12 |
| 18 | Uncertainty related to the use of the phantoms: | TR 25.914 | | | 0.00 |
| | a) Uncertainty of dielectric properties and shape of the hand phantom | A.12.3 | | | 0.00 |
| | b) Uncertainty related to the use of laptop ground plane phantom | A.12.4 | | | 0.00 |
| 19 | Random uncertainty (repeatability) | TS 34.114, E.14 | 0.20 | rect | 0.12 |
| 20 | Uncertainty associated with the stirring method and number of subframes (NOTE 3) | | see NOTE 3 | std | see NOTE 3 |
| | Stage 2-Calibration measurement | | | | 0.00 |
| 21 | Uncertainty of network analyzer - Receiver and Source VNA - Receiver VNA Calibration prior to measurement | TS 34.114, E.15 | 0.50 | rect | 0.29 |
| 22 | Mismatch of transmitter chain | TS 34.114, E.1-E.2 | 0.00 | u-shape | 0.00 |
| 23 | Insertion loss of transmitter chain | TS 34.114, E.3-E.5 | 0.00 | | 0.00 |

| | | | | | |
|----|--|---------------------|------|------|-------------|
| 24 | Mismatch in the connection of calibration antenna | TS 34.114, E.1 | 0.00 | rect | 0.00 |
| 25 | Influence of the calibration antenna feed cable | TS 34.114, E.6 | | | 0.00 |
| 26 | Influence of the transmitter antennas/probes cables | TS 34.114, E.6 | 0.00 | rect | 0.00 |
| 27 | Uncertainty of the absolute gain of the transmitter antennas/probes | TS 34.114, E.7 | 0.00 | rect | 0.00 |
| 28 | Uncertainty of the absolute gain/radiation efficiency of the calibration antenna | TS 34.114, E.16 | 0.50 | std | 0.50 |
| 29 | Chamber statistical ripple and repeatability | G.1.2.2 | 0.40 | std | 0.40 |
| 30 | Phase Center Offset (when using horn to calibrate) | TS 34.114, E.9 | N/A | | 0.00 |
| 31 | Quality of the quiet zone (Range Ref. Antenna) | TS 34.114, E.10 | N/A | | 0.00 |
| 32 | Impact of ATF pattern error on TP - DUT RSAP measurement uncertainty TR - DUT RSARP measurement uncertainty TR | TR 37.978 10.1&2 | N/A | | 0.00 |
| 33 | Impact of non-ideal isolation between streams in radiated 2nd stage (assuming 15 dB isolation) | | N/A | | 0.00 |
| | External Amplifiers | | | | 0.00 |
| 34 | Stability | B.7.1 | | | 0.00 |
| 35 | Linearity | B.7.2 | | | 0.00 |
| 36 | Noise Figure | B.7.3 | | | 0.00 |
| 37 | Mismatch | B.7.4 | | | 0.00 |
| 38 | Gain | B.7.5 | | | 0.00 |

NOTE 1: 0dB if fading for RTS is done in baseband; same as RC&CE and MPAC if fading is not in baseband

NOTE 2: assumption is that MU set to 0dB with channel model validation pass/fail limits (FFS) that have negligible impact on TP FOM; MU for channel model validation is FFS

NOTE 3: Analysis of the element associated with stirring method and number of subframes is based on existing harmonization test campaign data and can be further augmented by additional measurements. The following combinations of stirring modes and number of subframes have been identified as common use cases with the following standard uncertainties (different combinations require separate validation):

A: stepped stirring mode with 20k SF per stirring state: 0dB

B: stepped stirring mode with 400 SF per stirring state: 0.22dB

C: continuous stirring mode with 20k SF per sample: FFS

D: continuous stirring mode with 400 SF per sample: FFS

Until MU elements for continuous stirring modes have been defined, the test plan shall only consider stepped stirring approach

NOTE 4: As the applicability of SIR to MIMO OTA performance evaluation is FFS, the measurement uncertainty treatment for SIR related items will remain FFS. When the applicability of SIR is confirmed, the measurement uncertainty treatment defined in 3GPP TS 36.521-1 [12] Table F.1.4-1 for line item 8.2.1.3.1 should be considered along with the related test system constraints. Any adjustments to the test system limits or uncertainty definitions necessary for MIMO OTA performance testing should be applied.

B.6 Fading channel emulator output uncertainty

In the case where a fading channel emulator is used, the outputs of the fading channel emulator are used to drive signals through the amplifiers, if necessary, to the probe antennas in the MIMO OTA tests either as an absolute level or as a relative level. The receiving device used is a UE. Generally, an uncertainty contribution comes from the absolute level

accuracy, non-linearity, and output signal stability of the fading channel emulator. All of the contributions should be considered. However, the applicability of each contribution is contingent on the specific measurement implementation and calibration procedure.

This uncertainty should be determined from the manufacturer's data sheet expressed in dB with a rectangular distribution, unless otherwise informed (see clause 5.1.2 in [6]). Furthermore, the uncertainty of the non-linearity and the output signal stability of the device may be included in the absolute level uncertainty. If not, the non-linearity, output signal stability and output signal stability versus temperature should be determined from the manufacturer's data sheet. Once determined, the non-linearity uncertainty and the output signal stability uncertainties should be combined with the output uncertainty using the RSS method.

B.7 External Amplifiers Uncertainty Terms

Any components in the setup can potentially introduce measurement uncertainty. It is then needed to determine the uncertainty contributors associated with the use of such components. For the case of external amplifiers, the following uncertainties should be considered but the applicability is contingent to the measurement implementation and calibration procedure.

B.7.1 Stability

An uncertainty contribution comes from the output level stability of the amplifier. Even if the amplifier is part of the system for both measurement and calibration, the uncertainty due to the stability shall be considered. This uncertainty can be either measured or determined by the manufacturers' data sheet for the operating conditions in which the system will be required to operate.

B.7.2 Linearity

An uncertainty contribution comes from the linearity of the amplifier since in most cases calibration and measurements are performed at two different input/output power levels. This uncertainty can be either measured or determined by the manufacturers' data sheet.

B.7.3 Noise Figure

When the signal goes into an amplifier, noise is added so that the SNR at the output is reduced with regard to the SNR of the signal at the input. This added noise introduces error on the signal which affects the Error Rate of the receiver thus the EVM (Error Vector Magnitude). An uncertainty can be calculated through the following formula:

$$\varepsilon_{EVM} = 20 \cdot \log \left(1 + 10^{\frac{-SNR}{20}} \right)$$

where SNR is the signal to noise ratio in dB at the signal level used during the sensitivity measurement.

B.7.4 Mismatch

If the external amplifier is used for both stages, measurement and calibration the uncertainty contribution associated with it can be considered systematic and constant -> 0dB. If it is not the case, the mismatch uncertainty at its input and output shall be either measured or determined by the method described in [11].

B.7.5 Gain

If the external amplifier is used for both stages, measurement and calibration the uncertainty contribution associated with it can be considered systematic and constant -> 0dB. If it is not the case, this uncertainty shall be considered.

Annex C: Other Environmental Test conditions for consideration

C.1 Scope

This annex contains non standard channel models which are described for evaluation purposes. Approved channel models are described in Clause 4.2.

C.2 3D isotropic Channel Models

This clause proposes three 3D isotropic channel models. One of the models is based on the NIST channel model and two of the models are based on the temporal aspects and Base Station (BS) correlation properties of the SCME UMi and SCME UMa channel models.

The proposed 3D isotropic channel models are not directly based on real life operating conditions, rather, are an attempt to model the properties of the reverberation chamber which has been shown to represent a statistically isotropic environment provided sufficient averaging is performed using mode stirring. The instantaneous conditions within the reverberation chamber are not isotropic.

The following 3D isotropic model is based on the PDP and BS correlation of the SCME Urban Micro-cell model with isotropic AoAs and modified XPR values and Velocity.

Table C.2-1: Short delay spread low correlation channel model

| Cluster # | Delay [ns] | | | Power [dB] | | | AoD [°] | AoA ¹ |
|---|------------|-----|-----|------------|-------|-------|---------|---------------------------------------|
| 1 | 0 | 5 | 10 | -3.0 | -5.2 | -7.0 | 6.6 | Average isotropic ¹ |
| 2 | 285 | 290 | 295 | -4.3 | -6.5 | -8.3 | 14.1 | Average isotropic ¹ |
| 3 | 205 | 210 | 215 | -5.7 | -7.9 | -9.7 | 50.8 | Average isotropic ¹ |
| 4 | 660 | 665 | 670 | -7.3 | -9.5 | -11.3 | 38.4 | Average isotropic ¹ |
| 5 | 805 | 810 | 815 | -9.0 | -11.2 | -13.0 | 6.7 | Average isotropic ¹ |
| 6 | 925 | 930 | 935 | -11.4 | -13.6 | -15.4 | 40.3 | Average isotropic ¹ |
| Delay spread [ns] | | | | | | | | 294 |
| Cluster AS AoD / AS AoA [°] | | | | | | | | 5 / Average isotropic ¹ |
| Cluster PAS shape | | | | | | | | 3D uniform |
| Total AS AoD / AS AoA [°] | | | | | | | | 18.2 / Average isotropic ¹ |
| Mobile speed [km/h] | | | | | | | | 3, 30 |
| XPR ² | | | | | | | | 0 dB |
| NOTE 1: The angles of arrival are said to be Average Isotropic when the incoming field satisfies the Isotropy requirements established in [16]. | | | | | | | | |
| NOTE 2: V & H components based on assumed BS antenna array configurations in Clause 7.2. | | | | | | | | |

The following 3D isotropic model is based on the PDP and BS correlation of the SCME Urban Macro-cell model with isotropic AoAs and modified XPR values and velocity.

Table C.2-2: Long delay spread high correlation channel model

| Cluster # | Delay [ns] | | | Power [dB] | | | AoD [°] | AoA [°] |
|---|------------|------|------|------------|-------|-------|---------|--------------------------------------|
| 1 | 0 | 5 | 10 | -3 | -5.2 | -7 | 82.0 | Average isotropic ¹ |
| 2 | 360 | 365 | 370 | -5.2 | -7.4 | -9.2 | 80.5 | Average isotropic ¹ |
| 3 | 255 | 260 | 265 | -4.7 | -6.9 | -8.7 | 79.6 | Average isotropic ¹ |
| 4 | 1040 | 1045 | 1050 | -8.2 | -10.4 | -12.2 | 98.6 | Average isotropic ¹ |
| 5 | 2730 | 2735 | 2740 | -12.1 | -14.3 | -16.1 | 102.1 | Average isotropic ¹ |
| 6 | 4600 | 4605 | 4610 | -15.5 | -17.7 | -19.5 | 107.1 | Average isotropic ¹ |
| Delay spread [ns] | | | | | | | | 839.5 |
| Cluster AS AoD / AS AoA [°] | | | | | | | | 2 / Average isotropic ¹ |
| Cluster PAS shape | | | | | | | | 3D uniform |
| Total AS AoD / AS AoA [°] | | | | | | | | 7.9 / Average isotropic ¹ |
| Mobile speed [km/h] | | | | | | | | 3, 30 |
| XPR ² | | | | | | | | 0 dB |
| NOTE 1: The angles of arrival are said to be average isotropic when the incoming field satisfies the isotropy requirements established in [16]. | | | | | | | | |
| NOTE 2: V & H components based on assumed BS antenna array configurations in Clause 7.2. | | | | | | | | |

The following 3D isotropic model is based on the NIST model with isotropic AoAs and added XPR values and Velocity. The cluster model described below is a simplification of the full model, where a continuous exponential decaying power transfer function with an RMS delay spread of 80 ns is obtained.

Table C.2-3: Isotropic model based on the NIST channel model

| Cluster # | Delay [ns] | Power [dB] | AoD [°] | AoA [°] |
|---|------------|------------|---------|--------------------------------------|
| 1 | 0 | 0.0 | N/A | Average isotropic ¹ |
| 2 | 40 | -1.7 | N/A | Average isotropic ¹ |
| 3 | 120 | -5.2 | N/A | Average isotropic ¹ |
| 4 | 180 | -7.8 | N/A | Average isotropic ¹ |
| 5 | 210 | -9.1 | N/A | Average isotropic ¹ |
| 6 | 260 | -11.3 | N/A | Average isotropic ¹ |
| 7 | 350 | -15.2 | N/A | Average isotropic ¹ |
| Delay spread [ns] | | | | 80 |
| Cluster AS AoD / AS AoA [°] | | | | N/A / Average isotropic ¹ |
| Cluster PAS shape | | | | 3D uniform |
| Total AS AoD / AS AoA [°] | | | | N/A / Average isotropic ¹ |
| Mobile speed [km/h] | | | | 1 |
| XPR ² | | | | 0 dB |
| NOTE 1: The angles of arrival are said to be average isotropic when the incoming field satisfies the isotropy requirements established in [16]. | | | | |
| NOTE 2: V & H components based on assumed BS antenna array configurations in Clause 7.2. | | | | |

The parameters of the channel models are the expected parameters for the MIMO OTA channel models. However, the final channel model achieved for different methods could be a combined effect of the chamber and the channel emulator.

The Rayleigh fading may be implementation specific. However, the fading can be considered to be appropriate as long as the statistics of the generated Rayleigh fading are within standard requirement on Rayleigh fading statistics.

C.3 Verification of Channel Model implementations

Channel Models have been specified in Clause C.2.

This clause describes the MIMO OTA validation measurements, in order to ensure that the channel models are correctly implemented and hence capable of generating the propagation environment, as described by the model, within a test area. Measurements are done mainly with a Vector Network Analyzer (VNA) and a spectrum analyzer.

C.3.1 Measurement instruments and setup

The measurement setup includes the following equipment:

Table C.3.1-1: Measurement equipment list for the verification procedure

| Item | Quantity | Item |
|------|----------|-----------------------|
| 1 | 1 | Channel Emulator |
| 2 | 1 | Signal Generator |
| 3 | 1 | Spectrum Analyzer |
| 4 | 1 | VNA |
| 5 | 1 | Electric Dipole |
| 6 | 1 | Wideband test antenna |

C.3.1.1 Vector Network Analyzer (VNA) setup

Most of the measurements are performed with a VNA. An example set of equipment required for this set-up is shown in Figure C.3.1.1-1. VNA transmits frequency sweep signals through the MIMO OTA test system.

A test antenna, within the test area, receives the signal and VNA analyzes the frequency response of the system.

A number of traces (frequency responses) are measured and recorded by VNA and analyzed by a post processing SW, e.g., Matlab. Special care has to be taken into account to keep the fading conditions unchanged, i.e. frozen, during the short period of time of a single trace measurement. The fading may proceed only in between traces. This setup can be used to measure PDP, BS antenna correlation, Rayleigh fading and Isotropy of the Channel models defined in Clause C.2.

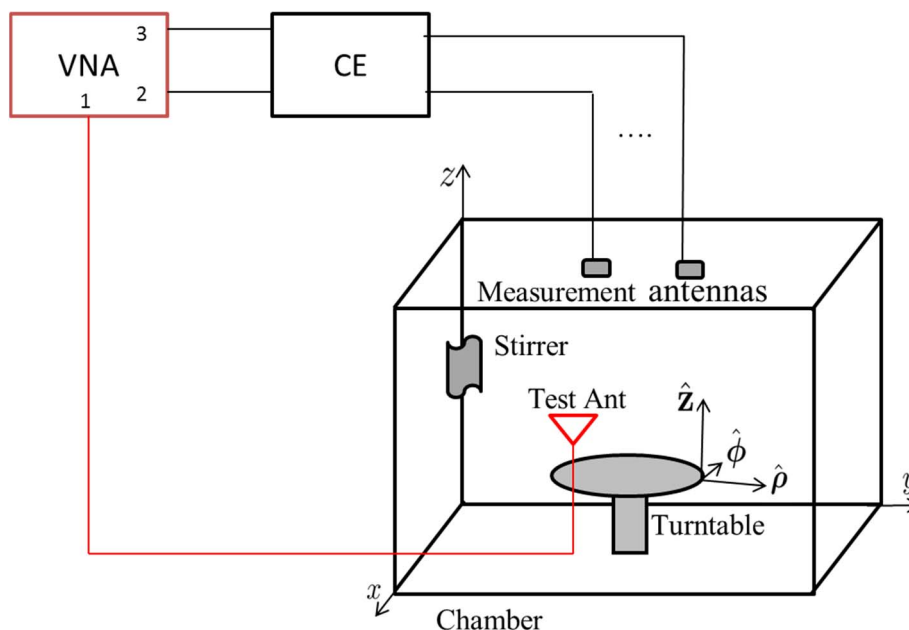


Figure C.3.1.1-1: Setup for VNA measurements for reverberation chamber and channel emulator methods

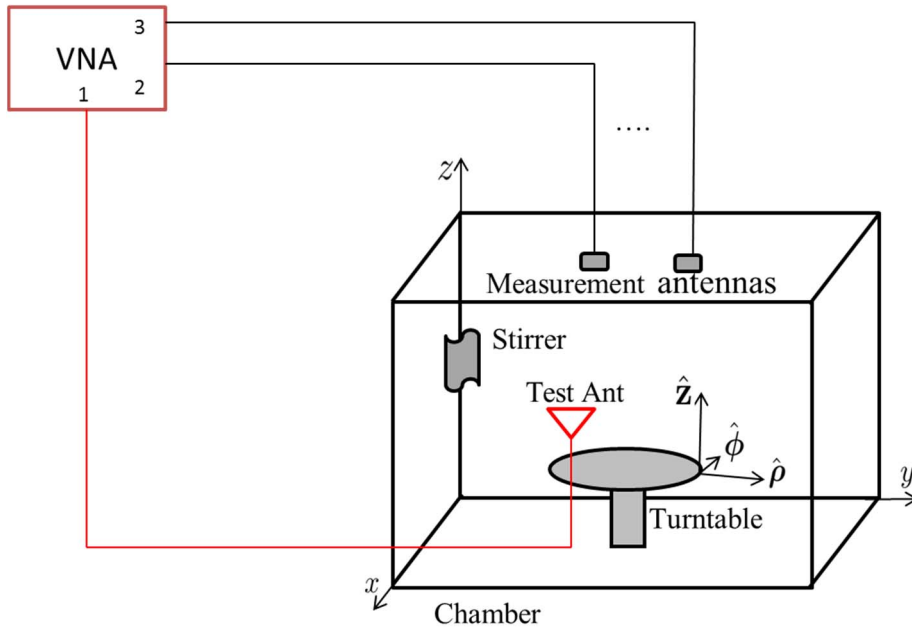


Figure C.3.1.1-2: Setup for VNA measurements for reverberation chamber-only methods

C.3.1.2 Spectrum Analyzer (SA) setup

The Doppler spectrum is measured with a Spectrum Analyzer as shown in Figure C.3.1.2-1. In this case a Signal generator transmits CW signal through the MIMO OTA test system. The signal is received by a test antenna within the test area. Finally the signal is analyzed by a Spectrum Analyzer and the measured spectrum is compared to the target spectrum. This setup can be used to measure Doppler Spectrum of the Channel models defined in Clause C.2.

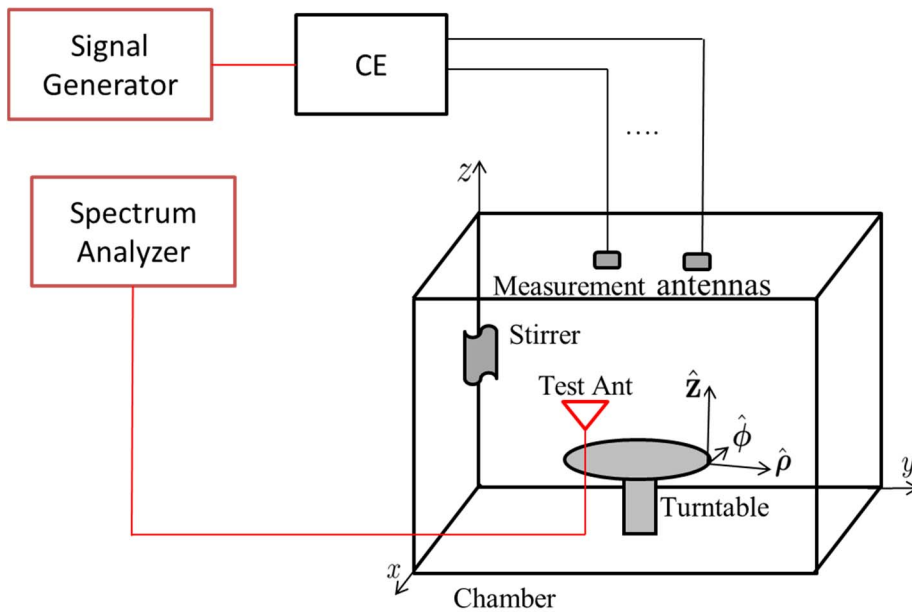


Figure C.3.1.2-1: Setup for SA measurements for reverberation chamber and channel emulator methods

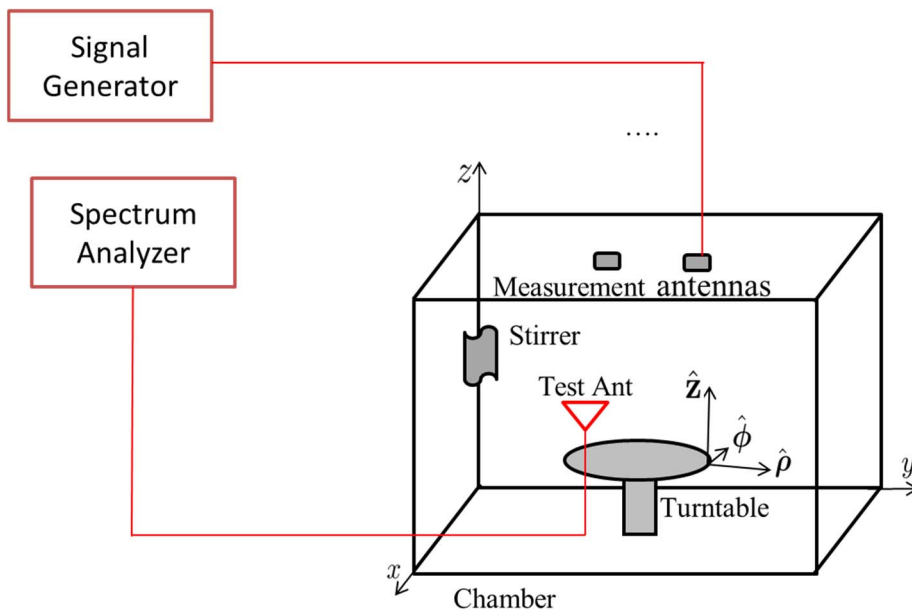


Figure C.3.1.2-3: Setup for SA measurements for reverberation chamber-only methods

C.3.2 Validation measurements

C.3.2.1 Power Delay Profile (PDP)

This measurement checks that the resulting Power Delay Profile (PDP) is as defined in the channel model.

Method of measurement:

Step the chamber stirring sequence and store traces from VNA measurements at each step until the Number of Traces specified in Table C.3.2.1-1 is obtained. For the RC+CE, also the channel model emulation will be stepped for each VNA trace.

The VNA sampling should be such that independent samples of the channel model impulse response are obtained. This is ensured if the effective distance travelled by the UE between faded samples of the channel model is as defined in the table below, regardless of the number of stirring positions in the chamber stirring sequence. To accurately emulate the longest PDP duration t_f of 5 μ s, the relationship $N/\text{Span} = t_f$ must be satisfied.

VNA settings:

Table C.3.2.1-1: VNA settings for PDP

| Item | Unit | Value |
|--|-------------------|---|
| Center frequency | MHz | Downlink Center Frequency in 36.508 [19] as required per band |
| Span | MHz | 200 |
| RF output level | dBm | 0 |
| Number of traces | | 1000 |
| Effective distance traveled by UE between faded channel model samples | wavelength (Note) | > 2 |
| Number of points in the trace | | 1101 |
| Averaging | | 1 |
| NOTE: Time [s] = distance [λ] / MS speed [λ /s] | | |
| MS speed [λ /s] = MS speed [m/s] / Speed of light [m/s] * Center frequency [Hz] | | |

Channel model specification:

Table C.3.2.1-2: Channel model specification for PDP

| Item | Unit | Value |
|-----------------------|------------|--|
| Center frequency | MHz | Downlink Center Frequency in 36.508 [19] as required per band |
| Channel model samples | wavelength | > 2000 |
| Channel model | | As specified in Clause C.2 |

Method of measurement result analysis:

Measured VNA traces (frequency responses $H(t,f)$) are saved into a hard drive. The data is read into, e.g., Matlab. The analysis is performed by taking the Fourier transform of each frequency response. The resulting impulse responses $h(t, \tau)$ are averaged in power over time (or samples):

$$P(\tau) = \frac{1}{T} \sum_{t=1}^T |h(t, \tau)|^2$$

Finally the resulting PDP is shifted in delay, such that the first tap is on delay zero.

The reference PDP plots from Table C.2-1, Table C.2-2 and Table C.2-3 are shown in Figure C.3.2.1-1.

In a reverberation chamber, when a channel emulator is not used and the PDP is therefore an exponential decay, such as the NIST channel model, only the inherent RMS Delay Spread of the reverberation chamber needs to be calculated. The selection of the $T h_i(t, \tau)$ measurements has to be performed when the absorber loading technique is used to tune the RMS DS in an RC. Alternatively, the sample selection technique allows for selecting a subset of $M h_i(t, \tau)$ measurements which provide the desired RMS DS, and in this case the averaging has to be performed only over the selected subset of M channel impulse responses.

The calculation of RMS delay spread is performed on the time domain data as the square root of the second central moment of the PDP, that is:

$$\sigma_{\tau} = \sqrt{\sum_{\tau} \tau^2 \frac{PDP(\tau)}{\sum_{\tau} PDP(\tau)} - \left(\frac{\sum_{\tau} \tau \frac{PDP(\tau)}{\sum_{\tau} PDP(\tau)}}{\sum_{\tau} PDP(\tau)} \right)^2}$$

Only PDP values above a threshold of -60 dB should be included in the calculation of the RMS delay spread.

The expected RMS delay spread for the NIST channel model is 80 ns.

OTA antenna configuration: Fixed measurement source antenna.

Measurement antenna:

A suitable wideband test antenna.

Tolerances:

Performance bounds of (cluster power ± 0.85 dB and excess delay ± 1 ns).

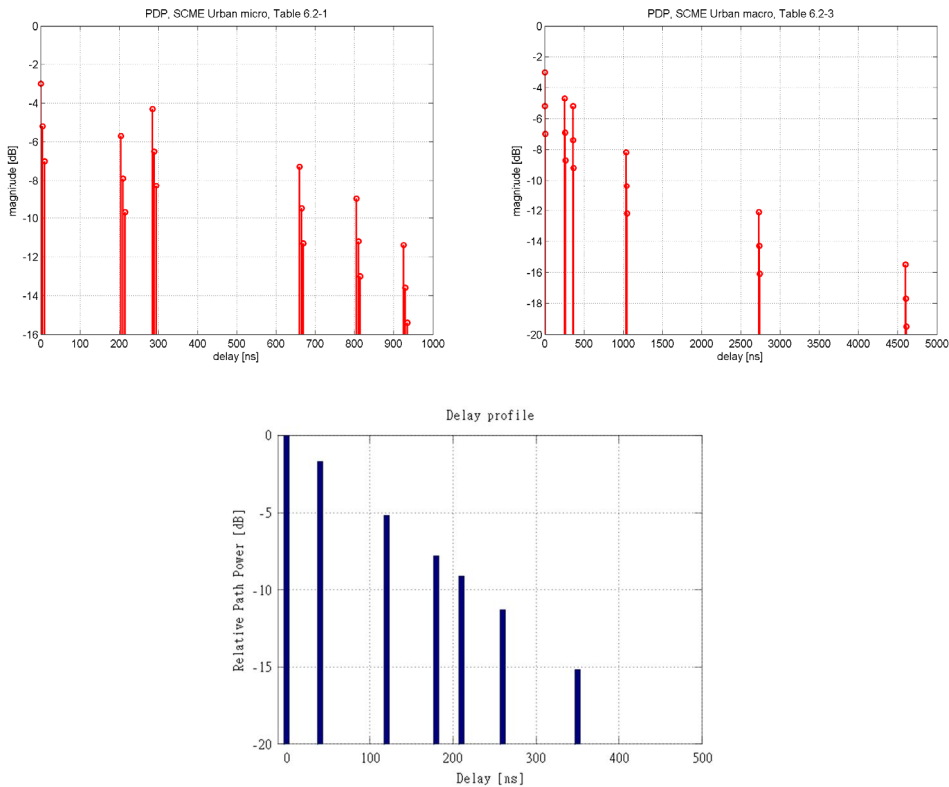


Figure C.3.2.1-1: Reference PDP values for the short delay spread low correlation and long delay spread high correlation and NIST channel models plotted from Table C.2-1, Table C.2-2 and Table C.2-3

C.3.2.2 Doppler for 3D isotropic models

This measurement checks that the resulting is as defined in the channel model.

Doppler. Method of measurement:

For Doppler validation, two methods could be used to measure the Doppler spectrum. The first uses a CW tone from the Signal Generator fed directly, or via the channel emulator if used, to the fixed measurement antennas and is recorded by the spectrum analyzer. For the second method, the input signal from the VNA is fed directly, or via the channel emulator if used, to the fixed measurement antennas of the chamber.

For the first method, a sine wave (CW, carrier wave) signal is transmitted from the signal generator. The signal is connected from the signal generator to the channel emulator via cables, or alternatively directly fed to the chamber measurement antenna for the RC methodology. For the RC+CE methodology, the channel emulator output signals are then transferred via cables to the fixed measurement antennas (possibly via amplifiers). The fixed measurement antennas radiate the signals over the air to the test antenna. The Doppler spectrum is measured by the spectrum analyzer having the stirring sequence and, if applicable, the channel emulation active and the trace is saved. The signal generator and the spectrum analyzer reference oscillators should be synchronized, in order to minimize frequency shift etc.

Alternatively, the Doppler spectrum can be measured with a VNA. Frequency sweeps are measured with the VNA for a complete stirring sequence, thus collecting samples of the chamber transfer function $H(f, s_n)$ for each fixed stirrer position s_n . To get a correct estimate of the Doppler power spectrum, the spatial distance between the stirrer positions should be small enough to satisfy Nyquist theorem. $H(f, s_n)$ is Fourier transformed according to

$$H(f, \rho) = FFT(H(f, s_n))$$

The Doppler spectrum $D(f, \rho)$ can then be calculated using

$$D(f, \rho) = |H(f, \rho)|^2$$

The discrete Doppler power spectrum will now have a frequency axis ranging from 0 to N-1, where N is the number of stirrer positions used. To convert this into a Doppler frequency domain, the sampling theorem gives a frequency axis in the interval $[-\rho_{\max}, \rho_{\max}]$, where

$$\rho_{\max} = \frac{1}{2\Delta t}$$

and the frequency step between each Doppler frequency sample is given by

$$\Delta\rho = \frac{\rho_{\max}}{N} = \frac{1}{2N\Delta t}$$

Δt is the time step between the measured samples.

Signal generator settings:

Table C.3.2.2-1: Signal generator settings for Doppler

| Item | Unit | Value |
|------------------|------|---|
| Center frequency | MHz | Downlink center frequency in 36.508 [19] as required per band |
| Output level | dBm | 0 |
| Modulation | | OFF |

Spectrum analyzer settings:

Table C.3.2.2-2: Spectrum analyzer settings for Doppler

| Item | Unit | Value |
|------------------|------|---|
| Center frequency | MHz | Downlink center frequency in 36.508 [19] as required per band |
| Span | Hz | 3x maximum Doppler |
| RBW | Hz | 1 |
| VBW | Hz | 1 |
| Number of points | | 101 |
| Averaging | | 100 |

VNA settings

Table C.3.2.2-3: VNA settings for Doppler

| Item | Unit | Value |
|------------------|------|---|
| Center frequency | MHz | Downlink center frequency in 36.508 [19] as required per band |
| Span | MHz | Downlink portion of frequency band |
| RF output level | dBm | 0 |
| Number of traces | | 600 |
| Number of points | | 1401 |
| Averaging | | 1 |

Channel model specification:

Table C.3.2.2-4: Channel model specification for Doppler

| Item | Unit | Value |
|------------------|------|---|
| Center frequency | MHz | Downlink center frequency in 36.508 [19] as required per band |
| Channel model | | As specified in Clause C.2 |

Method of Measurement Result Analysis:

Calculate the square root of the second central moment of the Doppler spectrum from center frequency to the frequency corresponding to -30 dB (make sure that no noise is included in the calculations). Use the value obtained (Δf) to calculate the equivalent speed (Δv) using the following equation:

$$\Delta v = \frac{\Delta f * c}{f_0}$$

where c is the speed of light and f_0 is the carrier frequency.

The reference classical Doppler spectrum is shown in figure C.3.2.2-1. B_d is the maximum Doppler shift expected for the mobile speed used for the measurements.

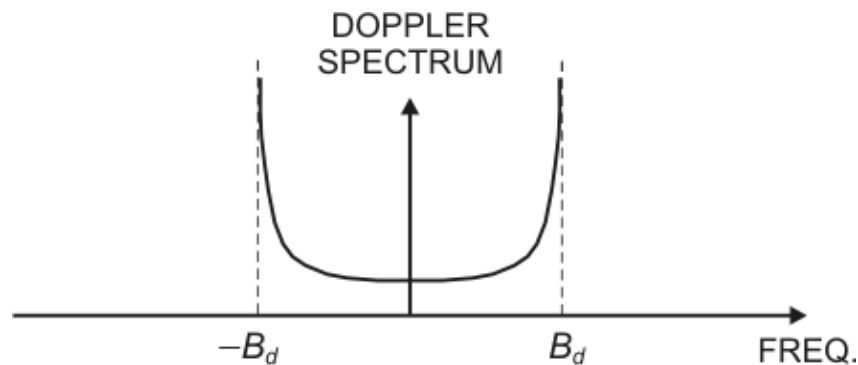


Figure C.3.2.2-1: Reference Doppler Spectrum for Jake's fading models

OTA antenna configuration: Fixed measurement source antennas.

Measurement antenna: A suitably wideband test antenna.

Tolerances:

The equivalent speed obtained shall be within 30 km/h +/- 5 km/h.

C.3.2.3 Base Station antenna correlation for 3D isotropic models

This measurement checks that the resulting Base Station (BS) antenna correlation follows the computed values from the channel parameters given in tables C.2-1, C.2-2 and C.2-3.

Method of measurement:

For correlation validation, the input signal from the VNA is fed directly (for table C.2.-3), or via the channel emulator (for tables C.2-1 and C.2-2), to the fixed measurement antennas of the reverberation chamber.

Step the chamber stirring sequence and store traces from VNA measurements at each step until the Number of Traces specified in Table C.3.2.3-1 is obtained. For the RC+CE, also the channel model emulation will be stepped for each VNA trace.

Each of the paths for the two transmit streams must be measured separately using the procedure above. The samples for each path must be taken for the exact same channel emulator and stirring positions.

The VNA sampling should be such that independent samples of the channel model impulse response are obtained. This is ensured if the effective distance travelled by the UE between faded samples of the channel model is as defined in the table below.

VNA settings:

Table C.3.2.3-1: VNA settings for BS antenna correlation

| Item | Unit | Value |
|---|-------------------|---|
| Center frequency | MHz | Downlink center frequency in 36.508 [19] as required per band |
| Span | MHz | Same as signal bandwidth |
| RF output level | dBm | 0 |
| Number of traces | | 600 |
| Effective distance traveled by UE between faded channel model samples | wavelength (Note) | > 2 |
| Number of points | | Configured to obtain 1 MHz step size |
| Averaging | | 1 |
| NOTE: Time [s] = distance [λ] / MS speed [λ /s] MS speed [λ /s] = MS speed [m /s] / Speed of light [m/s] * Center frequency [Hz] | | |

Channel model specification:**Table C.3.2.3-2: Channel model specification for BS antenna correlation**

| Item | Unit | Value |
|-----------------------|------------|---|
| Center frequency | MHz | Downlink center frequency in 36.508 [19] as required per band |
| Channel model samples | wavelength | > 2000 |
| Channel model | | As specified in Clause C.2 |

Method of Measurement Results Analysis

Compute the correlation between two traces (e.g. S21 and S31) which represents the correlation between two transmit streams. This correlation should match that of the channel model used.

OTA antenna configuration: Fixed measurement source antennas.

Measurement antenna: A suitably wideband test antenna.

Tolerances:

The amplitude of the complex correlation averaged over the channel bandwidth shall be within the interval 0.05 – 0.2.

C.3.2.4 Rayleigh fading

This measurement checks that the resulting fading of the MIMO OTA system is Rayleigh as per the channel model.

Method of measurement:

For Rayleigh Fading validation, the input signal from the VNA is fed to one of the two input ports of the channel emulator and further to the fixed measurement transmit antennas of the reverberation chamber. The same stirring sequence, number of active CE output ports, channel model and CE channel model emulation as used for the DUT measurement, as well as the chamber loading used for the DUT measurement and PDP validation, should be used for the validation measurement.

In order to achieve statistical significance, the number of samples should be >1000. If the DUT stirring sequence has less than 1000 steps, the number of measurements shall be increased proportionally without altering the fading envelope distribution. This is done reducing the CE IR, and the stirring step by dividing them by an N value such as the resultant number of measurements will be > 1000 while keeping the same amplitude distribution. e.g. if the stirring sequence has 120 steps, and for every measurement the stirrers move equally 9 degrees, then using N = 9 for 1080 samples will result in changing the stirring sequence to 1 degree per measurement for all the stirrers, and dividing the IR step by 9. If needed, the IR should be rounded to the closest integer.

Step the chamber stirring sequence and store traces from VNA measurements at each step until the Number of Traces specified in Table C.3.2.4-1 is obtained. For the RC+CE, also the channel model emulation will be stepped for each VNA trace.

The VNA sampling should be such that independent samples of the channel model impulse response are obtained. This is ensured if the effective distance travelled by the UE between faded samples of the channel model is as defined in the table below.

The procedure described above shall be performed in two of the extreme test volume validation positions (TVVPs) defined in Annex G. Observe that each TVVP consists of three orientations, which means that in total 6 Rayleigh validation measurements shall be performed and the results from each of these measurements shall pass the limits. The same stirring sequence, number of active CE output ports, channel model and CE channel model emulation shall be used at each of the chosen TVVPs.

VNA settings:

Table C.3.2.4-1: VNA settings for Rayleigh fading

| Item | Unit | Value |
|---|-------------------|---|
| Center frequency | MHz | Downlink center frequency in 36.508 [19] as required per band |
| Span | MHz | Same as signal bandwidth |
| RF output level | dBm | 0 |
| Number of traces | | >1000 |
| Effective distance traveled by UE between faded channel model samples | wavelength (Note) | > 2 |
| Number of points | | Configured to obtain 1 MHz step size |
| Averaging | | 1 |
| NOTE: Time [s] = distance [λ] / MS speed [λ /s] MS speed [λ /s] = MS speed [m /s] / Speed of light [m/s] * Center frequency [Hz] | | |

Channel model specification:

Table C.3.2.4-2: Channel model specification for Rayleigh fading

| Item | Unit | Value |
|-----------------------|------------|---|
| Center frequency | MHz | Downlink Center Frequency in 36.508 [19] as required per band |
| Channel model samples | wavelength | > 2 x Number of traces |
| Channel model | | As specified in Annex C.2 |

Method of Measurement Results Analysis

The primary performance criterion to evaluate Rayleigh fading is the Cumulative Distribution Function (CDF) of the received signal amplitude (x) at the DUT. CDF describes the probability of a signal level being less than the CDF parameter. The CDF of x in a set of measured samples in a reverberation chamber is defined as,

$$CDF(x) = Prob(X < x) = \int_0^x p_y dy$$

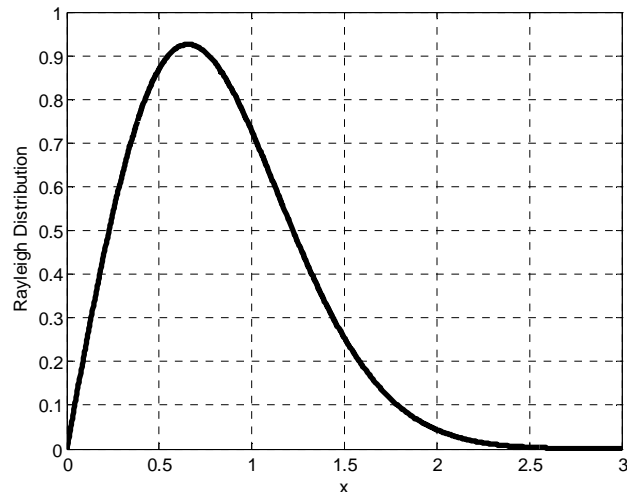


Figure C.3.2.4-1: Reference Rayleigh distribution

The difference between the measured histogram of CDF (also known as empirical CDF, ECDF) and ideal histogram is computed within the framework of the Chi-Square test [3] to determine if the chamber provides a Rayleigh fading. The Chi-Square test is a purely statistical test for determining if the observed data ECDF follows the theoretic CDF. The Chi-Square test is performed as follows [21].

1. Partition the measured sample space (N samples) into K disjoint intervals (bins).
2. Calculate the number m_i of samples that fall in each of these intervals. This is a measure of the probability that the outcome will fall in that interval.
3. Compare the Rayleigh CDF obtained from the measured data to the theoretical probability distribution using the Chi-Square test.

The Chi-Square statistic is defined as the “weighted square error” and is given by

$$\chi^2 = \sum_{i=1}^K \frac{(m_i - Np_i)^2}{Np_i}$$

Here, N is the number of samples, p_i is the theoretical probability of landing in the bin with index i, and m_i is the measured number of samples in the bin with index i. K=15 shall be used for the validation. The theoretical value p_i is given in Table C.3.2.4-3 below.

Due to the statistical variations of the chi-squared value, the final reported value should be obtained by averaging the chi-squared values obtained for each frequency point in the signal bandwidth. This averaged value should be compared to the limit.

Table C.3.2.4-3: Theoretical probability distribution for the Rayleigh distribution with 15 bins

| Bin limit (min) | Bin limit (max) | p_i |
|-----------------|-----------------|-------|
| 0.00000 | 0.06899 | 1/15 |
| 0.06899 | 0.14310 | 1/15 |
| 0.14310 | 0.22314 | 1/15 |
| 0.22314 | 0.31015 | 1/15 |
| 0.31015 | 0.40547 | 1/15 |
| 0.40547 | 0.51083 | 1/15 |
| 0.51083 | 0.62861 | 1/15 |
| 0.62861 | 0.76214 | 1/15 |
| 0.76214 | 0.91629 | 1/15 |
| 0.91629 | 1.09861 | 1/15 |
| 1.09861 | 1.32176 | 1/15 |
| 1.32176 | 1.60944 | 1/15 |
| 1.60944 | 2.01490 | 1/15 |
| 2.01490 | 2.70805 | 1/15 |
| 2.70805 | +infinity | 1/15 |

Note: These limits are given as Watt ratios.

According to [22], a chi-squared value less than or equal to 27.69 will mean that the numbers are Rayleigh distributed (1% significance level).

It also needs to be verified that there is no strong LOS component present. This is done by evaluating the ratio of the direct path component to the scattered component (also known as K-factor). If there is no direct component present, then $K = 0$, $K = -\infty$ dB.

$$K = \frac{(|\langle S_{21} \rangle|)^2}{(\langle |S_{21} - \langle S_{21} \rangle|^2 \rangle)}$$

The maximum allowed K-factor is -10dB, anything higher than will be considered a failure.

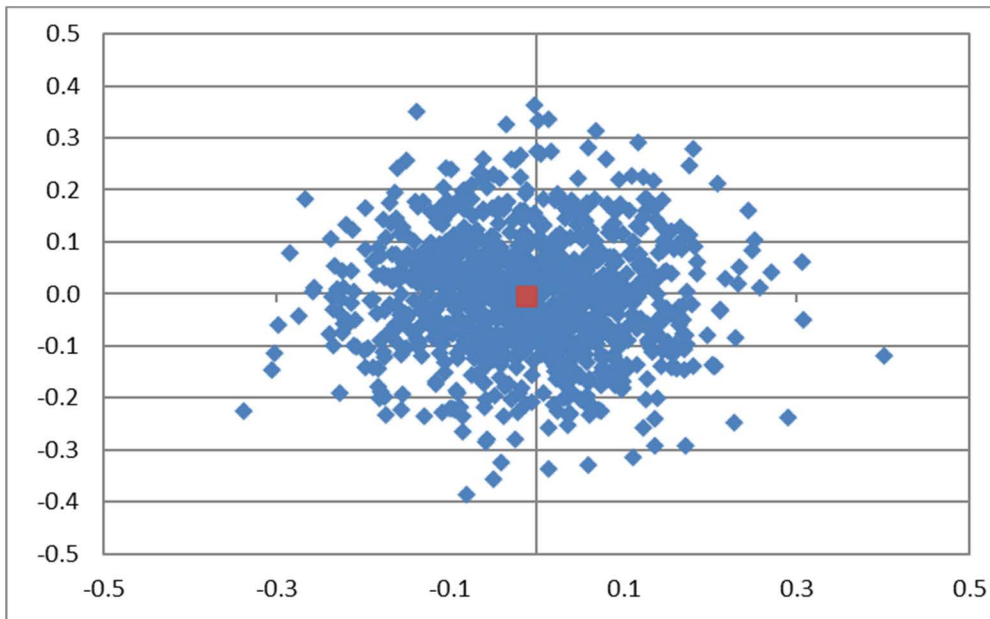


Figure C.3.2.4-2: Scattered Plot of Measured S21 with no LOS component present.

OTA antenna configuration: Fixed measurement source antennas.

Measurement antenna: A suitably wideband test antenna.

C.3.2.5 Isotropy for 3D isotropic models

This measurement checks that the resulting received signal characteristics are statistically spatially isotropic.

Method of measurement:

For isotropic validation, the input signal from the VNA is fed directly, or via the channel emulator, to the fixed measurement antennas of the reverberation chamber. If a channel emulator is used, it has to be placed in Bypass mode where no fading is used. An electric dipole is placed on the turn table.

Three orthogonal components of the electric field are recorded with the dipole in three different orientations. The same stirring sequence as used for the DUT measurement, as well as the chamber loading used for the DUT measurement and PDP validation, should be used for the validation measurement.

Step the chamber stirring sequence and store traces from VNA measurements at each step until the Number of Traces specified in Table C.3.2.5-1 is obtained. Repeat this procedure with the dipole in all three orthogonal orientations.

VNA settings:

Table C.3.2.5-1: VNA settings for isotropy

| Item | Unit | Value |
|--|------|---|
| Center frequency | MHz | Downlink center frequency in 36.508 [19] as required per band |
| Span | MHz | Same as signal bandwidth |
| RF output level | dBm | 0 |
| Number of traces per receive antenna orientation | | Same as in DUT measurement |
| Number of points | | Configured to obtain 1 MHz step size |
| Averaging | | 1 |

Method of Measurement Results Analysis

Compute and evaluate the anisotropy coefficients from the measured data as described in [2]. Using S parameters, the anisotropy coefficient that employs two orientations may be given as

$$A_{pq}(n) = (|S_{21,p}(n)|^2 - |S_{21,q}(n)|^2) / (|S_{21,p}(n)|^2 + |S_{21,q}(n)|^2),$$

where $p < q = 1, 2, 3$. The total anisotropy coefficient that takes into account all three orientations is given by

$$A_{\text{tot}}(n) = \sqrt{[A_{12}(n)]^2 + [A_{13}(n)]^2 + [A_{23}(n)]^2} / \sqrt{3}.$$

The cumulative distribution functions (CDFs) for the ideal anisotropy coefficients are shown in figure C.3.2.5-1, where the left plot applies to $A_{pq}(n)$ and the right plot applies to $A_{\text{tot}}(n)$.

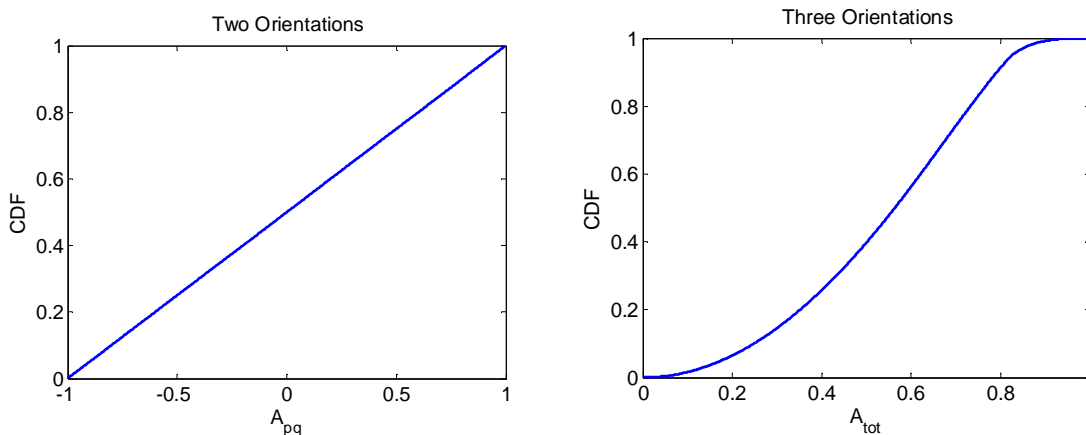


Figure C.3.2.5-1: Reference anisotropy coefficients for two orientations (A_{pq}) and for three orientations (A_{tot})

NOTE: These figures have been provided by the National Institute of Standards and Technology in USA.

The differences between the measured CDF of $A_{pq}(n)$, $A_{\text{tot}}(n)$ and their ideal CDF's are computed within the framework of the chi-square test [3] to determine if the chamber is isotropic. The chi-square test is a statistical test for determining whether the CDF of the observed data for $A_{pq}(n)$, and $A_{\text{tot}}(n)$ are significantly different from the ideal. The chi-square test is performed as follows [21].

1. Sort the N measured values of $A_{pq}(n)$, and A_{tot} into the K equal, disjoint intervals (bins) specified in the first two columns of Table C.3.2.5-1A and C.3.2.5-2, with $K = 10$, and $K = 11$ respectively.
2. Count the number M_k of measured samples of $A_{pq}(n)$, and A_{tot} that fall in the k th interval. It is necessary that at least 5 measured samples fall into each interval.
3. For $A_{pq}(n)$ the numbers of samples per bin are equal, therefore $p_i = N/10$. For $A_{\text{tot}}(n)$ calculate the probability p_k of samples for each bin from the ideal CDF in the k th interval. Table C.3.2.5-2 provides the values of p_k for $K = 11$ bins.
4. Compare the M_k with the expected number obtained from the ideal CDF p_k using the chi-square test as follows.

$$\chi^2 = \sum (M_k - Np_k)^2 / (Np_k).$$

The summation over bins goes from $k=1$ to K .

Due to the statistical variations of the chi-squared value, the final reported value should be obtained by averaging the chi-squared values obtained for each frequency point in the signal bandwidth. This averaged value should be compared to the limit.

Table C.3.2.5-1A: Expected Count for 2 Orientations Anisotropy Coefficients with 10 bins

| Bin limit (min) | Bin limit (max) | p_i |
|-----------------|-----------------|-------|
| -1.0 | -0.8 | 1/10 |
| -0.8 | -0.6 | 1/10 |
| -0.6 | -0.4 | 1/10 |
| -0.4 | -0.2 | 1/10 |
| -0.2 | 0.0 | 1/10 |
| 0.0 | 0.2 | 1/10 |
| 0.2 | 0.4 | 1/10 |
| 0.4 | 0.6 | 1/10 |
| 0.6 | 0.8 | 1/10 |
| 0.8 | 1.0 | 1/10 |

Table C.3.2.5-2: Expected Count for Total Anisotropy Coefficient with 11 Bins

| Bin limit (min) | Bin limit (max) | p_k |
|-----------------|-----------------|-------|
| 0.00000 | 0.09090909 | 0.013 |
| 0.09090909 | 0.18181818 | 0.040 |
| 0.18181818 | 0.27272727 | 0.066 |
| 0.27272727 | 0.36363636 | 0.093 |
| 0.36363636 | 0.45454545 | 0.118 |
| 0.45454545 | 0.54545454 | 0.140 |
| 0.54545454 | 0.63636363 | 0.157 |
| 0.63636363 | 0.72727272 | 0.163 |
| 0.72727272 | 0.81818181 | 0.150 |
| 0.81818181 | 0.90909090 | 0.053 |
| 0.90909090 | 1.00000000 | 0.006 |

According to [22], a chi-squared value less than or equal to 21.67 will mean that the 2 orientation anisotropy coefficients, $A_{pq}(n)$, are uniformly distributed as expected (1% significance level). For the Total anisotropy coefficients, $A_{tot}(n)$, a chi-squared value less than or equal to 23,21 will mean that there is no significant difference from the ideal reference (1% significance level).

OTA antenna configuration: Fixed measurement source antennas.

Measurement antenna: The electric dipole.

C.3.3 Reporting

Additionally, the results should be summarized in the following table (some entries like isotropy apply only to certain methods):

Table C.3.3-1: Template for reporting validation results

| Item | Parameter | Result | Tolerances (Note 1) | Comments |
|------|------------------------|--------|---------------------|----------|
| 1 | Power delay profile | | | |
| 2 | Doppler | | | |
| 3 | BS antenna correlation | | | |
| 4 | Rayleigh fading | | | |
| 5 | Isotropy | | | |

NOTE 1: The exact tolerances are for further study.

NOTE 2: In addition to the validation of channel model parameters stated here, in order to properly identify test tolerances it is important to verify test repeatability. Though not required for channel model verification, individual labs are encouraged to run test repeatability experiments, such as the one described in Annex G.A.2 in [4]. For future uncertainty analyses, test repeatability of all methodologies has to be reported.

C.4 Channel model validation results

Channel models have been specified in clause C.2.

This clause describes the MIMO OTA validation measurements, in order to ensure that the channel models are correctly implemented and hence capable of generating the propagation environment, as described by the model, within a test area. Measurements are done mainly with a Vector Network Analyzer (VNA) and a spectrum analyzer.

C.4.1 Scope

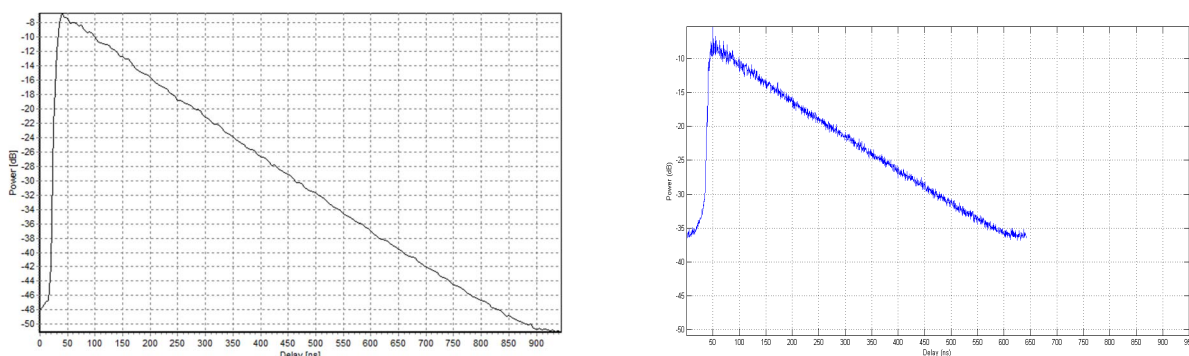
Clauses C.4.2-C.4.6 contain the validation results of channel models in Annex C.2 for companies using methods as described in Clause 6.3.2. These results are based on two different types of equipment vendors and both sets of results are included here for comparison.

C.4.2 Power Delay Profile (PDP) for 3D isotropic models

The power delay profiles of the channel models in Annex C.2 have been measured according to the procedures in Annex C.3.

Figure C.4.2-1 below illustrates the measured results for Band 13 for the isotropic channel model based on NIST for two different reverberation chambers.

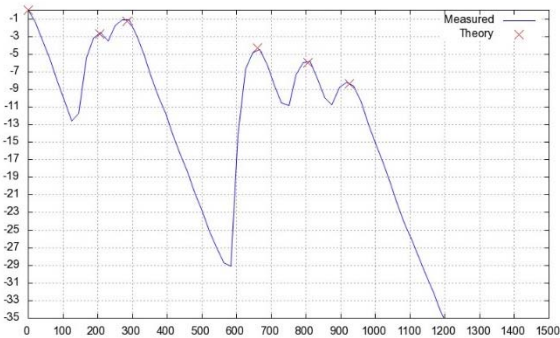
Figure C.4.2-2 illustrates the measured results for Band 13 for the short delay spread low correlation and long delay spread high correlation isotropic channel models for two different reverberation chambers and channel emulators.



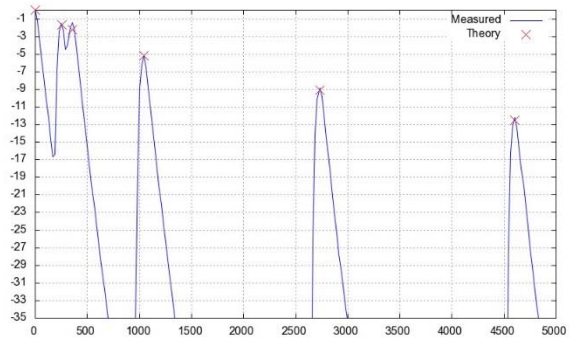
(a)

(b)

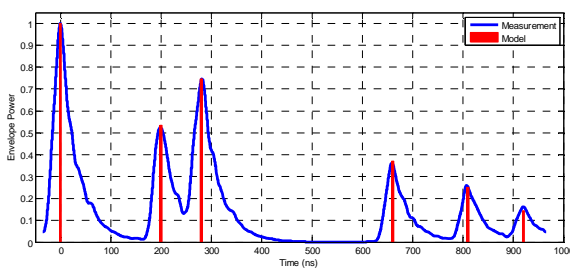
Figure C.4.2-1: For Band 13, isotropic channel model based on NIST PDP verification measurement for reverberation chamber A (a); isotropic channel model based on NIST PDP verification measurement for reverberation chamber B (b)



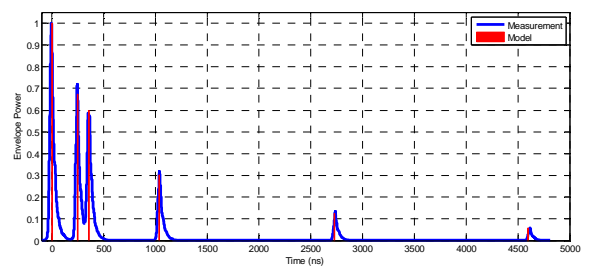
(a)



(b)



(c)



(d)

Figure C.4.2-2: For Band 13, short delay spread low correlation (a) and long delay spread high correlation (b) isotropic channel models PDP verification measurement for reverberation chamber and channel emulator setup A; short delay spread low correlation (c) and long delay spread high correlation (d) isotropic channel models PDP verification measurement for reverberation chamber and channel emulator setup C

Table C.4.2-1 and Table C.4.2-2 below summarize the PDP verification results.

Table C.4.2-1: Summary of PDP verification results at Band 13 for the isotropic channel model based on NIST for both equipment vendors

| Chamber | RMS Delay Spread measured [ns] | RMS Delay Spread theory [ns] | Delta [ns] |
|---------|--------------------------------|------------------------------|------------|
| 1 | 79.34 | 80 | - 0.66 |
| 2 | 82.21 | 80 | + 2.21 |

**Table C.4.2-2: Summary of PDP verification results at Band 13
for the short delay spread low correlation and long delay spread high correlation
isotropic channel models for both equipment vendors**

| Isotropic Long Delay Spread High Correlation | Reverberation Chamber and Channel Emulator A | | | Reverberation Chamber and Channel Emulator C | | |
|--|--|------------------------|---------------------|--|------------------------|---------------------|
| | Cluster | Theoretical Power (dB) | Measured Power (dB) | Delta | Theoretical Power (dB) | Measured Power (dB) |
| 1 | 0 | 0 | 0 | 0 | 0 | 0 |
| 2 | -2.2 | -1.44 | +0.76 | -2.2 | -2.31 | -0.11 |
| 3 | -1.7 | -1.48 | +0.22 | -1.7 | -1.43 | +0.27 |
| 4 | -5.2 | -5.19 | +0.01 | -5.2 | -4.98 | +0.22 |
| 5 | -9.1 | -8.86 | +0.24 | -9.1 | -8.75 | +0.35 |
| 6 | -12.5 | -12.20 | +0.30 | -12.5 | -12.45 | +0.05 |
| Isotropic Short Delay Spread Low Correlation | Reverberation Chamber and Channel Emulator A | | | Reverberation Chamber and Channel Emulator C | | |
| | Cluster | Theoretical Power (dB) | Measured Power (dB) | Delta | Theoretical Power (dB) | Measured Power (dB) |
| 1 | 0 | 0 | 0 | 0 | 0 | 0 |
| 2 | -1.3 | -1.11 | +0.19 | -1.3 | -1.26 | +0.04 |
| 3 | -2.7 | -2.57 | +0.13 | -2.7 | -2.79 | -0.09 |
| 4 | -4.3 | -4.47 | -0.17 | -4.3 | -4.42 | -0.12 |
| 5 | -6.0 | -5.79 | +0.21 | -6.0 | -5.86 | +0.14 |
| 6 | -8.4 | -8.18 | +0.22 | -8.4 | -7.88 | +0.52 |

C.4.2.1 Setup used by harmonization test lab

The measurement procedures and data analysis align with Annex C.3.2.1. The inherent RMS delay spread of the chamber (without channel emulator) is 50 ns and 1000 stirring positions are used (one per VNA trace).

Figure C.4.2.1-1 and Figure C.4.2.1-2 show the results from the PDP validation measurements for the SDLC channel model for 751 MHz and 2655 MHz, respectively. Table C.4.2.1-1 shows a summary of the delta between measured and ideal values.

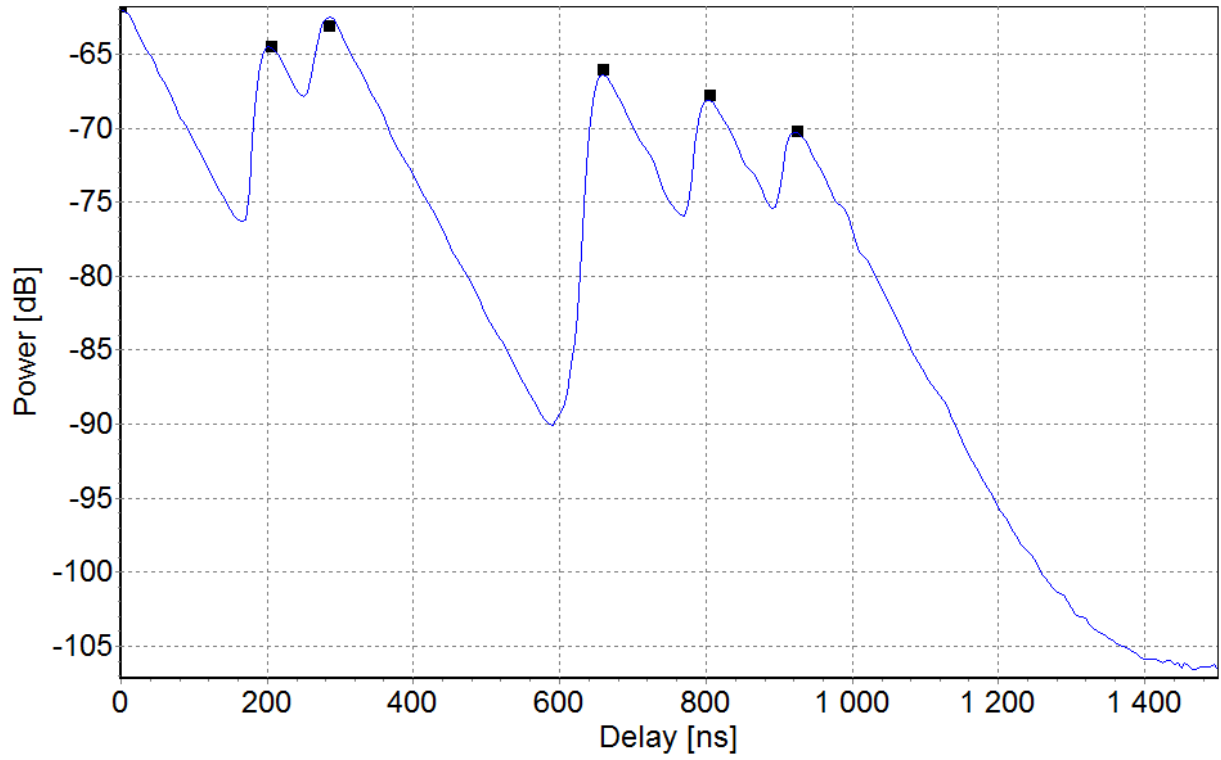


Figure C.4.2.1-1: Results from PDP validation measurements for the SDLC channel model and 751 MHz.

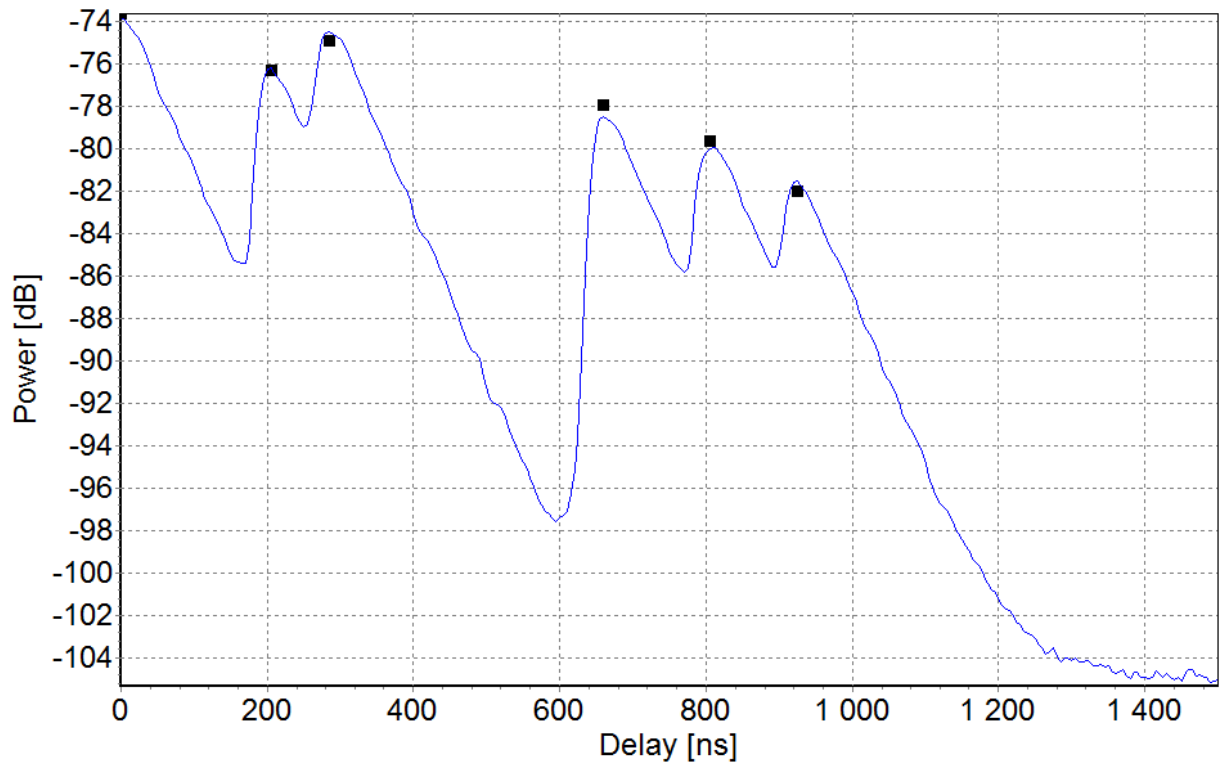


Figure C.4.2.1-2: Results from PDP validation measurements for the SDLC channel model and 2655 MHz.

Table C.4.2.1-1: Summary of deltas between measured and ideal values for the SDLC channel model for 751 MHz and 2655 MHz.

| Cluster | 751 MHz | | 2655 MHz | |
|---------|------------------|------------------|------------------|------------------|
| | Power delta [dB] | Delay delta [ns] | Power delta [dB] | Delay delta [ns] |
| 1 | 0 | 0 | 0 | 0 |
| 2 | -0.1 | -5 | +0.2 | 0 |
| 3 | +0.6 | 0 | +0.4 | 0 |
| 4 | -0.3 | 0 | -0.6 | 0 |
| 5 | -0.3 | 0 | -0.3 | +5 |
| 6 | -0.1 | -5 | +0.5 | 0 |

C.4.3 Doppler for 3D isotropic models

The Doppler spectrum of the channel models defined in Annex C.2 has been characterized according to Annex C.3. Figure C.4.3-1 illustrates the measured results for Band 13 for the isotropic channel model based on NIST and Figure C.4.3-2 shows the measured results for Band 13 for the short delay spread low correlation and long delay spread high correlation isotropic channel models.

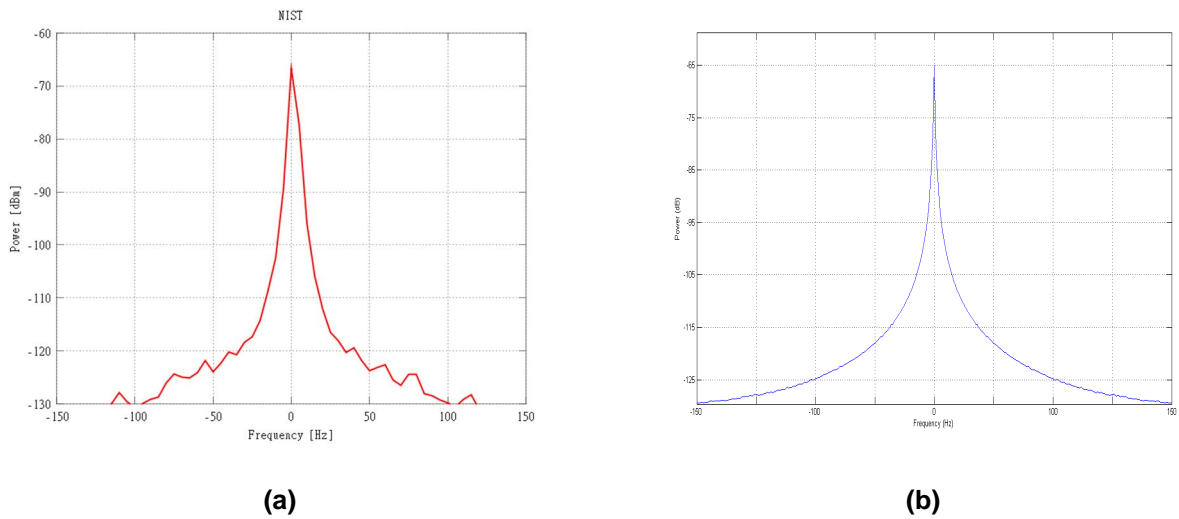
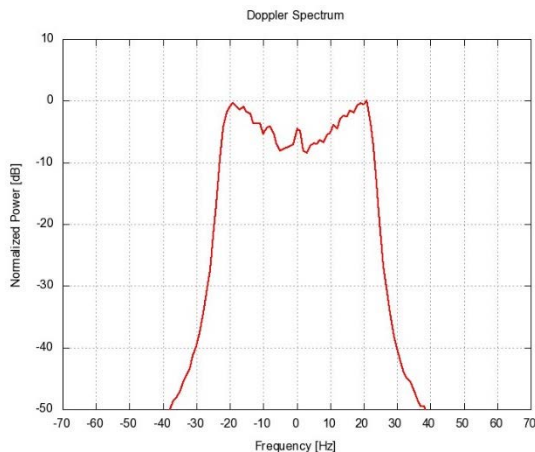
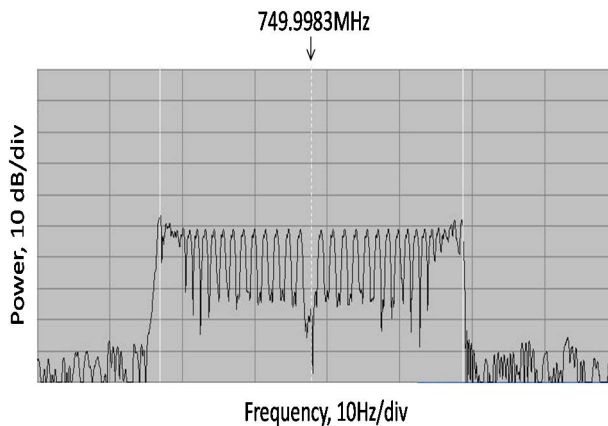


Figure C.4.3-1: For Band 13, Doppler spectrum for isotropic channel model based on NIST emulated by reverberation chamber A (a); Doppler spectrum for isotropic channel model based on NIST emulated by reverberation chamber B (b)



(a)



(b)

Figure C.4.3-2: For Band 13, Doppler spectrum for short delay spread low correlation and long delay spread high correlation isotropic channel models emulated by reverberation chamber and channel emulator setup A (a); Doppler spectrum for short delay spread low correlation and long delay spread high correlation isotropic channel models emulated by reverberation chamber and channel emulator setup C (b)

C.4.3.1 Setup used by harmonization test lab

The measurement procedures and data analysis align with Annex C.3.2.2. The inherent RMS delay spread of the chamber (without channel emulator) is 50 ns and 100 stirring positions are used (one per spectrum analyzer sweep).

Figure C.4.3.1-1 and Figure C.4.3.1-2 show the results from the Doppler validation measurements for the SDLC channel model for 751 MHz and 2655 MHz, respectively.

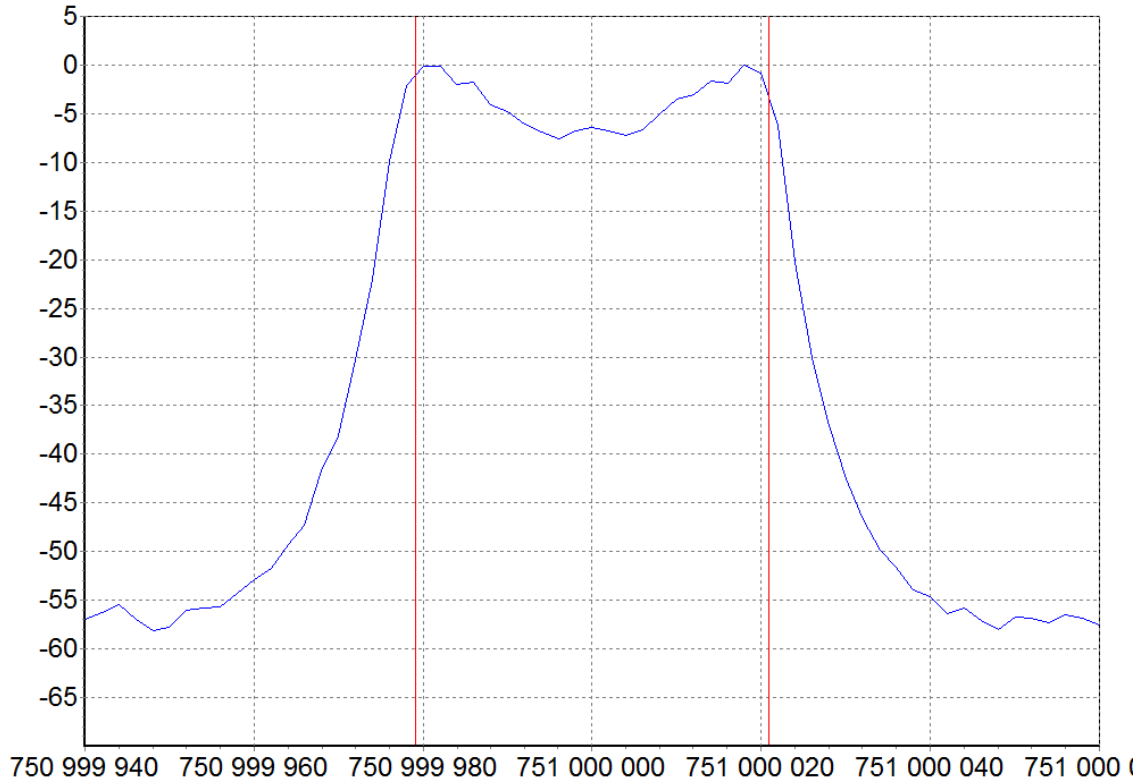


Figure C.4.3.1-1: Results from Doppler validation measurements for the SDLC channel model, 751 MHz. The red vertical lines represent the ideal maximum Doppler shift for 30 km/h (20.88 Hz).

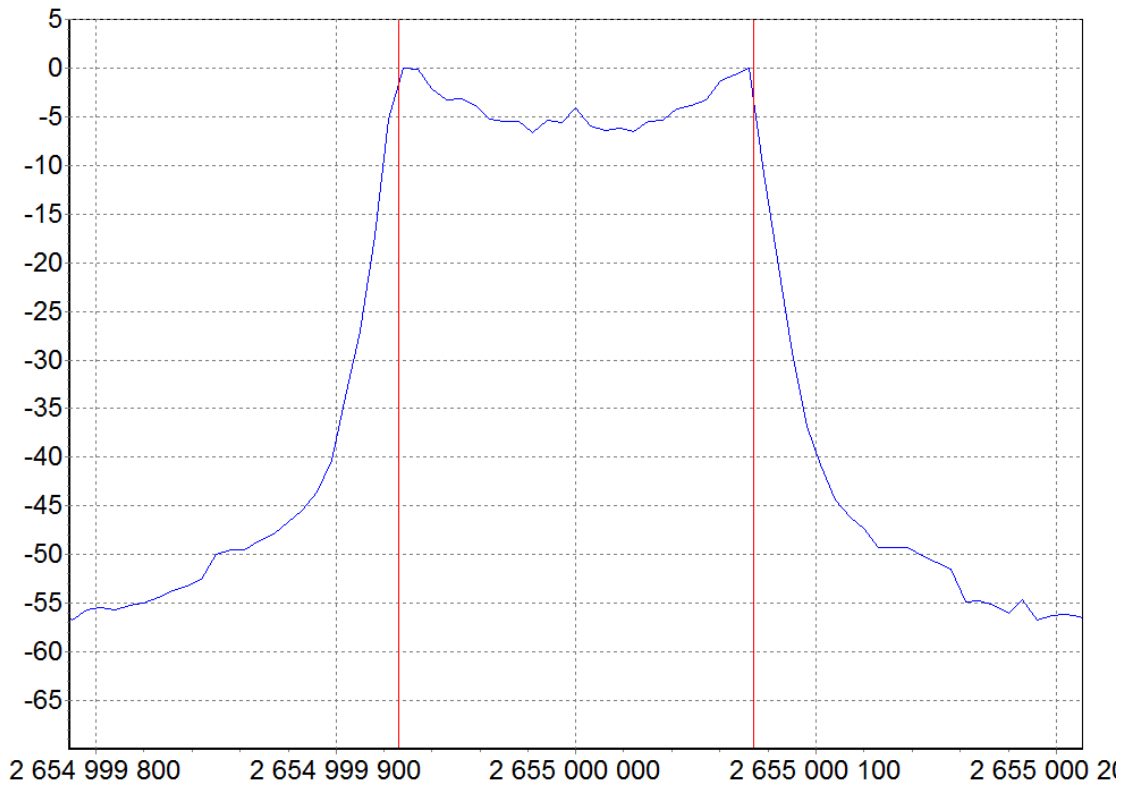
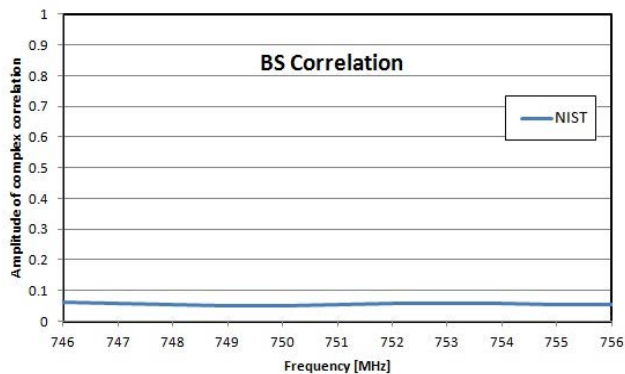


Figure C.4.3.1-2: Results from Doppler validation measurements for the SDLC channel model, 2655 MHz. The red vertical lines represent the ideal maximum Doppler shift for 30 km/h (73.80 Hz).

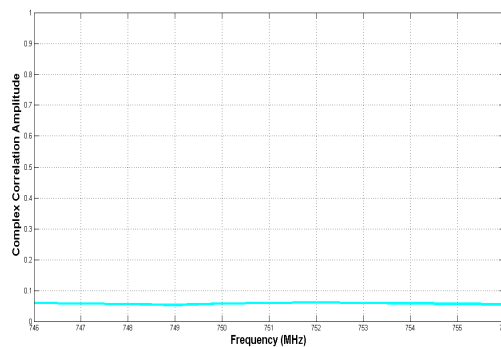
C.4.4 Base Station antenna correlation for 3D isotropic models

The Base Station (BS) antenna correlation of the models defined in Annex C.2 has been characterized according to Annex C.3.

Figure C.4.4-1 shows the measured results for the isotropic channel model based on NIST and Figure C.4.4-2 shows the measured results for the short delay spread low correlation and long delay spread high correlation isotropic channel models for Band 13.

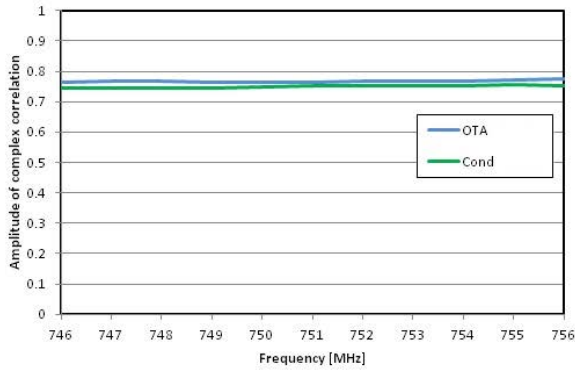


(a)

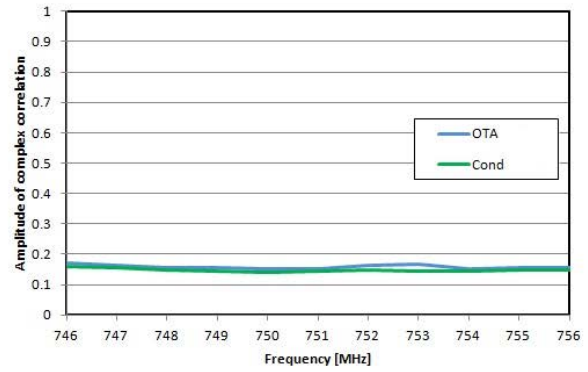


(b)

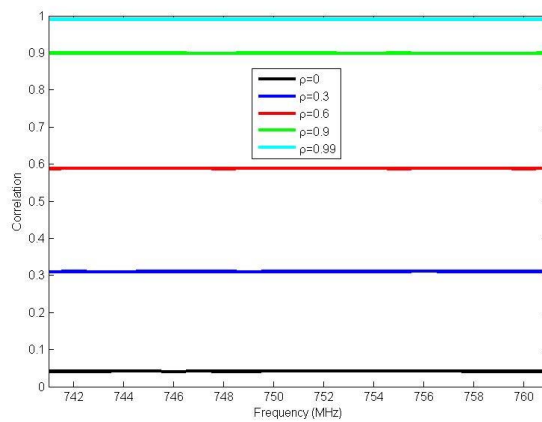
Figure C.4.4-1: For Band 13, base station antenna correlation for isotropic channel model based on NIST emulated by reverberation chamber A (a); base station antenna correlation for isotropic channel model based on NIST emulated by reverberation chamber B (b)



(a)



(b)



(c)

Figure C.4.4-2: For Band 13, base station antenna correlation for the long delay spread high correlation (a) and short delay spread low correlation (b) isotropic channel models emulated by reverberation chamber and channel emulator setup A; base station antenna correlation observed in the test volume for different values of base station antenna correlation imposed by the channel emulator for the reverberation chamber and channel emulator setup C (c)

C.4.4.1 Setup used by harmonization test lab

The measurement procedures and data analysis align with Annex C.3.2.3. The inherent RMS delay spread of the chamber (without channel emulator) is 50 ns and 600 stirring positions are used (one per VNA trace).

Figure C.4.4.1-1 and Figure C.4.4.1-2 show the results from the base station correlation validation measurements for the SDLC channel model for 751 MHz and 2655 MHz, respectively.

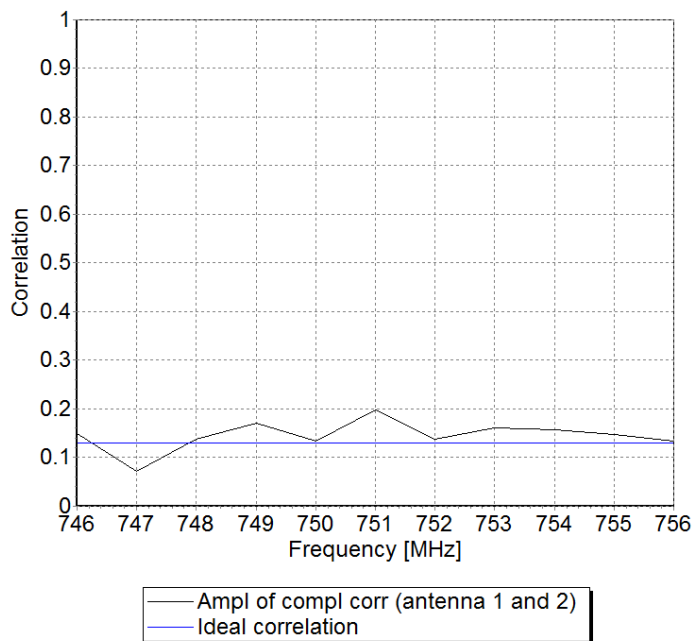


Figure C.4.4.1-1: Results from base station antenna correlation validation measurements for the SDLC channel model and 751 MHz.

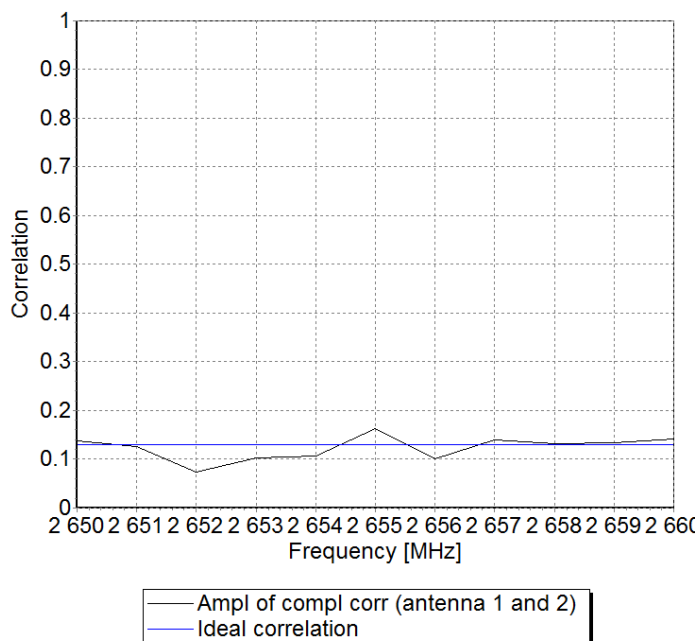
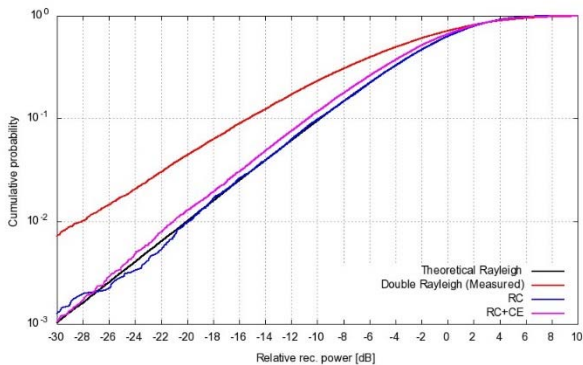


Figure C.4.4.1-2: Results from base station antenna correlation validation measurements for the SDLC channel model and 2655 MHz.

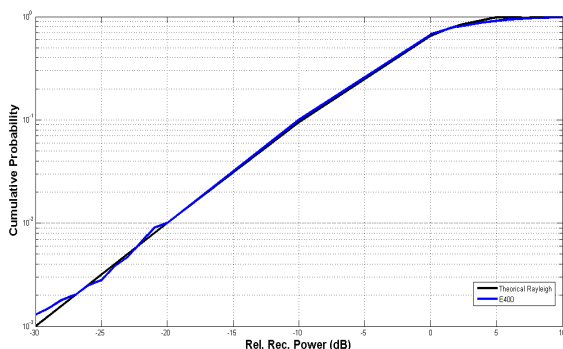
C.4.5 Rayleigh fading for 3D isotropic models

The Rayleigh fading of the models defined in Annex C.2 have been characterized according to Annex C.3. Figure C.4.5-1 shows the measured results for the short delay spread low correlation and long delay spread high correlation isotropic channel models for Band 13.



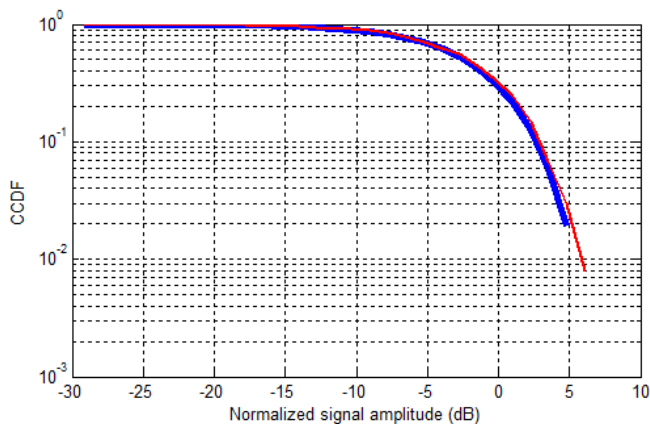
Max diff to theoretical +10 to -20 dB: < 1.5 dB
 Max diff to theoretical -20 to -30 dB: < 1.5 dB
 χ^2 for RC: 5.37
 χ^2 for RC+CE: 15.22

(a)



Max diff to theoretical +10 to -20 dB: < 1.0 dB
 Max diff to theoretical -20 to -30 dB: < 1.0 dB

(b)



Max diff to theoretical +10 to -20 dB: < 1.5 dB
 Max diff to theoretical -20 to -30 dB: < 1.5 dB

(c)

Figure C.4.5-1: For Band 13, Rayleigh fading for isotropic channel model based on NIST, short delay spread low correlation and long delay spread high correlation isotropic channel models emulated by reverberation chamber and channel emulator setup A (a); Rayleigh fading for isotropic channel model based on NIST emulated by reverberation chamber B (b); Rayleigh fading for short delay spread low correlation and long delay spread high correlation isotropic channel models emulated by reverberation chamber and channel emulator setup C (c)

C.4.5.1 Setup used by harmonization test lab

The measurement procedures and data analysis align with Annex C.3.2.4. The inherent RMS delay spread of the chamber (without channel emulator) is 50 ns and 1080 stirring positions are used (one per VNA trace).

Table C.4.5.1-1 shows the chi-squared values calculated for two different TVVPs (see Annex C.4.6.1) and three orientations for each TVVP for the SDLC channel model at 751 MHz and 2655 MHz. As can be seen from this table, the chi-squared value is within the limit (< 27.69) for all cases.

Table C.4.5.1-1: Chi-squared values for the SDLC channel model for 751 MHz and 2655 MHz.

| Frequency [MHz] | TVVP 1-1 | TVVP 1-2 | TVVP 1-3 | TVVP 9-1 | TVVP 9-2 | TVVP 9-3 |
|-----------------|----------|----------|----------|----------|----------|----------|
| 751 | 18,6 | 16,2 | 19,0 | 25,3 | 21,9 | 24,3 |
| 2655 | 22,6 | 18,4 | 20,9 | 18,2 | 23,1 | 21,1 |

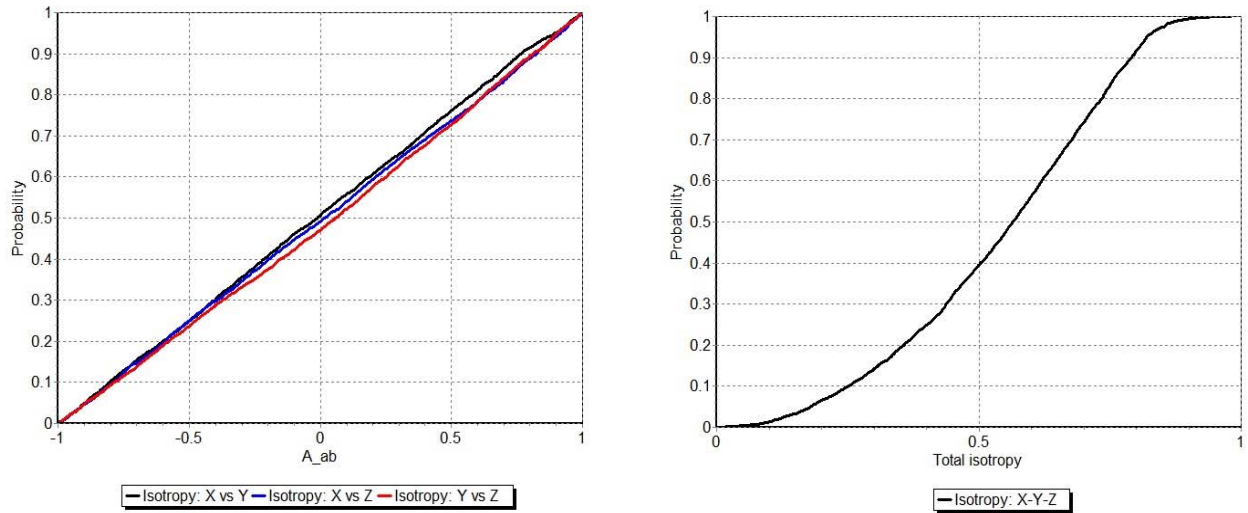
In addition, the K-factor was calculated for the same positions and orientations as described above. The result is shown in Table C.4.5.1-2 for the SDLC channel model at 751 MHz and 2655 MHz. All values are within the limit (< -10 dB).

Table C.4.5.1-2: K-factor for the SDLC channel model for 751 MHz and 2655 MHz.

| Frequency [MHz] | TVVP 1-1 | TVVP 1-2 | TVVP 1-3 | TVVP 9-1 | TVVP 9-2 | TVVP 9-3 |
|-----------------|----------|----------|----------|----------|----------|----------|
| 751 | -51,8 | -37,1 | -43,6 | -30,5 | -28,5 | -25,0 |
| 2655 | -41,4 | -31,8 | -26,3 | -30,0 | -26,7 | -26,6 |

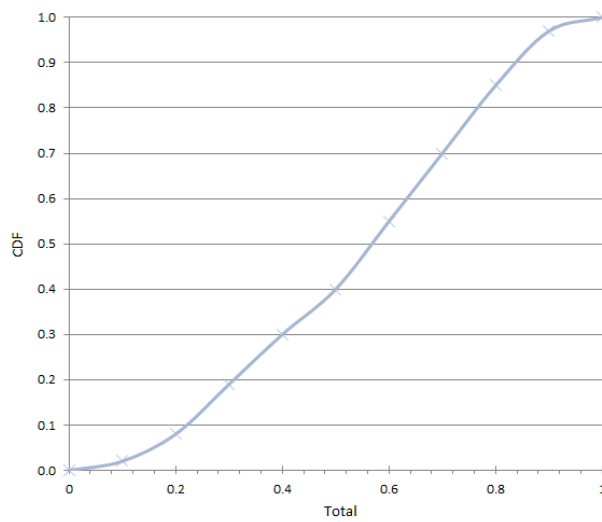
C.4.6 Isotropy for 3D isotropic models

The isotropy of the models defined in Annex C.2 has been characterized according to Annex C.3. Figure C.4.6-1 shows the measured results for the isotropic channel model based on NIST, short delay spread low correlation and long delay spread high correlation isotropic channel models for band 13.

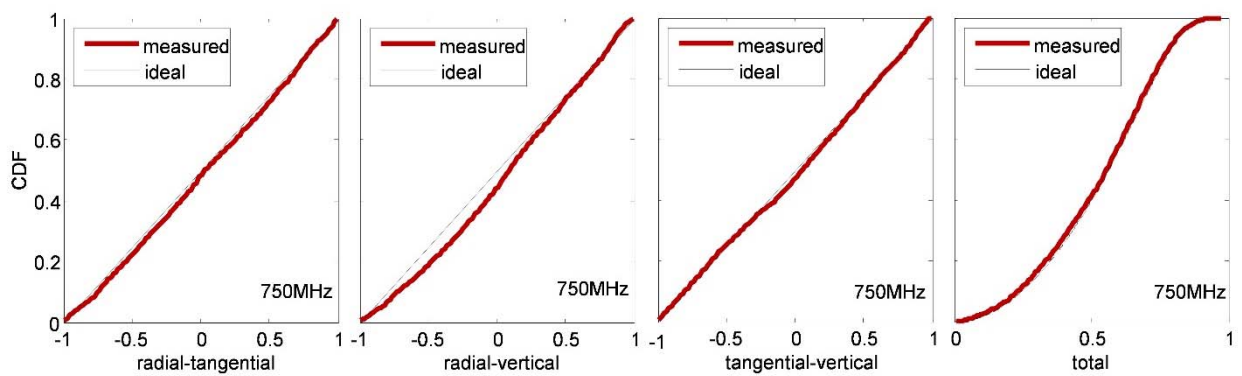


χ^2 : 7.89

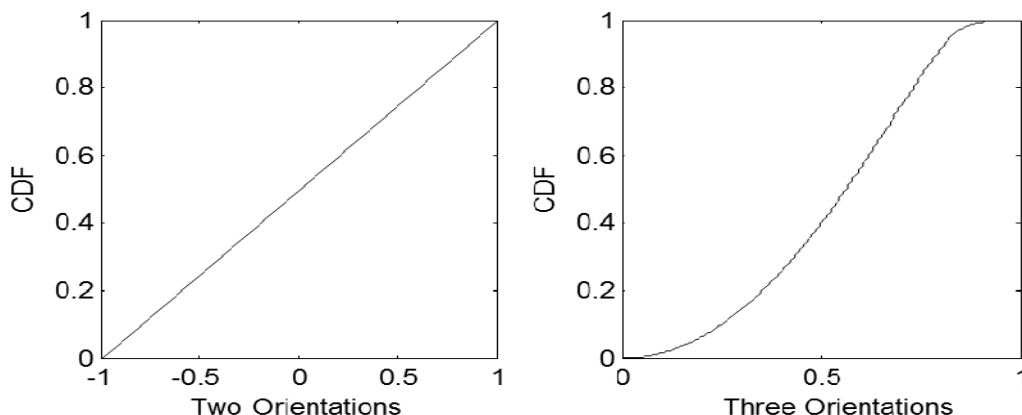
(a)



(b)



(c)



(d)

Figure C.4.6-1: For Band 13, isotropy for isotropic channel model based on NIST, short delay spread low correlation and long delay spread high correlation isotropic channel models emulated by reverberation chamber and channel emulator setup A (a); Isotropy for isotropic channel model based on NIST emulated by reverberation chamber B (b); Isotropy for short delay spread low correlation and long delay spread high correlation isotropic channel models emulated by reverberation chamber and channel emulator setup C (c); Reference anisotropy coefficients (d)

C.4.6.1 Setup used by harmonization test lab

The measurement procedures and data analysis align with Annex C.3.2.5. The inherent RMS delay spread of the chamber (without channel emulator) is 50 ns and 120 stirring positions are used (one per VNA trace).

The RC+CE setup used is a Type 1 RC, with a schematic setup as shown in Figure C.4.6.1-1. The TVVPs map to the physical dimensions as shown in Table C.4.6.1-1. For each TVVP three orthogonal orientations were used, denoted 1.1, 1.2 and 1.3 (and similarly for the other TVVPs).

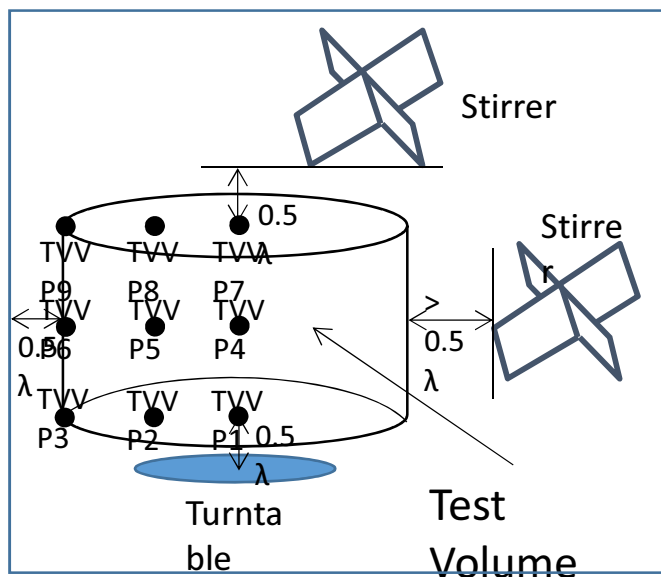


Figure C.4.6.1-1. Schematics of the RC+CE setup used for the harmonization testing and the corresponding TVVPs.

Table C.4.6.1-1. Physical dimensions of the TVVPs.

| Test Volume Validation Position | Height above reference point ¹ [cm] | Radius [cm] |
|---------------------------------|--|-------------|
| TVVP1 | 0 | 0 |
| TVVP2 | 0 | 16 |
| TVVP3 | 0 | 32 |
| TVVP4 | 30 | 0 |
| TVVP5 | 30 | 16 |
| TVVP6 | 30 | 32 |
| TVVP7 | 60 | 0 |
| TVVP8 | 60 | 16 |
| TVVP9 | 60 | 32 |

Note 1: Reference point at least 0.5λ above the turntable.

The chi-squared values for the 2 and 3 orientation anisotropy coefficients are given in Table C.4.6.1-2 and Table C.4.6.1-3 for 751 MHz and 2655 MHz, respectively. As can be seen, all values fall within the limits (< 21.67 and < 23.21 for 2 and 3 orientation anisotropy coefficients, respectively).

Table C.4.6.1-2. Chi-squared for 2 and 3 orientation anisotropy coefficients for all TVVPs for 751 MHz.

| | Chi-squared | | | | | | | | |
|-------------------|-------------|--------|--------|--------|--------|--------|--------|--------|--------|
| | TVVP 1 | TVVP 2 | TVVP 3 | TVVP 4 | TVVP 5 | TVVP 6 | TVVP 7 | TVVP 8 | TVVP 9 |
| 3 orientations | 16,86 | 15,36 | 13,08 | 12,19 | 15,81 | 12,67 | 13,08 | 14,97 | 14,56 |
| 2 orientations XY | 10,54 | 8,81 | 7,52 | 17,26 | 9,74 | 12,31 | 10,91 | 14,65 | 14,19 |
| 2 orientations XZ | 9,46 | 7,76 | 6,78 | 10,5 | 8 | 11 | 9,26 | 12,02 | 11,06 |
| 2 orientations YZ | 7,33 | 8,72 | 8,44 | 15,09 | 9,54 | 11,37 | 16,67 | 13,26 | 11,87 |

Table C.4.6.1-3. Chi-squared for 2 and 3 orientation anisotropy coefficients for all TVVPs for 2655 MHz.

| | Chi-squared | | | | | | | | |
|-------------------|-------------|--------|--------|--------|--------|--------|--------|--------|--------|
| | TVVP 1 | TVVP 2 | TVVP 3 | TVVP 4 | TVVP 5 | TVVP 6 | TVVP 7 | TVVP 8 | TVVP 9 |
| 3 orientations | 16,58 | 14,94 | 15,69 | 11,61 | 16,28 | 15,5 | 15,64 | 12,78 | 14,31 |
| 2 orientations XY | 9,2 | 9,24 | 12,87 | 9,33 | 9,11 | 8,28 | 10,33 | 6,74 | 11,44 |
| 2 orientations XZ | 10,54 | 9,78 | 9,5 | 9,37 | 7,76 | 10,31 | 9,78 | 9,46 | 8,59 |
| 2 orientations YZ | 8,83 | 7,93 | 8,2 | 8,81 | 11,83 | 7,61 | 7,67 | 9,19 | 6,76 |

C.4.7 Summary for 3D Isotropic Models

The summary of the channel model validation activity is provided in Table C.4.7-1 below.

Table C.4.7-1: Summary of channel model validation results

| Item | Parameter | Result | Tolerances | Comments |
|------|------------------------|-----------|-------------|----------|
| 1 | Power delay profile | See C.4.2 | See C.3.2.1 | |
| 2 | Doppler | See C.4.3 | See C.3.2.2 | |
| 3 | BS Antenna Correlation | See C.4.4 | See C.3.2.3 | |
| 4 | Rayleigh Fading | See C.4.5 | See C.3.2.4 | |
| 5 | Isotropy | See C.4.6 | See C.3.2.5 | |

Annex D: Environmental requirements

D.1 Scope

The requirements in this clause apply to all types of UE(s) and MS(s).

D.2 Ambient temperature

All the MIMO OTA requirements are applicable in room temperature e.g. 25°C.

D.3 Operating voltage

The device under test shall be equipped with a real battery that is fully charged (at the beginning of the test).

Annex E: DUT orientation conditions

E.1 Scope

This annex lists the testing environment conditions for all DUT types relevant to MIMO OTA testing. The use cases (positioning) discussed here are applicable for all methodologies, however the orientation and rotations described may be applicable for some methodologies only, and not for some other methodologies.

E.2 Testing environment conditions

Table E.2-1 below lists the testing environment conditions along with a diagram and applicable references.

The reference coordinate system and orientation of devices in that coordinate system is shown in Figure E.2-1 below, which includes the mechanical alignment of a phone.

For tablets the home button, charging connector and similar components can be used to define top and bottom.

For laptops the definitions specified in 3GPP TR 25.914 [11] (and repeated here in Table E.2-1) are used.

In the case of methodologies utilizing a spatial channel model in Figure E.2-1, the X axis points towards the channel model reference. For example in the case of an anechoic chamber utilizing 2D antenna array in the azimuth plane (XY plane from Figure E.2-1) this is the direction of the first probe at 0 degrees as shown in Figure 6.3.1.2.1-2.

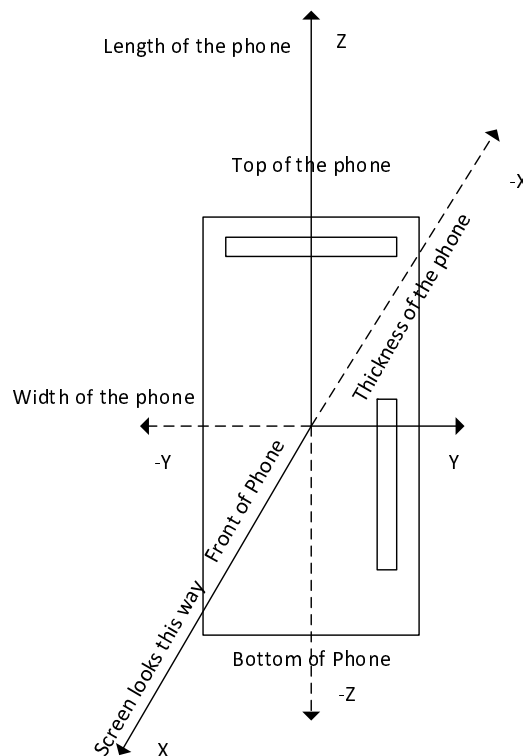


Figure E.2-1: Reference coordinate system and reference device orientation

First the terminology used below is defined here. Where possible consistency with [11], [17], [18] and [9] is sought.

Use Case (Position): the use case (position) indicates how the DUT is related to its environment. This includes the following example use cases: free space, beside head, beside head and hand, hand only etc.

Note that formerly this has been referred to as position in [4] as well as in [9]. Since to date only isotropic metrics have been used (TRP/TRS) the definition of positioning the device for a certain use case has been equivalent to orienting it

relative to the environment. With the introduction of spatial channel models, the positioning for a specific use case has to be separated from the actual orientation relative to the spatial incoming signals. For some methodologies not utilizing spatial channel models this distinction might not be necessary.

Orientation: The orientation of the device in three dimensional space is defined using the three Euler angles – Ψ -yaw; Θ -pitch; Φ -roll as defined in [17] and [18] and linked to the reference coordinate systems and reference orientation from Figure E.2-1. Note that for most use cases practical considerations of how to position the DUT together with the phantom may determine the DUT orientation.

Rotation: Once positioned for a specific use case and oriented within the reference coordinate system, the DUT and phantom are rotated within the test zone to measure the performance under various spatial channel illuminations. The rotation is defined with the same Euler angles but expressed as vectors of equal size. An example is given below:

EXAMPLE: Consider a DUT measured in an anechoic chamber as described in Clause 6. To measure the free space use case in the YZ plane (see Table E.2-1) for example at every 30 degrees the rotation vectors would be as follows:

$\Psi = [0\ 0\ 0\ 0\ 0\ 0\ 0\ 0\ 0\ 0\ 0\ 0]$ - a vector of 12 zeros indicating no rotation from the reference position for any phi value below

$\Theta = [-90\ -90\ -90\ -90\ -90\ -90\ -90\ -90\ -90\ -90\ -90\ -90]$ – a vector of 12 values equal to -90 indicating a constant pitch of -90 degrees for all phi values below

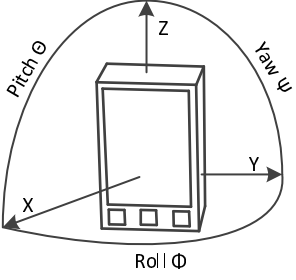
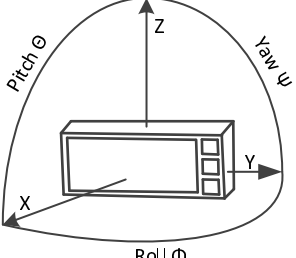
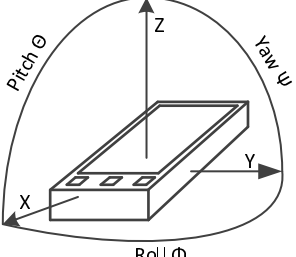
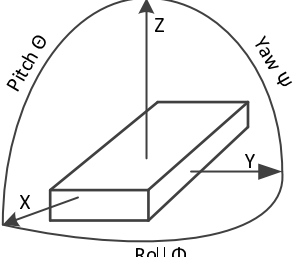
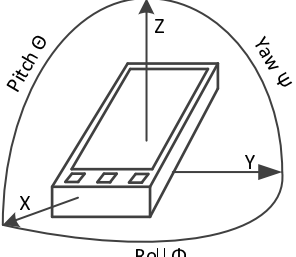
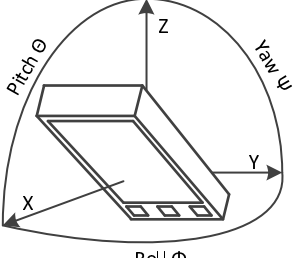
$\Phi = [0\ 30\ 60\ 90\ 120\ 150\ 180\ 210\ 240\ 270\ 300\ 330]$ – a vector of 12 distinct rotations from the reference position representing a rotation along the azimuth plane with a step of 30 degrees.

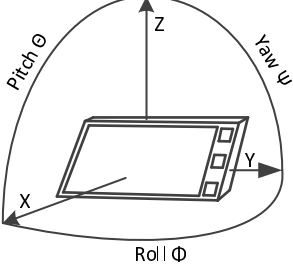
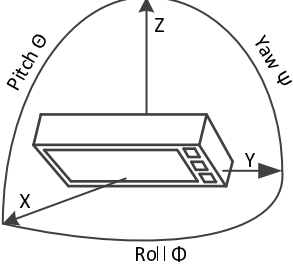
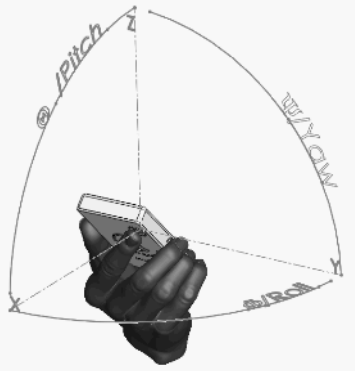
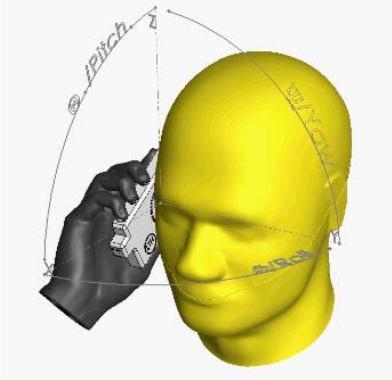
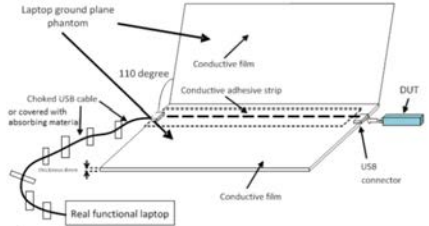
These vectors unambiguously define that the DUT is to be oriented with the screen up and rotated in azimuth every 30 degrees.

The principal antenna pattern cuts (XY plane, XZ plane, and YZ plane) are defined in [17].

The XY plane cut corresponds to the absolute throughput testing condition applied to the CTIA reference antennas for the IL/IT activity. The XZ plane and YZ plane cuts are shown for completeness and are not required for the absolute data throughput framework. The YZ plane cut corresponds to a device positioned with its screen up in a USB/WLAN tethering scenario and may be a useful testing point for handset devices expected to achieve performance metrics under such usage conditions.

Table E.2-1: Summary of possible testing environment conditions for devices supporting DL MIMO data reception

| DUT type and dimensions | Testing condition | DUT orientation angles | Diagram |
|--|---|--|--|
| Handset, tablet, CTIA reference antennas | XY plane or P0 | $\Psi=0;$ $\Theta=0;$ $\Phi=0$ |  |
| Handset, tablet, CTIA reference antennas | XZ plane or L0 | $\Psi=90;$ $\Theta=0;$ $\Phi=0$ |  |
| Handset, tablet, CTIA reference antennas | Free space data mode screen up (FS DMSU) or YZ plane or Face Up | $\Psi=0;$ $\Theta=-90;$ $\Phi=0$ |  |
| Handset, tablet | Face Down | $\Psi=0;$ $\Theta=-90;$ $\Phi=0$ |  |
| Handset, tablet | Free space data mode portrait (FS DMP) | $\Psi=0;$ $\Theta=-45;$ $\Phi=0$ |  |
| Handset, tablet | Free space portrait tilt down | $\Psi=0;$ $\Theta=45;$ $\Phi=0$ |  |

| | | | |
|---|--|---|--|
| <p>Handset, tablet</p> | <p>Free space data mode landscape (FS DML)</p> | <p>$\Psi=90;$ $\Theta=-45;$ $\Phi=0$ – left tilt</p> |  |
| <p>Handset, tablet</p> | <p>Free space landscape tilt down</p> | <p>$\Psi=90;$ $\Theta=45;$ $\Phi=0$ – left tilt</p> |  |
| <p>Handset, width < 56mm</p> | <p>Left/right hand narrow phantom data mode portrait (LH/RH DMP)</p> | <p>$\Psi=0;$ $\Theta=-45;$ $\Phi=0$</p> |  |
| <p>Handset, 56 mm < width < 72 mm</p> | <p>Left/right hand PDA phantom data mode portrait (LH/RH DMP)</p> | <p>$\Psi=0;$ $\Theta=-45;$ $\Phi=0$</p> | |
| <p>Handset width < 56 mm</p> | <p>Beside head and hand right/left (BHHR/BHHL)</p> | <p>$\Psi=60;$ $\Theta=6;$ $\Phi=-90$ – right side $\Psi=-60;$ $\Theta=-6;$ $\Phi=90$ – left side</p> |  |
| <p>Handset 56 < width < 72 mm</p> | <p>Beside head and hand right/left (BHHR/BHHL)</p> | <p>$\Psi=60;$ $\Theta=6;$ $\Phi=-90$ – right side $\Psi=-60;$ $\Theta=-6;$ $\Phi=90$ – left side</p> | |
| <p>LME</p> | <p>Laptop ground plane phantom</p> | <p>$\Psi=0;$ $\Theta=0;$ $\Phi=0$</p> |  |

| | | | |
|--|----------|--------------------------------------|--|
| LEE | XY plane | $\Psi=0;$ $\Theta=0;$ $\Phi=0$ | |
| <p>NOTE 1: The orientation angles given in the table define a set of use cases and orientations relative to the spatial channel model. The rotation angles to be used for measurements are FFS. Methodologies not utilizing spatial channel models might not need to define any rotations but are expected to measure for the given use cases.</p> <p>NOTE 2: The CTIA reference antennas have been defined for inter-lab inter-technique testing for the purposes of comparing MIMO OTA methodologies.</p> <p>NOTE 3: For DMP, other pitch positions can be considered FFS.</p> <p>NOTE 4: The absolute throughput usage mode is defined only within the framework of the CTIA reference antennas and is used for comparison of results within/across MIMO OTA methodologies.</p> <p>NOTE 5: Screen up flat positioning reference corresponds to a possible USB/WLAN tethering case, details of implementing this DUT orientation condition such as additional cabling, etc., are FFS.</p> <p>NOTE 6: Left/right/both hand phantoms for the DML usage scenario are not currently defined in 3GPP; until these phantom designs become available, is possible to only define a DML usage scenario in free space.</p> <p>NOTE 7: For a symmetric 2D coverage of testing points in azimuth, DML left and right tilts are expected to produce identical results in free space. Once phantom designs become available, we expect the interaction of the phantom with the antennas to be dependent on the tilt.</p> <p>NOTE 8: The 110 degree angle of the notebook screen opening is a standard reference for all measurements of antennas embedded in notebooks; as a result, the LEE measurement in free space is the principal XY plane cut with respect to this reference.</p> <p>NOTE 9: The orientation angles for the talk mode position are only approximate. The phone positioning is defined as in [11] and in [9] relative to the SAM phantom.</p> | | | |

The Data Mode Portrait (DMP) conditions are defined in TR 25.914 [11], and are included in this table for completeness. The Data Mode Landscape (DML) testing conditions are not currently defined in any standard testing methodology but benefit from a thorough treatment in academic literature [18]. This testing condition considers free space for all handset sizes until a DML phantom design becomes available, at which time the testing condition will be revisited.

The Laptop Mounted Equipment (LME) and Laptop Embedded Equipment (LEE) testing conditions are well defined in TR 25.914 [11] and constitute an XY plane cut measurement, given the proper orientation of the lid of the laptop ground plane phantom (in the case of LME) or of the laptop itself (in the case of LEE).

Given a 2D ring of symmetrically distributed probes (as in Clause 6):

- The XZ plane is similar to the DML mode except for the additional 45 degrees pitch in the DML casw
- For the phantom case the tilt of the DML case is very relevant since the interaction of the phantoms with the antennas will depend on it – see Figure E.2-2

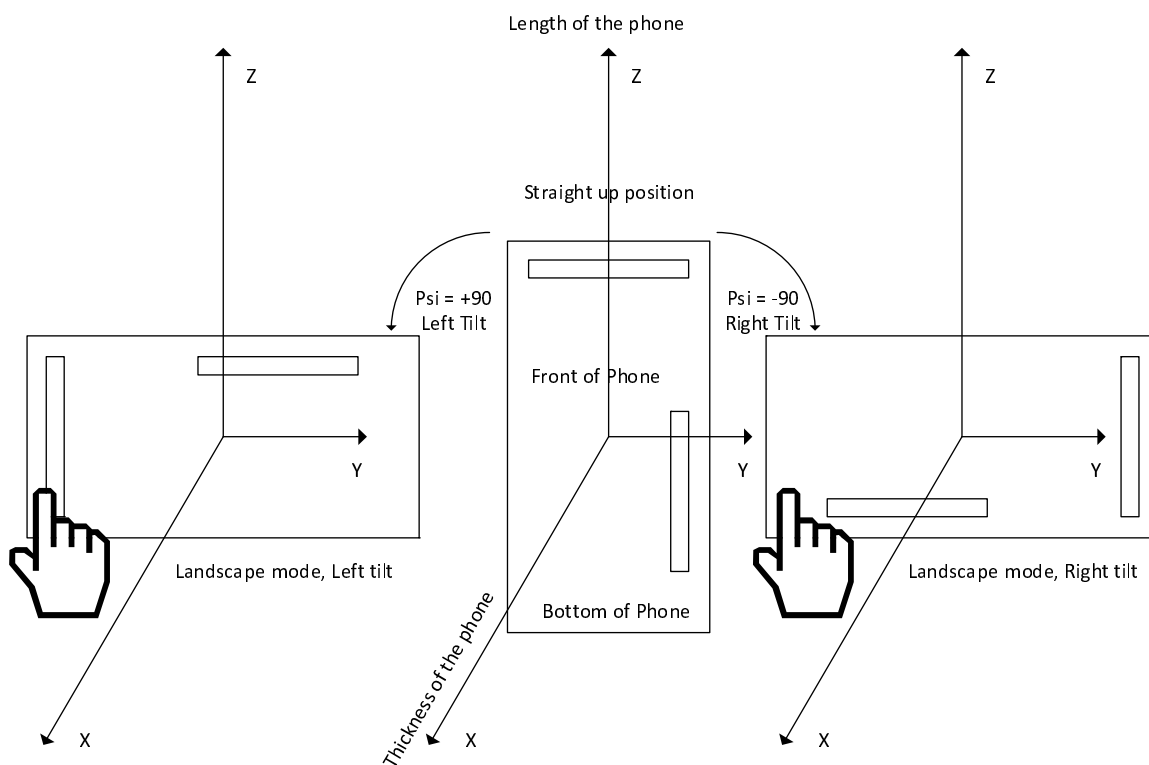


Figure E.2-2: Left and Right tilts for landscape mode with left hand phantom shown to interact differently with the antennas depending on the tilt

E.2.1 MPAC Positioning Guidelines

In order for the anechoic chamber multi probe system to emulate the intended propagation statistics within the region of space incident on the DUT antennas, two concepts determine the associated antenna spacing and positioning guidelines. The maximum antenna spacing in the DUT must be within the limit determined by the anechoic chamber multi probe system’s ability to emulate the spatial correlation function, and the power stability of the field incident on the DUT antennas must be verified.

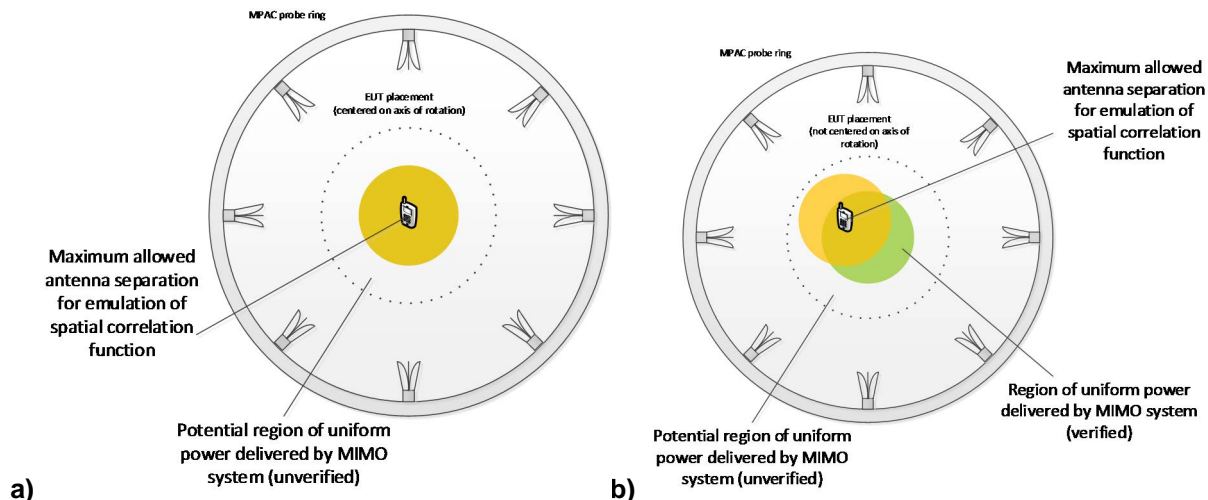


Figure E.2.1-1: Illustration of DUT antenna spacing and positioning guidelines; a) guideline in this specification, b) example with DUT meeting the maximum allowed antenna separation but not within the verified power stability region

As the channel model validation procedures for spatial correlation as defined in clause 8.3.2.3 are to be performed at the downlink center frequency in 3GPP TS 36.508 [19], the maximum antenna spacing in the DUT shall be defined by the wavelength per operating band center frequency of the middle channel of the downlink at the band under test. A verification of power stability can be derived from the spatial correlation verification results in clause 8.3.2.3. Given that this verification spans a region with a diameter of 1 wavelength centered on the axis of rotation in the chamber and that the performance demonstrated by multiple 8 dual-polarized probe MPAC implementations in clause 8.4.4 has shown good alignment up to 0.85 lambda for SCME UMi, the region where DUT antennas shall be placed (the MIMO OTA test zone) shall be defined in the same way (see Figure E.2.1-1a above) but further confined by the 0.85 lambda antenna separation limit for SCME UMi. Figure E.2.1-1b above provides an example of a DUT meeting the maximum allowed antenna separation but not within the verified power stability region; this placement of a DUT shall not be used. The optimization of the maximum allowed antenna spacing of the DUT and the verification of the test zone, as well as SCME UMa considerations, are expected as part of future work.

The region of uniform power delivered by the MIMO system (unverified) as shown in Figure E.2.1-1 is an indication of the region where the wavefront may maintain its uniformity. Therefore, it may be used to extend the test volume but is not allowed at this time. It is considered unverified because the validation of spatial correlation provides a verification that spans a region of 1 lambda. Any further extension of the verified test volume would require an update to the spatial correlation validation in clause 8.3.2.3.

The DUT maximum antenna spacing and placement within the test zone shall be defined by the following two-tier methodology due to the primary radiation modes below 1 GHz and above 1 GHz and how they relate to the device and/or antenna size.

When operating in frequency bands lower than 1GHz, the physical center of the DUT shall be placed in the chamber center, the DUT shall be completely contained within the volume defined by the respective operating band equivalent to a sphere with a radius equal to 0.425 wavelength as defined in Tables E.2.1-1 and Tables E.2.1-2 for SCME UMi.

When operating in frequency bands higher than 1 GHz the equidistant physical point between the DUT MIMO antenna system shall be placed in the chamber center following guidance defined in Figure E.2-2 and the DUT MIMO antenna system (further physical dimension or both antennas' maximum E-field regions) shall be completely contained within the volume defined by the respective operating band equivalent to a sphere with a radius equal to 0.425 wavelength defined in Tables E.2.1-1 and Tables E.2.1-2 for SCME UMi. The definition of the equidistant point between the DUT MIMO antennas shall be provided through manufacturer declaration for all operating bands where the maximum antenna separation requirement has been met. The location of the equidistant point(s) for each operating band shall be identified by the manufacturer by either marking the device utilized for MIMO OTA testing or by providing clear instructions to the test operator as to the physical location(s).

The two-tier approach is needed to be technically correct when defining the MPAC test volume. While the geometric center can be used in frequencies lower than 1GHz, the same methodology will add unnecessary limitations for test applicability in frequencies above 1GHz. In this case, manufacturers will need to provide further information to enable the proper definition of the test volume. Ideally, the same approach adopted in frequencies above 1 GHz could be used for all frequencies. However, the extra positioning work and need to identify the equidistant point between the DUT MIMO antennas isn't necessary for frequencies under 1GHz since the wavelength dimension is large enough for all handsets, phablets, and most tablets and laptops.

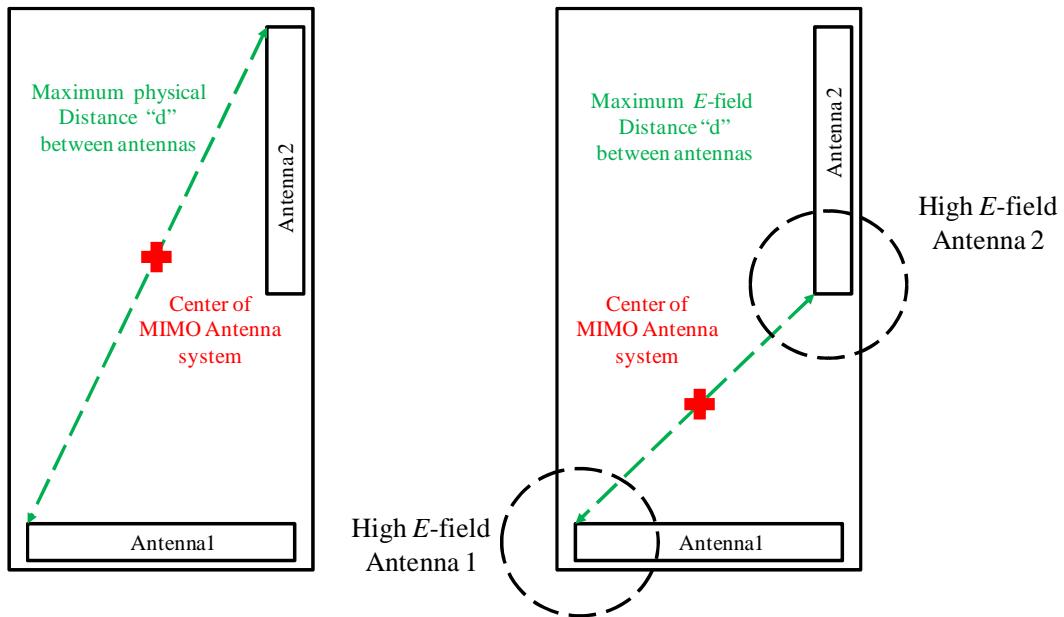


Figure E.2-2: Definition of distance between MIMO antennas and DUT center, maximum physical separation, or E-field maximum separation defined by manufacturer

Table E.2.1-1: Test zone dimension definition vs. FDD band of operation

| Band | DL middle channel frequency (MHz) | 0.85*Wavelength (m) middle channel | Test volume sphere radius (m) |
|------|-----------------------------------|------------------------------------|-------------------------------|
| 1 | 2140 | 0.119 | 0.060 |
| 2 | 1960 | 0.130 | 0.065 |
| 3 | 1842.5 | 0.138 | 0.069 |
| 4 | 2132.5 | 0.119 | 0.060 |
| 5 | 881.5 | 0.289 | 0.145 |
| 6 | 880 | 0.290 | 0.145 |
| 7 | 2655 | 0.096 | 0.048 |
| 8 | 942.5 | 0.270 | 0.135 |
| 9 | 1862.4 | 0.137 | 0.068 |
| 10 | 2140 | 0.119 | 0.060 |
| 11 | 1485.9 | 0.171 | 0.086 |
| 12 | 737.5 | 0.346 | 0.173 |
| 13 | 751 | 0.339 | 0.170 |
| 14 | 763 | 0.334 | 0.167 |
| 17 | 740 | 0.344 | 0.172 |
| 18 | 867.5 | 0.294 | 0.147 |
| 19 | 882.5 | 0.289 | 0.144 |
| 20 | 806 | 0.316 | 0.158 |
| 21 | 1503.4 | 0.169 | 0.085 |
| 22 | 3550 | 0.072 | 0.036 |
| 23 | 2190 | 0.116 | 0.058 |
| 24 | 1542 | 0.165 | 0.083 |
| 25 | 1962.5 | 0.130 | 0.065 |
| 26 | 876.5 | 0.291 | 0.145 |
| 27 | 860.5 | 0.296 | 0.148 |
| 28 | 780.5 | 0.326 | 0.163 |
| 29 | 722.5 | 0.353 | 0.176 |
| 30 | 2355 | 0.108 | 0.054 |
| 31 | 465 | 0.548 | 0.274 |
| 32 | 1474 | 0.173 | 0.086 |

Table E.2.1-2: Test zone dimension definition vs. TDD band of operation

| Band | DL middle channel frequency (MHz) | 0.85*Wavelength (m) middle channel | Test Volume Sphere Radius (m) |
|------|-----------------------------------|------------------------------------|-------------------------------|
| 34 | 2017.5 | 0.126 | 0.063 |
| 35 | 1880 | 0.136 | 0.068 |
| 36 | 1960 | 0.130 | 0.065 |
| 37 | 1920 | 0.133 | 0.066 |
| 38 | 2595 | 0.098 | 0.049 |
| 39 | 1900 | 0.134 | 0.067 |
| 40 | 2350 | 0.108 | 0.054 |
| 41 | 2593 | 0.098 | 0.049 |
| 42 | 3500 | 0.073 | 0.036 |
| 43 | 3700 | 0.069 | 0.034 |
| 44 | 753 | 0.338 | 0.169 |

The positioning of the device under test within the test volume shall be set as defined above and in Clause 9.4.

The environmental requirements for the device under test shall be set as defined in Annex D.

E.2.2 RTS Positioning Guidelines and test zone dimensions

For the RTS system, it can be seen from earlier analysis in the MU budget in Annex B.2 that the MU elements related to device size are linked to uncertainties in the field uniformity of the anechoic chamber used for the first stage antenna pattern measurement. The RTS MU budget was calculated with the assumption that the device size was within the limits defined by the chamber quiet zone defined in TS 34.114 Annex A2.3, TS 34.114 E.10 and as measured in TS 34.114 Annex G.2. The applicable device size for RTS is therefore the same as used for SISO TRS in the same chamber.

The second stage of the RTS method which involves a cable replacement radiated connection, is assumed in the MU budget to take place in the same anechoic chamber as was used for the first stage antenna pattern measurement, and there are no additional test zone considerations required. The use of a different chamber for the second stage is not precluded, but would require a recalculation of the impact of any difference between the anechoic chambers.

For device positioning within the test zone for the first stage the normal positioning accuracy assumed in Table B.2-1 of 0.5 degrees is considered insignificant compared to the raster used for the antenna measurement.

For the second stage positioning impact, and with the assumption the chamber is the same as used in the first stage, the issue is the repeatability of the position used from the first stage. This is likely to be less than the 0.5 degree absolute positioning error so is again assumed to be negligible.

Annex F: Calibration

F.1 Scope

Here the absolute power level calibration in the center of the test zone is described. Note that Clause 8.3 describes in detail the verification process for the various channel models however in addition to that an absolute power calibration needs to be performed as well. Note also that the channel model validation and absolute power calibration may have different renewal cycles.

F.2 Calibration Procedure – Anechoic chamber method with multiprobe configuration

The system needs to be calibrated in two steps in order to ensure that the absolute power is correct. The first calibration steps ensures the accurate generation of the channel model in the center of the chamber as required by Clause 8.3. The second step validates the total power as would be seen by the DUT and allows for that power to be scaled up or down if necessary.

Considering the complexity of the system various way to calibrate are possible. The end goals are however the same no matter the exact procedure. The two steps must achieve the following:

Step 1: This step is used to equalize the power in the center coming from the different probes. This being a relative measurement is very robust and with minimal uncertainty. It is sufficient to use instruments calibrated according to the manufacturer's specifications and the measurements require no additional calibration. This step is done for both vertical and horizontal polarizations. The relative differences between probe path losses are recorded and used (typically in the fading emulator) to adjust the generated fading signals for each probe. Example measurement set-up is shown in Figure 8.3.1.1-1.

NOTE 1: If Step 1 is performed as an absolute measurement accounting for the cable and reference antenna gains Step 2 can be omitted.

Step 2: This step is used to measure the total absolute power of at least one polarization in the center of the ring. Then assuming that validation of the channel models has been done, the total power available to the DUT in the center of the chamber can be computed. If necessary the power can be scaled up or down to achieve the desired power level. Since this is an absolute power measurement, the measurement cable and reference antenna gains have to be accounted for.

NOTE 2: To minimize measurement uncertainty the passive and active components of the system may be calibrated independently as well as at different intervals.

NOTE 3: Step 2 of the calibration should be performed with the channel model loaded and LTE signaling active. Sufficient amount of time averaging is required because of the fading nature of the models used.

NOTE 4: Various ways of performing the two steps may exist depending on the equipment used. The lab is responsible for providing a comprehensive calibration procedure.

NOTE 5: Steps one and two may be combined with the channel verification procedure.

NOTE 6: The calibration must be performed for all frequencies of interest.

F.2.1 Example Calibration Procedure

The calibration procedure outlined below is only one possibility based on a concrete measurement set-up. Improvements can be made to minimize measurement uncertainty.

Step 1:

1. Place a vertical reference dipole in the center of the chamber, connected to a VNA port, with the other VNA port connected to the input of the channel emulator unit – Figure 8.3.1.1-1.
2. Configure the channel emulator for bypass mode (NOTE this might not be available in all instruments)
3. Measure the response of each path from each vertical polarization probe to the reference antenna in the center.
4. Adjust the power on all vertical polarization branches of the channel emulator so that the powers received at the center are equal.
5. Repeat the steps 1 to 4 with the magnetic loop and horizontally polarized probes instead, and adjust the horizontal polarization branches of the channel emulator.

NOTE: At this stage all vertical polarization paths have equalized gains, and so do all horizontal polarization paths. The two polarizations however do not necessarily produce the same signal strength in the center of the chamber – this most commonly happens if two physically different channel emulators are used for the two polarizations. The resulting power imbalance can be accounted for either at this step or adjusted at point 7 of step 2.

Step 2 (see Figure F.2.1-1):

1. Place a vertical reference dipole in the center of the chamber connected to a spectrum analyzer via an RF cable.
NOTE: A power meter can also be used.
2. Record the cable and reference dipole gains.
3. Load the target channel model
4. Start the LTE signaling in the base station emulator with the required parameter identical to the measurements conditions (some special instrument options might be necessary).
5. Average the power received by the spectrum analyzer for a sufficient amount of time to account for the fading channel – one full channel simulation might be unnecessary.
6. Repeat steps 1 to 4 with a magnetic loop for the horizontal polarization (NOTE: this way no prior validation of the channel model is required)
7. Calculate the total power received at the test area as the sum of the power in the two polarizations.
8. Adjust the power in the two polarizations if necessary. The power adjustment can be a simple scaling of the power up or down or adjustment of the XPR due to slight differences in the fading unit's branches. Depending on the adjustment needed, it can be done at the base station emulator or the channel emulator or both.

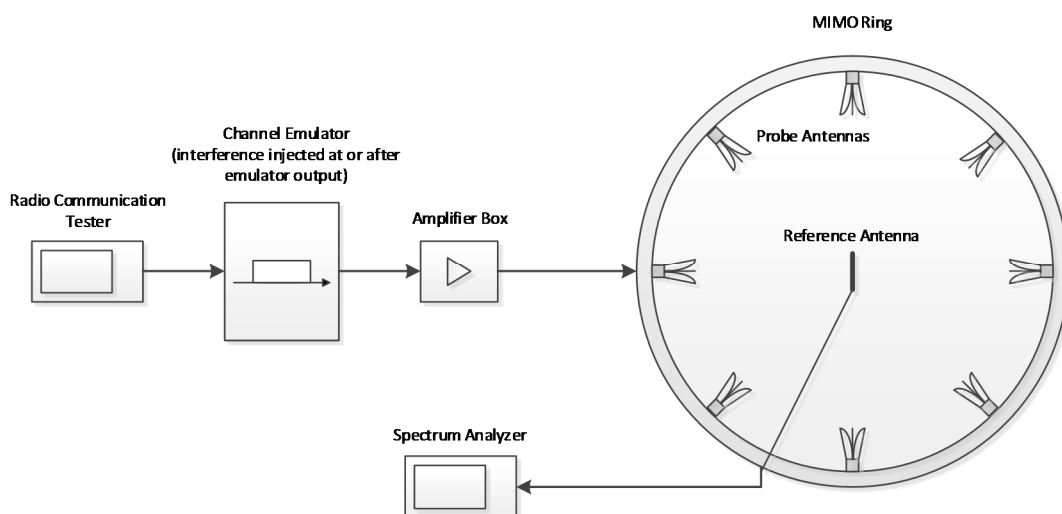


Figure F.2.1-1: – Example setup for step 2 of the calibration

F.3 Calibration Procedure – Reverberation chamber method

The purpose of the calibration measurement is to determine the average power transfer function in the chamber, mismatch of fixed measurement antennas and path losses in cables connecting the power sampling instrument and the fixed measurement antennas. Preferably a network analyzer is used for these measurements. Recommended calibration antennas are dipoles tuned to the frequency band of interest.

In general, the calibration of a reverberation chamber is performed in three steps:

1. Measurement of S-parameters through the reverberation chamber for a complete stirring sequence
2. Calculation of the chamber reference transfer function
3. Measurement of connecting cable insertion loss

If several setups are used (e.g. empty chamber, chamber with head phantom, etc.), steps 1 and 2 must be repeated for each configuration. The calibration measurement setup can be studied in Figure F.3-1.

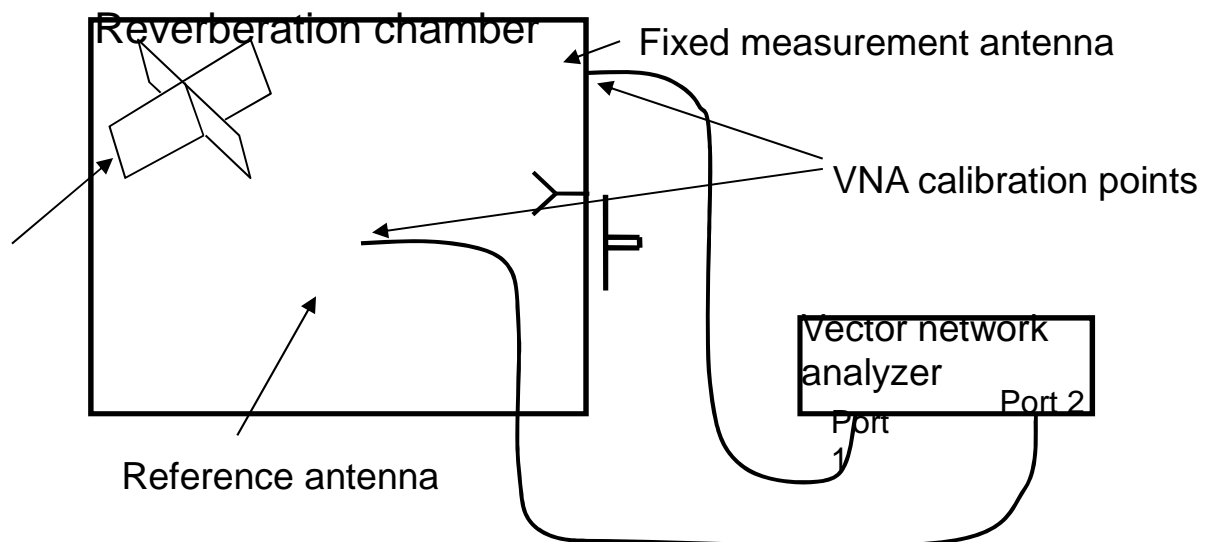


Figure F.3-1: Calibration measurement setup in the reverberation chamber, using a vector network analyzer

F.3.1 Measurement of S-parameters through the chamber for a complete stirring sequence

This step will measure S-parameters through the reverberation chamber through a complete stirring sequence. This information is required to determine the chamber's reference transfer function. The procedure must be performed separately for each measurement setup of which the loading of the chamber has been changed. The calibration procedure must be repeated for each frequency as defined above. Therefore, it is advantageous if the network analyzer can be set to a frequency sweep covering the defined frequencies, so that all frequencies of interest can be measured with a minimal number of measurement runs.

- i. Place all objects into the RC which will be used during the throughput measurements, including a head phantom, hand phantom and fixture for the EUT. This ensures that the loss in the chamber, which determines the average power transfer level, is the same during both calibration and test measurements. Also, if the EUT is large or contains many antennas, it may represent a noticeable loading of the chamber. It should then be present in the chamber and turned on during the calibration.
- ii. Place the calibration antenna inside the chamber. The calibration antenna is preferably mounted on a low-loss dielectric fixture, to avoid effects from the fixture itself which may affect the EUT's radiation efficiency and

mismatch factor. The calibration antenna must be placed in the chamber in such a way that it is far enough from any walls, mode-stirrers, head phantom, or other object, such that the environment for the calibration antenna (taken over the complete stirring sequence) resembles a free space environment. "Far enough away" depends on the type of calibration antenna used. For low gain nearly omni-directional antennas like dipoles, it is normally sufficient to ensure that this spacing is larger than 0.5 wavelengths. More directive calibration antennas should be situated towards the centre of the chamber. The calibration antenna should be present in the chamber during the throughput measurements.

- iii. Calibrate the network analyzer with a full 2-port calibration in such a way that the vector S-parameters between the ports of the fixed measurement antenna and the calibration antenna can be accurately measured. Preferably, the network analyzer is set to perform a frequency sweep at each stirrer position. This will enable calibration of several frequency points during the same stirring sequence, thereby reducing calibration time. This will also enable frequency stirring, i.e., averaging the measured power transfer function over a small frequency bandwidth around each measured frequency point (moving frequency window). This will increase accuracy at the expense of frequency resolution.
- iv. Connect the antennas and measure the S-parameters for each stirrer position and each fixed measurement antenna.

The number of stirrer positions in the chosen stirring sequence, i.e. the number of S-parameter samples at each frequency point, should be chosen in such a way that it is large enough to yield an acceptable statistical contribution to the total measurement uncertainty.

F.3.2 Calculation of the chamber reference transfer function

From the S-parameters obtained in the calibration measurement, the chamber reference transfer function for fixed antenna n can be calculated. The reflection coefficient for fixed antenna n can be calculated as

$$R_n = \left| \frac{1}{M} \sum_{m=1}^M S_{11,n,m} \right|^2 = \left| \overline{S_{11,n}} \right|^2$$

Thus, the chamber reference transfer function can be calculated as

$$P_{ref,n} = \frac{1}{M} \sum_{m=1}^M \frac{|S_{21,n,m}|^2}{(1 - R_n)(1 - |\overline{S_{22}}|^2)} \cdot \frac{1}{e_{ref}}$$

where M is the total number of samples of the transfer function measured for each fixed measurement antenna and $S_{21,n,m}$ is sample number m of the transfer function for measurement antenna n. Moreover, $\overline{S_{22}}$ is the complex average of the calibration antenna reflection coefficient. Finally, e_{ref} is the radiation efficiency of the calibration antenna.

Note that the radiation efficiency of the fixed antenna is not corrected for, because it will be the same both during calibration and measurements. Therefore the fixed antenna's radiation efficiency will not affect the final results. The same can be said about the mismatch factor of the fixed measurement antennas, but it is still advantageous to correct for this factor if frequency stirring is applied to improve accuracy.

F.3.3 Cable calibration

This measurement step will calibrate the power loss of the cables needed to connect the instrument to the reverberation chamber.

- i. Disconnect the cables between the VNA and the chamber.
- ii. Connect the cables one-by-one between the two ports of the network analyzer. The VNA must be calibrated at its own two ports.
- iii. Measure the frequency response of the transmission S-parameter (S_{21} or S_{12}) of the cable.

- iv. Save the power transfer values ($|S_{21}|^2$) of the frequency response curve for the test frequencies, and cables positions, etc).

F.4 Calibration Procedure: RTS method

For the RTS method, only the DUT reporting RSAP calibration is to perform. The RTS method depends on reported RSAP to do the antenna pattern measurement, and the power calibration for radiated second-stage throughput test. Since these reported readings do not come from a calibrated measurement instrument, their accuracies are often subject to questioning. Below procedure provides method for proper calibration to validate the reported RSAP accuracy.

- DUT reporting RSAP calibration calibration:

With proper spherical coordinate definition of mobile terminal setup, the receive antenna pattern at any coordinate (θ_i, ϕ_i) can be expressed as:

$$P(\theta_i, \phi_i) = \text{RS}_i \quad (1)$$

The test point (θ_i, ϕ_i) can be at any point on the 4π solid angle of the coordinate. More precisely, the reported RS of the UE can be expressed as:

$$\text{RS}_i(x) = m(x) \cdot x + c \quad (2)$$

where $m(x_i)$ and c is a function of signal strength independent of testing point angular coordinates. x is the actual incident field power density that can be derived from the signal power and test range loss. The above equation (2) assumes that the signal variables in both sides of the equation are expressed in decibels or dB's. When $m(x)=1$ and $c=g_0$, where g_0 is the received antenna gain at the test point, we would have declared that the RS report is a true reading of the signal strength. But in reality, $m(x)$ can be biased by either the signal level relative to the receiver's detector operating condition, or by application software programming errors. Meanwhile, the offset constant c can also be biased by either the noise floor of the receiver and/or other artificial factors in the UE RS reporting. Therefore, a Taylor's series can be introduced to have a better representation of the RS report value:

$$\text{RS}_i(x) = c + ax + bx^2 + dx^3 + ex^4 + \dots \quad (3)$$

In theory, equation (3) may require many terms to represent the RS report accurately. However, since the reported RS reading in the receive antenna pattern in (1) has a limited signal dynamic range, the following three term expression is enough to correct for the reporting errors:

$$\text{RS}_i(x) = c + ax + bx^2 + o(x^3) \quad (4)$$

The third order term $o(x^3)$ is ignored since it is not significant for limited signal dynamic range.

The RS pattern in (1) will need to be calibrated for its possible reporting errors. One practical method is to introduce signal correction terms in equation (4) to enhance the accuracy. This process is also referred to as the linearization. The following steps describe what is needed to linearize the RS report and the RS antenna pattern in (1):

- 1). Find the maximum RS reading in the pattern obtained in (1) from all angular test points, and at all polarizations. Set this point as the reference point and record signal generator power P_0 and let $x_0 = P_0 - \text{Test Range Path Loss}$ (in dB), and note the maximum RS reading as r_0 .
- 2). At the reference test point, decrease the signal generator's output power P_i , and let $x_i = P_i - \text{Test Range Path Loss}$ (in dB), starting from P_0 with a step size (1.0 dB by default) to a power range so as to obtain the full RS reading range while searching from the reference point r_0 when the test system dynamic range allows, or to 20 dB by default when the system dynamic range is known to be limited, whichever is lower in range. Record the corresponding RS reading of the UE as r_i . Repeat this process until all angular test points are completed as required.
- 3). Use those pairs of data obtained in Step 2) (r_i, x_i) as the input of the quadratic fitting curve in (4) to formulate the Algorithm LSF (Least Square Fit) to calculate the three coefficients (a, b , and c) in:

$$\text{Err}(a,b,c) = \sum (c + ax_i + bx_i - r_i)^2 \quad (5)$$

Please note that the power range of the linearization can be limited to 20 dB as stated in Step 2) since the lower RS readings than the processed range do not contribute to the overall receive antenna pattern as much.

Once the three coefficients (a,b, and c) are obtained in LSF of (5), the use of the inverse function of Equation (4) to convert RS pattern in (1) into the normalized incident power pattern. This process completes the error correction for both constant biased and the non-linearity in the RS report from the UE within the limited signal dynamic range as tested in (1) and Step 1. Similar steps can be applied for error corrections if multiple receiver RS are involved in the testing.

Of course, the reference test point can also be further tested for the threshold of the receiver sensitivity and/or throughput knee-point for the required calibrated reference power level.

Annex G: Test Volume Validation

This annex describes the procedures for validating the test volume for the different methodologies.

G.1 Test Volume Validation for the RC+CE Methodology

The crucial parameters for defining the RC+CE test volume are the isotropy and the standard deviation of the power transfer function. The validation procedure will thus consist of the following:

- Isotropy measurements in the extreme positions (boundaries) of the test volume, as well as in positions within the boundaries of the test volume.
- Standard deviation of the power transfer function measured in the same positions as defined for the isotropy measurements.

This is described in detail below.

G.1.1 Test Volume Validation Setup

There are two main RC configurations available in the industry. The first configuration utilizes a turntable for the stirring sequence and thus to emulate the desired environment. Additional stirring procedures might also exist to further improve the accuracy of the emulated channel properties. The DUT is kept on the turntable throughout the measurement sequence, thus moved around in the test volume.

The second configuration does not utilize a turntable, thus instead relying on other stirring procedures for emulating the desired environment. For this case the DUT is kept at a fixed position in the test volume throughout the measurement sequence.

In order to define a generic test volume validation procedure, it is needed to differentiate between these two types of RCs.

G.1.1.1 Type 1 Reverberation Chamber – With Turntable

For RCs utilizing a stirring configuration with a turntable, the test volume will consist of a cylinder as depicted in Figure G.1.1.1-1. The Test Volume Validation Positions (TVVPs) in this test volume consist of extreme positions, e.g. minimum distances to other metallic and/or absorbing objects and the location on the turntable, as well as additional positions representative to DUT test positions. Based on Figure G.1.1.1-1, the following baseline TVVPs are identified:

- TVVP1-3: These three positions correspond to the lower extremes of having the DUT as close as possible to the metallic turntable plate and still fulfil the 0.5 lambda guideline from [22].
 - o TVVP1 will experience a minimum of statistics, given that a DUT in this position will be kept at the same position throughout the measurement. This position could also be shifted away from the centre of the turntable, if needed for the accuracy of the measurements. For such case, the test volume would be a cylinder with the centre excluded.
 - o TVVP2 corresponds to additional test position representative to DUT test position for gathering sufficient statistics.
 - o TVVP3 is the edge of the test volume. This is the position farthest away from the turntable centre that still fulfils the requirement in [22] of being 0.5 lambda separated from other metallic or absorbing objects in the chamber (e
- TVVP4-6: These three positions correspond to additional test positions in the centre azimuth cut of the cylinder representative to DUT test positions, in order to gather sufficient statistics for the validation. The individual points correspond to the same distances from the centre of the turntable as TVVP1-3.

- TVVP7-9: These three positions correspond to extreme points at the upper edge of the test volume, which still satisfy the requirements in [22] of being 0.5λ away from metallic or absorbing objects (in this case the metallic stirrer plate; it can also be bounded by the roof of the chamber). The individual points correspond to the same distances from the centre of the turntable as TVVP1-3.

One azimuth cut consisting of 3 TVVPs is shown in Figure G.1.1.1-2 for clarity.

In addition to metallic surfaces and objects, different amount of absorbing objects can be used for obtaining the desired chamber characteristics. If such objects exist the boundaries of the test volume must be set as to take these into account. This case is depicted in Figure G.1.1.1-3, where the absorber located on the chamber wall decreases the size of the test volume.

The 9 positions defined above will be the TVVPs for Type 1 RCs and will define the valid test volume. The test system vendor should declare these 9 TVVPs for each implementation.

Having nine individual measurements will provide a sufficient statistical ground for concluding on the RC test volume characteristics. It matches the minimum number of points adopted for characterizing the uncertainty related to the chamber statistical ripple and repeatability in TS34.114 [4]. Observe however that there will be three orientations measured for each position, in order to calculate the anisotropy coefficients. This means that there will be 27 individual estimates of the power transfer function and all of these shall be used for the standard deviation calculation.

In order to pass the test volume validation, the isotropy in all TVVPs must satisfy the requirements and standard deviation of the power transfer function must result in an acceptable overall uncertainty once combined with the other uncertainty sources. If any of the positions fail the isotropy test or the resulting uncertainty exceeds acceptable limits, the test volume boundaries, and thus the TVVPs, must be redefined and the procedure repeated in the new TVVPs.

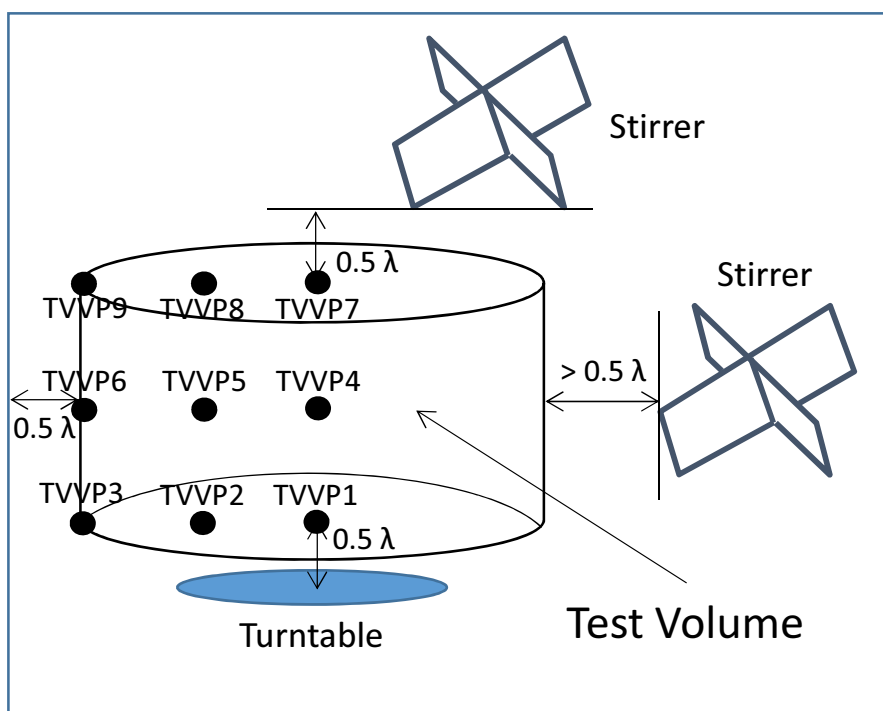


Figure G.1.1.1-1: Schematics of the test volume and baseline TVVPs for Type 1 RC.

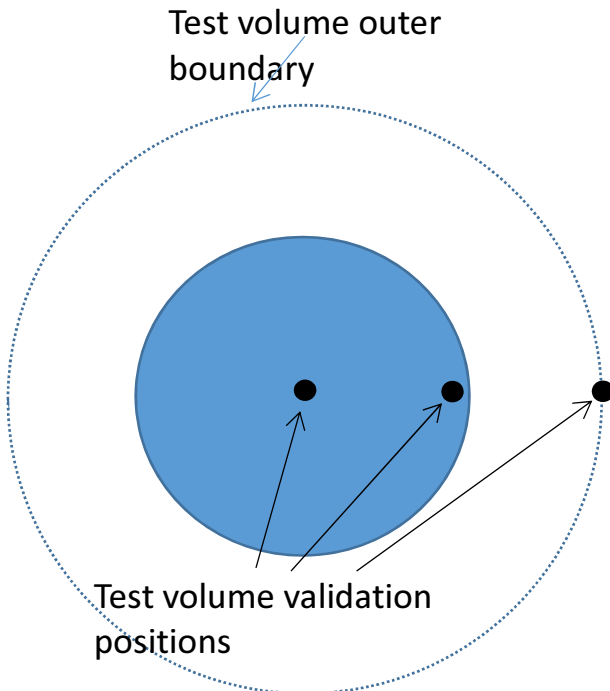


Figure G.1.1.1-2: Top view schematics of one azimuth cut of the test volume consisting of 3 TVVPs for Type 1 RC.

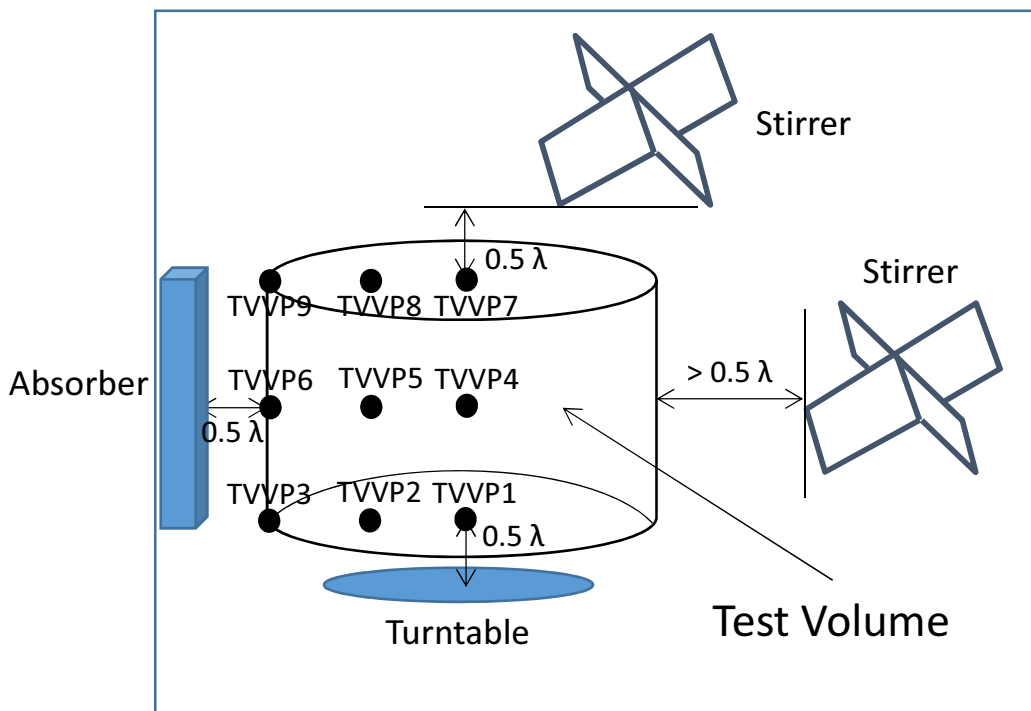


Figure G.1.1.1-3: Schematics of the test volume and TVVPs for Type 1 RC, when the test volume is bounded by an absorber on the chamber wall.

G.1.1.2 Type 2 Reverberation Chamber – Without Turntable

For RCs utilizing a stirring configuration without a turntable, the test volume will consist of a rectangular box as depicted in Figure G.1.1.2-1. As for Type 1 chambers, the TVVPs correspond to extreme positions, e.g. minimum distances to other metallic and/or absorbing objects and the location on the turntable, as well as additional positions representative to DUT test positions. Based on Figure G.1.1.2-1, the following baseline TVVPs are identified:

- TVVP1-4: These four corner positions correspond to the lower extremes of having the DUT as close as possible to the metallic floor as well as two additional walls of the chamber (or stirrers and other metallic objects) and still fulfil the 0.5λ guideline from [22].
- TVVP5-8: These four corner positions correspond to the upper extremes of having the DUT as close as possible to the metallic roof as well as two additional walls of the chamber (or stirrers and other metallic objects) and still fulfil the 0.5λ guideline from [22]. The individual points correspond to the same distances from the chamber walls as TVVP1-4.
- TVVP9: This is the centre position of the test volume and represents an additional point representative to DUT test position and provides additional statistics.

In addition to metallic surfaces and objects, different amount of absorbing objects can be used for obtaining the desired chamber characteristics. If such objects exist the boundaries of the test volume must be set as to take these into account, as for Type 1 RCs.

The 9 positions defined above will be the TVVPs for Type 2 RCs and will define the valid test volume. The test system vendor should declare these 9 TVVPs for each implementation.

Having nine individual measurements will provide a sufficient statistical ground for concluding on the RC test volume characteristics. It matches the minimum number of points adopted for characterizing the uncertainty related to the chamber statistical ripple and repeatability in TS34.114 [4]. Observe however that there will be three orientations measured for each position, in order to calculate the anisotropy coefficients. This means that there will be 27 individual estimates of the power transfer function and all of these shall be used for the standard deviation calculation.

In order to pass the test volume validation, the isotropy in all TVVPs must satisfy the requirements and standard deviation of the power transfer function must result in an acceptable overall uncertainty once combined with the other uncertainty sources. If any of the positions fail the isotropy test or the resulting uncertainty exceeds acceptable limits, the test volume boundaries, and thus the TVVPs, must be redefined and the procedure repeated in the new TVVPs.

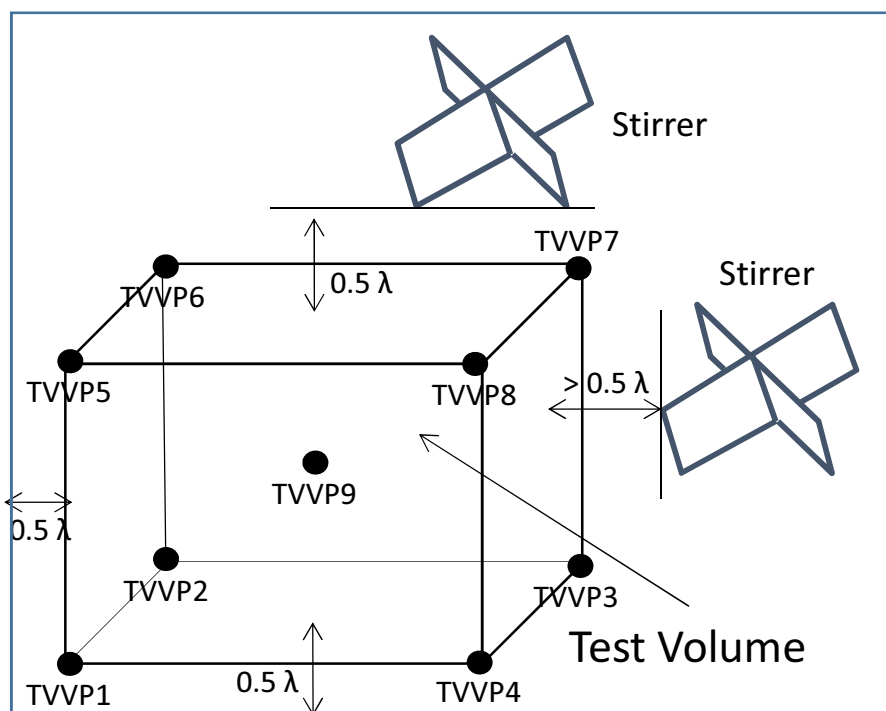


Figure G.1.1.2-1: Schematics of the test volume and baseline TVVPs for Type 2 RC.

G.1.2 Test Volume Validation Procedure

In each of the positions defined above, the procedure described in Clause C.3.2.5 of TR37.977 shall be used to obtain the test volume validation data. From this data it is possible to calculate the metrics of interest, as described below.

G.1.2.1 Isotropy

The procedure described in Annex C.3.2.5 shall be used to evaluate the isotropy in each TVVP.

G.1.2.2 Chamber Statistical Ripple and Repeatability

From the data obtained with the procedure above the chamber transfer function G_{ref}^j is calculated for each TVVP. The normalized standard deviation is then calculated as

$$\sigma = \sqrt{\frac{1}{M-1} \sum_{j=1}^M (G_{ref}^j - G_{ref}^{mean})^2}$$

where

$$G_{ref}^{mean} = \frac{1}{M} \sum_{j=1}^M G_{ref}^j$$

M is the number of antenna positions used for the estimate, in this case 27 (9 TVVPs and 3 orientations in each TVVP).

The total standard deviation is then given by

$$\sigma_{tot} = \sigma * K_p$$

where K_p is 1.05.

The standard measurement uncertainty estimate is obtained by selecting the worst case for each band/channel combination. The value obtained should be inserted into the uncertainty budget in Annex B.5 as the “chamber statistical ripple and repeatability”.

Annex H: Change history

| Change history | | | | | | | |
|----------------|-----------|-----------|----|-----|-----|---|-------------|
| Date | Meeting | TDoc | CR | Rev | Cat | Subject/Comment | New version |
| 2012-03 | R4#62bis | R4-121734 | | | | Blank report: initial content to be incorporated from TR 37.976 v1.8.0 | 0.0.1 |
| 2012-03 | R4#62bis | R4-122118 | | | | Updated TR incorporating agreed text proposals R4-122096, R4-122097, and R4-122099. | 0.1.0 |
| 2012-05 | R4#64 | R4-124568 | | | | Updated TR incorporating agreed text proposals: R4-123526 (proposed change to 6.4 is applied to Clause 8.3) R4-123271. | 0.2.0 |
| 2012-11 | R4#65 | R4-126204 | | | | Updated TR incorporating agreed text proposals: R4-125975 R4-125939 | 0.3.0 |
| 2013-01 | R4#66 | R4-130645 | | | | Updated TR incorporating agreed text proposals: R4-126911 R4-126926 | 0.4.0 |
| 2013-02 | RAN #59 | RP-130342 | | | | Presentation of TR 37.977 v0.4.0: Verification of radiated multi-antenna reception performance of User Equipment (UE) Moved to Release 12 | 0.4.0 |
| 2013-04 | R4 #66bis | R4-131665 | | | | Updated TR incorporating agreed text proposals: R4-131672 R4-131673 R4-131674 | 0.5.0 |
| 2013-05 | R4 #67 | R4-132685 | | | | Updated TR incorporating agreed text proposals: R4-131993 R4-131211 Agreed text proposals from R4#66 R4-130881 R4-130710 R4-130742 R4-130751 | 0.6.0 |
| 2013-08 | R4 #68 | R4-133205 | | | | Updated TR incorporating agreed text proposals: R4-133086 R4-133000 R4-133088 R4-133133 R4-132843 R4-132161 R4-132887 | 0.7.0 |
| 2013-09 | - | - | | | | MCCclean-up | 0.7.1 |
| 2013-09 | RP#61 | RP-131221 | | | | Presented to RP#61 for information | 1.0.0 |
| 2013-10 | R4 #68bis | R4-135392 | | | | Updated TR incorporating agreed text proposals: R4-134445 R4-134502 R4-134435 R4-134233 R4-134429 R4-134501 R4-134511 R4-134497 R4-133208 R4-133297 R4-133288 | 1.1.0 |

| | | | | | | | |
|---------|--------|-----------|------|---|---|---|--------|
| 2013-11 | R4 #69 | R4-136755 | | | | Updated TR incorporating agreed text proposals: R4-135719 R4-135720 R4-135738 R4-135725 R4-135466 R4-135736 R4-135735 R4-135749 R4-135733 R4-135722 R4-135734 R4-135368 R4-135566 R4-135766 | 1.2.0 |
| 2013-11 | R4 #69 | R4-137114 | | | | R4-136805 R4-136186 R4-136859 R4-137060 R4-137111 R4-136765 R4-137063 R4-137136 | 1.3.0 |
| 2013-12 | RP#62 | RP-131819 | | | | Presented to RP#62 for approval | 2.0.0 |
| 2013-12 | - | - | | | | TR approved by RAN | 12.0.0 |
| 03-2014 | RP-63 | RP-140376 | 001 | 1 | | Clarifications to Single Cluster Channel Model in TR 37.977 Clause 6 | 12.1.0 |
| 03-2014 | RP-63 | RP-140376 | 002 | | | Significant Figures for AoAs and AoDs for UMa-based Channel Models in TR 37.977 | 12.1.0 |
| 03-2014 | RP-63 | RP-140376 | 004 | | | Clarifications to Channel Model Validation in TR 37.977 Clause 8 | 12.1.0 |
| 07-2015 | RP-68 | RP-150966 | 011 | | | Change of TDD eNodeB emulator settings for MIMO OTA test | 13.0.0 |
| 07-2015 | RP-68 | RP-150966 | 012 | 1 | | Addition of the ATF to the two-stage method description | 13.0.0 |
| 07-2015 | RP-68 | RP-150966 | 015 | | | Addition of the ATF to the two-stage method description | 13.0.0 |
| 09-2015 | RP-69 | RP-151493 | 0016 | 1 | | CR to 37.977 on harmonization outcome | 13.1.0 |
| 09-2015 | RP-69 | RP-151493 | 0019 | - | | Addition of SIR Control for MIMO OTA test methods | 13.1.0 |
| 12-2015 | RP-70 | RP-152145 | 0023 | 1 | | CR to 37.977 on harmonization test campaign | 13.2.0 |
| 12-2015 | RP-70 | RP-152145 | 0025 | | | CR to 37.977 to clarify BS antenna assumptions for channel model validation | 13.2.0 |
| 12-2015 | RP-70 | RP-152145 | 0026 | | | CR to TR37.977: Measurement uncertainty budget for AC and RC Methodologies. This CR replaces Table B.1-1, Table B.2-1 and Table B.3-1 with new tables. However the deletion of tables B.1-1, B.2-1 and B.3-1 is not shown with track changes. | 13.2.0 |
| 03/2016 | RP-71 | RP-160471 | 0028 | | F | CR to TR37.977: Further updates to channel model validation procedures for the RC and RC+CE methodologies | 13.3.0 |
| 03/2016 | RP-71 | RP-160471 | 0030 | | F | CR for Definition of Fading Channel Emulator Output Uncertainty Term | 13.3.0 |
| 03/2016 | RP-71 | RP-160471 | 0031 | | F | CR for SIR Related Uncertainty Terms | 13.3.0 |
| 03/2016 | RP-71 | RP-160471 | 0032 | | F | Update of channel model validation results for RTS | 13.3.0 |
| 03/2016 | RP-71 | RP-160471 | 0033 | | F | Update of terminology | 13.3.0 |
| 03/2016 | RP-71 | RP-160471 | 0034 | 1 | F | CR for Definition of External Amplifiers Uncertainty Terms | 13.3.0 |
| 03/2016 | RP-71 | RP-160471 | 0027 | 1 | B | CR to TR 37.977 on harmonization outcome | 13.3.0 |
| 06/2016 | RP-72 | RP-161142 | 0035 | 1 | F | CR to TR37.977: RC+CE Test Volume Validation | 13.4.0 |
| 06/2016 | RP-72 | RP-161142 | 0037 | - | F | CR to TR37.977: RC+CE Validation Updates | 13.4.0 |
| 06/2016 | RP-72 | RP-161142 | 0036 | 2 | F | Definition of device positioning within the Multi Probe Anechoic Chamber test volume | 14.0.0 |
| 09/2016 | RP-73 | RP-161635 | 0038 | 1 | F | CR to TR37.977: Clarification to the Rayleigh Validation | 14.1.0 |
| 12/2016 | RP-74 | RP-162389 | 0040 | | F | Correction of DUT testing conditions | 14.2.0 |
| 12/2016 | RP-74 | RP-162436 | 0043 | 1 | F | CR to TR37.977: RC+CE Channel Model Validation Results | 14.2.0 |
| 03/2017 | RP-75 | RP-170556 | 0046 | 2 | F | CR to TR 37.977 on lab alignment test plan | 14.3.0 |
| 03/2017 | RP-75 | RP-170602 | 0047 | - | F | CR to TR37.977: RC+CE Channel Model Validation Requirements | 14.3.0 |
| 03/2017 | RP-75 | RP-170602 | 0048 | 2 | B | UMi Channel Model validation limits | 14.3.0 |
| 03/2017 | RP-75 | RP-170556 | 0049 | - | F | CR to 37.977 to add test zone size for RTS | 14.3.0 |
| 03/2017 | RP-75 | RP-170556 | 0050 | 2 | F | Correction of uplink power control setting | 14.3.0 |

History

| Document history | | |
|-------------------------|------------|-------------|
| V14.3.0 | April 2017 | Publication |
| | | |
| | | |
| | | |
| | | |